Generation of neuronal diversity in the mammalian cerebral cortex

Llorca Molina, Alfredo

Awarding institution:
King's College London

Generation of neuronal diversity in the mammalian cerebral cortex

Alfredo Llorca Molina

A thesis for the degree of Doctor of Philosophy

September 2019

Centre for Developmental Neurobiology

King's College London

"*Desafortunadamente la naturaleza parece inconsciente de nuestra necesidad intelectual de conveniencia y unidad, y muy frecuentemente se deleita con la complicación y la diversidad*." – **Santiago Ramón y Cajal**

"Unfortunately, nature seems unaware of our intellectual need for convenience and unity, and very often takes delight in complication and diversity." – ***Santiago Ramón y Cajal***

"*Que siguin moltes les matinades que entraràs en un port que els teus ulls ignoraven, i vagis a ciutats per aprendre dels que saben."*– **Lluís Llach, *Itaca.***

"Let them be many the mornings that you will enter a port that your eyes ignored, and go to cities to learn from those who know." – **Lluís Llach, *Itaca.***

ABSTRACT

The mammalian cerebral cortex is one of the most complex cellular machineries developed by nature, containing a wide diversity of neuronal cell types that present unique structural and functional features. These diverse cell types are, moreover, heterogeneously distributed across different regions of the cortical territory, assembling region-specific cellular architectures. Despite decades of study, the developmental mechanisms that originate this diversity are not completely understood. In this thesis, I have studied the mechanisms underlying the origin of the diverse types of excitatory pyramidal cells and inhibitory interneurons that populate the murine cortex.

Our results indicate that cortical progenitor cells exhibit heterogeneous neurogenic behaviours, generating progenies composed by a wide range of sizes and fates. These results are compatible with a stochastic model of cortical neurogenesis, in which cortical progenitor cells, despite sharing common molecular programmes, undergo a series of probabilistic decisions that lead to the specification of very heterogeneous progenies. Such mechanism would allow the flexible tuning of the neuronal output of cortical progenitor cells, supporting the generation of diverse region-specific cytoarchitectures without the requirement of region-specific intrinsic programmes.

We also investigated the mode of division of progenitor cells in the embryonic subpallium. Our observations suggest the existence of expansive

intermediate progenitor cells in the medial ganglionic eminence, which divide several times to produce small groups of post-mitotic neurons.

Finally, we designed and tested a novel high-resolution lineage tracing method that will allow us to map interneuron origins from development to adult life. Used in appropriate experimental conditions, this method will represent a powerful tool for the identification of interneurons derived from individual progenitor cells. This tool will open the opportunity for an in-depth description of the neuronal outputs of subpallial progenitor cells at single cell resolution.

ACKNOWLEDGEMENTS

I would like to first thank the director of my thesis, Oscar Marín, for giving me the opportunity to work in his lab. He has been a real mentor in science, and has constantly helped me to develop and independent way of thinking, and to grow as a scientist. From him I learned the importance of doing a proper work, no matter the costs in time or effort. His constant support and positivism also made me learn to enjoy science all the way, even in the hardest moments. I would also like to thank my second supervisor, Beatriz Rico, who has been very supportive during all these years, and has also provided useful feedback to our work. Third, I would like to thank Gabriele, who has strongly contributed to the projects presented in this thesis, and who helped me with these firsts steps in the lab, which were also the most difficult. His guidance at these moments was very important for me, and I will always be thankful for it. I also own a special mention to both Marian and Elena, who importantly contributed to this work, and with their care and loyalty to both me and the project had made my project our project. The opportunity to work together allowed us to build a relationship that is, by now, way further than just professional.

I should not forget to thank all my colleagues in both the Marín and Rico labs. From those I met in Alicante (Trini, Virtu, Nines, Carol, Ricardo, Nathalie, Cristina, Giorgia, Jorge, Amanda, Malik, Isabel, Ana, Aida, Diana, Sandra and Ana) to those that accompanied me during most of my time in the Marín Lab (Clemence, Lynette, Mi Da, Asha, Sunny, Ian, Martijn, Varun, Veronique,

Alberto, Claudia, Catarina, Charlotte, Adrián, Julie, Tim, Nancy, Laura, and Maddalena) and also the people who recently join (Alicia, Risto, Giuseppe, Noemi, Fernando, and Alfonso). Please forgive me if I forgot to mention anyone. Together they created a great environment, making very pleasant to work in the lab, and I'm sure that all of them have, one way or another, contributed to this thesis. From all of them, I would like to specially thank Fong Kuan, David and Monika, with whom I enjoyed passionate scientific discussions, and who have specially supported me in the moments of doubt and uncertainty. Working with you has been a great privilege.

Among all my colleagues, there are a few that stand out, those that shared the move from Alicante to London, those I would not doubt to call friends. Rubén, who taught me almost everything I now about cloning and molecular biology, and who has been a great example of ethics and integrity in science. Emilia, who has been an example of effort and critical thinking, and with whom I shared many fun and useful discussions about big picture neuroscience, that I miss a lot now. And Antonio, who was an example of fight and courage in the worst moments, and from who I learned that passion and ideas are the most important part of our work. Together with the already mentioned Marian they have been a great support during all these years.

I believe that Patri requires an individual mention. She has certainly been my closest friend during all these years, and the only one that has accompanied me during my entire thesis. She has been my "Sam" in this story, always loyal, always supportive, always present. She has helped me to enjoy this time, and

also to believe in myself in the hardest times. It would not have been the same without her.

No somos sino la suma de las experiencias y las personas que han marcado nuestra vida. En este sentido, hay tres personas que han tenido enorme peso en la mía, haciendo de de mi lo que soy ahora; mi padre, mi madre y mi hermana Adri. Los tres, con su vida incansable, han conseguido que me sienta querido cada día de mi vida, y me han mostrado lo que es verdaderamente importante, y cómo alguien puede poner en segundo plano sus sueños, ambiciones y deseos sólo para cuidar y ayudar a los seres queridos. Espero reunir algún día la fuerza y el valor para parecerme más a ellos. Ningún hijo tendrá nunca mejores padres. Ningún hermano tendrá nunca mejor hermana.

También quisiera recordar a mis amigos, aquellos que han estado siempre a mi lado y me han hecho disfrutar de todo el camino hasta hoy; Andrés, Ernesto, Guillem, Pablo, Amanda y Violeta. También a Guille y a Nico, quienes comparten mi pasión por la ciencia. Ellos, junto a muchos otros, siempre estuvieron presentes y creyeron en mí, haciendo de estos años un tiempo mucho más sencillo de lo que habría sido sin ellos. Juntos vivimos momentos inolvidables que ya serán para siempre parte de este trabajo, !Y no cambiamos un solo minuto!.

It has been a long journey, but I have enjoyed every single bit of it, and that as only been possible because of the care and support of all these people, and the ones I could have forgot. All of them are part of this and deserve their place in this thesis.

CONTRIBUTION STATEMENT

This thesis contains published work that includes experiments and analysis performed by our collaborators. I will therefore clearly state the individual contribution of each person to the presented work:

Alfredo Llorca performed all the experiments presented in this thesis, with the exception of lineage tracing experiments using retrovirus and Mosaic Analysis with Double Markers (MADM). Gabriele Ciceri carried the retroviral work (Figures 2.1, 2.2, 2.3 and 2.9 Top). MADM experiments (Figures 2.5, 2.6 and 2.9 Bottom) where done by Robert Beattie in the Hippenmeyer Lab. However, MADM experiments were designed, and their results analysed by Alfredo Llorca.

Mathematical models were also product of collaborative work. Bayesian inference of progenitor types (Figure 2.13) was done by Giovanni Diana under constant supervision and dialog with Alfredo Llorca. Both Alfredo Llorca and Miguel Maravall contributed directly to the generation of explicit models of progenitor cell behaviour (Figures 2.12, 2.14 and 2.15). Miguel Maravall was in charge of generating the code for those models.

Text on results chapter I is identical to the later published paper on this matter. Both Alfredo Llorca and Oscar Marín contributed to write this text. The first draft of it originally written by Alfredo Llorca.

TABLE OF CONTENTS

Abstract……3
Acknowledgements……5
Contribution statement ……8
Table of contents……9
List of figures…….. 12
Abbreviations……14
Key definitions……15
Introduction……16
1. Neuronal diversity and brain function……17
2. General mechanisms for the generation of neuronal diversity….18
2.1 Patterning and cell specification…….18
2.2 Spatial patterning: The vertebrate spinal cord as a model….19
2.3 Temporal patterning: Deterministic and stochastic models…25
3. Developmental origin of neuronal diversity in the mammalian cerebral cortex……40
3.1 Cellular composition of the mammalian cortex……41
3.2 Early patterning of the mammalian telencephalon……50
3.3 Developmental origins of cortical PC diversity……57
3.4 Developmental origins of cortical IN diversity……67
4. Thesis Aims……78
Materials & Methods……79
Mice……80
Generation of *c-Binbow* and *n-Binow* mouse strains……81
Generation of retroviral vectors……81
In utero infection and electroporation……82
Inducible genetic labelling……82
Histology……83
Cell culture and *in vitro* tests……84
Alternative recombination i*n vitro* test……85
Imaging……85
In silico modelling of cortical development ……85

Bayensian inference of progenitor types..…….……..87

Quantification and statistical analysis…….……89

Data and software availability..……..……93

Results..…… 94

Chapter I : A stochastic framework of neurogenesis underlies the assembly of neocortical cyoacrhitectures……..……94

1. Introduction……..……..……95

Retroviral tracing of pyramidal cell lineages…….……98

2. Results……..…..……..……..104

A small fraction of progenitors generates laminar-restricted lineages. ……104

Pyramidal cell lineages acquire diverse configurations..……111

Heterogeneous lineage configurations arise directly from neurogenesis…..……..……...115

Laminar densities do not predict lineage structure……117

Stochastic models reproduce the diversity of progenitor outputs……119

A small number of progenitor identities underlie lineage diversity……..……121

3. Discussion……..…..……..……..126

Methodological considerations…….……..……127

Diversity of neocortical lineages...…….……129

A stochastic model of cortical neurogenesis…..…….……131

Chapter II : Mapping the origins of cortical interneuron diversity…...…134

1. Introduction……..……..……..……135

2. Results...……..……..……139

Progenitor cell diversity in the MGE…...…….…….……139

Mode of division of IN progenitor cells…...……..……141

SVZ expansion of MGE lineages…….……..……144

A novel strategy to map IN lineages: The *Binbow* system …148

Identification of four incompatible lox sites..…..……151

Combinatorial labelling with four distinguishable reporters..153

Functional characterisation of *Binbow* cassettes…...…..……155

3. Discussion……158

Cellular logic of IN genesis……158

Lineage tracing in cortical INs……161

Discussion……165

Stochastic generation of PC diversity……166

Development of IN lineages……176

Fate and freedom in cortical neurogenesis: An integrated view of PC and IN fate-specification……178

References……186

Appendix……216

LIST OF FIGURES

INTRODUCTION

Figure 1.1 Neuronal diversity in the vertebrate ventral spinal cord
Figure 1.2 Spatial patterning in the ventral spinal cord
Figure 1.3 Temporal patterning in *Drosophila* neuroblasts
Figure 1.4 Fate specification in the vertebrate retina
Figure 1.5 Pyramidal cell diversity in the mammalian cerebral cortex
Figure 1.6 Interneuron diversity in the mammalian cerebral cortex
Figure 1.7 Spatial patterning in the mammalian telencephalon
Figure 1.8 Developmental origins of neocortical pyramidal cells
Figure 1.9 Fate specification of cortical pyramidal cells
Figure 1.10 Development of cortical interneurons
Figure 1.11 Fate specification of cortical interneurons

RESULTS: CHAPTER I

Figure 2.1 Identification of pyramidal cell lineages with low-titer conditional reporter retroviruses
Figure 2.2 Sparse labelling of neuronal clones with low-titer retroviral infection
Figure 2.3 Retroviral-based lineage tracing reveals diverse lineage outcomes
Figure 2.4 Lineage tracing of Tbr2+ intermediate progenitor cells
Figure 2.5 Lineage tracing using MADM identifies a small fraction of deep layer-restricted cortical lineages
Figure 2.6 Large MADM subclones reveal a small fraction of artifactual superficial layer-restricted lineages in the retroviral dataset
Figure 2.7 A fraction of early-quiescent cortical progenitors generates superficial layer-restricted lineages
Figure 2.8 Translaminar lineages adopt very heterogeneous configurations
Figure 2.9 Retrovirus and MADM labeled lineages reproduce laminar configuration diversity
Figure 2.10 Identification of pyramidal cell subclasses
Figure 2.11 Subtle impact of pyramidal neuron cell death in final configurations of cortical neuron lineages
Figure 2.12 Laminar densities of pyramidal neurons do not predict lineage structure
Figure 2.13 A stochastic model of cortical neurogenesis
Figure 2.14 A small number of progenitor identities underlie lineage diversity

Figure 2.15 Stochastic models considering single and multiple programmes corroborate Bayesian inference

RESULTS: CHAPTER II

Figure 3.1 Progenitor cell diversity in the embryonic subpallium
Figure 3.2 MGE progenitor cells generate complex expansive lineages
Figure 3.3 SVZ expansion of MGE lineages
Figure 3.4 The *Binbow* system
Figure 3.5 Identification of four incompatible pairs of lox sites
Figure 3.6 Selection of distinguishable reporters for combinatorial labelling
Figure 3.7 Functional characterisation of *Binbow* cassettes

ABBREVIATIONS

AC: Amacrine cell

APN: Associative projection neuron

BC: Bipolar cell

BMP: Bone morphogenic protein

bRGC: Basal radial glia cell

CCK: Coleocistokinin

CFuPN: Corticofugal projection neuron

CGE: Caudal ganglionic eminence

CNS: Central nervous system

CP: Cortical plate

CPN: Commissural projection neuron

CR: Calretinin

CSrPN: Corticostriatal projection neuron

CThPN: Corticothalamic projection neuron

FGF: Fibroblast growth factor

FT: Flashtag

GABA: Gamma amino-butyric acid

GCL: Ganglion cell layer

Gdf: Growth differentiation factor

GMC: Ganglion mother cell

HPN: Heterogeneous projection neuron

HZ: Horizontal cell

IN: Interneuron

INL: Inner nuclear layer

IPC: Intermediate progenitor cell

IPL: Inner plexiform layer

iSVZ: Inner subventricular zone

ITPN: Intra-telencephalic projection neuron

IZ: Intermediate zone

LGE: Lateral ganglionic eminence

L-HD: Lim-Homeodomain

MACRM: Mosaic analysis with repressive cell marker

MADM: Mosaic analysis with double markers

MGE: Medial ganglionic eminence

MN: Motorneuron

MZ: Marginal zone

NB: Neuroblast

NEC: Neuroepithelial cell

NOS: Nitric oxide synthase

NPY: Neuropeptide Y

ONL: Outer nuclear layer

OPL: Outer plexiform layer

oRGC: Outer radial glial cell

oSVZ: Outer subventricular zone

PC: Pyramidal cell

POA: Preoptic area

POH: Preoptic-hypothalamic border domain

PV: Parvalbumin

RA: Retinoic acid

RPC: Retinal progenitor cell

RGC: Retinal ganglion cell

RGC: Radial glial cell

tTF: Temporal transcription factor

S1: Primary somatosensory cortex

SC: Spinal cord

SCPN: Subcerebral projection neurons

SNP: Short neural precursor

SP: Subplate

SST: Somatostatin

SVZ: Subventricular zone

VS: Ventricular surface

VZ: Ventricular zone

KEY DEFINITIONS

Cell type: Basic unit of cell identity. Consists in a group of cells that share morphological, physiological, anatomical and/or neurochemical features that make them unequivocally distinguishable form others.

Cell class: Higher category in the hierarchical classification of cell identities, which encloses a number of cell types based in their phenotypic similarity.

Lineage: The entire set of post-mitotic cells derived from a single progenitor cell

Sub-lineage: The set of cells originated from one of the two daughter cells resulting from a cell division. In MADM clones, sub-linage reflects to the group of cells expressing each reporter in G2-X lineages, and all yellow cells in G2-Z lineages.

Cell fate: The set of phenotypic features that define the identity of a cell. In progenitor cells, fate refers to their commitment to generate specific cell outputs.

Reprogramming: Induced change in the molecular program of a progenitor cell that leads to a variation in the cell fate of their nascent progenies.

INTRODUCTION

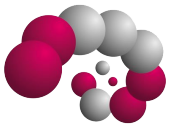

1. Neuronal diversity and brain function

Following the proposition of the cell theory by Schwann and Schleiden in 1839, a prolific generation of scientists (including Purkinje, Valentin, Remark and others) focused their research efforts in the study of the cells that compose the nervous system. These efforts lead to the proposition of the neuron doctrine, supported by the decisive work of Santiago Ramón y Cajal and Heinrich Wilhelm Gottfried Waldeyer, among others, in the last decades of the 19th Century. The word "neuron" was then coined by Waldeyer as a way to identify nerve cells. Since then, scientists have been fascinated by the wide diversity of neuronal morphologies that exists in the central nervous system (CNS) of animal species. The brain is, indeed, one of the best examples of biological diversity in nature, containing a large number of cell types that integrate into complex brain networks and play specific roles in neural computation. Our understanding of adult brain function is therefore as good as our knowledge of the neuronal diversity that populates it, and this will likely remain the case during the next decades. In mammals, such diversity of cell types has its origin in the embryonic and early postnatal life of the animal. During this period, diverse cellular and molecular mechanisms are responsible for the generation of the adult diversity of neuronal types. Despite decades of study, our current understanding of these mechanisms remains incomplete. Remarkably, malfunction of the developmental mechanisms underlying the origin of this neuronal diversity have been linked to a large number of human disorders, highlighting the importance of such processes for the correct function of the adult brain. Consequently, the study of

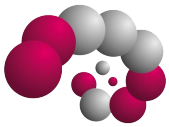

the cellular diversity that constitutes the mammalian brain, as well as the mechanisms underlying its appearance, is of outstanding importance in modern neuroscience. Research efforts in this direction will largely contribute to our future knowledge of brain function and dysfunction, having, in addition, potential applications in the diagnosis and treatment of neurological and psychiatric disorders.

Deciphering the cellular and molecular rules that underlie the generation of cell diversity is a challenge in developmental neurobiology. Here, I will describe our current knowledge of these mechanisms, using the biological systems in which these processes have been more extensively studied as an example. I will also discuss how the combined action of diverse mechanisms coordinates the assembly of our central system of study: the murine cerebral cortex.

2. General mechanisms for the generation of neuronal diversity

2.1 Patterning and cell specification

The many different neuronal types of the nervous system originate from mitotically active cells named neural progenitors. These progenitor cells are therefore responsible for the generation of neuronal diversity, which is accomplished by two main mechanisms known as spatial patterning and temporal patterning. Spatial patterning uses positional information within the developing tissue to establish the identity of the nascent neurons. In contrast, temporal patterning refers to the mechanism through which cell fate is specified by birthdate. In this framework, neurons originate from a particular point inside a

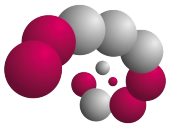

tetra-dimensional matrix established by the three spatial coordinates and the temporal line. Their point of origin within such matrix would suffice to predict their cell fate. While this seems to be the case for the simplest neurological systems, such as for example the nervous system of the nematode *C. elegans*, predicting cell fate has proven far more complex in more sophisticated nervous systems.

Spatial and temporal patterning have been extensively studied in many different biological systems. For instance, the vertebrate spinal cord represents an exquisite example of how neural progenitors utilise spatial information for the specification of the diverse neuronal identities. On the other hand, the development of *Drosophila* nervous system and the vertebrate retina illustrate two different ways in which time is used to define the identity of nascent neurons. I will use these systems to describe our current understanding of spatial and temporal patterning, respectively.

2.2 Spatial patterning: The vertebrate spinal cord as a model

Cell diversity in the ventral spinal cord

The developing spinal cord can be divided into two main regions in the dorsoventral axis, the basal plate located ventrally to the sulcus limitans, and the alar plate above. In the basal plate, two main classes of neurons can be distinguished: Motor neurons (MNs) innervate different muscle groups to execute motor commands, while locally-connected interneurons (INs) coordinate the activity of MNs by linking afferent sensory information with precise MN groups. Both these classes can be further divided into several cell subclasses.

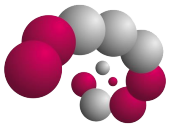

Spinal INs, for instance, can be divided in four main subclasses named V0, V1, V2 and V3 (FIG 1.1A). These IN subclasses can, in turn, be further divided into a larger number of cell types based on the expression of specific molecular markers (Alvarez et al., 2005; Sapir et al., 2004). For example, recent findings revealed the existence of deep transcriptional heterogeneity in murine spinal INs at lumbar levels, which may comprise as many as fifty different types of V1 INs based on their transcriptional signature (Bikoff et al., 2016). In addition, a recent study has reported regional variations in the composition of V1 INs at different rostrocaudal levels of the murine spinal cord (Sweeney et al., 2018). This highlights that the extent of IN diversity in the ventral SC may be larger than previously anticipated. Thus, while it is clear that spinal cord INs represent a very diverse group of neurons, our current knowledge about the cell types that compose such group remains incomplete.

Motor neurons, on the other hand, can be classified into different motor columns based on their position and projection targets (FIG 1.1B). For example, MNs in the lateral motor column are present at limb levels and project to limb muscles, while medial motor column neurons are present along the entire rostrocaudal dimension and innervate dorsal axial musculature. Motor columns can be further subdivided into different divisions and pools based in their precise muscle innervation (FIG 1.1C).

Dorsoventral patterning in the vertebrate ventral spinal cord

During embryonic development, the activity of several signalling gradients delineates the identity of different progenitor pools along the dorsoventral axis of

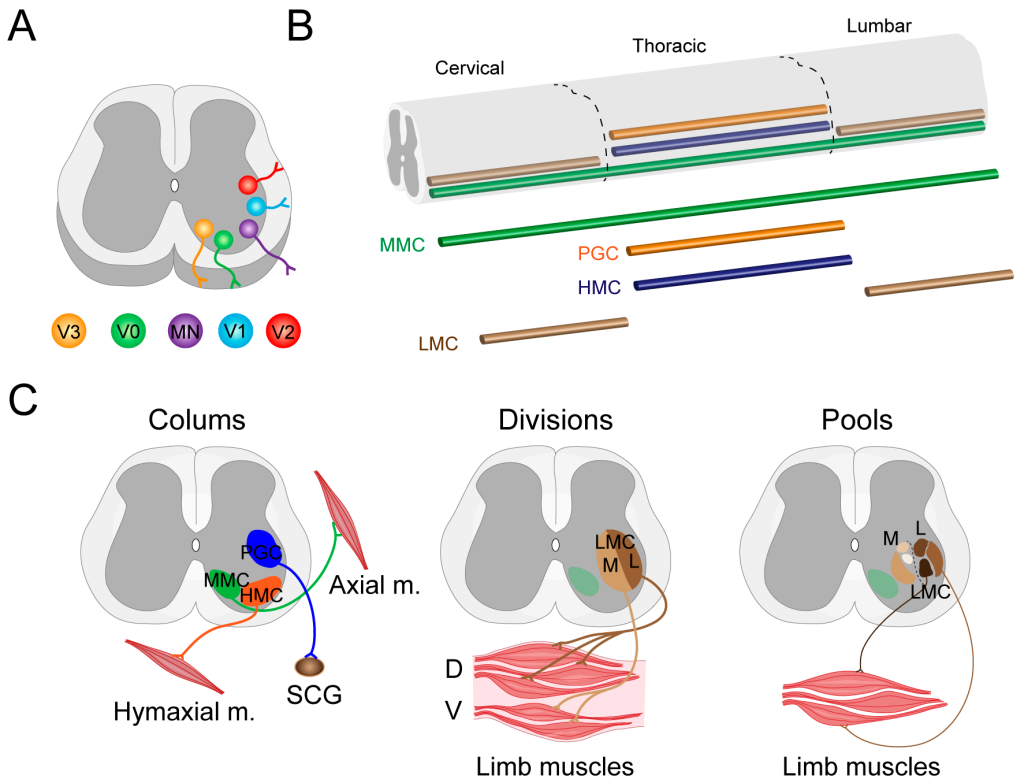

Figure 1.1. Neuronal diversity in the vertebrate ventral spinal cord
(**A**) Schematic representation of the neuronal identities populating the ventral spinal cord of vertebrates. Four types of interneurons (V0, V1, V2 and V3) can be observed along with MNs. (**B**) Principal motor columns present at different rostrocaudal levels of the spinal cord. (**C**) Motor columns are defined on the bases of their target muscle groups. These columns can be further subdivided in divisions and pools regarding their precise muscle innervation. As an example, MNs of the LMC project to limb muscles. This column is split in two divisions: the lateral division (L) projects to dorsal flexor muscles, the medial division (M) projects to ventral extensor muscles. Both divisions can be subdivided in MN pools innervating individual muscle groups. MN, motor neuron. MMC, medial motor column. PGC, visceral preganglionic column. HMC, hypaxial motor column. LMC, lateral motor column. *Figure inspired by Dansen and Jessel 2009*.

the vertebrate SC. For instance, the diffusive signal sonic hedgehog (Shh) is secreted from the mesodermal notochord, an embryonic structure located ventrally to the neural tube (Placzek, 1995). In amniotes, Shh induces the formation of the floor plate in the ventral-most part of the developing SC. Subsequently, cells constituting the floor plate also commence to secret Shh. The ventral position of both signalling centres and the diffusible nature of the protein leads to the generation of a dorsoventral gradient of Shh, which expose dorsal

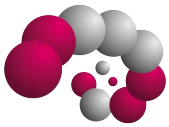

regions of the SC to progressively smaller doses of this signal (FIG 1.2A) (Jessell, 2000). This ventral-to-dorsal signalling gradient triggers downstream events that induce the specification of diverse neuronal fates in a dose-dependent manner. Consistently, exposure of chick embryonic SC explants to different doses of Shh *in vitro* induces the appearance of diverse cell identities (Ericson et al., 1996; Roelink et al., 1995; Ericson et al., 1997a; 1997b), while blocking of Shh signalling disrupts the genesis of these identities both *in vitro* and *in vivo* (Ericson et al., 1996). Besides Shh, other signals are known to take part in this process, including retinoic acids (RAs) secreted from the paraxial mesoderm (Pierani et al., 1999).

Shh plays its role by regulating the expression of different Homeodomain (HD) transcription factors (Briscoe et al., 2000; 1999; Ericson et al., 1997a; 1997b). In brief, Shh represses the expression of Class I HD proteins and induces the expression of Class II HD proteins. Since the expression of each HD protein is induced by a specific dose of Shh, this process leads to the expression of different HD transcription factors in different dorsoventral regions of the SC (FIG 1.2A) (Balaskas et al., 2012). These transcription factors subsequently interact through negative gene regulatory feedback loops, restricting the expression of each HD protein to a spatially defined territory (Briscoe et al., 2000). This pattern of expression leads to the segregation of progenitor cells into different dorsoventral domains, and instructs them to generate specific classes of neurons. Five spatially-organised progenitor pools, named p0, p1, p2, pMN and p3 are delineated along the dorsoventral dimension of the ventral embryonic SC.

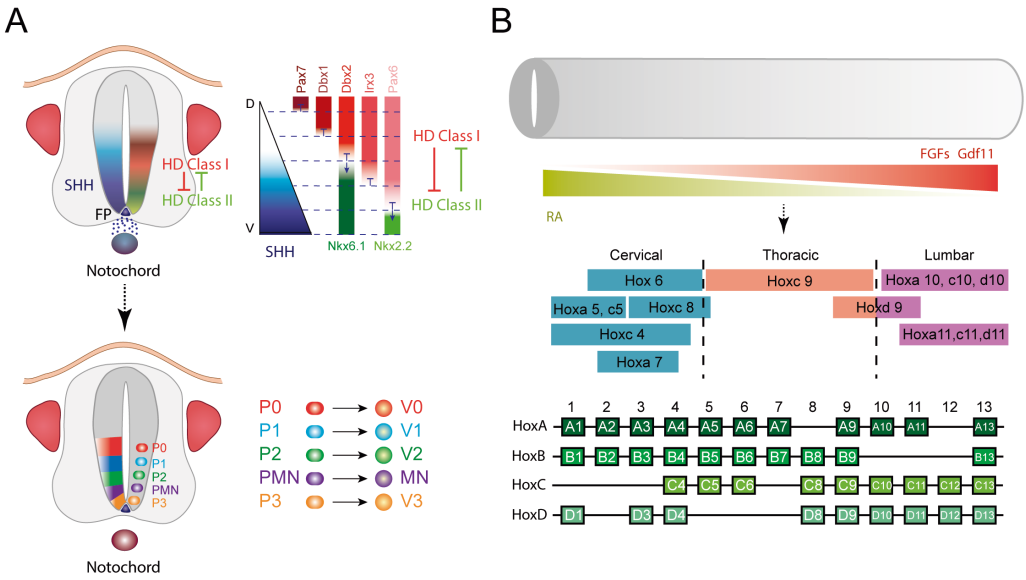

Figure 1.2. Spatial patterning in the ventral spinal cord
(**A**) Schematic representation of dorsoventral pattering mechanisms in the embryonic ventral spinal cord. The notochord and the FP secrete the diffusive signal Shh, generating a ventral-to-dorsal gradient of this protein. The exposure to different levels of Shh induces the expression of diverse HD proteins at different dorsoventral levels of the spinal cord. Feedback interactions between the different HD proteins further refine these expression patterns, delineating five progenitor domains with distinctive gene expression profiles. Each of these progenitor domains (P0, P1, P2, PMN & P3) is then committed for the generation of the corresponding neuronal identity. (**B**) Schematic representation of rostrocaudal pattering mechanisms in the embryonic ventral spinal cord. *Top*: Signalling gradients of diverse diffusive cues in opposite directions induce the expression of different *Hox* genes along the rostrocaudal axis of the spinal cord. This initial expression triggers complex downstream events leading to the specification of MN columnar identities. *Bottom;* Genome-clustered organisation of *Hox* genes. The rostrocaudal order of expression of *Hox* genes recapitulates their genomic organisation. Shh, sonic hedgehog. FP, floor plate. RA, retinoic acid. FGFs, fibroblast growth factors. Gdf, growth differentiation factor 11. *Figure inspired by Jessel 2000.*

Each of these pools expresses a particular combination of HD proteins, and is tuned for the generation of their homonymous cell class (i.e., progenitor cells of the p0 domain will exclusively generate V0 INs, while progenitors of the pMN domain would be committed to generate spinal motorneurons) (FIG 1.2A) (Briscoe et al., 1999; Ericson et al., 1997b; Pierani et al., 1999). Consistently, ectopic expression of these HD proteins is sufficient to generate the corresponding neuronal classes (Briscoe et al., 2000). Through this process, progenitors cells acquire the capacity to generate specific neuronal fates via the

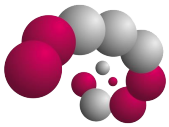

expression of certain combinations of transcription factors which, in turn, relies entirely on spatial information.

Rostrocaudal patterning in the vertebrate spinal cord

The mechanisms regulating the specification of different columnar identities among motor neurons are similar to those use for the dorsoventral patterning of the SC. In chick and mouse embryos, two opposite gradients of morphogens provide positional information along the rostrocaudal dimension of the neural tube. Proteins from the fibroblast growth factor family (FGFs) as well as Growth differentiation factor 11 (Gdf11) are secreted by the caudal Hensen's node and the embryonic tail bund, while RAs are synthesised by the rostral paraxial mesoderm (Berggren, 1999; Crossley and Martin, 1995; Liu et al., 2001; Mahmood et al., 1995; Dubrulle et al. 2004; Nakashima et al., 1999; Niederreither et al., 1997; Niswander and Martin, 1992; Riese et al., 1995). These signals therefore establish morphogen gradients in opposite directions (FIG 1.2B). Similarly to HD proteins in the dorsoventral axis, these diffusive signals negatively regulate the expression of each other. This establishes a scenario of molecular competence that causes the exposure of different rostrocaudal territories in the SC to different doses of these signals (Del Corral and Storey, 2004).

These signalling gradients induce the expression of a family of genome-clustered genes encoding for Hox transcription factors in a dose-dependent manner. In other words, exposure to different doses of FGFs and Gdf11 induces the expression of specific combinations of *Hox* genes along the SC rostrocaudal

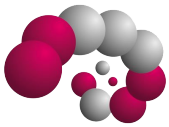

axis (Bel-Vialar, 2002; Liu et al., 2001). Interestingly, the rostrocaudal order of expression of these genes recapitulates their genomic organisation (FIG 1.2B) (Carpenter, 2002; Fernald, 2006; Kmita and Duboule, 2003). This heterogeneous gene expression pattern is then transmitted from progenitor cells to the nascent MNs, in which it triggers a complex regulatory pathways that leads to the appearance of progressively more defined gene expression profiles, and ultimately the acquisition of MN columnar identities (Dasen et al., 2003). Thus, expression of a specific combination of *Hox* genes seems to be causally linked to the specification of a particular MN columnar identity. In line with these view, misexpression of specific *Hox* genes in SC progenitor cells is sufficient to redefine their columnar fate (Dasen et al., 2003; Shah et al., 2004).

In summary, these mechanisms use the spatial distribution of progenitor cells to regulate the generation of neuronal diversity, endowing spinal progenitors with the capacity to produce distinct neuronal fates depending on their position along the dorsoventral and rostrocaudal axes of the developing SC.

2.3 Temporal patterning: Deterministic and stochastic models

If the vertebrate SC represents an great example of the use of positional information for the specification of neuronal identities, the development of *Drosophila* CNS and the vertebrate retina constitute good models for understanding how temporal information is used to generate cell diversity. While these mechanisms govern the genesis of stereotyped progenies in *Drosophila*

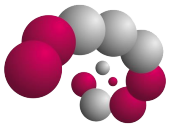

neuroblasts, more complex the regulatory logic underlying the generation of retinal neurons leads to the generation of highly heterogeneous lineages.

Temporal patterning in Drosophila neuroblasts

Several types of neuroblasts in the Drosophila CNS

In *Drosophila*, a large number of spatially organised neuroblasts (NBs) are responsible for the generation of both neurons and glial cells. These NBs can be classified in three main categories based on their mode of cell division (FIG 1.3A). Type 0 neuroblasts undergo several rounds of asymmetric self-renewing cell division, generating one postmitotic neuron in each round (Baumgardt et al., 2014). This mode of division is common during late embryogenesis. In contrast, type I NBs undergo sequential rounds of asymmetric cell division in which they generate ganglion mother cells (GMCs), a different type of neural progenitor that subsequently divides once to generate two postmitotic cells. These progenitors are especially abundant during early embryogenesis (Kohwi and Doe, 2013). Finally, type II NBs show a more complex mode of division, generating ramified lineages. This is due to the production of self-renewing NBs and intermediate progenitor cells (IPCs) in every round of division. IPCs, in turn, divide multiple times, extending a parallel sub-lineage that typically contains several postmitotic cells (Bello et al., 2008; Boone and Doe, 2008). This mode of division seems to be restricted to only six NBs in the larval central brain.

Temporal patterning in Drosophila type I neuroblasts

During early embryonic development, spatial patterning mechanisms, similar to those described in the vertebrate SC, delineate *Drosophila* neuroepithelium into different segments. These events specify different NB identities that can be

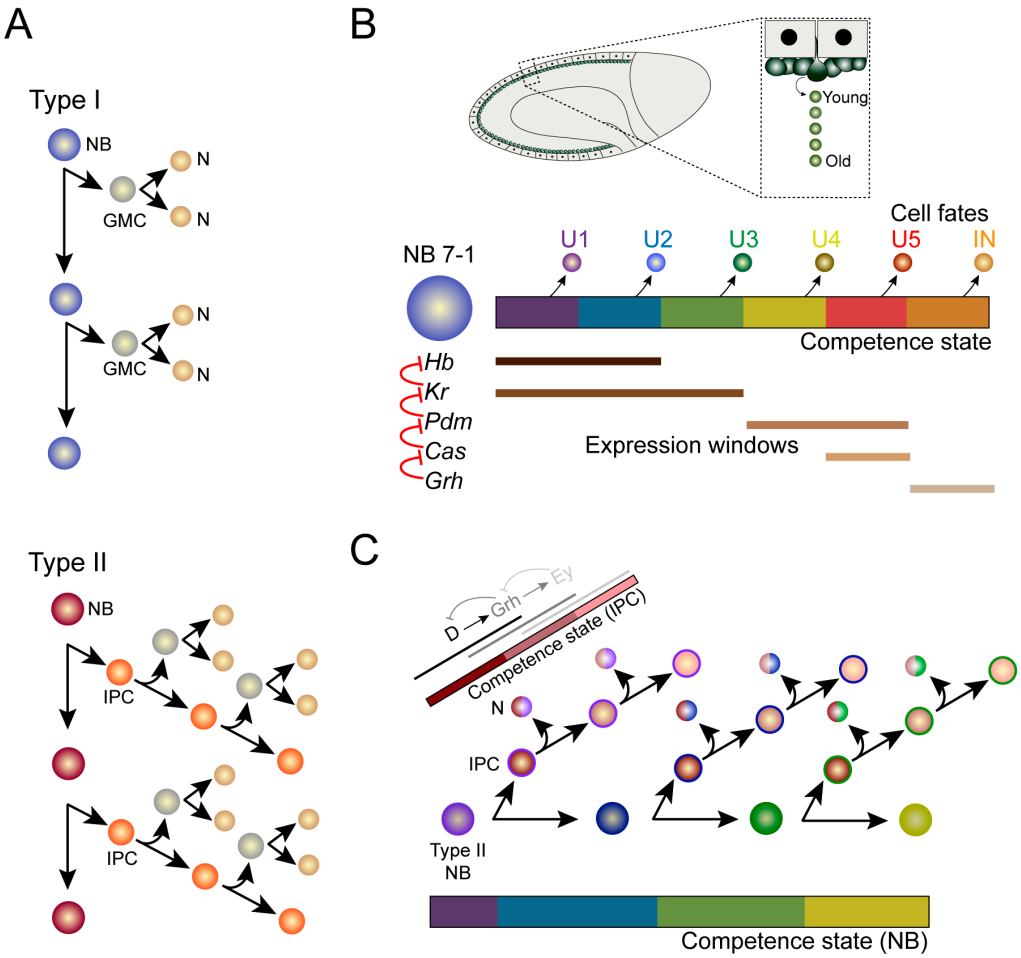

Figure 1.3. Temporal patterning in *Drosophila* neuroblasts
(**A**) Schematic representation of mode of cell division in type I (*top*) and type II (*bottom*) NBs. (**B**) Temporal patterning in *Drosophila* embryonic type I NBs. *Top*: Embryonic neuroblasts in *Drosophila* ventral nerve cord delineate from neuroepithelium and generate stereotyped progenies that adopt columnar organisation above their stem cells. These progenies are generated in an inside out pattern correlated with birthdate, with younger progenies progressively displacing their earlier counterparts. *Bottom*: The expression of five transcription factors in sequential temporal windows (brown lines) promotes the progression of the NB through different competence states (coloured squares). In each competence window, NBs are instructed to generate specific cell fates (coloured circles). Example shows the different cell identities derived from the NB7-1 NB in each competence window (U1, U2, U3, U4, and U5 motorneurons, and INs). (**C**) Temporal patterning in *Drosophila* larval type II NBs. In addition to the temporal progression of the NB (coloured squares), the expression of three tTFs (grey lines) creates a secondary temporal progression in IPCs (red squares). Thus, progenies of type II NBs are instructed by the interaction of two nested temporal patterning mechanisms. NB, neuroblasts. GMC, ganglion mother cell. N, neuron. IPC, intermediated progenitor cell. INs, interneurons. tTFs, temporal transcription factors. Hb, *Hunchback*. Kr, *Krüppel*. Cas, *Castor*. Grh, *Grainy head*. D, *Dichaete*. E, *Eyeless*. *Figure inspired by Doe 2017*.

named and recognised based on their position within the neuroepithelium. Hence, each NB of the embryonic nerve cord can be conveniently identified with

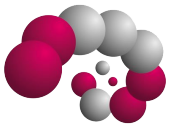

a row and column number, and their activity traced during development (Kohwi and Doe, 2013; Skeath and Thor, 2003). At the onset of neurogenesis, NBs detach from the germinal layer and begin to divide generating heterogeneous progenies, consisting of different types of neurons and glia that organise radially above their stem cells (Doe and Technau, 1993). As neurogenesis proceeds, early progenies are progressively displaced by their younger counterparts, so that an inside-out pattern emerges that correlates with their birthdate (FIG 1.3B) (Isshiki et al., 2001). Intriguingly, each NB gives rise to a reproducible set of cell types in a stereotyped birth order (A Schmid, 1999; Bossing et al., 1996). Although the cellular identities specified vary between different NBs, the progeny of each individual NB contains an invariant combination of cell types generated in a precise temporal sequence. Of note, the number of neurons of each type arising from individual NBs, however, is slightly variable.

The ability of single NBs to generate diverse types of neurons and glia during development is achieved through the progressive restriction of their neurogenic potential. In other words, *Drosophila* type I NBs progress across different temporal windows over the course of development in which they are competent to generate a specific cell fate (FIG 1.3B). The progression along these competence windows is highly organised in time, which leads to the generation of diverse cell types in a highly stereotyped sequence (Cleary and Doe, 2006; Pearson and Doe, 2003). Hence, developmental time is used as a rule for the generation of neuronal diversity in the *Drosophila* CNS.

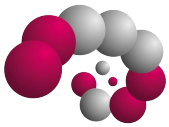

The sequential expression of five temporal transcription factors (tTFs): *Hunchback* (*Hb*), *Krüppel* (*Kr*), *Nubbin/Pdm2* (*Pdm*), *Castor* (*Cas*) and *Grainy head* (*Grh*) has been proposed to govern this process (Isshiki et al., 2001). Accordingly, the generation of a given group of cell types in NB lineages is correlated with the window of expression of corresponding tTFs (FIG 1.3B). Although these tTFs represent a core "canonical" pathway that seems to be common to all NB lineages mapped to date, the number of transcription factors involved, the relative length of each expression window and the cell identities specified during those windows are known to vary for different NBs (Doe, 2017; Isshiki et al., 2001; Tran and Doe, 2008).

Several lines of evidence provide a causal link between the expression of tTFs and the generation of specific progenies. For instance, a series of elegant loss of function experiments have shown that interfering with the expression of these genes prevent the generation of their corresponding cell fates (Grosskortenhaus, et al. 2006; Novotny, et al. 2002). In contrast, their sustained expression leads to an excessive generation of the corresponding cellular identities (Grosskortenhaus et al., 2005). In addition, the sequential progression among competence windows seems to be, at least in part, based on the regulatory roles of these tTFs. Indeed, multiple studies indicate that these genes repress the expression of their preceding counterparts (FIG 1.3B), promoting the closure of each expression window while progressing to the next (Baumgardt et al., 2009; Grosskortenhaus, et al. 2006; Tran and Doe, 2008). In contrast, there is no clear evidence of a feedforward activation mechanism driving the progression of the

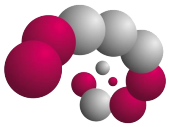

pathway. While some tTFs, have been shown to activate the succeeding gene in the pathway (Isshiki et al., 2001), removal of single or multiple tTFs does not seem to block the temporal progression (Benito-Sipos et al., 2010; Grosskortenhaus, et al. 2006; Grosskortenhaus et al., 2005; Isshiki et al., 2001), indicating that the expression of early genes is not necessary for the activation of the following. This suggests the existence of alternative transcriptional activators for each gene that remain unknown.

It should be noted, however, that multiple cell fates often arise during the expression window of each tTF, which indicates that additional mechanisms exist for the specification of each precise fate. Consistently, several other tTFs have been implicated in this process. Some of these genes are known to subdivide temporal windows into smaller segments to drive the specification of precise cell types (Baumgardt et al., 2009; Stratmann et al., 2016; Tsuji et al., 2008), while others seem to act as temporal switchers between different widows (Benito-Sipos et al., 2011). Whether the progression of this pathway is somehow linked to the mitotic activity of NBs remains unclear. Some transitions in the pathway seem to depend on cell division, while others are independent of the cell cycle (Grosskortenhaus et al., 2005; Mettler, 2006).

Ultimately, *Drosophila* NBs use tTFs to direct postmitotic neurons towards a particular differentiation program. These genes are transmitted from NBs to the nascent neurons, where they trigger complex molecular programmes that lead to their final differentiation into a specific cell fate (Allan and Thor, 2015; Baumgardt et al., 2007). Some of these programmes include secondary roles of

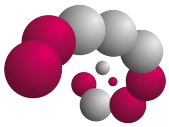

the before mentioned tTFs in postmitotic cells (Stratmann et al., 2016), but also additional secondary actors (Lundgren et al., 1995; Thor and Thomas, 1997; Wolfram et al., 2014). Remarkably, despite intense research efforts, the regulatory logic governing the transition from tTF expression to the final establishment of neuronal identity remains elusive.

Temporal patterning in Drosophila type II neuroblasts

As discussed above, type II NBs generate several IPCs in their successive rounds of division, which, in turn, divide multiple times to generate small cohorts of neurons and glia. Through this process, NBs generate distinct neuronal identities, with unique projection patterns and molecular profiles, in variable numbers (Ito et al., 2013). Similar to their embryonic counterparts, larval type II NBs use a set of tTFs for the temporal specification of their progenies (FIG 1.3C) (Ren et al., 2017; Syed and Doe, 2017). Interestingly, clonal labelling experiments using twin spot mosaic analysis with repressive cell markers (tsMARCM) have shown that IPC progenies are highly heterogeneous, containing several cell identities with different projection patterns. These findings raised the question about the mechanisms underlying the fate specification of IPC-derived cohorts.

An elegant study from the Doe lab has recently helped to illuminate this issue. The authors identified a sequence of three transcription factors, Dichaete (D), Eyeless (E), and Grainy head (Grh), as been responsible for the specification of ICP-derived sub-lineages (FIG 1.3C) (Bayraktar and Doe, 2014). Specific groups of neurons and glia are generated during the expression window of each transcription factor, and disruption of this temporal sequence leads to loss of the

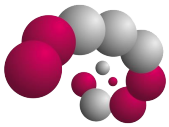

corresponding cell fates. Intriguingly, overexpression of these genes created more complex phenotypes, suggesting that these tTFs may be necessary but not sufficient for the specification of cell identities. These genes seem to play dual roles in the regulation of temporal progression: each tTF represses the preceding and activates the next (FIG 1.3C). Hence, this system draws a model in which two orthogonal temporal sequences regulate the fate of type II NB progenies. A first pathway takes place in the NBs themselves, committing the nascent IPCs to generate certain fates according to the progenitor birthdate. Subsequently, IPCs progress through their own temporal sequence using similar mechanisms. The combined action of these two temporal sequences therefore provides a complex molecular code for the specification of post-mitotic cell fates with increased resolution for the generation of a wide diversity of cell types.

These two examples illustrate the use of temporally regulated molecular cascades as powerful mechanisms for the generation of reproducible progenies following a precise birth order. Such mechanisms are used in a great number of biological systems to generate cellular diversity. In some cases, however, similar mechanisms are coupled with complex regulatory machineries, leading to the generation of more unpredictable progenies. The vertebrate retina represents a wonderful model of these complex interactions.

Fate specification in the vertebrate retina

Cell composition of the vertebrate retina

Seven major cell types populate the mature vertebrate retina, distributed among three cellular layers (FIG 1.4A) (Livesey and Cepko, 2001). The most external layer, named outer nuclear layer (ONL), contains photoreceptor cells, which are

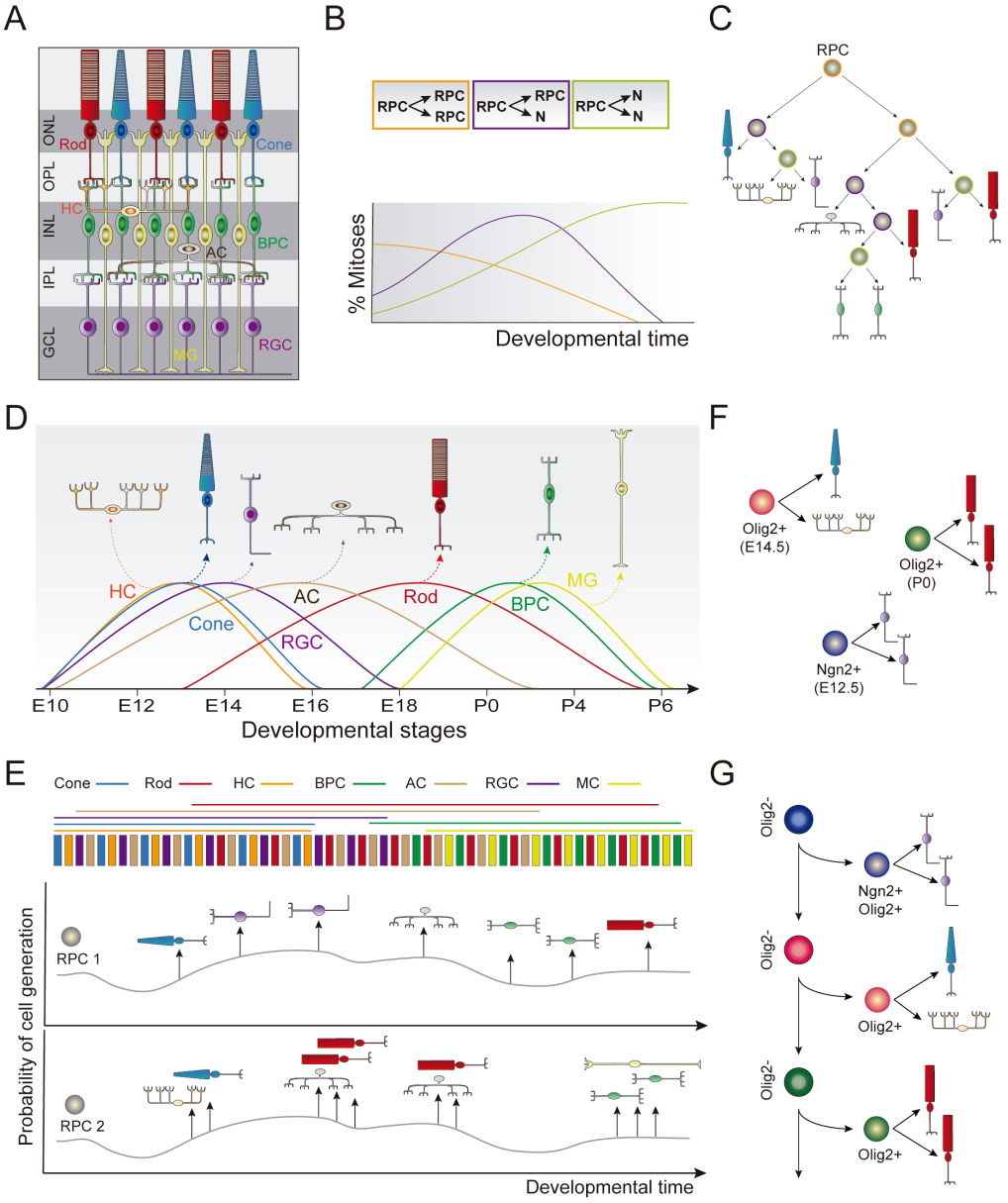

Figure 1.4. Fate specification in the vertebrate retina

(**A**) Schematic representation of cellular diversity in the vertebrate retina. (**B**) *Top:* The three alternative types of progenitor cell divisions observed in the mammalian retina. *Bottom:* The relative frequencies of the different cell division patterns experience changes along development. (**C**) Example of a retinal lineage tree in which RPCs divide following the patterns described in B. (**D**) Retinal cells are generated in a stereotyped temporal sequence. The different retinal cell types are generated in sequential but overlapping temporal windows (coloured lines). (**E**) Stochastic generation or retinal cell diversity. *Top:* Coloured lines represent the temporal windows for the generation of each retinal cell type. Coloured bars represent the theoretical neurogenic potential of RPCs across developmental stages. The partial overlap of temporal windows allows RPCs to generate diverse cell identities at a given stage. *Bottom*: During the different temporal windows, RPCs seem to take a number of stochastic 'decisions' for the specification of their progenies, leading to the genesis of flexible and unpredictable outcomes. The probability to generate neurons during the different temporal windows (grey lines) could have an important impact in the outcome of progenitor cells, ensuring the genesis of balanced ratios of cell types at population levels.

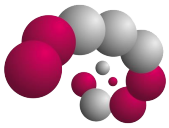

(**F**) Fate-restriction in RPC terminal divisions. Terminally dividing progenitor cells expressing specific marker genes seem to exhibit strong biases towards the generation of certain cell types, generating stereotyped and predictable progenies. (**G**) A unified model of retinal development. A population of self-renewing progenitor cells could progress through sequential temporal windows of competence, taking a number of stochastic 'decisions' for the generation of diverse retinal cell types as described in E. This could be achieved through the generation of several waves of terminally dividing progenitor cells that express known marker genes, and are committed for the generation of specific retinal types. GC L, ganglion cell layer. IPL, inner plexiform layer. OPL, outer plexiform layer. INL, inner nuclear layer. ONL, outer nuclear layer. HC, horizontal cell. RGC, retinal ganglion cell. AC, amacrine cell. BPC, bipolar cell. RPC, retinal progenitor cell. N, neuron. *Figure inspired by Cepko 2014*.

further classified into rods and cones, whose role is to encode light into electrical signals. The inner nuclear layer (INL) contains bipolar cells, the cell bodies of Müller glia, and two types of retinal interneurons, horizontal and amacrine cells. This layer is the first step in visual information processing, linking photoreceptors with retinal ganglion cells (RGCs). This last cell type populates the most internal layer of the retina, known as ganglion cell layer (GCL). This layer represents the output channel of the retina, from where visual information is transmitted to several brain centres. Two neuropil layers exist between the cellular layers. The outer plexiform layer (OPL) is located between ONL and INL, and contains the neurites of photoreceptors, bipolar and horizontal cells as well as their synaptic contacts. The inner plexiform (IPL) layer separates the INL from the GCL and hosts the synaptic contacts between bipolar cells, amacrine cells and RGCs. It should be noted that growing evidence supports the existence of further diversity within these major groups. Over 60 different subtypes have been recently identified based on their transcriptional profiles and functional properties (Masland, 2012).

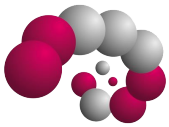

Cell biology of retinal neurogenesis

The complete set of retinal cell types arises from mitotic cells known as retinal progenitor cells (RPCs). The cell bodies of these progenitors move radially as they progress through the cell cycle, a process commonly known as interkinetic nuclear migration, and divide at the apical surface of the retinal neuroepithelium (Baye and Link, 2008; 2007). RPCs are known to divide following three different patterns: symmetrically to generate two RPCs, asymmetrically to generate one RPC and one post-mitotic cell, and terminally to generate two post-mitotic cells (FIG 1.4B) (Baye and Link, 2007; J. He et al., 2012; Jensen, 1997). Although RPCs are known to use these modes of division indiscriminately during neurogenesis, their relative frequency changes as development proceeds (FIG 1.4B,C). At early developmental stages, symmetrical divisions are prominent, leading to an expansion of the progenitor pool prior to the onset of neurogenesis. At the onset of retinogenesis, all three division patterns are present, but asymmetric divisions become more prevalent. Finally, at late developmental stages, progenitor cell numbers reduce progressively as a result of terminal divisions, leading to the final exhaustion of the progenitor cell population (Alexiades and Cepko, 1996; Livesey and Cepko, 2001).

Fate specification in the vertebrate retina

The vertebrate retina represents perhaps the best example of how temporal patterning mechanisms, endowed with sufficient flexibility, can lead to the generation of very complex cellular systems. In the retina, each progenitor cell generates variable and unpredictable outcomes, but the collective sum of

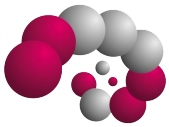

progenitor cells build a structure that is almost identical among different individuals.

The first evidence of temporal patterning in the vertebrate retina derives from classic birth dating studies. These experiments revealed that, at the population level, retinal cells are generated in a stereotyped temporal sequence conserved among vertebrate species (FIG 1.4D) (Belecky-Adams et al., 1996; Holt et al., 1988; Rapaport et al., 2004; Young, 1985). These studies also revealed that distinct cell fates are generated simultaneously at certain stages, which led to the conclusion that the diverse cell types that populate the adult retina are generated in sequential but overlapping developmental windows (FIG 1.4D). Two non-mutually exclusive hypotheses have been proposed to explain this fact. First, it has been suggested that RPCs could progress through a common temporal sequence as in *Drosophila* NBs, but such progression could not be synchronous among different progenitor cells, which would lead to the generation of different cell types at any given developmental time point. Consistently, different zones of the developing retina have been reported to mature asynchronously in a number of species (Martinez-Morales et al., 2005; Neumann and Nuesselein-Volhard, 2000). Second, it has been hypothesised that different types of RPCs could operate different developmental programmes in parallel, generating different cell identities simultaneously.

Few studies have aimed to clarify this question by studying the output of RPCs at clonal resolution. Lineages derived from early RPCs were found to be highly variable in size and composition, typically ranging between 1-16 cells per

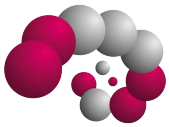

clone in *Xenopus* (Holt et al., 1988) and between 1 and over 200 cells in mice (Turner et al., 1990), and apparently containing random samples of retinal diversity organised in radial units (Holt et al., 1988; Turner et al., 1990; Weits and Fraser, 1988; Wong and Rapaport, 2009). This high degree of variability led to the premature conclusion that cell fate determination in the retina is established at the postmitotic state, and primarily driven by the local environment. Such mechanism has been also proposed for other cells, like those derived from the neural crests. However, experiments testing the influence of environmental signals in retinal cell fate specification have revealed a limited role of such signals in regulating RPC output. First, RPCs isolated *in vitro* generate temporally appropriate cell types (Reh and Kljavin, 1989) and recapitulate the *in vivo* sequence of cell identities both when cultured alone or in the presence of other retinal cells (Cayouette et al., 2003). In addition, embryonic rat RPCs co-cultured with postnatal retinal cells maintain their neurogenic fate, generating cells typically born during embryonic temporal windows *in vivo* (Cepko, 1999). This study, however, identified regulatory feedback loops controlling the production of balanced ratios of each cell type, since the presence of amacrine cells reduce the amount of these cells obtained from cultured progenitors. Conversely, co-culture with embryonic retinal cells seems unable to reprogram postnatal RPCs for the generation of cell fates typically produced in embryonic stages, although the fraction of postnatal cell fates generated differs from those observed *in vivo* (Belliveau et al., 2000). Thus, exposure to heterochronic environments *in vitro* seems unable to instruct the neurogenic behaviour in RPCs. The local environment, however, seems capable to regulate

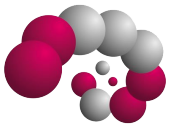

the precise output of these progenitors, impacting the ratios of each type of cell generated during development.

These observations led to the proposition of the so-called competence model of retinal development. According to this model, the competence to generate the different cell types that populate the adult retina is intrinsically encoded in RPCs. Thus, similar to *Drosophila* NBs, RPCs would progress through an invariant number of sequential competence states, each of which endowing them with the capacity to generate a specific cell fate (Cepko et al., 1996). Consistently, murine genes homologous to those encoding for tTFs in *Drosophila* have been reported to play similar roles in the mouse retina (Elliott et al., 2008). Environmental cues might, in addition, regulate the progression of the intrinsic timer and/or the mitotic activity of RPCs within each competence state, ultimately controlling the output of these progenitors. This environmental control of RPC activity would lead to the generation of heterogeneous progenies, matching the results obtained in clonal experiments. In agreement with this idea, recent studies have shown that the progenies of rat RPCs in culture, as well as those derived from zebrafish RPCs, are easily predicted by a simple stochastic model of retina development, in which the outcome of each RPC is established via a series of probabilistic "decisions" during development (Gomes et al., 2010; He et al., 2012). In such model, the probability to generate the different cell fates would be directly linked to the relative fraction of those fates generated across development (FIG 1.4E). Consequently, this mechanism would ensure an appropriated balance of cell types in the adult retina, while allowing a high

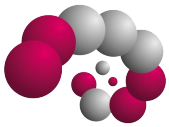

degree of freedom in the activity of individual RPCs. The nature of the biological identity behind these probabilities remains to be elucidated, although it probably requires the interaction of intrinsic programmes and environmental signals, as discussed above.

Intriguingly, the generation of some types of retinal cells in appropriate numbers does not seem to be faithfully predicted by stochastic models (Gomes et al., 2010), which suggest the presence of parallel developmental mechanisms underlying the appearance of such fates. These findings led to proposal of the existence of distinct pools of RPCs with different neurogenic properties. Several lines of evidence support the existence of multiple populations of RPCs. For instance, several studies using a variety of methods have reported heterogeneous gene expression profiles among progenitor cells in the murine retina (Blackshaw et al., 2004; Guillemot and Joyner, 1993; Jasoni and Reh, 1996; Nakamura et al., 2006; Trimarchi et al., 2008). In addition, the expression of few key marker genes in RPC subpopulations has been linked to the generation of specific cell fates in terminal divisions (Brzezinski et al., 2011; Emerson et al., 2013; Godinho et al., 2007; Hafler et al., 2012; Nakamura et al., 2006; Suzuki et al., 2013) (FIG 1.4F). Finally, RPCs expressing *Cdh6* have been recently shown to preferentially generate specific subtypes of RGCs throughout their lineage (la Huerta et al., 2012). Most of the observed biases towards the generation of specific cell fates, however, occur at terminal divisions, while non-terminally dividing RPCs seem to specify diverse progenies consistently. These results are thus compatible with a scenario in which multipotent RPCs generate sequential

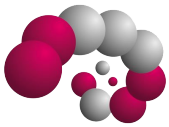

cohorts of terminally dividing progenitors programmed to generate specific cell types, as proposed previously (FIG 1.4G) (Hafler et al., 2012). Therefore, although the existence of several types of RPCs following different developmental programmes cannot be excluded, conclusive evidence supporting this idea is currently missing, and additional studies are required to shed light into this problem.

In conclusion, while temporal progression in *Drosophila* NBs leads to the appearance of stereotyped progenies in a fix birth order, temporal progression in the vertebrate retina seems to be linked to stochastic mechanisms that allow progenitor cells to generate a wide diversity of outcomes. These stochastic mechanisms are likely based on a sophisticated regulatory logic that controls the generation of correct numbers of retinal cells, ensuring the construction of organised structures from apparently disorganised individual progenitor behaviours. Such mechanisms confer a high degree of flexibility and robustness to the process (Johnston and Desplan, 2010), and may represent an adequate path for the assembly of very complex cellular systems.

3. Developmental origin of neuronal diversity in the mammalian cerebral cortex

The mammalian cerebral cortex is one of the most complex machineries of the mammalian brain. It can be further subdivided in three main structures, archicortex, paleocortex and neocortex. Among these cortices, the neocortex is the most recent evolutionary invention. It is composed by a wide diversity of cell

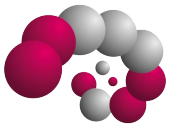

types and is responsible for several high-order functions, including sensory processing, cognition and learning, among others. The development of neocortex involves many diverse mechanisms, including different forms of spatial and temporal patterning. Collectively, these mechanisms generate the cellular elements that assemble the neuronal circuits involved in cortical function. Here I will describe how these mechanisms are combined for the generation of cortical neuronal diversity, using the mouse as a model organism.

3.1 Cellular composition of the mammalian neocortex

Architecture of the mammalian cortex: Layers & columns

The mammalian cerebral cortex is a regionalised structure that can be divided into several areas with differential cytoarchitectonic organisation, which contain different neuronal populations. Despite this complexity, two main axes of organisation are common across the diverse regions of the neocortex, representing the primary structural and functional organisation of the cerebral cortex.

In the tangential dimension, the neocortex is organised in six layers (named I to VI) defined by their differential cellular composition and relative position across the thickness of the cortex. The diverse neuronal populations residing in these layers are known to perform different computational functions, constituting sequential steps in cortical information flow. In broad terms, these layers can be classified in superficial (II/III-IV) and deep (V-VI) layers. Homologs of deep layers seem to be present in the brains of amphibians, reptiles and birds. In contrast, a remarkable expansion of superficial layers characterise the complex

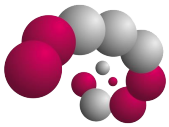

cortices of mammals (Molnár et al., 2006; Sùper and Uylings, 2001) been one of the most distinctive features of the primate brain.

In the radial dimension, the cerebral cortex is formed by repeated columnar modules that represent vertical samples of the six cortical layers. These columns are thought to work as independent information processing modules, constituting the primary functional organisation of the mammalian neocortex (Hubel and Wiesel, 1969; 1968; 1963; Mountcastle, 1997), although the universality of this organisation has been questioned (Horton and Adams, 2005). Inside these modules, information seems to flow across the different layers following a canonical directional circuit that is common in all mammalian species (Douglas and Martin, 2004; Thomson and Bannister, 2003).

Two major groups of neurons populate the mammalian neocortex

The neuronal population of the cerebral cortex can be classified into two broad classes. Excitatory pyramidal cells (PCs) constitute the majority (~80%) of the entire population of neurons. These neurons connect both locally and to distal targets, controlling communication between diverse brain regions, and use glutamate as their neurotransmitter. On the other hand, inhibitory GABAergic interneurons (INs) account for the remaining ~20% of the neuronal population. They establish local connections with surrounding neurons, primarily regulating the activity of local groups of PCs and other INs.

Pyramidal cells populate all layers of the neocortex with the exception of layer 1. They can be classified into different subclasses and types based on their projection patterns and gene expression profile (Greig et al. 2013; Lodato and

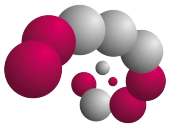

Arlotta, 2015; Y. Wang et al., 2018). Hence, two main subclasses of PCs populate the cerebral cortex (FIG 1.5A): Intratelecephalic projection neurons (ITPNs), also known as cortico-cortical projection neurons, exclusively target telencephalic structures, mostly projecting inside the cerebral cortex. In contrast, corticofugal projection neurons (CFuPNs) project to diverse targets outside the neocortex. The formers are found across all cortical layers, while the laters are commonly restricted to deep cortical layers. These subclasses can be, in turn, subdivided in different cell types heterogeneously distributed among cortical layers.

Different types of ITPNs are found across cortical layers (FIG 1.5B); commissural projection neurons (CPNs) send projections to the contralateral hemisphere, crossing the midline through the corpus callosum or the anterior commissure. In turn, associative projection neurons (APNs) connect locally and with diverse territories within the ipsilateral hemisphere. In layer IV, granular neurons, a morphologically defined group of locally-connecting APNs is dominant, and shares the niche with other types of associative and commissural neurons. In layer V, a third population of ITPNs, named corticostriatal projection neurons (CStPNs), send their axons to the ipsilateral striatum, often combining this connection with projections to the contralateral hemisphere. ITPNs are often identified by the expression of high levels of the transcription factor Satb2.

CFuPNs can also be subdivided in two main groups (FIG 1.5C); subcerebral projection neurons (SCPNs) reside in neocortical layer V, from where they extend their projections towards diverse targets in the brainstem and

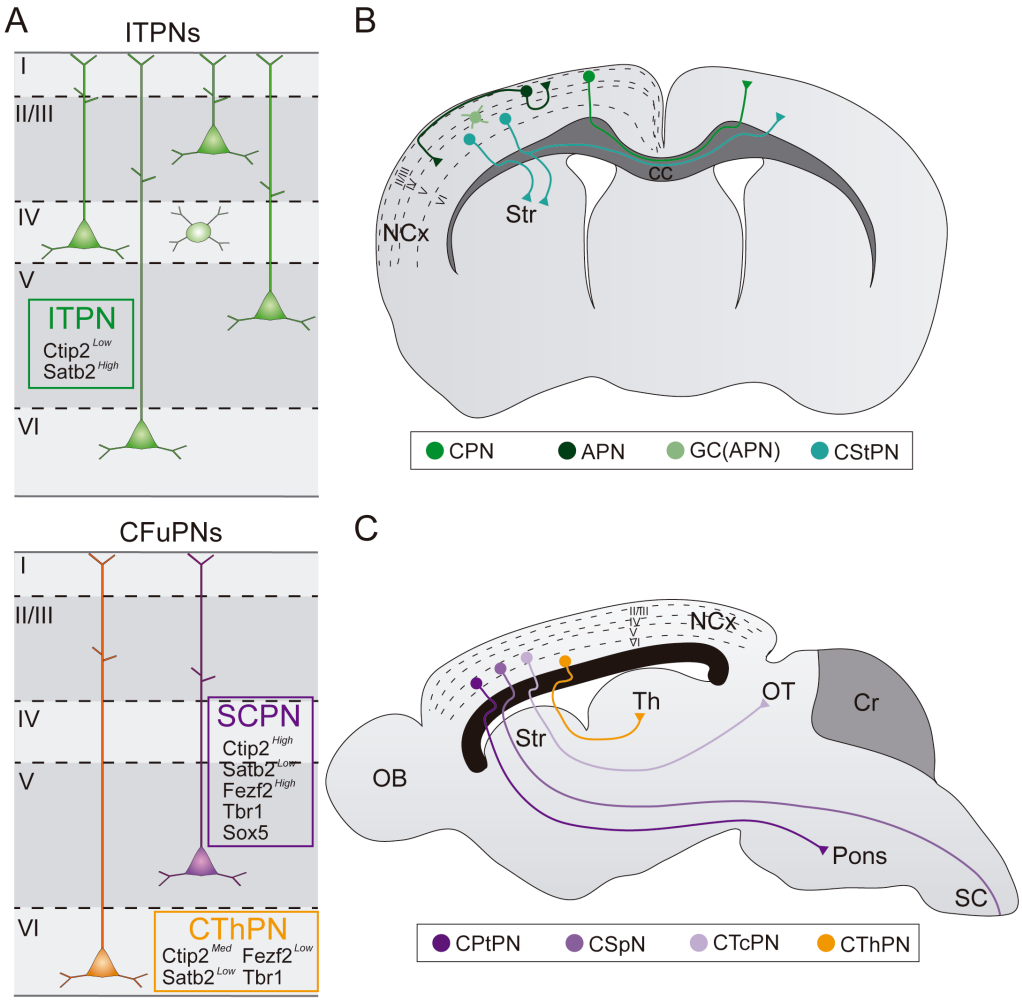

Figure 1.5. Pyramidal cell diversity in the mammalian cerebral cortex
(**A**) Two main PC subclasses populate the cerebral cortex. *Top:* ITPNs populate all cellular layers of the neocortex. *Bottom:* CFuPNs are typically confined in deep cortical layers. These subclasses can be identified on the bases of their distinctive gene expression patterns. (**B**) ITPNs can be classified in different types based on their projection patterns. (**C**) CFuPNs can be classified in different groups and types based on their projection patterns. ITPN, intratelencephalic projection neuron. CFuPN, corticofugal projection neuron. CThPN, corticothalamic projection neuron. SCPN, subcerebral projection neuron. CPN, commissural projection neuron. APN, associative projection neuron. GC, granular cell. CStPN, corticostriatal projection neuron. CPtPN, corticopontine projection neuron. CSpPN, corticospinal projection neuron. CTcPN, corticotectal projection neuron. NCx, neocortex. Str, striatum. cc, corpus callosum. OB, olfactory bulb. Th, thalamus. OT, optic tectum. Cr, cerebellum. SC, spinal cord. *Figure inspired by Molyneaux et al. 2007.*

the spinal cord. This group consists in turn of a number of different PC types, defined by their precise targets. Corticopontine (CPtPN), corticotectal (CTcPN), corticobulbar, and corticospinal (CSpPN) projection neurons are examples of those types. Layer V SCPNs are often recognised by their expression of the transcription factor Ctip2 at high levels. Corticothalamic projection neurons

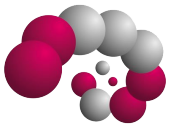

(CThPNs) are primarily found in layer VI, although a small population is also present in the deep strata of layer V. These cells project to diverse thalamic nuclei, and are often identified by the expression of the transcription factors Tle4 and Tbr1.

Although these two main subclasses agglutinate the vast majority of PC types, some PCs combine multiple connections and can be thus categorized in multiple groups. As an example, some layer V cells in the prefrontal cortex project to both subcerebral and cortical targets.

The different combinations of transcription factors expressed by these PC subclasses have been extensively used as marker genes for their identification (Alcamo et al., 2008; Arlotta et al., 2005; Bedogni et al., 2010; Britanova et al., 2008; Greig et al., 2013; McKenna et al., 2011; Molyneaux et al., 2007; 2015; Woodworth et al., 2016). It is worth noting, that although the expression of such genes is often considered subclass-specific, this assumption is frequently inaccurate. Instead, these genes seem to be dynamically regulated during development. At birth, immature PCs seem to co-express these transcription factors, exhibiting an undifferentiated state. Subsequently, the expression of these genes is segregated as neurons mature, driving the molecular programmes for their subclass specification (Greig et al., 2013; Molyneaux et al., 2007). Once development is completed, co-expression of these markers can be found in some PCs. Indeed, the expression of certain combinations of these genes has been proposed to identify further PC subpopulations (Harb et al., 2016).

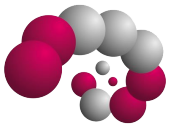

Increasing evidence supports the existence of a deeper diversity of PC identities. Many cell types can be further subdivided into a larger number of subtypes, present within and across cortical regions (Wang et al., 2018). These findings are not surprising, since the precise connectivity and projection patterns of each type are subject to variation within different cortical regions. In other words, neurons of a given type residing in different areas project to different targets, suggesting that PCs are indeed an extremely diverse group of neurons whose heterogeneity may escape our current understanding.

Cortical INs are also a highly diverse group of neurons that are commonly classified using a combination of morphological, neurochemical and functional criteria (De Felipe et al., 2013). In the rodent cortex, these neurons can be divided in three non-overlapping groups known as cardinal subclasses, based on the expression of specific markers: Parvalbumin- (PV), Somatostatin- (SST) and 5HT3aR-expressing interneurons (FIG 1.6).

PV cells account for ~40% of all cortical INs, receive their name due to the expression of the homonymous calcium binding protein, and present characteristic fast spiking firing properties. This IN class can be further subdivided in three main cell types. Soma-targeting basket cells are the most abundant among PV INs. These cells are widely distributed across cortical areas and layers, and extend tortuous local axonal arborisations that allow them to connect onto the cell bodies and proximal dendrites of surrounding PCs as well as other INs (Hu et al., 2014). Axo-axonic chandelier cells are a small group of PV interneurons heterogeneously distributed among cortical regions and layers,

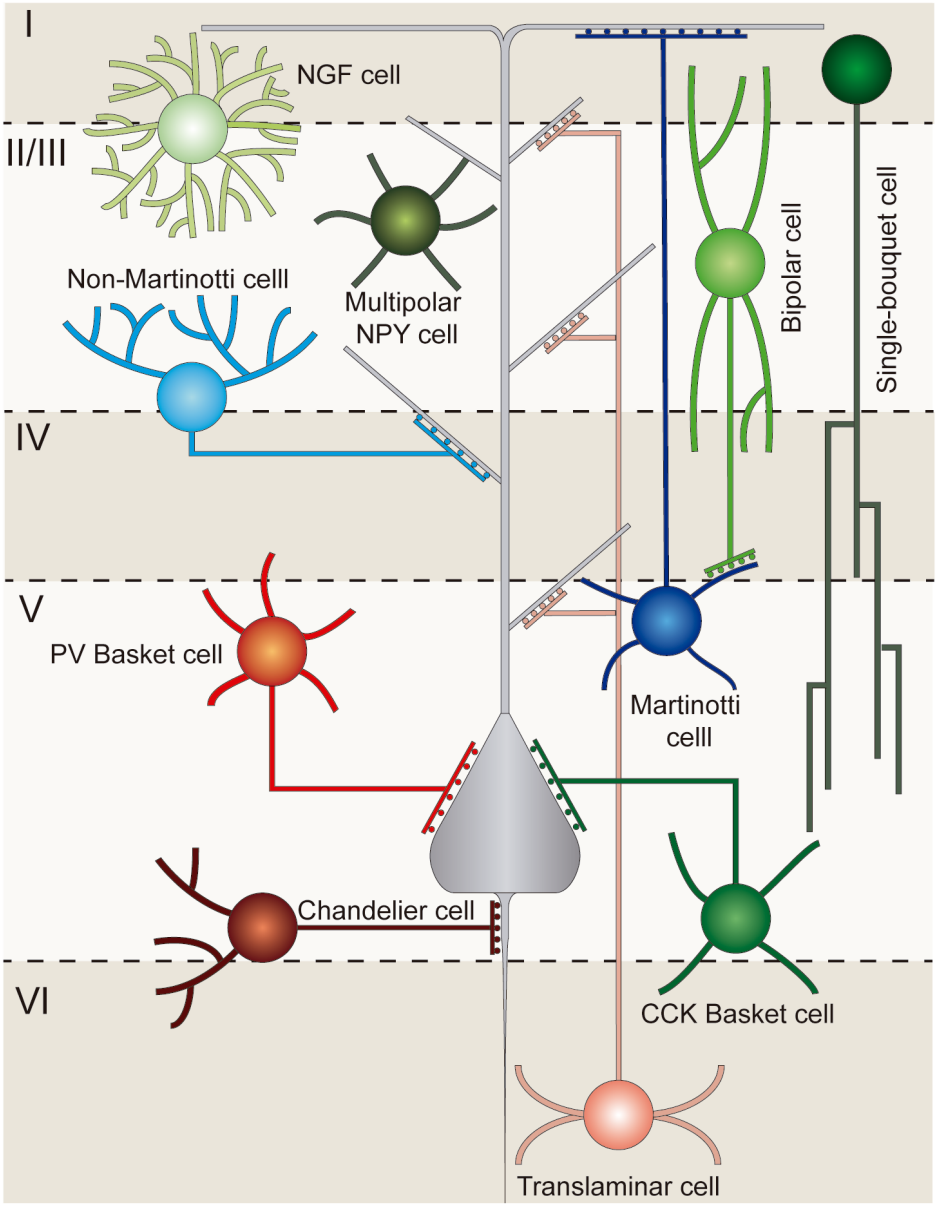

Figure 1.6. Interneuron diversity in the mammalian cerebral cortex
Cortical interneurons can be classified in three main subclasses: PV interneurons (red), SST interneurons (blue); and the heterogeneous group of 5HT3aR interneurons (green). Each of these subclasses can be further subdivided into the different types illustrated in the figure based on their distinctive features. Such features include gene expression, morphology, connectivity patterns and functional properties. *Figure inspired by Marín et al 2013*.

abounding in layers VI and II of prefrontal cortical regions. These cells specifically inhibit the axon initial segment of surrounding PCs, providing strong inhibition onto these cells (Somogyi et al., 1982). Their axonal arbours adopt very stereotyped morphologies, resembling the shape of a candlestick. Although

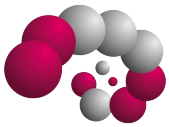

always considered part of this subclass given the important similarities with other types PV cells, an important fraction of chandelier cells in the murine cortex do not express detectable levels of PV (Taniguchi et al., 2013). Finally, translaminar INs are a rare type of PV cells particularly abundant in deep cortical layers, from where they send their axons upwards across cortical thickness, targeting PCs of different layers (Bortone et al., 2014).

A second cardinal subclass of cortical INs expresses the neuropeptide somatostatin, and specialises in specifically targeting the dendrites of their postsynaptic partners. These cells account for ~30% of total cortical INs, and can be divided in three different types. Martinotti cells are the most abundant (~60%) among SST INs, and are particularly abundant in neocortical layer V, although they can also be found in superficial layers, where they often express the calcium binding protein calretinin (CR). These cells are distinguishable by their characteristic morphology, extending their axons vertically to reach layer I, where they arborize profusely to target the distal dendrites of local PCs. (Hilscher et al., 2017; Maximiliano José et al., 2018; Wang et al., 2004). Unlike PV cells, these SST INs exhibit heterogeneous firing patterns. Non-Martinotti SST cells are present in all cortical layers, although they are particularly abundant in layer IV, where they primarily target PV basket INs (Xu et al., 2013). These cells extend their axons locally, lacking projections to layer I, and present higher firing frequencies than their Martinotti counterparts, but not as high as PV interneurons (Maximiliano José et al., 2018). In addition to SST INs, a small population of GABAergic projection neurons also express somatostatin, together

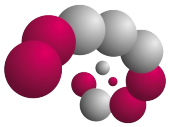

with other markers as nitric oxide synthase (NOS), and neuropeptide Y (NPY). These cells primarily populate deep cortical layers, from where they project to other cortical regions (He et al., 2016).

Finally, the third major subclass of cortical interneurons, which accounts for the remaining ~30% of cortical INs, and expresses the serotonin receptor 5HT3aR, represents a conglomerate of diverse cell types. Vasointestinal peptide (VIP) expressing bipolar INs are the most abundant type of 5HT3aR INs. These cells are abundant in the superficial layers II and III and have disinhibitory functions, since they mainly input onto SST and PV INs (Jiang et al., 2015; Pfeffer et al., 2013). They often co-express CR and display continuously adapting firing properties (Prönneke et al., 2015). Coleocistokinin (CCK) expressing basket cells constitute a group of 5HT3aR INs that can be divided into two types of basket cells. The first type also expresses VIP, and is more abundant in superficial layers in the cerebral cortex. The second type is negative for the expression of VIP, and resides primarily in layers V and VI. Both types of CCK basket cells are multipolar and, alike their PV mates, synapse onto the cell bodies of surrounding PCs and other INs. Unlike PV cells, however, these cells exhibit regular or burst spiking firing (Kawaguchi and Kubota, 1998). Neurogliaform cells are the most prominent group of layer I INs (Schuman et al., 2018), although they can be rarely found in other layers. They extend local tortuous axons, and often co-express reelin and NPY (Lee et al., 2010). They exhibit late spiking properties and have been implicated in volumetric GABA transmission (Oláh et al., 2007). Neurogliaform cells share layer I with 5HT3aR+

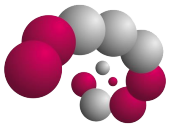

reelin+ double bouquet cells, which extend their axons towards deep cortical layers, where they ramify profusely (Jiang et al., 2015). NYP+ multipolar interneurons constitute a different type of cortical INs, which is frequently found in the top border of layer II (Gelman et al., 2009; Miyoshi et al., 2010). Finally, Meis2+ intersticial INs reside in the white matter, and their axons innervate deep cortical layers (Engelhardt et al., 2011; Frazer et al., 2017).

Current view of interneuron diversity and classification has been reviewed elsewhere (Lim et al., 2018a; Tremblay et al., 2016). Nevertheless, despite the multiple efforts in the characterisation and classification of cortical INs, our understanding of IN diversity remains very limited. Recent single cell transcriptomic data suggest the existence of ~50 different IN identities in murine V1 cortex based on gene expression profile (Tasic et al., 2016). Contrary to PCs, however, IN identities seem to be common across different regions of the mammalian brain (Tasic et al., 2018), although the relative numbers of the diverse types seem to vary across these regions.

3.2 Early patterning of the mammalian telencephalon

The development of the cerebral cortex commences with the spatial patterning of the rostral-most part of the neural tube, named telencephalon. This leads to the division of the telencephalic neuroepithelium into several regions committed to the generation of different classes of neurons.

Dorsoventral patterning in the rostral telencephalon

In the earliest stages of brain development the mammalian telencephalon consists of a single layer of neural progenitor cells. At this stage, the activity of diverse

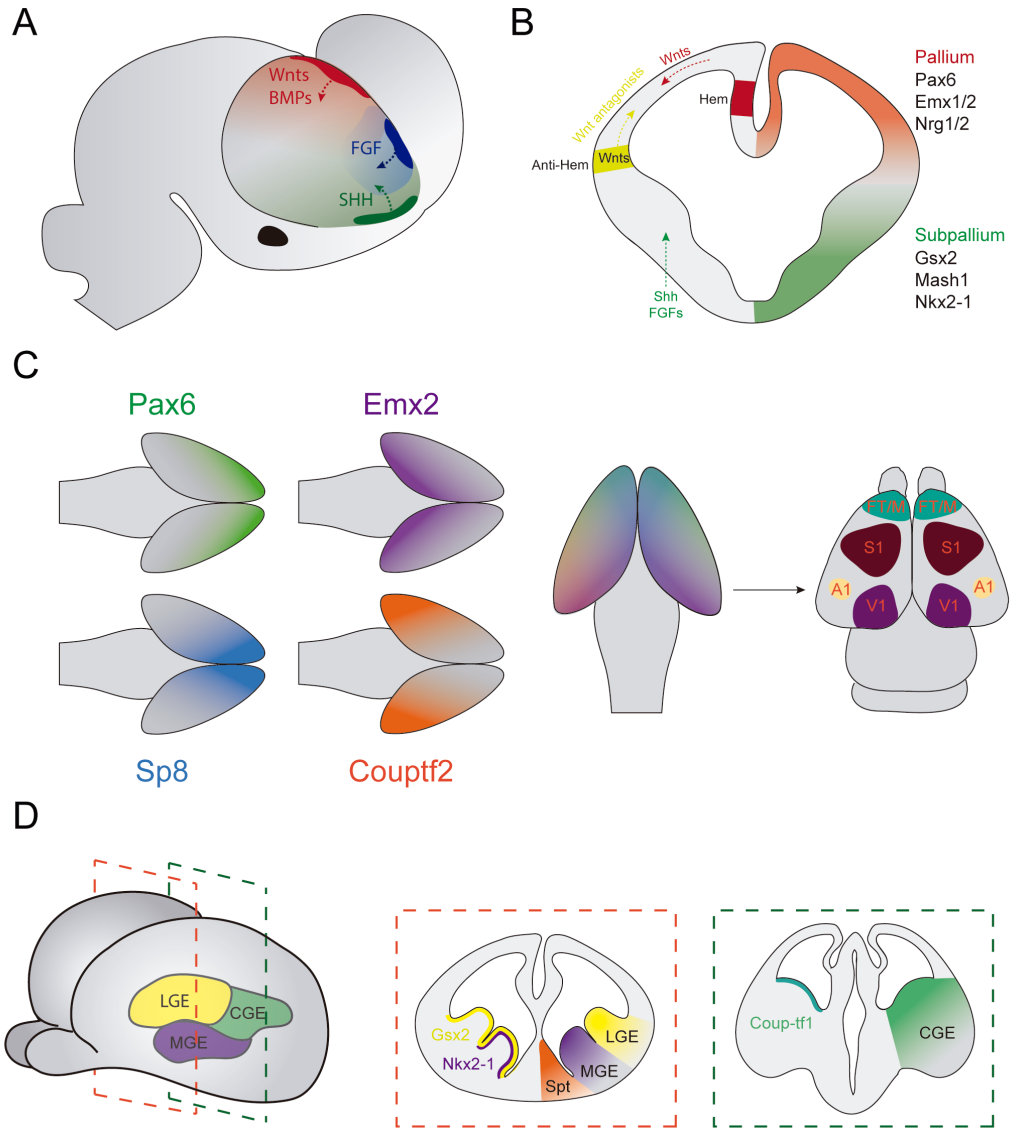

Figure 1.7. Spatial patterning in the mammalian telencephalon
(**A**) Schematic representation of the mammalian telencephalon at early developmental stages. Three main signalling gradients play primary roles in the initial spatial patterning of the telencephalon. (**B**) The activity of these signalling gradients segregates the rostral telencephalon into two main regions, the dorsal pallium and the ventral subpallium. The secretion of Wnts by the cortical hem contributes to the establishment of the pallial territory, which is delimited by the secretion of Wnt antagonists from the anti-hem. The subpallial territory is also established by the action of diverse signals, including Shh and FGFs. These initial patterning events lead to the expression of few core genes that define the identities of these two regions. (**C**) Within the dorsal pallium, the activity of four main signalling gradients creates a complex gene expression grid that exposes different regions of the presumptive neocortex to different dose of these signals. This would then lead to the appearance of different cortical areas that compose the adult cortex. (**D**) Within the ventral subpallium, four main structures are segregated based in the expression of key instructive genes that endow them with differential neurogenic capabilities. BMP, bone morphogenic protein. FGF, fibroblast growth factor. Shh, sonic hedgehog. LGE, lateral ganglionic eminence. MGE, medial ganglionic eminence. CGE, caudal ganglionic eminence. Spt, septum. *Figure inspired by Greig et al. 2014.*

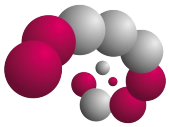

signalling gradients along the dorsoventral axis lay the groundwork for the division of the telencephalic neuroepithelium into two big domains, the dorsal pallium and the ventral subpallium (FIG 1.7A,B). Most importantly, the expression of Gli3 and Shh in opposing dorsoventral gradients is known to play central roles in the segregation of these embryonic regions.

In the dorsal telencephalon, the expression of the transcription factor Gli3 induces the secretion of Wnts and Bone morphogenic proteins (BMPs) by the cortical hem at the dorsal midline. Such secretion establishes a dorsoventral gradient of Wnt expression across the presumptive pallial territory. The expression of these cues is restricted to the dorsal aspect of the telencephalon by the action of an opposing signalling gradient of Wnt antagonists derived from the anti-hem, an embryonic patterning centre located in lateral positions at the level of the presumptive pallial/subpaliall boundary (Azzarelli et al., 2015). Via molecular mechanisms that have not been completely unravelled, these signals induce the expression of a handful of genes, that are responsible for the specification of pallial identity in the dorsal telencephalon. These include, among others, *Empty spiracles homolog 2* (*Emx2*), *Paired box gene 6* (*Pax6*) and Neurogenines 1 and 2 (*Ngn1/2*).

In the ventral telencephalon, the expression of Shh seems to be critical for the establishment of subpallial identity. This morphogen seems to act as a repressor of the transcription factor Gli3, confining its expression to the dorsal aspect of the embryonic telencephalon, preventing the dorsalisation of the ventral region (Hébert and Fishell, 2008). As Gli3 exhibits repressive effects in the

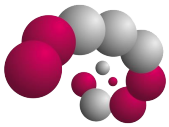

expression of proteins of the Fibroblast growth factor (FGF) family, its blockage by Shh allows the secretion of these cues from the anterior neural ridge. These proteins seem to participate in indirect feedback regulatory loops, inducing the expression of Shh. Ultimately, Shh and FGFs induce the expression of several transcription factors in the ventral telencephalon that establish the subpallial identity in this region. These include *Nkx2-1*, *Gsx2*, *Mash1*, and several members of the *Dbx* family.

The dorsal pallium gives raise to the paleocortex, archicortex and neocortex, while the ventral subpallium originates the basal ganglia structures such as the striatum and the globus pallidus (Hébert and Fishell, 2008; Rallu et al., 2002), as well as the full complement of cortical INs (Anderson et al., 1997; Tamamaki et al., 1997). Subsequent spatial patterning will subdivide these structures into diverse regions with specific developmental roles.

Regionalisation of the embryonic pallium

After the delineation of the pallial territory, the expression of the Lim-Homeodomain transcription factor *Lhx2* in the dorsomedial region of the pallium differentiates the presumptive neocortex from the adjacent medial archicortex and lateral paleocortex. The embryonic neocortex is then patterned into different regions via the activity of several morphogen gradients expressed in orthogonal directions (Greig et al., 2013). In brief, several members of the FGF family are secreted by the commissural plate, generating a rostro-medial to caudo-lateral gradient (Garel et al., 2003; Toyoda et al., 2010). Furthermore, Wnts and members of the BMP family are secreted from the cortical hem at caudo-medial

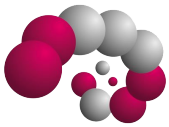

positions. Finally, the anti-hem expresses secreted frizzled-related protein 2 (SFRP2) and epidermal growth factors (EGFs) at lateral positions. These signals induce the expression of several transcription factors (Pax6, Emx2, Couptf1, and Sp8) in four complementary gradients which, collectively, generate a spatial matrix of gene expression that defines the entire cortical primordium (FIG 1.7C).

The expression of these TFs in cortical progenitors establishes a presumptive proto-map that ultimately controls the size and position of the different cortical areas that constitute the adult cerebral cortex (FIG 1.7C). Consequently, manipulating the activity of these genes is sufficient to alter cortical regionalisation (Armentano et al., 2007; Bishop et al., 2000; Hamasaki et al., 2004; Muzio et al., 2002; Zembrzycki et al., 2007). It should be noted, however, that although the position and size of cortical areas are severely disrupted when the expression of these patterning genes is altered, subsequent developmental processes seem to remain unaltered. Indeed, ectopic areas develop appropriate cell identities, establish correct projection patterns, and even generate properly configured sensory representations (Armentano et al., 2007). This suggests an early role of these genes in encoding positional information, triggering regional developmental programmes in specific positions within the expression matrix. Once triggered, these programmes would be free to progressively unfold downstream events in both progenitors and postmitotic cells, controlling the acquisition of appropriate cell identities and regional connectivity patterns independently from the early expression code.

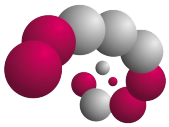

Regionalisation of the embryonic subpallium

While regionalisation in the pallial territory induces the origin of the different cortical areas, spatial patterning in the subpallium is linked to the generation of different neuronal identities (Butt et al., 2005; Gelman and Marín, 2010; Xu, 2004). Following the delineation of pallial and subpallial territories, the signalling gradients involved in such patterning also induce differential gene expression patterns in the subpallium, leading to the appearance of several major subpalliall structures (FIG 1.7D) (Flames et al., 2007; Mayer et al., 2018; Xu et al., 2010). The most dorsal aspect of the subpallium expresses the transcription factor *Gsh2* and forms the lateral ganglionic eminence (LGE), which gives rise to striatal GABAergic projection neurons, and olfactory bulb INs. The domain immediately ventral to the LGE expresses *Nkx2-1* and originates the medial ganglionic eminence (MGE) and the preoptic area (POA). These structures are responsible for the generation of two of the cardinal subclasses of cortical INs, PV and SST cells, as well as striatal INs (Lavdas et al., 1999; Wonders and Anderson, 2006; Xu et al., 2008). In addition, these embryonic structures also generate the diverse set of GABAergic neurons that populates the globus pallidus (Nobrega-Pereira et al., 2010). Finally, the most caudal aspect of the LGE, although lacking an anatomically distinguishable border with the rostral LGE, is defined by the expression of a different combination of genes, including diverse members of the *Coup-tf* family. This distinctive gene expression pattern endows this region with differential neurogenic properties. This structure, known as the caudal ganglionic eminence (CGE), gives rise to the third major group of cortical INs, those expressing the serotonin receptor 5HT3aR (Nery et al., 2002).

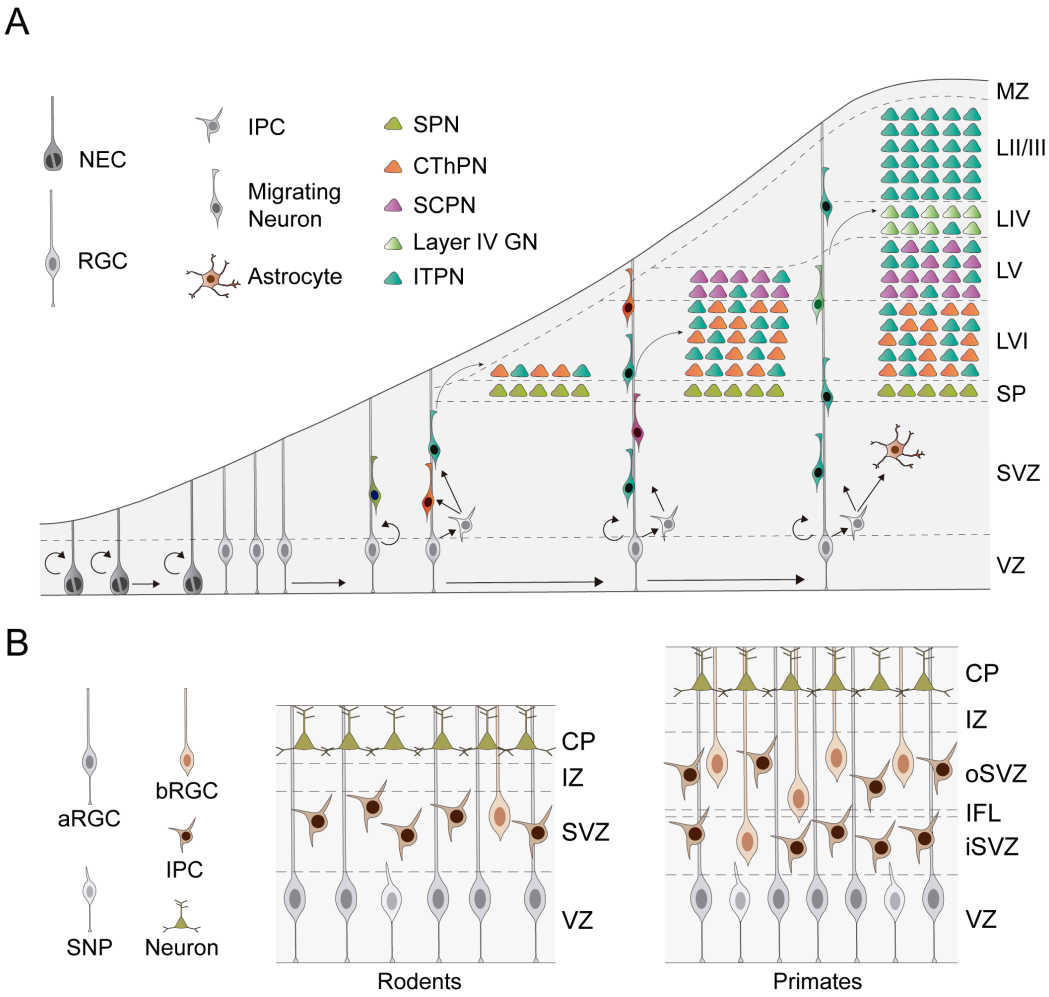

Figure 1.8. Developmental origins of neocortical pyramidal cells
(**A**) Schematic representation of cortical neurogenesis. Prior neurogenesis, NEC divide intensely to expand the pool of progenitor cells in the presumptive cortex. At the onset of neurogenesis, NEC become RGCs and generate excitatory PCs either directly or through the specification of mitotically-restricted IPCs. At population levels, RGCs sequentially generate waves of PCs of different fates. Such progenies migrate following the basal processes of RGCs and organise following an inside-out pattern that correlates with birthdate. (**B**) *Left:* Progenitor cell diversity in the rodent developing neocortex. *Right:* Progenitor cell diversity in the primate developing neocortex. NEC, neuroepithelial cell. RGC, radial glia cell. IPC, intermediated progenitor cell. SPN, subplate neuron. CThPN, Corticothalamic projection neuron. SCPN, subcerebral projection neuron. GC, granular cell. ITPN, intratelencephalic projection neuron. aRGC, apical radial glia cell. bRGC, basal radial glia cell. SNP, short neural precursor. CP, cortical plate. IZ, intermediate zone. SVZ subventricular zone. oSVZ, outer subventricular zone. iSVZ, inner subventricular zone. VZ ventricular zone. IFL, inner fibre layer. *Figure inspired by Greig et al. 2014.*

Ventrally to the CGE, a caudal extension of the POA named preoptic-hypothalamic border domain (POH), exhibits gene expression patterns that match better with the CGE than with those observed in the rostral POA (i.e. lacks

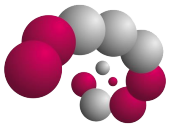

expression of *Nkx2-1*). This structure is the main source of neurogliaform cells and NPY multipolar INs (Niquille et al., 2018).

Hence, spatial patterning mechanisms in the embryonic subpallium delineate several regions with unique neurogenic properties, whose combined action underlies the appearance of cortical IN diversity. Although most of these evidences arise from experimental work in the rodent cortex, recent data indicate that similar principles underlie IN development in the primate and human brain (Hansen et al., 2013; Ma et al., 2013). In the human brain, however, there has been reported a remarkable increase in 5HTR3a INs. Consistently, an enlargement of of the CGE and an intensification of the mitotic activity in this structure has also been observed (Clowry 2015; Arshad et al., 2016).

3.3 Developmental origins of cortical PC diversity

Cell biology of PC neurogenesis

Before the generation of the first excitatory neurons in the murine cortex, the pallial neuroectoderm is populated by a large pool of neural progenitors named neuroepithelial cells. These cells are distinguishable by their characteristic bipolar morphology, as they extend an apical process that contacts the ventricular surface (VS) and a basal process whose extreme is attached to the pia. As described for RPCs, the cell bodies of these progenitors undergo interkinetic nuclear migration, ultimately dividing at the VS. (Götz and Huttner, 2005; Taverna et al., 2014). At early developmental stages, neuroepithelial cells undergo several rounds of symmetric divisions, consequently expanding the progenitor pool (FIG 1.8A). Later, cortical progenitors lose some of their

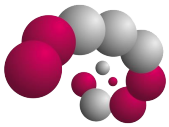

epithelial features and acquire a glial-like molecular phenotype defined by the expression of several genes, such as *Pax6* (Götz et al., 1998; Heins et al., 2002), and are known as radial glial cells (RGCs). RGCs maintain the characteristic bipolar morphology of neuroepithelial cells and also undergo interkinetic nuclear movements as they cycle (FIG 1.8A). Concurrently to this phenotypic transition, a change in their mode of division marks the start of the neurogenic process. From this point, RGCs divide asymmetrically to generate post-mitotic PCs following two alternative routes. In the first route, named direct neurogenesis, RGCs divide generating a self-renewing RGC and a post-mitotic neuron. In the second route, denominated indirect neurogenesis, RGC divisions generate a self-renewing RGC and a mitotically-restricted progenitor, named intermediate progenitor cell (IPC) (FIG 1.8A) (Miyata, 2004; Noctor et al., 2004). IPCs, also known as basal progenitors, lack contacts with the ventricular surface and the pia. In addition, these cells quickly downregulate the expression of *Pax6* and upregulate the expression of the transcription factor *Tbr2* as they migrate away from the VZ, forming an layer of progenitor cells immediately superficial to the VZ named subventricular zone (SVZ) (FIG 1.8A) (Englund et al., 2005; Haubensak et al., 2004; Noctor et al., 2004; Pontious et al., 2008). The generation of a self-renewing RGC in every round of division allows these cells to continue generating cells during embryogenesis. At the end of the neurogenic process, some RGCs become gliogenic and generate astrocytes and oligodendrocytes. Finally, most cortical progenitors undergo terminal divisions to generate postmitotic cells and/or IPCs exclusively, which leads to the disappearance of the embryonic population of progenitor cells.

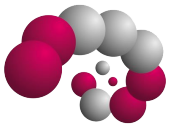

Although RGCs are the most abundant progenitor cells in the developing cortex, they are not the unique residents of the VZ. Recent studies have identified a second type of apical progenitor cell, which is mainly distinguishable by their characteristic morphology and their molecular profile. These progenitors are known as short neural precursors (SNPs) based on their monopolar morphology, with an apical process contacting the ventricular surface and a short basal process that does not reach the pial surface (Gal, et al. 2006) (FIG 1.8B). Unlike RGCs, SNPs seem to exclusively generate post-mitotic neurons through direct neurogenesis. Also, their neuronal output is thought to be smaller than that of RGCs (Stancik et al., 2010; Tyler and Haydar, 2013).

Human and non-human primates, as well as other gyrencephalic species, contain many more neurons in superficial layers than lissencephalic animals, a feature that has been linked to the acquisition of the gyrencephalic phenotype. This seems to be achieved through an intensification of the mitotic activity in the SVZ during late neurogenesis, when superficial neurons are typically generated. Indeed, the SVZ of gyrencephalic species is enlarged and split into two sub-layers, the inner SVZ (iSVZ) and the outer SVZ (oSVZ) (Lui et al., 2011; Smart et al., 2002; Zecevic et al., 2005). This process is, to some extent, due to the existence of an additional type of basal progenitor, named outer radial glia (oRGC) or basal radial glia (bRGC) which, together with some multipolar IPCs constitute the cellular population of the oSVZ (FIG 1.8B) (Fietz et al., 2010; Hansen et al., 2010; Reillo et al., 2010). These cells have a characteristic radial morphology and are typically attached to the pia by a long basal process, but lack

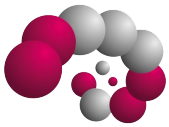

contact with the VZ. In contrast to their multipolar neighbours, bRGCs undergo several rounds of cell division, generating larger cohorts of neurons. Their molecular profile seems to be similar but distinguishable from the VZ RGCs (Pollen et al., 2015) and their progenies are thought to contribute primarily to the population of PCs in the superficial layers. Of note, a small population of bRGCs has also been described in the murine cortex, but their contribution to murine neurogenesis is considered residual (Wang et al., 2011).

Cortical neurogenesis begins with the generation of a first cohort of excitatory neurons that migrate above the germinal layers and constitute the preplate (PP). These cells share their niche with Cajal-Retzius cells, which are generated from discrete pallial structures such as the cortical hem (Bielle et al., 2005). Starting at embryonic stages E11-E12 in the mouse, cortical progenitors generate sequential waves of PCs. Neurons generated during this period use the basal process of RGCs to migrate radially away from the germinal regions. These cells split the PP into the superficial marginal zone (MZ), populated by Cajal-Retzius cells, and the deep subplate (SP), populated by the earliest cohort of excitatory neurons, named subplate cells. Subsequent cohorts of PCs occupy the space between these two layers and form the cortical plate (CP), which progressively grows with the invasion of new PCs as development proceeds.

The migratory behaviour of PCs is controlled by a complex code of adhesive and diffusive signals (Marin et al., 2010). Most importantly, the diffusive signal Reelin secreted by the transient population of Cajal-Retzius cells at the marginal zone is known to regulate PC migration (Caviness, 1982; Rice

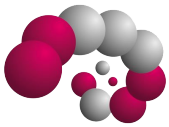

and Curran, 1999). Newly born PCs migrate beyond older neurons to reach the most superficial position in the cortical plate, forming radial columns. This mode of migration organises PCs following an inside-out pattern that correlates with their birthdate, which ultimately underlies the appearance of cortical lamination (FIG 1.8A). Consistently, classic birthdating studies in the murine cortex indicate that early-born PCs populate deep cortical layers, while late-born PCs progressively occupy more superficial positions (Fairén et al., 1986).

Fate specification of cortical PCs

Different populations of PCs occupy the six neocortical layers. While the laminar structure of the mammalian neocortex is established via their inside-out migratory pattern, developmental mechanisms underlying the acquisition of laminar-specific identity run in parallel to this process. Two main models have been proposed to explain the genesis of PC diversity (Marín and Müller, 2014).

The first model, commonly known as the progressive fate restriction model, shares the principles of the temporal patterning mechanisms described previously. According to this model, a homogeneous population of cortical progenitor cells undergo progressive changes in competence over the course of development, generating different neuronal identities during sequential temporal windows. Thus, a RGC would first generate deep laminar fates, and subsequently progress to generate cell identities destined for more superficial layers. This would result in the generation of a radially aligned ontogenic column of cells, derived from a common progenitor cell, and containing the entire complement of PC types found in the mature cortex. Such clonal column receives the name of

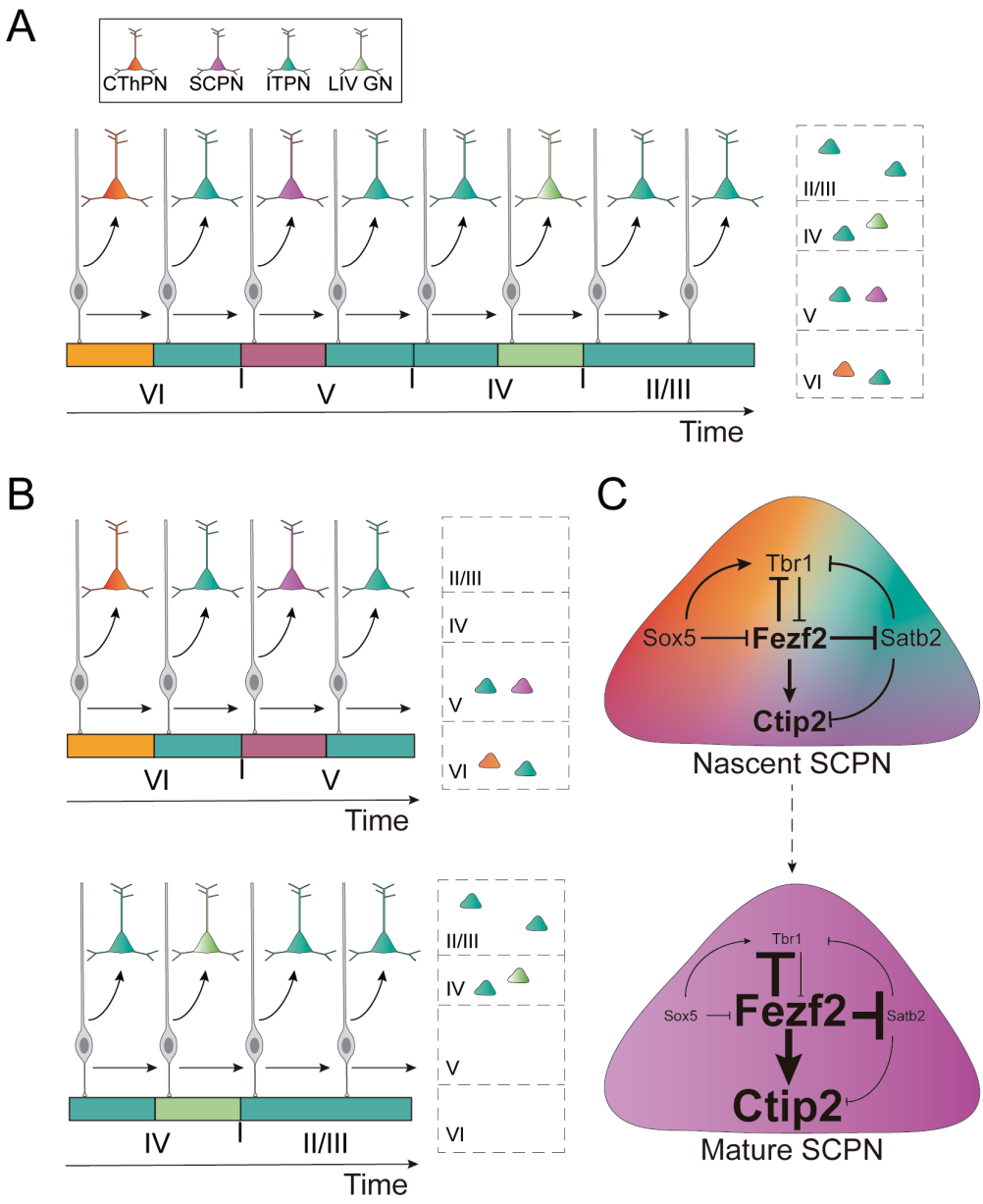

Figure 1.9. Fate specification of cortical pyramidal cells
(**A**) The progressive fate restriction model. RGCs progress through sequential competence windows. During each of these windows, cortical progenitors generate specific cell identities. (**B**) The multiple fate-restricted progenitors model. Different RGCs pools, restricted for the generation of specific PC types collectively generate the PC population of the cerebral cortex. (**C**) Post-mitotic refinement of PC identity. *Top:* Progenitor cells "prime" the nascent neurons via the transmission of unbalanced doses of key transcription factors. *Bottom:* These factors interact through competitive regulatory networks, leading to the total dominance of certain molecular programmes. These programmes then trigger diverse downstream molecular pathways that ultimately establish the identity of the neuron. Bold letters and letter sizes represent transcription factor doses. RGC, radial glia cell. CThPN, Corticothalamic projection neuron. SCPN, subcerebral projection neuron. GC, granular cell. ITPN, intratelencephalic projection neuron.

"radial unit", and would be the basis of the homonymous hypothesis. According

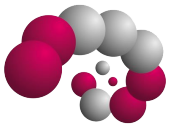

to this theory, the development of the cerebral cortex would depend on multiple replicates of this radial unit (FIG 1.9A) (Rakic, 1988).

Several lines of evidence support this hypothesis. First, as discussed above, classic studies using S-phase markers correlate birthdate with laminar fate acquisition (Fairén et al., 1986). Second, RGCs isolated in culture are capable of reproducing the sequence of neuronal types generated in vivo (Gaspard et al., 2008; Shen et al., 2006a). Third, both classic and recent fate-mapping experiments using a variety of methods to trace the progeny of RGCs at clonal resolution, have shown columnar outputs containing multiple cell types, as predicted by the model (Eckler et al., 2015; Gao et al., 2014; Guo et al., 2013).

The most common view regarding the progressive fate restriction model proposes that the sequence of competence states encoded in cortical progenitors is a consequence of the temporally organised expression of different sets of tTFs, as described in *Drosophila*. In other words, the sequential expression of different combinations of genes establishes temporal windows in which cortical progenitors are capable to generate specific cell types. Moreover, environmental influences have been proposed to regulate the progression of this intrinsic molecular clock. Accordingly, progenitor cells from early developmental stages are reprogrammed to generate late neuronal fates when transplanted into late developmental stages in the ferret cortex (Desai and McConnell, 2000). In contrast, heterochronic transplantation of late progenitors into early cortical environment seems unable to reprogram these progenitors to generate early neuronal fates. Thus, the competence windows encoded in cortical progenitors

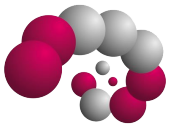

are thought to get locked as progenitors move to the next state. Hence, progenitor cells would progressively lose their capacity to generate earlier neuronal fates as neurogenesis proceeds. Although the molecular basis of this "lock" remains largely unknown, epigenetic regulation of gene expression has been proposed as a possible mechanism. It should be noted, however, that recent work in the mouse cortex has challenged some of these conclusions (Oberst et al., 2019). Specifically, late progenitor cells transplanted into early cortices seem capable to recapitulate their entire developmental program, returning to previous competence windows for the generation of early PC fates. Whether the discrepancy between the two studies reflects species-specific features or technical differences remains to be elucidated.

A second alternative model, known as the multiple fate-restricted progenitors model, has been recently proposed based on intriguing genetic fate-mapping studies in the mouse cortex. This model proposes the existence of several pools of fate-restricted cortical progenitors, specialised in the generation of particular cell types, whose joined action would accomplish the generation of PC diversity (FIG 1.9B) (Franco and Müller, 2013). In this paradigm, the expression of some key genes would establish progenitor cell identity prior neurogenesis, locking them to the generation of specific types of PCs (Franco et al., 2012; García-Moreno and Molnár, 2015). However, the interpretation of these results is not devoid of controversy (Eckler et al., 2015; Gil-Sanz et al., 2015). In addition, despite the existence of diverse morphotypes of cortical progenitors, and their apparently different contribution to cortical neurogenesis,

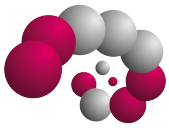

evidence of wide transcriptomic heterogeneity among cortical progenitor cells has not been found (Pollen et al., 2015).

Although the two models of cortical neurogenesis have been the object of intense discussion over the past years, they are not necessarily incompatible. Scenarios combining the existence of fate-restricted progenitors with others undergoing temporal progression are easy to imagine. Since the evidence supporting fate-restriction mostly derives from the analysis of progenitor cell output at the population level (Franco et al., 2012; García-Moreno and Molnár, 2015), it is possible that they may actually reflect progenitor fate biases towards the generation of certain neuronal identities, rather than an absolute restriction of their lineage. For this reason, additional studies characterising RGC output at the single progenitor level would be necessary to shed light into this controversial topic.

Progressive refinement of PC identity

It is presently clear that the first stages of PC fate determination take place in progenitor cells, but downstream events are also known to occur in postmitotic neurons, contributing to the refinement and maintenance of cellular identities. A handful of transcription factors are known to regulate these processes in postmitotic PCs, some of which are also expressed in cortical progenitor cells and have been linked to progenitor fate restriction (Franco et al., 2012). For instance, the zinc-finger transcription factor *Fezf2* is known to be a master regulator of corticofugal projection neuron (CFuPN) identity (Chen et al., 2005; Chen et al., 2005; Molyneaux et al., 2005).This gene is expressed at high levels

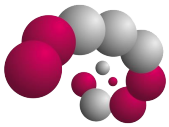

in subcortical projection neurons (SCPNs) and in lower levels in corticothalamic projection neurons (CThPNs). The cortices of *Fezf2* null mice exhibit a complete absence of layer V SCPNs along with an excessive number of intratelencephalic projection neurons (ITPNs) and CThPNs. CThPNs in these brains are however severely disorganised and lack the expression of several cell identity markers. Thus, although *Fezf2* seems to play a prominent role in the establishment of the SCPN identity, it is also required for the proper acquisition of the CThPN fate. *Coup-tf* interacting protein two (*Ctip2*) is a downstream target of *Fezf2* that plays a central role in the specification of SCPN identity (Arlotta et al., 2005). Consistently, putative SCPNs in *Ctip2* mutant mice have aberrant projection patterns that never reach their presumptive targets. CThPNs express high levels of the transcription factor T-box brain protein 1 (*Tbr1*). This gene seems to act in opposition to *Fezf2* and *Ctip2* for the establishment of CThPN fate (Bedogni et al., 2010; Han et al., 2011; McKenna et al., 2011). In the absence of *Tbr1*, layer VI cells adopt SCPN identities. The specification ITPN identity, in turn, requires the action of AT-rich sequence binding protein 2 (*Satb2*), a transcription factor expressed in virtually all cortical ITPNs. *Satb2* null mice have a severe loss of axons crossing the cerebral commissures, and putative ITPNs seem to acquire an incomplete SCPN fate (Britanova et al., 2008; Leone et al., 2015).

The transcription factors described above are initially co-expressed by immature PCs, in which they promiscuously interact with each other creating negative feedback regulatory loops. These interactions will then drive the transition from an early undefined state to a fate-determined state, in which a

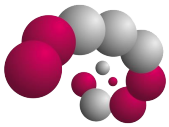

particular molecular program will dominate over the rest, directing neuronal differentiation towards a specific fate (FIG 1.9C) (Greig et al., 2013). Hence, cortical progenitors would prime postmitotic neurons via transmission of unbalance doses of diverse master regulatory genes, triggering downstream regulatory events in postmitotic cells. This would lead to the dominance of a particular molecular program in the subsequent competition, and ultimately, drive the differentiation of the nascent neuron into a particular fate.

3.4 Developmental origins of cortical IN diversity

Cortical INs originate from the embryonic subpallium, far from their place of residence in the adult brain. This structure also originates cortical oligodendrocytes, as well as other neurons and glial cells destined to diverse structures, such us the striatum, the globus pallidus or the olfactory bulb. Once generated, these cells migrate tangentially form their embryonic sources to reach the developing cortex. This migratory behaviour has made the study of their developmental history particularly challenging, limiting our understanding of the mechanisms underlying the genesis of the diverse IN fates.

Cell biology of IN neurogenesis

Three main subpallial structures are responsible for the genesis of all cortical interneurons: MGE, CGE and preoptic region (POA/POH). As discussed previously, progenitor cells in each of these regions are committed to the generation of specific classes of INs (FIG 1.10A). In brief, MGE and POA produce PV and SST interneurons, while the CGE and POH generate the heterogeneous group of 5HT3aR cells.

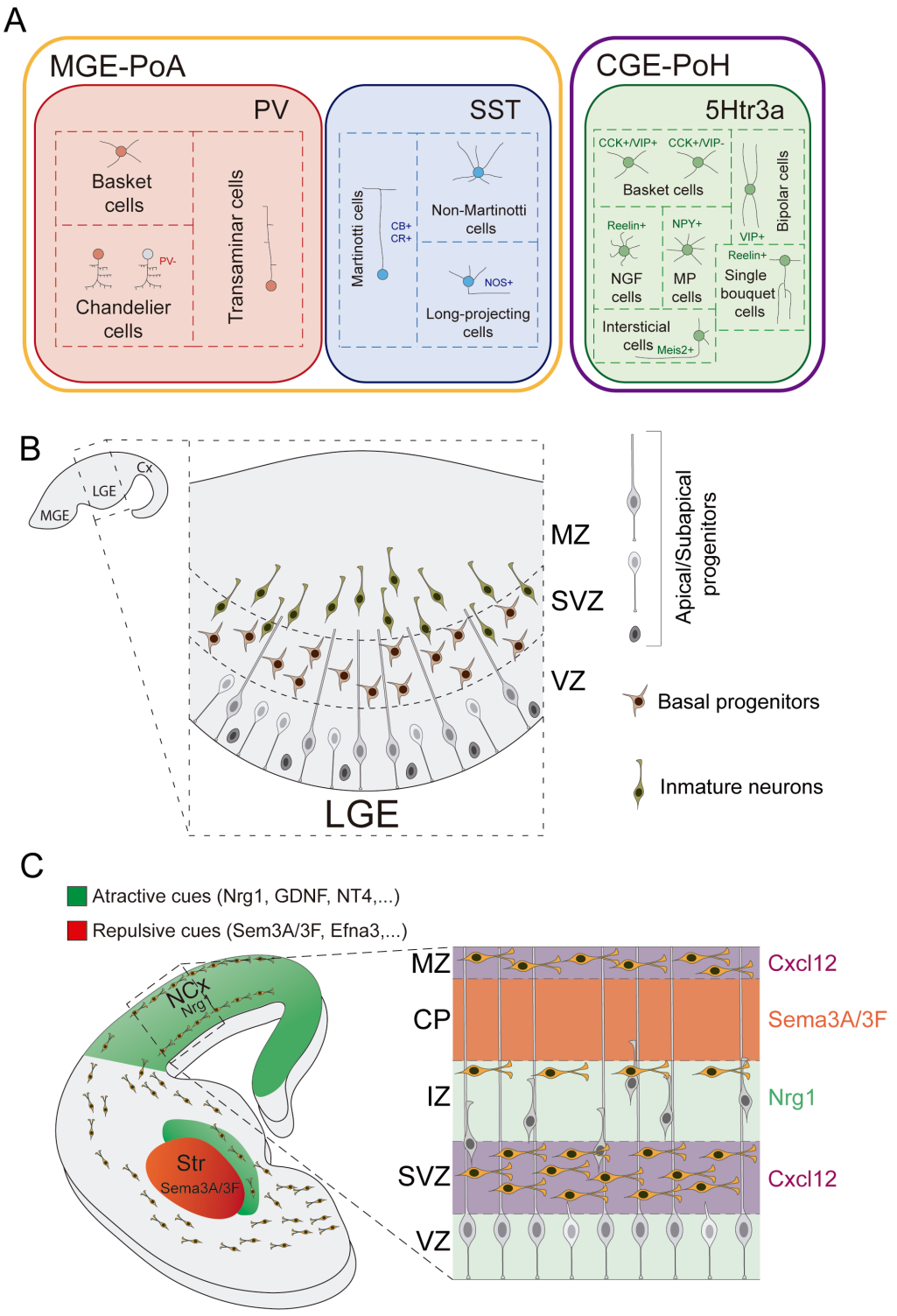

Figure 1.10. Development of cortical interneurons

(**A**) Cortical interneuron diversity. The different interneuron types that populate the adult cerebral cortex can be grouped in three non-overlapping subclasses distinguishable for the expression of specific neurochemical markers. These three subclasses also differ in their embryonic origin. PV and SST interneurons derive from the MGE and the POA, while 5Htr3a are generated in the CGE and the POH. (**B**) Schematic representation of progenitor cell diversity in the LGE. Diverse morphotypes of VZ progenitors have been described in this structure.

(**C**) Tangential migration of cortical interneurons in the developing mammalian brain. Diverse attractive and repulsive signals guide the migration of interneurons to the cerebral cortex, avoiding the invasion of other structures, like the striatum. Once they reached the cortical territory, other signals confine their migration in two main streams, the MZ and the SVZ. LGE, lateral ganglionic eminence. MGE, medial ganglionic eminence. CGE, caudal ganglionic eminence. POA, preoptic area. POH, preoptic-hipothalamic border domain. CP, cortical plate. IZ, intermediate zone. SVZ subventricular zone. VZ ventricular zone. NCx, neocortex. Str, striatum. *Figure inspired by Lim et al. 2018.*

Similarly to the developing cortex, these regions of the subpallium are populated by a large number of apical and basal progenitor cells, which reside in the VZ and SVZ, respectively. Unlike the homologous process in the pallial territories, however, the division patterns and lineage progression dynamics of cortical IN progenitor cells remain largely unknown. Intriguingly, it has been reported that VZ progenitors in the LGE and MGE divide inside this germinal layer, away from the ventricular surface, in sharp contrast to the apical progenitor cells of the developing pallium (Pilz et al., 2013). Since the location of mitosis is one of the main criteria for the classification of progenitor cells in the CNS (Taverna et al., 2014), this finding has led to the classification of these subpallial progenitor cells as an additional population of sub-apical progenitors, which are absent in the cerebral cortex. In addition, recent time-lapse imaging analysis of LGE progenitors have revealed the existence of a wide diversity of progenitor morphologies (FIG 1.10B), whose division patterns lead to an extraordinary complex and ramified lineage development. In brief, LGE lineages emerge from apical progenitors in the VZ and seem to progress through the generation of several rounds of sub-apical and basal progenitors, prior to the final generation of postmitotic INs (Pilz et al., 2013). It is conceivable that the complex neurogenic behaviour of LGE progenitor cells responds to the spatial constrains

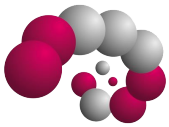

in this structure. Since the area contacting the ventricular space in the LGE is significantly smaller than it is in the pallium, an enhancement in sub-apical and basal mitotic activity may compensate this limitation. According to this hypothesis, similar division patterns should be expected to take place in the MGE. Unfortunately, the dynamics of progenitor cell divisions in this region have not yet been described in detail.

Cortical INs arising from the embryonic subpallium migrate tangentially across the subpallial mantle zone to reach the cerebral cortex. During this journey, they make use of diverse signalling mechanisms that allow them to move towards the developing cortex avoiding the invasion of other structures such as the nascent striatum (FIG 1.10C). Such signalling mechanisms include attractive cues produced by the developing cortex, such as neuregulin 1 (*Nrg1*), as well as repulsive cues expressed in the presumptive striatum, such as class III semaphorins (for a review in this matter see Marín and Rubenstein, 2001). Once they reach the cortical territory, migrating INs confine their movement to two main migratory routes, a superficial route through the marginal zone and a deeper route via the pallial SVZ (Fig 1.10C) (Lavdas et al., 1999). A smaller fraction of cortical INs migrate tangentially through the subplate. Following these routes, INs continue their tangential migration, dispersing across the developing cerebral cortex. After reaching their target regions, INs switch their migratory behaviour to invade radially the cortical plate.

Several lines of evidence suggest that cortical INs interact with local PCs for their final laminar allocation and integration into nascent circuits. First, INs

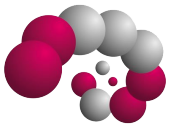

only begin the invasion of the cortical plate once PCs are in place. Second, disruption of PC lamination leads to aberrant laminar distribution of cortical INs (Pla et al., 2006). Finally, PCs in ectopic positions below the cortical plate are able to recruit migrating INs (Lodato et al., 2011). The type-specific laminar distribution of cortical INs indicates that interactions with local PCs may work in combination with IN intrinsic programmes to orchestrate the precise laminar allocation of these cells.

Fate specification of cortical INs

Although the origin of the different cardinal classes of cortical INs is spatially segregated, a wide diversity of IN subclasses and types arises from each major subpallial division: MGE and POA generate several types of PV and SST cells, whereas 5HTaR INs originated from the CGE and POH constitute a highly heterogeneous group of INs. This fact stresses the necessity of additional mechanisms for the specification of the precise identity of cortical INs, which likely involve further spatial patterning within the subpallial structures that give rise to cortical INs, as well as temporal patterning and lineage specification.

Multiple evidences support the spatial segregation of progenitor cells inside the MGE, CGE and preoptic region. Several transcription factors are expressed in heterogeneous patterns within the MGE, delineating up to five different spatial domains along its dorsoventral axis (FIG 1.11A) (Flames et al., 2007). For instance, the transcription factors *Nkx6-2* and *Er81* are expressed in opposite dorsoventral gradients within the MGE. The expression of these genes thus defines two spatial domains at the extremes of the dorsoventral axis, which

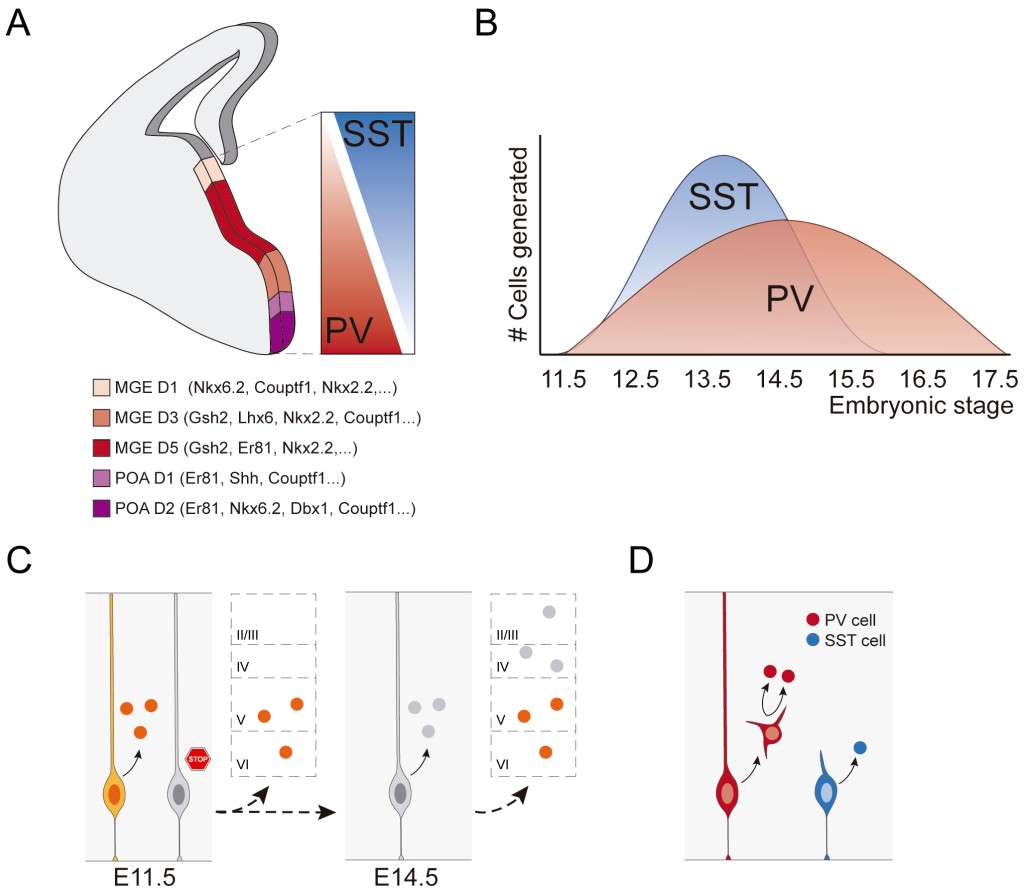

Figure 1.11. Fate specification of cortical interneurons
(**A**) Spatial bias in the origin of cortical interneuron fates. Differential gene expression patterns delineate spatial domains inside the MGE and the POA. These differences in gene expression correlate with the preferential generation of SST or PV subclasses in different regions of the MGE. Hence, dorsal MGE generates dominant numbers of SST interneurons, while ventral seems bias towards the generation of PV cells. (**B**) Temporal bias in the origin of interneuron fates. SST interneurons are primarily generated during early embryonic stages, while PV cells are born at constant ratios during the entire neurogenic period. (**C**) Two consecutive waves of MGE progenitor cells generate cortical interneurons. Early progenitor cells are responsible of the generation of deep layer interneurons, while a later wave of progenitor cells generates interneurons destined to superficial cortical layers. (**D**) Two different pools of progenitor cells generate different interneuron identities. A first type of progenitor cell preferentially generates PV interneurons through indirect neurogenesis, while a second type primarily generates SST interneurons through direct neurogenesis. Adapted from Petros et al 2015. MGE. Medial ganglionic eminence. POA, preoptic area. *Figure inspired by Flames et al. 2007.*

generate unbalanced fractions of IN classes. The dorsal, Nkx6-2 expressing domain generates mostly SST cells, while the ventral Er81 domain preferentially generates PV INs (Fogarty et al., 2007; He et al., 2016). Transplantation of dorsal and ventral pieces of MGE donor tissue into the cortex or MGE of host animals

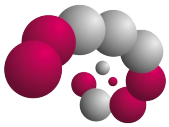

recapitulates this pattern, further supporting the existence of a spatial bias for the origin of PV and SST INs. Importantly, experiments returning cells into host MGEs are not expected to reliably introduce these cells in the specific sub-regions from where they were originally obtained. This will lead to the exposure of the transplanted cells to a different local environment after transplantation. Thus, these data implies that the developmental programmes responsible for the preferential generation of IN classes are intrinsically encoded, and unable to be reprogrammed in response to environmental influences (Flames et al., 2007; Wonders et al., 2008).

Heterogeneous gene expression patterns in the rostrocaudal axis have also been linked to the generation of different IN fates. For instance, *Couptf1* and *Couptf2* are expressed in the most caudal region of the MGE, which has been reported to generate dominant fractions of SST INs. Similar spatial biases have also been reported in the CGE. A study from the Muramaki group described striking differences in the IN fates derived from indiscriminately targeting of CGE ventricular wall via *in utero* electroporation (Torigoe et al., 2016), suggesting that different IN populations derive from different regions of this structure. In sum, although subpallial progenitor pools do not seem to segregate as sharply as in other neuronal epithelia such as in the spinal cord, it seems clear that the different embryonic sources of cortical INs are further regionalised into smaller regions, which follow specific neurogenic programmes.

Temporal patterning mechanisms also seem to be integral in IN development. Although a temporal progression of IN progenitors across several

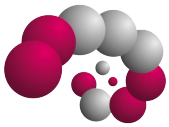

competence windows, as proposed for cortical progenitors, has not yet been described, several pieces of evidence support the existence of temporal biases in the generation of specific IN fates. SST cells are known to be produced in larger numbers during early embryonic stages, while PV INs are generated at constant rates throughout the neurogenic period (Inan et al., 2012; Miyoshi et al., 2007) (FIG 1.11B). In addition to the specification of these two cardinal classes, chandelier cells are an excellent example of temporal restriction in the origin of specific IN types. These cells are known to be generated during a specific time window in late development (Taniguchi et al., 2013). Finally, as described for PCs, INs are also generated in an inside-out pattern that largely correlates with their birthdate (Pla et al., 2006; Rymar and Sadikot, 2007; Valcanis and Tan, 2003). This is consistent with the gradient of generation of SST and PV cells, since SST INs are more abundant in deep cortical layers, while PV INs seem to adopt a homogeneous laminar distribution.

In conclusion, although the precise mechanisms underlying the origin of the diverse IN fates remain unclear, current evidence support the existence of both spatial and temporal patterning mechanisms interacting in subpallial progenitors for the specification of precise IN types, mirroring the development of PCs in the developing cortex.

Detailed analysis of MGE/POA progenitor outputs revealed that INs derived from individual progenitor cells seem to share common features, suggesting possible roles of lineage relationships in the development of these cells. Consistent with a progressive restriction model of neurogenesis, recent

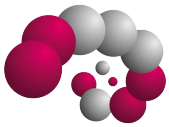

retrovirus-mediated lineage tracing data revealed that single MGE/POA progenitors generate multiple IN types, often including cells belonging to both PV and SST classes (Brown et al., 2011; Ciceri et al., 2013; Harwell et al., 2015; Mayer et al., 2015). However, superficial and deep layer INs seem to originate from independent lineages, reflecting a certain degree of lineage restriction in MGE progenitors (FIG 1.11C) (Ciceri et al., 2013). These findings are also supported by the discovery of heterogeneous patterns of gene expression among MGE progenitors (Mi et al., 2018).

Further evidences regarding fate-tuning in MGE progenitors arise from fate-mapping experiments mapping the progenies of specific progenitor populations. For example, Petros and colleagues proposed that a population of SNP-like cells in the MGE generate progenies enriched in SST INs, while RGC-like progenitors preferentially generate PV cells (Petros et al., 2015) (FIG 1.11D). Since SNPs are thought to generate neurons through direct neurogenesis, while RGCs seem to generate postmitotic neurons mostly through IPCs, the genesis of SST and PV fates has also been causally linked to these modes of division. Consistent with this idea, cyclin D1 KO mutants, which show reduced mitotic activity at the SVZ (Glickstein et al., 2009), present a severe loss of PV INs (Glickstein et al., 2007).

The appearance of these putatively different progenitor pools, and their distinguishable neurogenic activities, remain a matter of intense research. Such processes could be nested into a general temporal progression, with some lineages ramified into different branches, set for the generation of specific groups

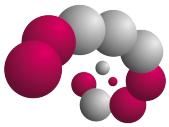

of cells (i.e., different laminar fates). Also, some temporal windows could be enriched in the generation of IPCs over others in which direct neurogenesis dominates, linking these modes of division with the generation of specific fates. Alternatively, this segregation could occur as a consequence of interactions between different progenitor cells through mechanisms involving Notch signalling, representing a novel source of diversity in the developing subpallium. At any rate, despite decades of study, our current understanding of the developmental mechanisms underlying IN diversification remains remarkably immature, and only a orchestrated research effort, involving diverse approaches and disciplines, will help to clarify our vision.

Progressive refinement of IN identity

Despite the multiple lines of evidence regarding fate specification occurring prior to IN birth, it should be highlighted that cortical INs only acquire their distinctive features once they have completed their migration and have settled in the cortex. This has led to the idea that cortical INs may be specified into cardinal subclasses at birth, but remain plastic to differentiate into specific identities progressively, as they become exposed to the cortical environment and interact with nascent circuits (Kepecs and Fishell, 2014; Wamsley and Fishell, 2017). Consistently, recent single-cell RNA-seq data identified genetic signatures linking nascent INs to cardinal subclasses, but lacking the specificity of cell types (Mayer et al., 2018). In sharp contrast, a contemporaneous study reported deeper transcriptional heterogeneity among cortical INs within hours of their generation (Mi et al., 2018). These authors reported the existence of early molecular signatures in nascent interneurons that seem to correlate with those

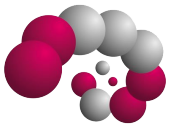

observed in adult IN types, suggesting that cortical INs may be directed towards differentiation into specific types from the moment they are generated. In line with this view, different IN types seem to be tuned to preferentially transit through different migratory streams when they invade the cortex. This is the case for different types of SST INs: Martinotti cells seem to migrate through the marginal zone route more frequently than non-Martinotti cells (Lim et al., 2018b). Importantly, the experimental reduction of the number of cells migrating through the marginal zone does not impact the normal ratio of Martinotti/non-Martinotti cells in the adult cortex, suggesting that early fate determination is the cause, rather than the consequence, of their migratory choice.

Exposure to the cortical environment is, however, undoubtedly required for the appropriate maturation of cortical INs. For example, neurogliaform cells require activation via interaction with thalamic afferents to acquire their mature properties (De Marco García et al., 2012; 2011). In addition, local PC activity has been shown to be important for the survival of immature INs (Wong et al., 2018). This seems to constitute a critical mechanism for the selection of those INs that have properly integrated into functional circuits. Finally, despite cell fate is commonly considered as an invariant feature, INs of a particular type often exhibit variations in some of their cellular attributes considered as 'states' within a given type. Some of these states have been linked to neuronal activity, reflecting adaptive changes in response to network states (Dehorter et al., 2015; 2017). Thus, it is not surprising that single-cell RNA-seq studies report a continuum of gene expression variations among some cortical IN types (Harris et

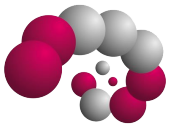

al., 2019; Tasic et al., 2018). These findings suggest that the diverse IN types generated during development are indeed flexible and adaptable to tune cortical function, and therefore their role in cortical computation goes far beyond their classification into particular categories.

4. Thesis Aims

We have discussed how the interaction of spatial and temporal patterning mechanisms accounts for the generation of neuronal diversity in different neural systems. In the cerebral cortex, these mechanisms reach a high degree of complexity, underlying the assembly of one of the most intricate and diverse cellular machineries in nature. In order to achieve a detailed understanding of these developmental mechanisms, three central aims are pursued in this thesis:

1. To achieve a detailed understanding of the developmental mechanisms underlying the appearance of the different types of neocortical PCs, and how these mechanisms lead to the precise building of the diverse regional cytoarchitectures that define cortical areas.

2. To understand the cellular principles of cortical IN generation in the embryonic subpallium.

3. To develop and validate an experimental strategy to map IN lineages derived from individual progenitor cells from development to adult life.

MATERIALS & METHODS

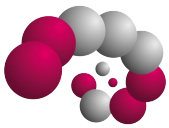

Mice

The following transgenic mouse lines were used in this study: *Nex-Cre* (Neurod6tm1(cre)Kan) (Schwab et al., 2000), *Emx1-Cre*^{ERT2} (B6.CBA-Tg(Emx1-cre/ERT2)1Kess/SshiJ), *Tbr2-Cre*^{ERT2} (C57BL/6J; 129S-Eomestm1.1(cre/ERT2)Sjar) (Pimeisl et al., 2013), *Nkx2.1- Cre*^{ERT2} (Nkx2-1$^{tm1.1(cre/ERT2)Zjh}$) (Taniguchi et al., 2011) , *Ai9*(B6.Gt(ROSA)26Sor$^{tm9(CAG-tdTomato)Hze}$) (Madisen et al., 2009), *RCE* (Gt(ROSA)26Sortm1.1(CAG-EGFP)Fsh) (Sousa et al., 2009), *MADM-TG* (Gt(ROSA)26Sortm4(ACTB-tdTomato,-EGFP)Luo) (Hippenmeyer et al., 2010), *MADM-GT* (Gt(ROSA)26Sortm4(ACTB-EGFP,-tdTomato)Luo) (Hippenmeyer et al., 2010) and *CAG-Fucci* (Gt(ROSA)26Stortm1 (CAG-Venus/GMNN,-Cherry/CDT1)Jnk) (Mort et al., 2014). All adult mice were housed in groups and kept on reverse light/dark cycle (12/12h) regardless of genotypes. Only time-mated pregnant female mice that have undergone in utero surgeries were house individually. Both male and female mice were used in all experiments. *In utero* experiments were performed at different developmental stages that range from E9.5 to E14.5. For histological analyses, mouse ages range from E12.5 to P30. All procedures were approved by King's College London and IST Austria, and were performed under UK Home Office project licenses, and in accordance to the Austrian Federal Ministry of Science and Research license, and European regulations (EU directive 86/609, EU decree 2001-486). The day of vaginal plug was considered as embryonic day (E) 0.5 and the day of birth as postnatal day (P) 0.

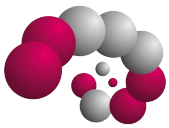

Generation of *c-Binbow* and *n-Binbow* mouse strains

The construction of *Binbow* cassettes recapitulated the structure of the original cassettes used for the generation of *Brainbow* mice (Livet et al., 2007), modified by introducing an additional reporter protein and adding homology arms to target the construct specifically into *Rosa26* locus. Recombination of the resulting conditional allele would lead to the random expression of one of the four reporter proteins in each individual cell expressing Cre, so we named this allele *binary brainbow* (*Binbow*). We generated two *Binbow* versions, one in which all reported proteins are cytosolic (*cBinbow*), and another one in which the reporter proteins have a sequence that retain them in the nucleus (*nBinbow*). Both vectors were constructed using a combination of Gibson assembly and standard cloning methods. Targeting vectors were introduced into murine C57BL/6 ES cells via electroporation, and validation of positive clones was performed by PCR and Southern blotting. ES cells were introduced into recipient blastocysts that were transferred into pseudo-pregnant females to obtain recombinant chimeras. Heterozygous F1 mice were genotyped by PCR and Southern blotting. Homologous recombination in ES cells and the subsequent generation of F1 mice was subcontracted to GenOway under my direct supervision.

Generation of retroviral vectors

Retroviral stocks encoding mCherry and EGFP (Ciceri et al., 2013) were produced as previously described (Tashiro et al. 2006). In brief, Moloney murine leukemia viruses (MoMLV) were produced by transfecting HEK293FT cells with retroviral plasmids (Rv::mCherry/EGFP, pCMV-Vsvg, and pCMV-GAG-

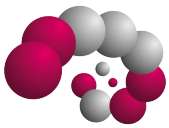

pol) using lipofectamine 2000. Forty-eight hours post transfection the supernatant was collected, concentrated and purified by two sequential rounds of ultracentrifugation. The viral pellet was re-suspended in sterile PBS and stored in aliquots at -80°C. Retroviral vectors used in this study were made by Gabriele Ciceri.

In utero infection and electroporation

Pregnant females were deeply anaesthetised with isofluorane and the abdominal cavity was incised to expose the uterus. For *in utero* infection, retroviruses were injected at low-titer into the telencephalic ventricles of mouse embryos. For *in utero* electroporation, 1µg/µl plasmid solution was injected into the telencephalic ventricles. Square electric pulses of 45V and 50ms were applied five times spaced 950ms, using a square pulse electroporator (Nepa21 Super electroporator, Nepagene). For FlashTag injections, a 10 mM solution of Cell Trace CFSE (Thermo Fisher, cat. no. C34554) dissolved in DMSO was injected into the telencephalic ventricles of E12.5 embryos. Following the procedure, the uterine horns were placed back in the abdominal cavity and the wound was surgically sutured. The female was then placed in a 32°C recovering chamber for 30 mins post-surgery before returning to standard housing conditions.

Inducible genetic labelling

For short-term fate mapping experiments in the MGE, *Nkx2.1-Cre ^{ERT2}, Ai9* pregnant females were injected with a single peritoneal injection of 5mg/kg tamoxifen dissolved in corn oil at E11.5. For clonal labelling, *Emx1-Cre^{ERT2}, RCE* and *Tbr2-Cre^{ERT2}, RCE* pregnant females received a single intraperitoneal

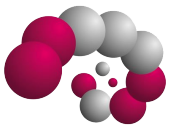

injection of low dose (1 ng/kg) tamoxifen dissolved in corn oil at E12.5. MADM clones were generated as described previously (Beattie et al., 2017; Hippenmeyer et al., 2010). In brief, timed pregnant females were injected intraperitoneally with tamoxifen dissolved in corn oil at E12.5 at a dose of 2-3 mg/pregnant dam. Live embryos were dissected at E13.5-E14.5, or recovered at E18–E19 through caesarean section, fostered, and raised for further analysis at P21.

Histology

Postnatal mice were perfused transcardially with 4% paraformaldehyde (PFA) in PBS and the dissected brains were fixed for 2h at 4°C in the same solution. Embryonic brains were dissected and fixed via overnight immersion in 4% PFA. Brains were serially sectioned at 60-100 µm on a vibratome (VT1000S, Leica) or on a freezing microtome (SM 2010R, Leica) and free-floating coronal sections were subsequently processed for immunohistochemistry as previously described (Pla et al., 2006). 1h incubation in 0.01M citrate buffer +10% glycerol at 70°C was used for antigen retrieval when required.

The following primary and secondary antibodies were used: chicken anti-GFP (1:2000 Aves lab cat. no. GFP-1020), rabbit anti-DsRed (1:500 Clonetech cat. no. 632496), goat anti-mCherry (1:500 Antibodies-Online cat. no. ABIN1440057), rat anti-RFP (1:500; ChromoTek cat. no. 5f8-100), rabbit anti-PhiYFP (1:500, Ervogen cat. no. AB604), ginea pig anti-TagRFP (1:1000, KeraFAST cat. no. EMU108), mouse IGG2a anti-β-Galactosidase (1:500 Pormega cat. no. Z3781), mouse anti-Cre (1:500, Millipore cat. no. MAB3120), rat anti-Ctip2 (1:500 Abcam cat. no. Ab18465), mouse anti-Sabt2 (1:500Abcam

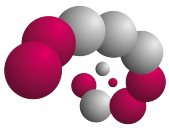

cat. no. Ab51502), rabbit anti-Sabt2 (1:1000 Abcam cat. no. Ab34735), goat anti-Tle4 (1:200 gift from Stefano Stifani), rabbit anti-Ki67 (1:500 Abcam cat. no. Ab113076), mouse anti-Tuj1 (1:500 Covance cat. no MMS-435P), rabbit anti-phospho-histone H3 (1:500 Sigma-Aldrich cat.no. 06-570), rat anti-BrdU (1:500 Abcam cat. no. ab6326), anti-chicken IgY (H+L) 488 (1:400 Molecular Probes cat. no. A-11039), anti-mouse IgG1 647 (1:400 Molecular Probes cat. no. A-21240), anti-mouse IgG (H+L) biotinylated (1:400 Vector laboratories cat. no. BA-2000), anti-rabbit IgG (H+L) biotinylated (1:400 Vector labs cat. no. BA-1000), anti-rat IgG (H+L) 555 (1:400 Molecular Probes A-21434), anti-goat IgG (H+L) 555 (1:400 Molecular Probes cat. no. A-21432), anti-rabbit IgG (H+L) 488 (1:400 Molecular Probes cat. no. A-21206), anti-rabbit IgG (H+L) 555 (Molecular Probes cat. no. A-31572), anti-ginea pig IgG (H+L) biotinylated (Jackson cat. no. 706-065-148), streptavidin 647 (Jackson, cat. no. 016-600-084), and streptavidin Dyligth 405 (Jackson, cat. no. 016-470-084).

Cell culture and *in vitro* tests

COS7 cells were maintained in DMEM (Dulbecco's modified Eagle's medium, GIBCO) medium supplemented with 10% Fetal bovine serum (FBS, GIBCO), 1% Glutamax (GIBCO) and 1% Penicilin/Streptomicin (GIBCO) at 37^{o}C, 5% CO_2. The day before transfection, 2.5x10^{5} cells were plated onto 12 mm autoclaved glass coverslips using multi-well plates. Cells were transfected with 1µg of the indicated plasmid using lipofectamine 2000 transfection reagent (Invitrogen) and incubated with DNA-lipid complex in Opti-MEM medium. In the case of co-transfection with two different plasmids, cells were transfected

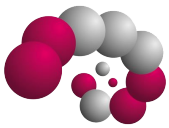

with 1µg of each plasmid. Five hours after transfection, the cell medium was replaced with the supplemented DMEM described above and cells were incubated for 48-72h. Cell cultures were fixed with a solution containing 4% paraformaldehyde (PFA) and 4% Sucrose in supplemented DMEM, for 20 minutes. Cells were labelled with standard immunocytochemistry methods and mounted in glass slides using Mowiol-Dabko (Sigma) solution.

Alternative recombination in vitro test

cBinbow circular vectors were recombined in vitro using Cre recombinase protein (New England Biolabs, cat. no. M0298). Recombinant clones were transfected into XL-Blue competent cells to obtain isolated clones. Plasmid DNA was purified from 106 individual bacterial clones, and resulting plasmids were classified into one of the four alternative configurations obtainable by Cre recombination based on enzymatic restriction analysis.

Imaging

Images were acquired using fluorescence microscopes (DM5000B, CTR5000 and DMIRB from Leica or Apotome.2 from Zeiss) coupled to digital cameras (DC500 or DFC350FX, Leica; OrcaR2, Hamamatsu) with the appropriate emission filter sets, or in inverted confocal microscopes (Leica TCS SP8 and Zeiss LSM800 Airyscan).

In silico modelling of cortical development

All modelling of progenitor behaviour was performed using Matlab (Mathworks).

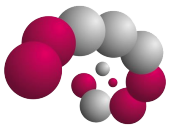

To avoid overfitting variability that could correspond to differences in progenitor behaviour across cortical areas, simulations were compared to the lineages observed in somatosensory cortex (SSCx), using our *Emx1-CreER^{T2}* ; RCE experimental dataset.

The structural similarity of model results to experimental data was assessed based on three parameters: proportion of cells per layer, clonal size distribution and Spearman correlation (r) values for number of cells in upper versus lower layers. For each parameter, we computed a normalised z-score measure by taking the difference between the experimental value and the average value across simulation repeats, and then dividing it by the standard deviation across simulation repeats. Thus, z-score values over 1 would reflect a distance between experimental and modelled data larger than the standard deviation between simulation repeats.

To generate randomly permuted cortical lineages, neurons observed in our *Emx1-CreER^{T2}* ; RCE experimental dataset were permuted among lineages while maintaining their laminar identities. This operation was repeated 1000 times, providing average and standard deviation values that were then used to compare with the experimental dataset.

Probabilistic models 1 and 2 simulated 100 progenitors undergoing cell generation sequentially, following the in vivo inside-out pattern. In each layer, *in silico* progenitors took a number of stochastic decisions for neuron generation; at each decision, a new neuron could be generated, or alternatively, the chance could be skipped without neuron generation. Sequential generation of neurons

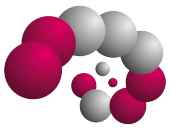

thus used the following parameters. Number of opportunities per layer was set randomly and could vary between a minimum of one and a maximum equal to the maximum number of cells found for that layer in any single experimental lineage across our three experimental datasets. This parameter establishes the number of stochastic decisions available to the progenitor and reflects the size of the temporal "window" within which a progenitor can generate neurons for a given layer. Probability of cell generation, also layer-specific, gave the likelihood that a neuron is actually generated at each decision point. Simulations were repeated 100 times. Lineages smaller than three cells or larger than 12 cells were discarded from analysis.

For each model, the set of laminar division probabilities was adjusted to fit the experimental data regarding clonal size and laminar fractions of cells. Model 1 used a unique progenitor, i.e. a single set of laminar division probabilities. Model 2 incorporated an additional population and was fit by varying both the relative size of the two populations and the values of their division probabilities, including how probabilities varied across layers.

Bayesian inference of progenitor types

To perform statistical inference on the number of categories required to explain the distribution of lineages throughout cortical layers, we employed a statistical model where N observed lineages are grouped in K progenitor types. Each type $t = 1, \ldots, K$ is associated to a vector of four probabilities $p_t = \{p_t^{(II/III)}, p_t^{(IV)}, p_t^{(V)}, p_t^{(VI)}\}$ representing the probabilities of any progenitor in the class to generate neurons in each of the four layers. We assume that each observed lineage can be

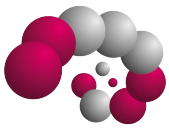

assigned to a unique progenitor type based on its occupancy distribution. Progenitor types are associated with frequencies f_t, reflecting how likely a lineage is to belong to type t. The occupancy probabilities and the relative frequencies for each type as well as the number of types K required can be obtained using Bayesian inference according to the Bayes' theorem

$$P\left(t_{1:N}, p_{1:K}, f_{1:K} \middle| S\right) = \frac{\overbrace{P\left(t_{1:N}, S \middle| p_{1:K}, f_{1:K}\right)}^{likelihood} \cdot \overbrace{P\left(p_{1:K}; f_{1:K}\right)}^{prior}}{\underbrace{P(S)}_{marginallikelihood}}$$

where S is the count matrix whose elements S_{ij} indicates how many neurons in lineage i belong to layer j. Bayes' theorem provides the posterior distribution of the model parameters p and f as well as the type assigned to each lineage conditional to the observations.

Our Bayesian model can be viewed as the following two-step generative process:

1. Each lineage i is assigned to a progenitor type t_i drawn independently from a categorical distribution with frequencies f.

2. The occupancy vector S_{ij} of each lineage i at each layer j is drawn from a binomial distribution $Binomial\left(p_{t_i}^{(j)}; N_{max}\right)$ where N_{max}=20 is the maximum number of cells that can occupy each layer.

The likelihood of a given lineage assignment and count matrix can be written as

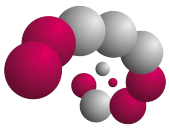

$$P\left(t_{1,\ldots,K}, S \middle| p_{1,\ldots,K}, f_{1:K}\right) = \left(\prod_{t=1}^{K} f_t^{n_t}\right) \prod_{i=1}^{N} \prod_{j \in layers} \left[p_{t_i}^{S_{ij}} \left(1 - p_{t_i}^{N_{max} - S_{ij}}\right)\right]^{\sigma_{ij}},$$

where we introduced the binary variable σ_{ij} to denote whether the matrix element S_{ij} is included in the likelihood (in which case $\sigma_{ij} = 1$) or not ($\sigma_{ij} = 0$). In particular, the selection variable σ_{ij} for each lineage was set in such a way to exclude for each lineage the most superficial empty layers not followed by an occupied layer. The corresponding zero counts in the matrix S might be spurious due to external processes stopping the lineage at early stages.

To perform Bayesian inference, we used Dirichlet priors on the relative frequencies and Beta distributions as priors on the occupancy probabilities $p_{1,\ldots,K}$. To draw samples of model parameters and progenitor types from the posterior distribution we implemented a Gibbs sampler (custom code written in C++, available upon request) which combines data likelihood and prior distributions to explore the parameter space efficiently. In order to draw statistical samples of the number of classes K we employed the Dirichlet process prior technique which allows us to remove existing classes or introduce new ones when assigning lineages to classes within the Gibbs sampler.

Quantification and statistical analysis

Quantification of cell distribution and clonal spatial configuration

In all the experiments, brain sections were sequentially analysed in rostral-to-caudal order. Pyramidal cell clones throughout the entire neocortex were

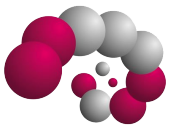

identified as sparse, spatially separated cell clusters. The boundaries between cortical layers were traced based on nuclear (DAPI) staining and the laminar position of each cell was recorded accordingly. Pyramidal cell clones were classified as translaminar, infragranular and supragranular clones according to the laminar position of the neurons belonging to each clone. Cortical areas were identified based on the reference atlas of adult mouse brain (Allen Brain Atlas; http://www.brain-map.org). In *Emx1^{CreER};MADM* experiments, lineages derived from symmetric divisions (defined as lineages with three or more cells expressing each reporter) were excluded. In the *Emx1^{CreER};RCE* experiments, lineages derived from symmetric divisions (defined as lineages containing more than twelve neurons) were excluded., Lineages containing one or two cells were also excluded in the *Emx1^{CreER} ;MADM* and *Emx1^{CreER};RCE* experiments. In the *Nkx2.1^{CreER};MADM* experiments, MGE lineages were mapped across the entire structure, and segregated based in colour code and spatial relationships. Cells were classified as polar progenitors, postmitotic neurons, and multipolar cells regarding morphology.

Classification of pyramidal cell subtypes

Brain sections were stained for markers of cortical projection neuron identity and classified based on the relative expression of the transcription factors Ctip2 and Satb2 in four main subtypes: Cortico-cortical (CCPN), Sub-cerebral (SCPN), CorticoThalamic (CthPN) and Heterogeneous (HPN) Projection neurons. This last type was defined as layer V cells expressing both Ctip2 and Satb2 markers, which have been recently described as a separate PC identity (Harb et al., 2016).

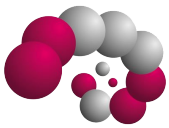

Images were captured using a confocal microscope and analysed using a custom algorithm written in Matlab (Mathworks). In brief, cell nuclei were segmented using the disk morphological function based on size and thresholds of fluorescence intensity over background. Cells were categorised as expressing high or low levels of the transcription factors Ctip2 and Satb2 and further subclassified as CCPN ($Ctip2^{Low}$ / $Satb2^{High}$), SCPN ($Ctip2^{High}$ / $Satb2^{Low}$) or HPN ($Ctip2^{High}$ / $Satb2^{High}$), based on the combination of marker expression. To distinguish between CThPN from CCPN in layer VI we used the following criteria: CCPN ($Ctip2^{Low}$ / $Satb2^{High}$ OR $Ctip2^{Low}$ / $Satb2^{Low}$) or CThPN ($Ctip2^{High}$ / $Satb2^{Low}$). This allowed for the subclassification of layer V and layer VI cells based on the same set of markers. We verified these criteria by staining brain sections for the transcription factor Tle4 (Figure S6), a well-established specific marker of cortical CThPN identity (Molyneaux et al. 2015). Layer VI cells expressing high levels of both transcription factors were not classified, and lineages containing such cells were excluded from our quantification.

Quantification of relative laminar ratios of pyramidal cells

To quantify the relative densities of PCs in different cortical layers, Nex^{Cre} mice were crossed with *Fucci2a* reporter mice (Mort et al., 2014). The density of labelled red nuclei in each cortical layer was quantified from 5 representative serial sections of the somatosensory and visual cortex. Z-stacks were then 3d reconstructed and quantified using Imaris 8.1.2 (Bitplane). A total of three animals were analysed, and each animal was considered a biological replicate.

Morphological classification of MGE progenitor cells

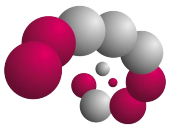

Embryonic brain slices were stained with specific antibodies (Ki67 and Tuj1) to delineate germinal zones (VZ, SVZ, MZ) and distinguish Ki67+ progenitor cells from Tuj1+ postmitotic neurons. Ki67 expressing progenitor cells present in the VZ and SVZ were then classified into different morphotypes on the basis of the presence or absence of apical and basal processes. Colocalisation of Ki67 and tdTomato fluorescent signals was measured via manual segmentation using commercial software (ImageJ). Three animals were analysed, and each animal was considered a biological replicate.

Histological analysis

Detection of specific markers and reporter genes was achieved via immunostaining. Quantifications of positive objects was performed via segmentation and colocalisation functions following semi-automatic approaches using custom-written software in MATLAB (Mathworks) or manually using commercially available software (ImageJ). Each animal was considered a biological replicate. When needed, regions of interest (ROI) were established based on the expression of specific markers or using cellular densities based on nuclear (DAPI) staining.

In vitro analysis

Quantification and colocalisation of positive objects in *in vitro* experiments was performed as described for histological analysis. For each condition, ten random fields were imaged for each one of three independent cultures, that were considered as biological replicates.

Statistical tests

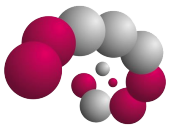

Error bars in all graphs indicate standard deviation (std) unless is otherwise stated in the legends. Comparisons of distributions over fractions of a total (as in Fig 6 E, F and Figure S5 C-E) were analysed using Fisher's exact test or Chi-square test. Comparisons of average measurements were analysed using t-Student test or ANOVA when parametric methods were applicable, and using U-Man Withney test or Kolmogorov-Smirnoff test when data distribution deviated from normality. All statistical tests applied in our analysis are specified in the figure legends.

Data and software availability

Custom-written MATLAB (Mathworks, USA) codes used for quantification are available upon request.

RESULTS

CHAPTER I:

A stochastic framework of neurogenesis underlies the assembly of neocortical cytoarchitectures

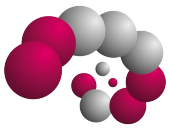

SUMMARY

The cerebral cortex contains multiple areas with distinctive cytoarchitectonic patterns, but the cellular mechanisms underlying the emergence of this diversity remain unclear. Here, we have investigated the neuronal output of individual progenitor cells in the developing mouse neocortex using a combination of methods that together circumvent the biases and limitations of individual approaches. Our experimental results indicate that progenitor cells generate pyramidal cell lineages with a wide range of sizes and laminar configurations. Mathematical modelling indicates that these outcomes are compatible with a stochastic model of cortical neurogenesis in which progenitor cells undergo a series of probabilistic decisions that lead to the specification of very heterogeneous progenies. Our findings support a novel mechanism for cortical neurogenesis whose flexibility makes it capable to generate the diverse cytoarchitectures that characterise distinct neocortical areas.

1. INTRODUCTION

The mammalian cerebral cortex contains a wide diversity of neuronal types heterogeneously distributed across layers and regions. The most abundant class of neurons in the cerebral cortex are excitatory projection neurons, also known as pyramidal cells. In the neocortex, PCs can be further classified into several subclasses with unique laminar distributions, projection patterns and electrophysiological properties (Greig et al., 2013; Jabaudon, 2017; Lodato and Arlotta, 2015), and currently available data suggest that several dozen distinct

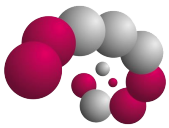

transcriptional signatures can be distinguished among them (Tasic et al., 2018). The relative abundance of the different types of PCs largely determines the distinct patterns of cytoarchitecture observed across different regions of the mammalian neocortex (Brodmann and Garey, 2006).

The diversity of excitatory neurons emerges from progenitor cells in the ventricular zone (VZ) of the developing neocortex known as radial glial cells (RGCs) (Miyata et al., 2001; Noctor et al., 2001; Malatesta, et al. 2000). RGCs divide symmetrically to expand the progenitor pool during early stages of corticogenesis. Subsequently, they undergo asymmetric cell divisions to generate clones of PCs directly or indirectly via intermediate progenitor cells (IPCs) (Lui et al., 2011; Taverna et al., 2014). The characteristic vertical organisation of migrating PCs in the developing neocortex led to the "radial unit hypothesis", which postulates that individual RGCs generate an ontogenic column of PCs organised radially, that contains neurons of diverse laminar fates (Rakic, 1988). According to this hypothesis, the construction of the cerebral cortex lies on multiple repeats of this ontogenic unit. However, the precise mechanisms through which RGCs generate diverse patterns of cytoarchitecture throughout the neocortex remain to be elucidated.

The most commonly accepted view of cortical neurogenesis is based on the notion that RGCs are multipotent and generate all types of excitatory neurons following an exquisite inside-out temporal sequence (Leone et al., 2008; Molyneaux et al., 2007, Rakic et al. 1994). Consistently, progenitor cells cultured in vitro reproduce the temporal sequence of cortical neurogenesis (Gaspard et al.,

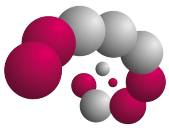

2008; Shen et al., 2006b), and genetic fate mapping experiments have shown that cortical progenitors identified by the expression of the transcription factors Fezf2 and Sox9 are multipotent in vivo (Guo et al., 2013; Kaplan et al., 2017). In contrast to this view, other studies have suggested the existence of fate-restricted cortical progenitors, which would only generate PCs for certain layers of the neocortex (Franco et al., 2012; García-Moreno and Molnár, 2015). Nevertheless, these results, and their appropriate interpretation, remain controversial (Eckler et al., 2015; Gil-Sanz et al., 2015).

Our current framework for understanding cortical neurogenesis largely relies on studies that consider RGCs as a homogeneous population. Consistent with this view, recent clonal analyses of the developing neocortex led to the conclusion that progenitor cell behaviour conforms to a deterministic program through which individual RGCs consistently generate the same neuronal output (Gao et al., 2014). This would suggest that variations in the organisation of cortical areas would exclusively rely on mechanisms of lineage refinement at postmitotic stages, such as programmed cell death. Alternatively, the absence of detailed quantitative data of individual PC lineages or methodological caveats may have prevented the identification of a certain degree of heterogeneity in the neuronal output of individual RGCs.

In this study, we have complement previous retroviral tracing data obtained in the lab with two additional experimental approaches. The combined use of these three complementary strategies allows the circumvention of some of the intrinsic technical biases associated with each of the previously used methods to

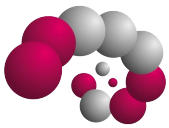

systematically investigate the clonal organisation of PC lineages in the cerebral cortex. Our results provide a detailed quantitative assessment of the neurogenic fate of individual VZ progenitor cells that reveal a large diversity of PC lineage configurations. These findings support a stochastic model of cortical neurogenesis through which a limited number of progenitor cell identities would generate the entire diversity of cytoarchitectonic patterns observed in the neocortex.

Retroviral tracing of pyramidal cell lineages

To study the cellular mechanisms underlying the generation of PCs in the neocortex, previous work in our laboratory began to analyze the organisation of neuronal lineages generated by individual progenitor cells. To this end, they used replication-deficient retroviral vectors that integrate indiscriminately in mitotic cells but only identify cell lineages with fluorescent proteins following Cre-dependent recombination (Ciceri et al., 2013). To specifically label PC lineages, they injected a very low titer cocktail of conditional reporter retroviruses (*rv::dio-Gfp* and *rv::dio-mCherry*) into the lateral ventricle of *Nex-Cre* mouse embryos (*Neurod6*$^{Cre/+}$), in which Cre expression is confined to postmitotic PCs (Goebbels et al., 2006) (FIG 2.1A). Using this approach, they achieved sparse labelling and avoided biasing the tagging of progenitor cells by the expression of specific genetic markers (Cepko et al., 2000).

To identify the developmental stage at which progenitor cells become neurogenic in the cortex, they injected retroviruses at different embryonic days (E9.5 to E14.5) and analysed the organisation of individual PC clusters at

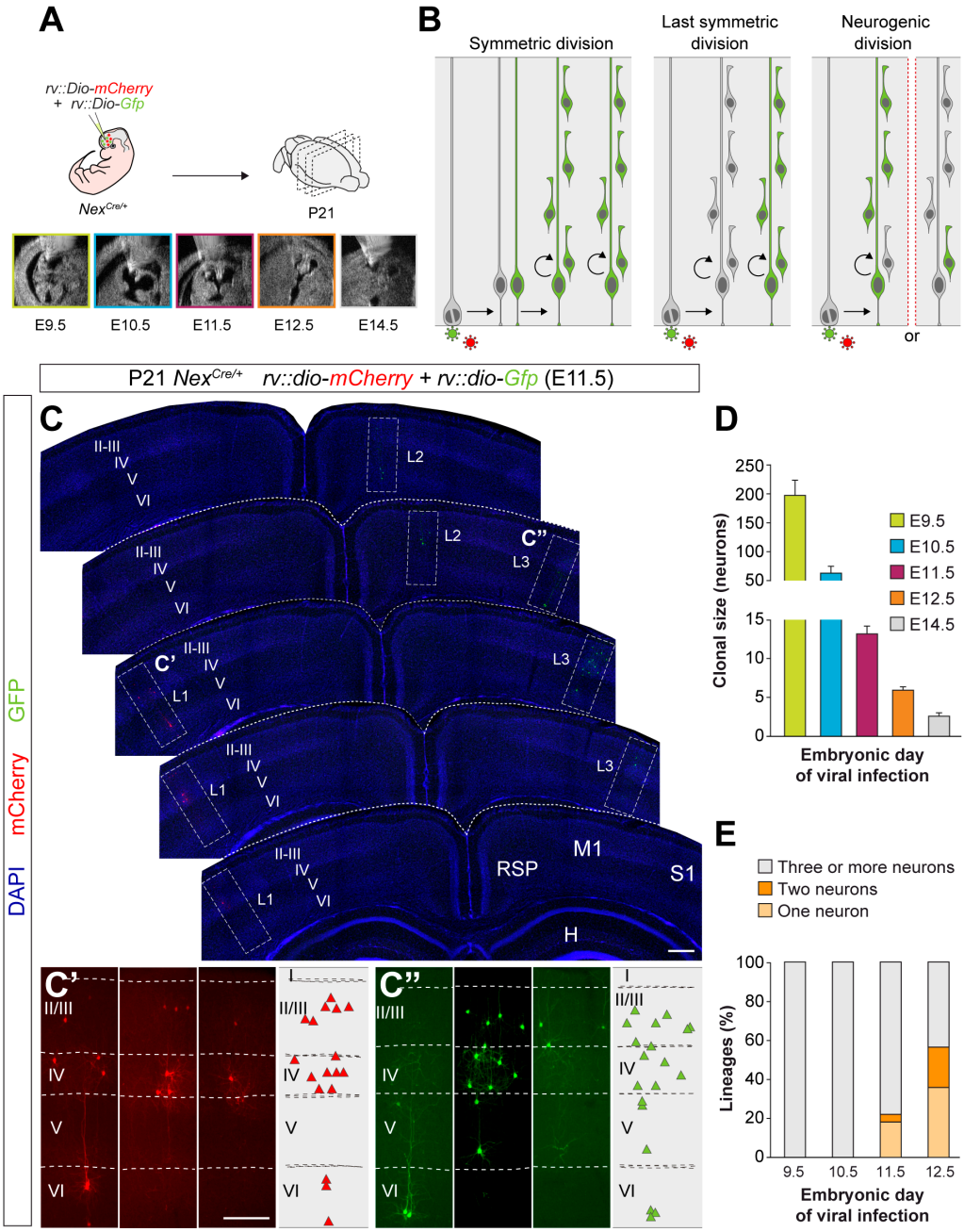

Fig. 2.1. Identification of pyramidal cell lineages with low-titer conditional reporter retroviruses.

(**A**) Experimental paradigm. (**B**) Schematic representation of the expected labelling outcomes in retroviral lineage tracing experiments. (**C–C”**) Serial coronal sections through the telencephalon of P21 *Nex*$^{Cre/+}$ mice infected with low-titer conditional reporter retroviruses at E11.5. Lineages (L) 1 and 3 are shown at high magnification in C’ and C”, respectively. Dashed lines define external brain boundaries and cortical layers. The schemas collapse lineages spanning across several sections into a single diagram. (**D**) Quantification of the number of PCs per lineage in P21 *Nex*$^{Cre/+}$ mice infected with conditional reporter retroviruses at different embryonic stages. (**E**) Quantification of the fraction of cortical lineages containing one, two or three or more neurons in P21 *Nex*$^{Cre/+}$ mice infected with conditional reporter retroviruses at different embryonic stages. Data are presented as mean ± sem. n = 13 lineages in 3 animals at E9.5; 21 lineages in 3 animals at E10.5; 64 lineages in 5 animals at E11.5; 166 lineages in 7 animals at E12.5; 32 lineages in 4 animals at E14.5. I–VI, cortical layers I to VI; H, hippocampus area; M1, primary motor cortex; RSD, retrosplenial cortex; S1, primary somatosensory cortex. Scale bars equal 100 μm (C) and 300 μm (C’ and C”).

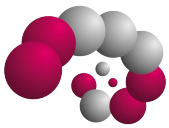

postnatal day (P) 21 (FIG 2.1A). Since a single copy of the viral vector is stably integrated into the host genome, retroviral infection leads to the labelling of only one of the two daughter cells resulting from the division of the infected progenitor cell. Consequently, infection of progenitor cells in the ventricular zone (VZ) of the pallium labels PC lineages in three main configurations depending of the mode of division of the infected progenitor (FIG 2.1B): (1) a large cluster containing more than one lineage, which results from the infection of a self-renewing progenitor cell dividing symmetrically; (2) a single lineage, which results from the infection of a progenitor cell undergoing its last symmetric division; and (3) a partial lineage, which results from a neurogenic division of a progenitor cell. In this later case, partial lineages may contain the majority of neurons in the clone, if integration occurs in the progenitor cell, or one or two neurons, if the integration occurs in a neuron or an IPC, respectively.

They observed clusters of neurons with the characteristic morphology of PCs at all stages examined. Systematic mapping at P21 revealed very sparse labelling and widespread distribution of clones throughout the entire neocortex (FIG 2.1C–C" and FIG 2.2). The spatial segregation of the lineages was confirmed by the virtual absence of green and red clones within 500 µm of each other in all experiments analysed (FIG 2.2B). They quantified the number of PCs per clone at P21 following viral infection at different embryonic stages and observed that lineages contained progressively smaller progenies (FIG 2.1D). This is consistent with the notion that VZ progenitors undergo proliferative symmetric cell divisions early during corticogenesis before they become

neurogenic and begin self-renewing via asymmetric divisions (Götz and Huttner, 2005; Kriegstein and Götz, 2003). Since neurogenic divisions label one or two neurons in 50% of the cases (FIG 2.1B), the fraction of one- and two-cell clones found after retroviral infection is indicative of the proportion of neurogenic VZ progenitor cells at each embryonic stage. They observed that these clones represent ~50% of the lineages at E12.5 (FIG 2.1E). Consistent with previous reports using other methods (Gao et al., 2014), these results indicate that the onset of cortical neurogenesis begins immediately before E12.5, and that at this

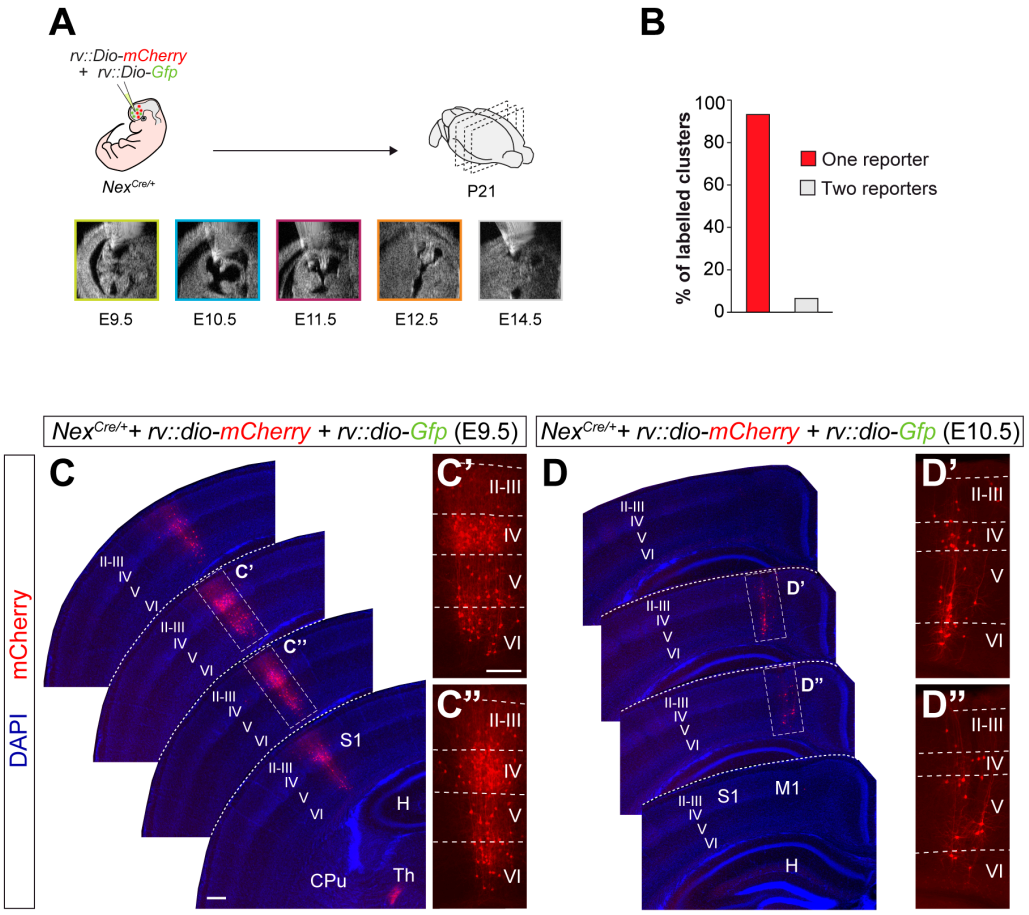

Fig. 2.2. Sparse labelling of neuronal clones with low-titer retroviral infection. **(A)** Experimental paradigm. **(B)** Fraction of neuron clusters containing cells labeled with one or two reporters. **(C-D)** Serial coronal sections through the telencephalon of P21 *Nex*$^{Cre/+}$ mice infected with low-titer conditional reporter retroviruses at E9.5 (C) and E10.5 (D). The high magnification pictures shown in (C'-C") and (D'-D") correspond to the clones shown in (C) and (D), respectively. n = 296 lineages in 19 animals across all ages. Scale bars equal 100 μm (C-D) and 300 μm (C', C", D', D").

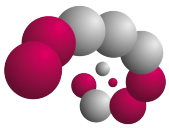

stage most VZ progenitor cells are already neurogenic. Thus, they focused subsequent analyses on this stage.

They first examined lineages labeled at E12.5 that contained more than two cells, which correspond to the progeny of a VZ progenitor cell (FIG 2.3A). Consistent with classical models of cortical neurogenesis, they found that most VZ progenitor cells (63%) infected with retroviruses at E12.5 produce translaminar lineages containing neurons in both deep (V and VI) and superficial (II-III and IV) layers of the neocortex (FIG 2.3B,E). However, they also observed a substantial fraction of lineages in which PCs were confined to either deep (FIG 2.3C,E) or superficial (FIG 2.3D,E) layers (15% and 22%, respectively).

The distribution of single-cell and two-cell clones following infection of VZ progenitor cells at E12.5 further supported the existence of cortical lineages restricted to superficial layers of the neocortex. As expected from the normal progression of neurogenesis in translaminar lineages, most single-cell and two-cell clones (which result from the labelling of a neuron or an IPC, respectively) were located in deep layers of the cortex (FIG 2.3F-M). However, in these experiments they also identified a small fraction of single-cell and two-cell clones in superficial layers of the neocortex (FIG 2.3F-M). This suggested that some VZ progenitor cells generate PCs for superficial layers of the neocortex in their earliest neurogenic divisions.

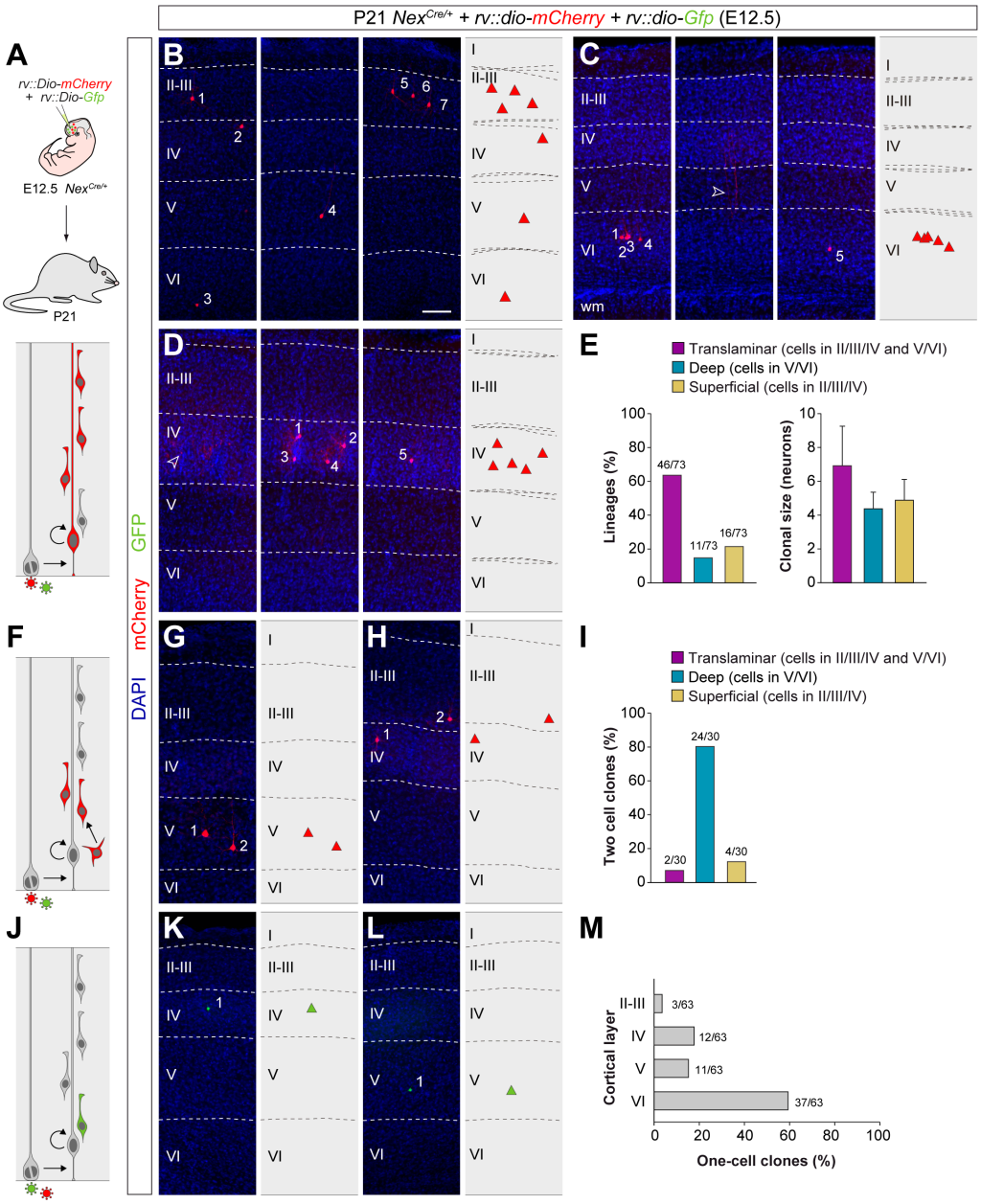

Fig. 2.3 Retroviral-based lineage tracing reveals diverse lineage outcomes.
(A) Experimental paradigm. The bottom panel illustrates the expected labelling outcome following retroviral infection of an RGC undergoing a neurogenic cell division in which the viral integration occurs in the self-renewing RGC. **(B-D)** Serial coronal sections through the cortex of P21 *Nex*$^{Cre/+}$ mice infected with low-titer conditional reporter retroviruses at E12.5. The images show examples of translaminar (B), deep-layer restricted (C) and superficial-layer restricted (D) lineages containing three or more cells. Dashed lines define external brain boundaries and cortical layers. The schemas collapse lineages spanning across several sections into a single diagram. **(E)** Quantification of the fraction of translaminar, deep- and superficial-layer restricted lineages containing three or more cells, and clonal size. Clonal size data are presented as mean ± standard deviation. **(F)** Expected labelling outcome following retroviral infection of an RGC undergoing a neurogenic cell division in which the viral integration occurs in an IPC (indirect neurogenesis). **(G-H)**, Coronal sections through the cortex of P21 *Nex*$^{Cre/+}$ mice infected with low-titer conditional reporter retroviruses at E12.5. The images show examples of superficial and deep layer-restricted two-cell clones. **(I)** Quantification of the fraction of translaminar, deep and superficial layer-restricted two-cell lineages.

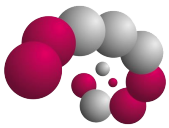

(**J**) Expected labelling outcome following retroviral infection of an RGC undergoing a neurogenic cell division in which the viral integration occurs in a postmitotic neuron (direct neurogenesis). (**K-L**) Coronal sections through the cortex of P21 $Nex^{Cre/+}$ mice infected with low-titer conditional reporter retroviruses at E12.5. The images show examples of superficial and deep layer-restricted single-cell clones. (**M**) Laminar distribution of single-cell clones. n = 166 lineages in 7 animals. Scale bar equals 100 μm.

2. RESULTS

A small fraction of progenitors generates laminar-restricted lineages

We noted that the clonal size of laminar-restricted lineages in previous retroviral tracing experiments was typically smaller than that of translaminar clones (FIG 2.3E). One explanation for this difference could be that laminar-restricted lineages represent sub-clones resulting from the labelling of IPCs that undergo more than one round of cell division, generating four to five neurons with a laminar-restricted distribution. To test this hypothesis, we carried out lineage tracing experiments at single cell resolution using low-dose tamoxifen administration in $Tbr2^{CreER};RCE$ pregnant mice at E12.5 (FIG 2.4A), which led to the sparse labelling of IPCs and their progenies (Pimeisl et al., 2013). We analysed 73 IPC-derived lineages at P21 and exclusively found one-cell and two-cell clones, with no evidence for larger clones within our sample (FIG 2.4B-D). Although the existence of IPCs that undergo more than one cell division, as reported in other studies (Vasistha et al., 2015) cannot be completely excluded, these results indicate that this is not common at this developmental stage. Consequently, IPCs are unlikely to be the origin of laminar-restricted lineages. These results show discrepancies with those Vasistha et al. 2015., where the existence of larger cellular outputs arising form individual IPCs was reported.

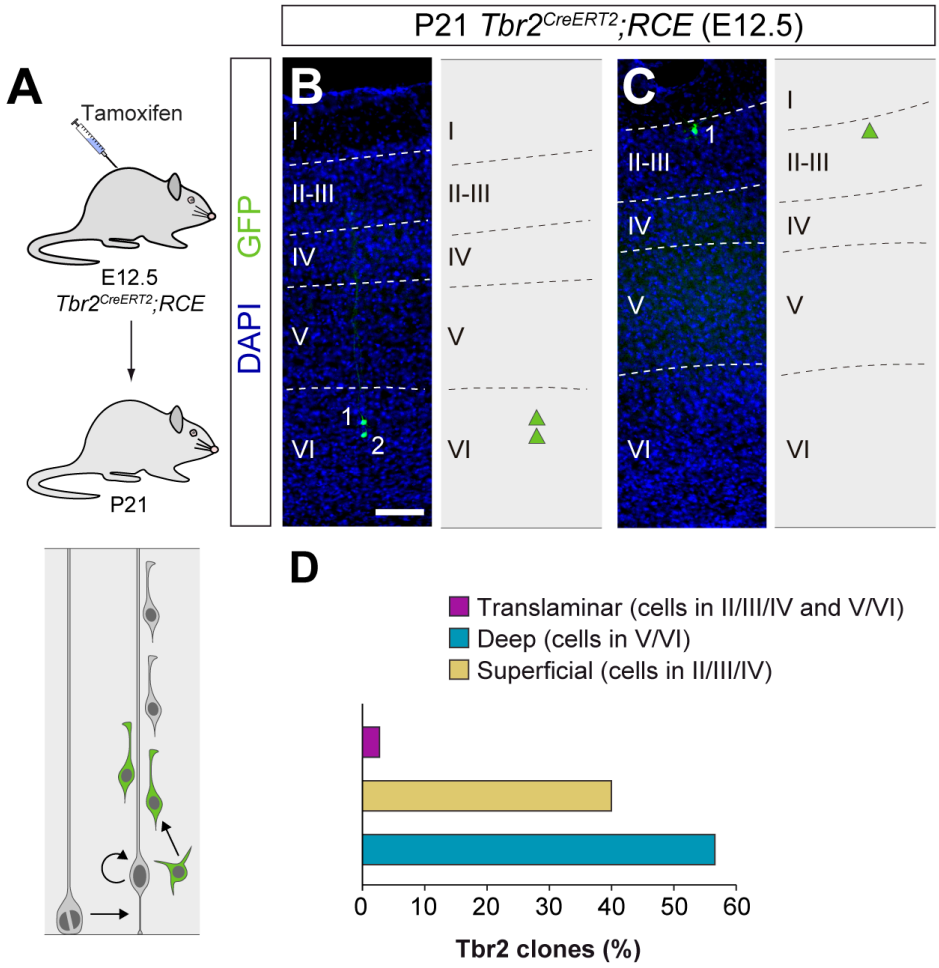

Fig. 2.4. Lineage tracing of Tbr2+ intermediate progenitor cells. **(A)** Experimental paradigm. The bottom panel illustrates the expected labelling outcome of the division of a Tbr2+ intermediate progenitor cell. **(B-C)** Coronal sections through the cortex of P21 *Tbr2*^{CreERT2}*;RCE* mice treated with low-dose tamoxifen at E12.5. The images show examples of deep and superficial layer-restricted Tbr2-derived lineages. The schemas collapse lineages spanning across several sections into a single diagram. **(D)** Fraction of translaminar, deep and superficial layer-restricted Tbr2-derived lineages. n = 73 lineages in 12 animals. Scale bar equals 100 μm.

Further studies will help to clarify these concepts. In our perspective, several factors can lead to these differential observations, such as the sample size of both experimental datasets, and/or in the different techniques used to map the outputs of individual IPCs.

Retroviral tracing experiments suggested that the neurogenic output of neocortical VZ progenitor cells is significantly more heterogeneous than

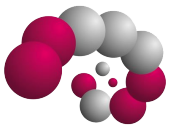

previously described, including translaminar, deep- and superficial-layer restricted lineages. However, several technical limitations may contribute to the observation of laminar-restricted lineages, as retroviral tracing may lead to the incomplete labelling of neuronal lineages. For example, the existence of deep layer-restricted lineages might be due to the silencing of the viral cassette after a few rounds of cell division (Cepko et al., 2000), which would prevent the expression of GFP or mCherry in superficial layer PCs. There are also alternative explanations for the observation of superficial layer-restricted lineages in the retroviral tracing experiments. First, infected progenitors might have become neurogenic at slightly earlier stages and have already produced a wave of deep layer PCs before infection, which would therefore not be labeled by the retrovirus. Second, the entire set of deep layer neurons might have been generated during the first neurogenic division of a VZ progenitor cell, which would not be labeled in some cases due to the retroviral integration mechanism.

To overcome these technical limitations, we took advantage of the Mosaic Analysis with Double Markers (MADM) technique, a genetic method widely used to fate-map cellular lineages at high resolution (Hippenmeyer et al., 2010; Zong et al., 2005). We used the *Emx1-CreER*^{T2} mice (Kessaris et al., 2006) to induce MADM sparse labelling of VZ progenitor cells following tamoxifen administration at E12.5 (FIG 2.5A). This set of experiments was performed by our collaborators in the Hippenmeyer Lab, being us in charge of the data analysis. We specifically focused our analysis on G2-X MADM segregation events that result in the labelling of an unbalanced number of daughter cells with

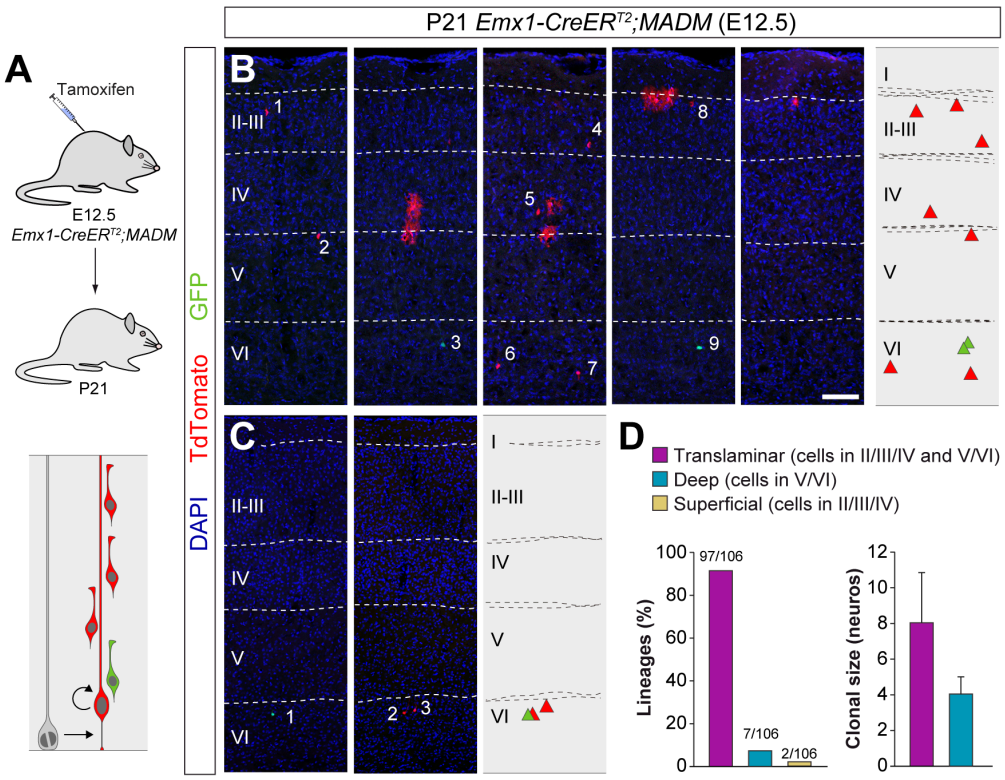

Fig 2.5. Lineage tracing using MADM identifies a small fraction of deep layer-restricted cortical lineages.
(**A**) Experimental paradigm. The bottom panel illustrates the expected labelling outcome of a neurogenic RGC division following inducible MADM-based lineage tracing in which two subclones are labeled with different reporters. (**B-C**) Serial coronal sections through the cortex of P21 Emx1-CreERT2;MADM mice treated with tamoxifen at E12.5. The images show examples of translaminar (B) and deep layer-restricted (C) lineages. The schemas collapse lineages spanning across several sections into a single diagram. (**D**) Quantification of the fraction of translaminar, deep and superficial layer-restricted lineages, and clonal size in MADM lineages derived from a neurogenic (asymmetric) RGC division. Clonal size data are presented as mean ± standard deviation. n = 106 neurogenic lineages in 28 animals. Scale bar equals 100 μm.

either green or red fluorescent proteins and report the outcome of asymmetric divisions in VZ progenitor cells (Zong et al., 2005). Consistent with the retroviral lineage tracing experiments, we found that the vast majority of MADM lineages adopt a translaminar configuration (FIG 2.5B,D). In addition, we also identified some lineages in which PCs were confined to layers V and VI, thereby confirming the existence of lineages restricted to deep layers of the neocortex (FIG 2.5C,D). We observed that the fraction of deep layer-restricted lineages

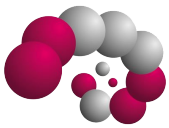

labeled with MADM (~7%) is smaller than that obtained with retroviral tracing (15%), which suggested that reporter silencing might exist in some clones in the retroviral lineage tracing experiments. In contrast, we did not recover a significant number of superficial layer-restricted lineages in MADM experiments (FIG 2.5D).

The MADM experiments suggested that the observation of superficial layer-restricted lineages in retroviral experiments might be artifactual, a result of the incomplete retroviral labelling of neuronal lineages. We reasoned that if this were the case, the analysis of the MADM sub-clones (i.e., only one of the two colors in the lineage) containing more than two cells should lead to a similar fraction of 'artifactual' lineages, since these would essentially correspond to those labeled by retroviral infection missing the first division of VZ progenitor cells (FIG 2.6). This analysis indeed identified a small fraction of MADM sub-clones as 'apparent' superficial layer-restricted lineages (~12%), which was nevertheless significantly smaller than those identified in the retroviral experiments (22%). This indicated that although some of the superficial layer-restricted lineages observed in retroviral experiments were artifactual, others might not be.

One important difference between both approaches is that MADM G2-X recombination events occur exclusively in mitotic cells (Zong et al., 2005), while retroviral labelling does not strictly depend on cell division. Retroviruses require cell division for their integration into the genome, but the infection is independent of cell cycle stage (Cepko et al., 2000). Thus, we hypothesized that

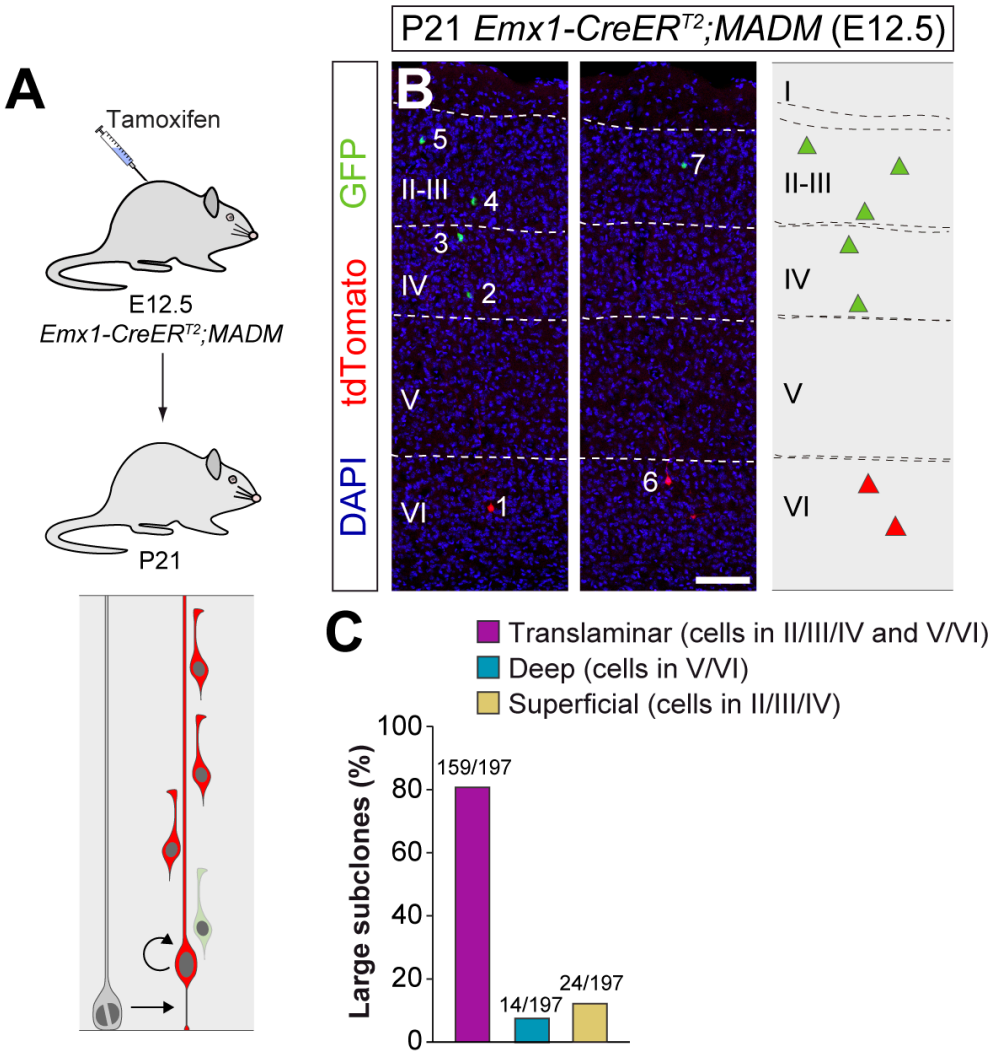

Fig. 2.6. Large MADM sub-clones reveal a small fraction of artifactual superficial layer-restricted lineages in the retroviral dataset.
(**A**) Experimental paradigm. The bottom panel illustrates the expected labelling outcome of a neurogenic RGC division following inducible MADM-based lineage tracing in which two sub-clones are labeled with different reporters. (**B**) Serial coronal sections through the cortex of P21 *Emx1-CreER^{T2};MADM* mice treated with tamoxifen at E12.5. The images show an example of a translaminar lineage containing a large superficial layer-restricted sub-clone. The schemas collapse lineages spanning across several sections into a single diagram. **(C)** Relative fraction of translaminar, deep and superficial layer-restricted MADM large sub-clones. n = 196 sub-lineages in 28 animals. Scale bar equals 100 μm.

MADM may not consistently label a fraction of quiescent or slowly dividing progenitors, which could otherwise be targeted by retroviral infection. To test this idea, we carried out a new set of lineage tracing experiments using a third, complementary method. In brief, we traced cortical lineages at single cell resolution using low-dose tamoxifen administration in *Emx1-CreER^{T2};RCE*

pregnant mice at E12.5 (FIG 2.7A), in which labelling of VZ progenitor cells should be independent of cell cycle dynamics. Since this method does not distinguish between lineages derived from symmetric or asymmetric cell divisions, we limited our analysis to lineages with a maximum of 12 cells, the larger clonal size of neurogenic lineages in the *Emx1-CreER^{T2};MADM* dataset (clones with more than 12 cells account for less than 5% of the neurogenic lineages and largely include [87%] the outcome of symmetrically-dividing progenitor cells).

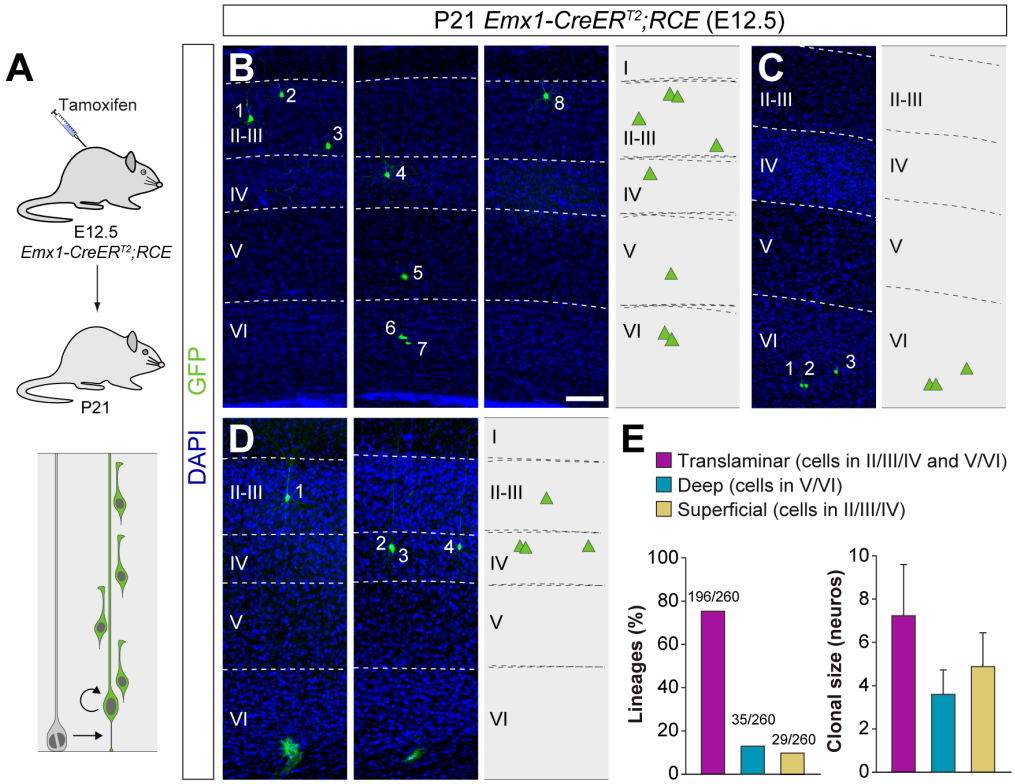

Fig 2.7. A fraction of early-quiescent cortical progenitors generates superficial layer-restricted lineages.
(**A**) Experimental paradigm. The bottom panel illustrates the expected labelling outcome of a neurogenic RGC division following inducible conditional reporter lineage tracing in Emx1-CreERT2;RCE mice. (**B-D**) Serial coronal sections through the cortex of P21 Emx1-CreERT2;RCE mice treated with low-dose tamoxifen at E12.5. The images show examples of translaminar (B), deep layer-restricted (C) and superficial layer-restricted (D) lineages. The schemas collapse lineages spanning across several sections in a single diagram. (**E**) Quantification of the fraction of translaminar, deep and superficial layer-restricted lineages, and clonal size in inducible conditional reporter lineage tracing experiments. Clonal size data are presented as mean ± standard deviation. n = 260 neurogenic lineages in 25 animals. Scale bar equals 100 μm.

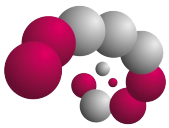

Consistent with the other approaches, the majority of lineages (~75%) labeled by injection of *Emx1-CreER^{T2};RCE* mice with low tamoxifen doses at E12.5 were translaminar (FIG 2.7B,E). We also confirmed that ~13% of the lineages were restricted to deep cortical layers (FIG 2.7C,E). In addition, we found that ~11% of the lineages consist of PCs confined to superficial layers of the neocortex (FIG 2.7D,E). In sum, the combined results of three different sets of lineage tracing experiments suggested that translaminar (~80%), deep layer-restricted (~10%) and superficial layer-restricted (~10%) lineages are generated at the onset of neurogenesis in the developing neocortex.

Pyramidal cell lineages acquire diverse configurations

We next explored the precise organisation of cortical lineages derived from VZ progenitor cells at E12.5. In lineage tracing experiments using *Emx1-CreER^{T2};RCE* mice (FIG 2.8A), we observed that only about a quarter of traced lineages contain neurons in every cortical layer from II to VI, and every other clone lacks neurons in one or multiple cortical layers (FIG 2.8B-D,F). For instance, a significant proportion of translaminar lineages lacks PCs in layer V (FIG 2.8B,F) or layer IV (FIG 2.8C,F) but, considered collectively, PC lineages adopt every possible configuration of laminar distributions in the neocortex (FIG 2.8F). The heterogeneous organisation of cortical lineages was not exclusively observed in the experiments performed in *Emx1-CreER^{T2};RCE* mice; similar results were obtained in retroviral lineage tracing and MADM experiments (FIG 2.9). Although the clonal size of these lineages also exhibits great heterogeneity, it seems to follow a bimodal distribution, with maximums at approximately 4

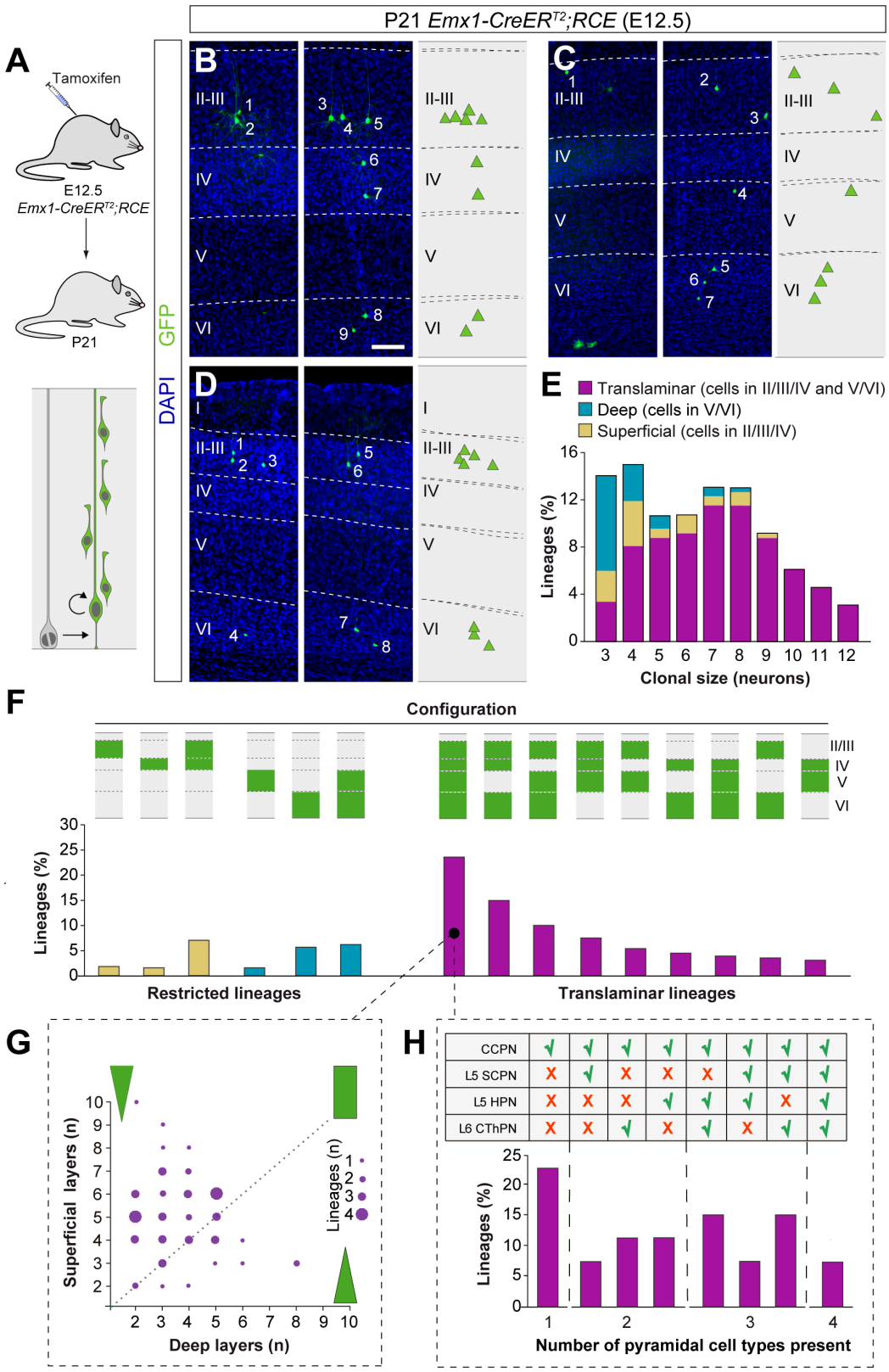

Fig 2.8. Translaminar lineages adopt very heterogeneous configurations.
(**A**) Experimental paradigm. The bottom panel illustrates the expected labelling outcome of a neurogenic RGC division following inducible conditional reporter lineage tracing in Emx1-CreERT2;RCE mice.

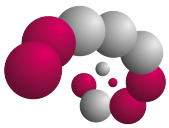

(**B-D**) Serial coronal sections through the cortex of P21 Emx1-CreERT2;RCE mice treated with low-dose tamoxifen at E12.5. The images show examples of translaminar lineages with various laminar configurations. The schemas collapse lineages spanning across several sections into a single diagram. (**E**) Clonal size distribution of translaminar, deep and superficial layer-restricted lineages. (**F**) Relative frequency (expressed as percentage over the total number of lineages) of the different laminar configurations (green and grey schemas) in inducible conditional reporter lineage tracing experiments. (**G**) Relative abundance of PCs in superficial and deep layers from translaminar lineages containing cells in every layer. Lineages are represented as circles in a bi-dimensional space, indicating the number of cells in superficial versus deep layers. The size of the circle indicates the number of lineages that shown a particular configuration. Green shapes schematically represent lineage configurations. A rectangular shape illustrates lineages with a balanced number of superficial and deep PCs; triangular shapes represent configurations of lineages biased towards superficial or deep layer neurons. (**H**) Fraction of translaminar lineages with neurons in every layer containing one, two, three or four subclasses of PCs. n = 260 neurogenic lineages in 25 animals. CCPN, cortico-cortical projection neuron; SCPN, subcortical projection neuron; HPN, heterogeneous projection neuron; CThPN, cortico-thalamic projection neuron. Scale bar equals 100 μm.

and 8 cells (FIG 2.8E, FIG 2.9). Intriguingly, these two maximums largely correspond to restricted and translaminar lineages respectively, reinforcing the previously described link between clonal size and laminar configuration.

We characterised the organisation of translaminar lineages with PCs in every layer by quantifying the relative proportion of neurons in deep and superficial layers. This analysis revealed that these cortical lineages typically showed a bias toward the production of PCs for superficial layers, although a minority of lineages displayed a preference towards deep layers or a balanced distribution across deep- and superficial layers (FIG 2.8G). In general, the total amount of cells in superficial and deep cortical layers was slightly anti-correlated. To further explore the molecular diversity of PCs in these lineages, we stained P21 brain sections from *Emx1-CreER^{T2};RCE* mice induced at E12.5 with antibodies against Ctip2 and Satb2, two transcription factors whose relative expression defines different types of PCs with unique patterns of axonal projections (Greig et al., 2013; Lodato and Arlotta, 2015). We identified four PC

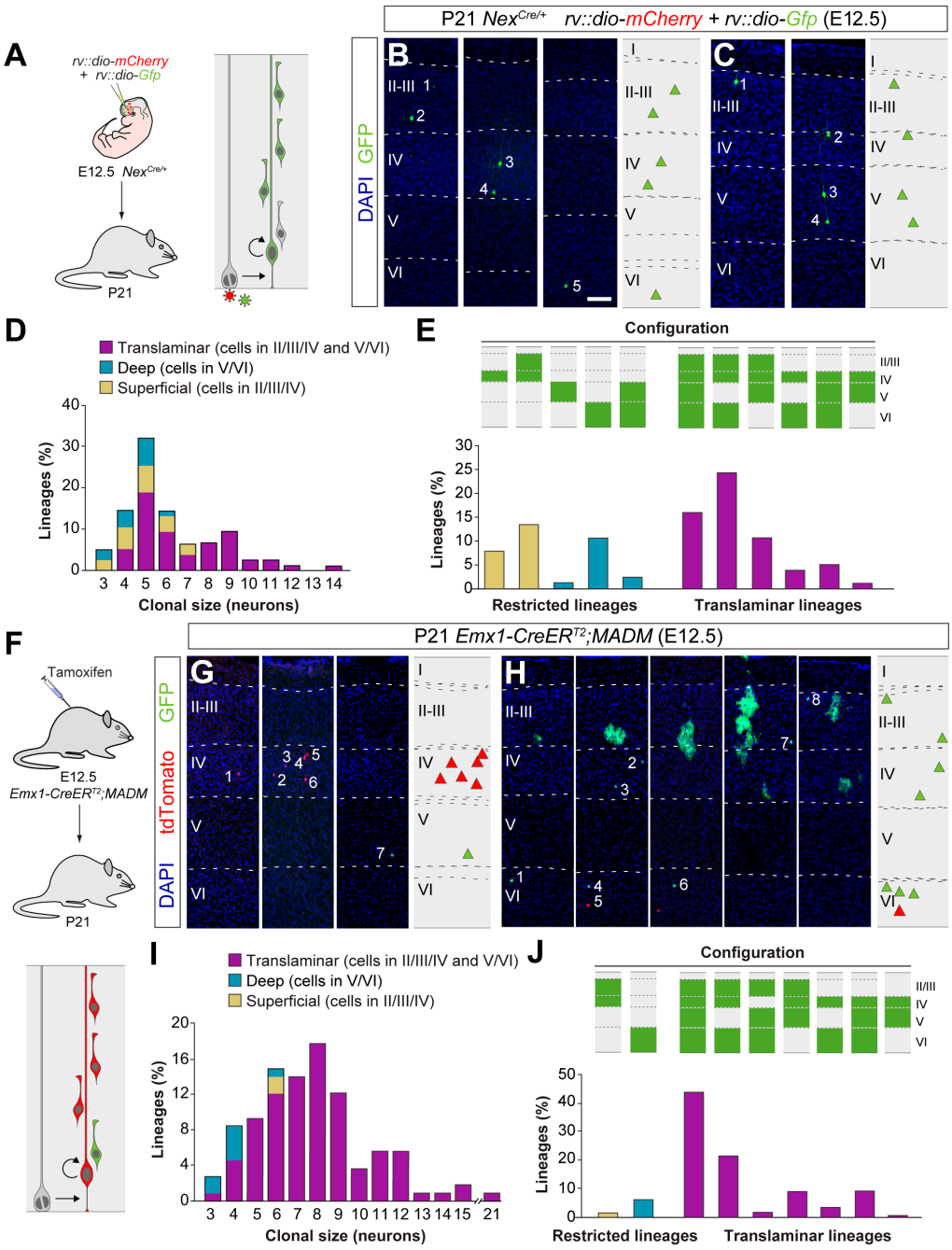

Fig. 2.9. Retrovirus and MADM labeled lineages reproduce laminar configuration diversity. (**A**) Experimental paradigm. The right panel illustrates the expected labelling outcome following retroviral infection of an RGC undergoing a neurogenic cell division in which the viral integration occurs in the self-renewing RGC. (**B-C**) Serial coronal sections through the cortex of P21 *Nex*$^{Cre/+}$ mice infected with low-titer conditional reporter retroviruses at E12.5. The images show examples of layer V (B) and layer 6 (C) skipping lineages. Dashed lines define cortical layers. The schemas collapse lineages spanning across several sections into a single diagram. (**D**) Clonal size distribution of translaminar, deep and superficial layer-restricted lineages in retroviral experiments. (**E**) Relative frequency (expressed as percentage over the total number of lineages) of the different laminar configurations (green and grey schemas) in retroviral labelling experiments. (**F**) Experimental paradigm. The bottom panel illustrates the expected labelling outcome of a neurogenic RGC division following inducible MADM-based lineage tracing in which two subclones are labeled with different reporters.

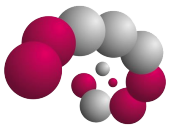

(**G-H**) Serial coronal sections through the cortex of P21 *Emx1-CreER^{T2};MADM* mice treated with tamoxifen at E12.5. The images show examples of layer IV and V restricted (G) and layer V skipping (H) lineages. The schemas collapse lineages spanning across several sections into a single diagram. (**I**) Clonal size distribution of translaminar, deep and superficial layer-restricted lineages in MADM experiments. (**J**) Relative frequency (expressed as percentage over the total number of lineages) of the different laminar configurations (green and grey schemas) in MADM experiments. n = 166 lineages in 7 animals in retrovirus experiments (D-E); 106 neurogenic lineages in 28 animals in MADM experiments (I-J). Scale bar equals 100 μm. Retrovirus experiments carried by Gabriele Ciceri.

types based on the expression of these markers and their laminar distribution (FIG 2.10): Cortico-cortical projection neurons (CCPN), subcerebral projection neurons (SCPN), cortico-thalamic projection neurons (CThPN) and heterogeneous projection neurons (HPN) (Harb et al., 2016). Using this classification, we found that nearly a quarter of all-layer translaminar lineages were composed exclusively by CCPNs, while multiple different combinations of PC identities comprise the remaining lineages (FIG 2.8H). Of note, only a minor fraction of all cortical lineages contains the entire complement of types identified. Altogether, our experiments revealed that PC lineages exhibit a great degree of heterogeneity in the number and identities they comprise.

Heterogeneous lineage configurations arise directly from neurogenesis

The observed heterogeneity in cortical lineages likely emerges during neurogenesis. However, it is possible that selective cell death of specific PCs might contribute to the heterogeneous organisation of cortical lineages. Recent studies have shown that PCs undergo apoptosis during early postnatal stages (Blanquie et al., 2017; Wong et al., 2018). To explore the contribution of cell death to the heterogeneous configuration of cortical lineages, we labeled clones by injecting a low dose of tamoxifen in *Emx1-CreER^{T2};RCE* mice at E12.5 and

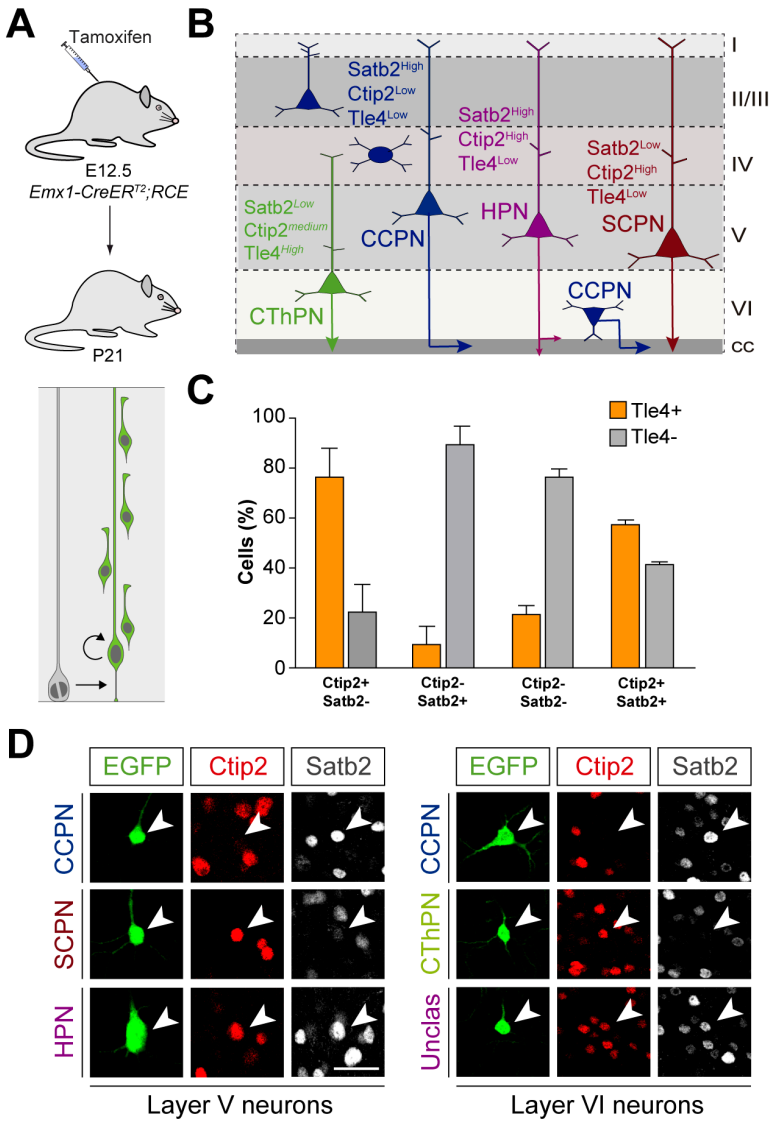

Fig. 2.10. Identification of pyramidal cell types.
(**A**) Experimental paradigm. The bottom panel illustrates the expected labelling outcome of a neurogenic RGC division following inducible conditional reporter lineage tracing in *Emx1-CreER^{T2};RCE* mice. (**B**) Schematic of PC types based on their laminar distribution and expression of specific markers. (**C**) Fraction of Tle4+ and Tle4- layer VI PCs that express the transcription factors Satb2 and Ctip2. Data are represented as mean ± standard deviation. (**D**) Pyramidal cell types in lineages traced in *Emx1-CreER^{T2};RCE* mice. Neurons are classified according to their laminar allocation and expression of Satb2 and Ctip2. n = 1123 cells in twenty slices from two brains. CCPN, cortico-cortical projection neuron; SCPN, subcortical projection neuron; HPN, heterogeneous projection neuron; CThPN, cortico-thalamic projection neuron. Scale bar equals 35 μm.

analysed their laminar organisation at P2, prior to the period of PC death (Wong et al., 2018). We detected no significant differences in the average clonal size or

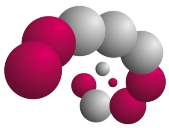

in the relative frequency of P2 translaminar and laminar-restricted lineages compared to P21 (FIG 2.11A-D). In addition, we observed that the diversity of lineage patterns was remarkably similar between P2 and P21 (FIG 2.11E). We also noted a tendency (χ^2 test, $p = 0.099$) for the fraction of lineages with PCs in every layer to be larger and the frequency of lineages lacking PCs in layer 5 to be smaller at P2 compared to P21 (FIG 2.11E). These experiments suggested that although cell death may have a subtle impact in refining the final diversity of lineages and their relative proportion, such heterogeneity should arise directly during the process of cortical neurogenesis.

Laminar densities do not predict lineage structure

The variability in size and composition of PC lineages raises questions about the developmental mechanisms underlying their genesis. We first asked whether lineage structure is relevant for cortical cytoarchitectural development. It is formally possible that the diversity in laminar composition of cortical lineages is simply the consequence of a random process of PC generation in which the only boundary condition is the relative number of PCs that populate each layer of the cortex. To test this, we used the lineages mapped in the primary somatosensory cortex (S1) of *Emx1-CreER^{T2};RCE* mice, which are meant to collectively generate a common pattern of laminar densities. We randomly permuted the PCs obtained from the different lineages while maintaining each neuron's laminar identity and the total number of cells in each lineage. If lineage structure were to exclusively affect the control of PC laminar fractions at population level, permuted lineages should be expected to match experimental data. As expected,

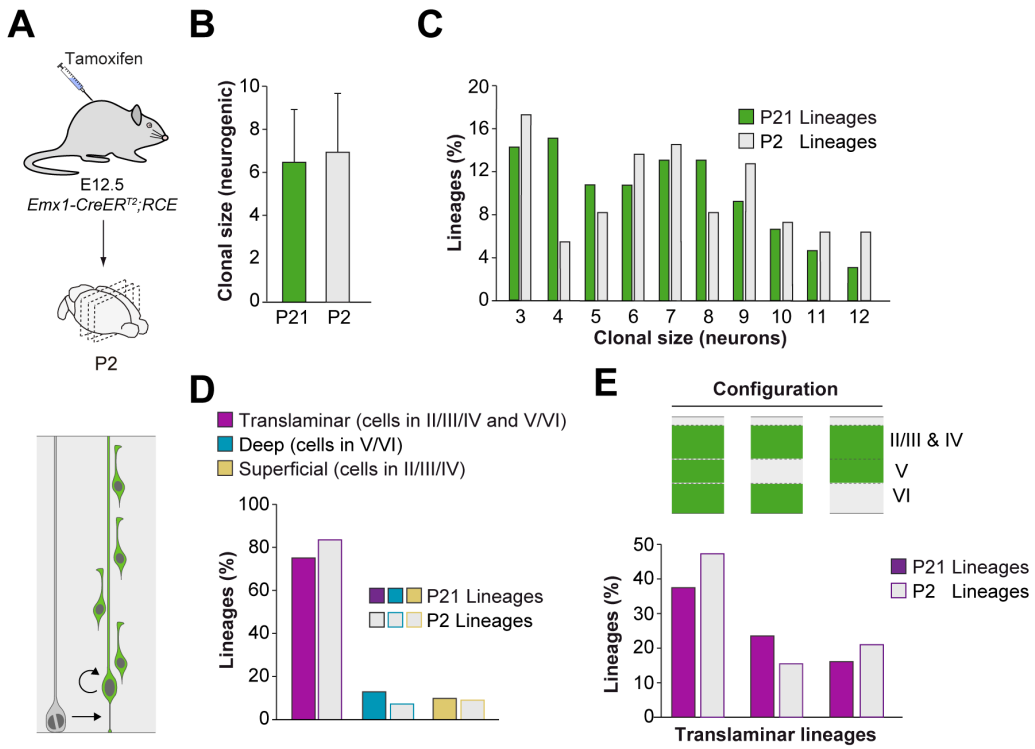

Fig. 2.11. Subtle impact of pyramidal neuron cell death in final configurations of cortical neuron lineages.
(**A**) Experimental paradigm. The bottom panel illustrates the expected labelling outcome of a neurogenic RGC division following inducible conditional reporter lineage tracing in *Emx1-CreER^{T2};RCE* mice. (**B**) Clonal size of cortical lineages at P2 and P21 following low-dose tamoxifen in *Emx1-CreER^{T2};RCE* mice at E12.5. Data are represented as mean ± standard deviation. (**C**) Clonal size distribution of cortical lineages at P2 and P21 in inducible conditional reporter lineage tracing experiments. (**D**) Quantification of the fraction of translaminar, deep and superficial layer-restricted lineages at P2 and P21 in inducible conditional reporter lineage tracing experiments. (**E**) Relative frequency (expressed as percentage over the total number of lineages) of the different laminar configurations (green and grey schemas) in inducible conditional reporter lineage tracing experiments at P2 and P21. At this age, layers II/II and IV cannot be reliably distinguished and are consequently considered as a single cortical layer. n = 110 neurogenic lineages in 11 animals at P2; n= 260 neurogenic lineages in 25 animals at P21.

the permutation process left unaltered the clonal size distribution and number of cells per layer observed in the experimental data (FIG 2.12 A,B). However, it failed to replicate the observed anti-correlation in neuron numbers between superficial and deep layers (FIG 2.12C). In addition, we observed that the laminar configuration of the permuted lineages differed from the experimental data (data not shown). These results indicated that the laminar distribution of

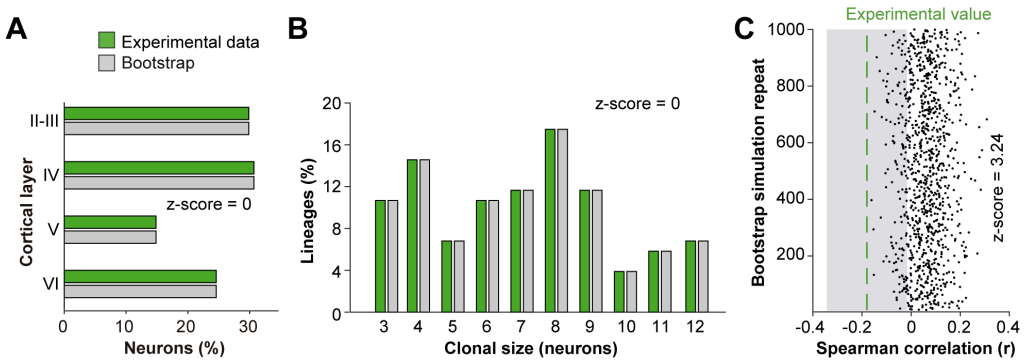

Fig. 2.12. Laminar densities of pyramidal neurons do not predict lineage structure.
(**A**) Fraction of cells in each cortical layer (expressed as percentage of total) in experimental and bootstrapped lineages. (**B**) Clonal size distribution in experimental and bootstrapped lineages. (**C**) Spearman correlation (r) values for the fraction of superficial and deep layer neurons in modeled lineages. Each dot represents an r value for one simulation. The green line shows the experimental value; the shadow area around the experimental data represents a 95% confidence interval for the experimental value. Histograms represent mean ± standard deviation. Z-scores represent the distance between experimental and simulated datasets for each parameter, which is calculated as the difference between the averages of model and experimental data divided by the standard deviation within model simulations (see methods for details). n = 103 neurogenic lineages in the somatosensory cortex of 25 animals.

neurons within each lineage arises specifically from an organised pattern of neurogenesis.

Stochastic models reproduce the diversity of progenitor outputs

One possibility to explain lineage diversity is the existence of multiple different VZ progenitor cell types with restricted potential to generate specific classes of PCs (Franco and Müller, 2013). However, the observed heterogeneity in lineage configurations may also arise from equipotent VZ progenitor cells that are subject to stochastic factors controlling their output, as proposed for the retina (He et al., 2012). To establish the feasibility of the latter scheme, we used a Bayesian approach to model the outcome of cortical progenitor cells following stochastic developmental programmes. This method involved using a set of probabilistic rules for generating lineages, and subsequently inferring the number

of rules required for the assignment of all lineages observed in the experimental data (see Methods for details). To avoid having to account for variability potentially attributable to differences in the distribution of lineages across areas of the neocortex, we only considered experimental data obtained from lineages mapped in S1 of *Emx1-CreER^{T2};RCE* mice. A total of 103 lineages was counted

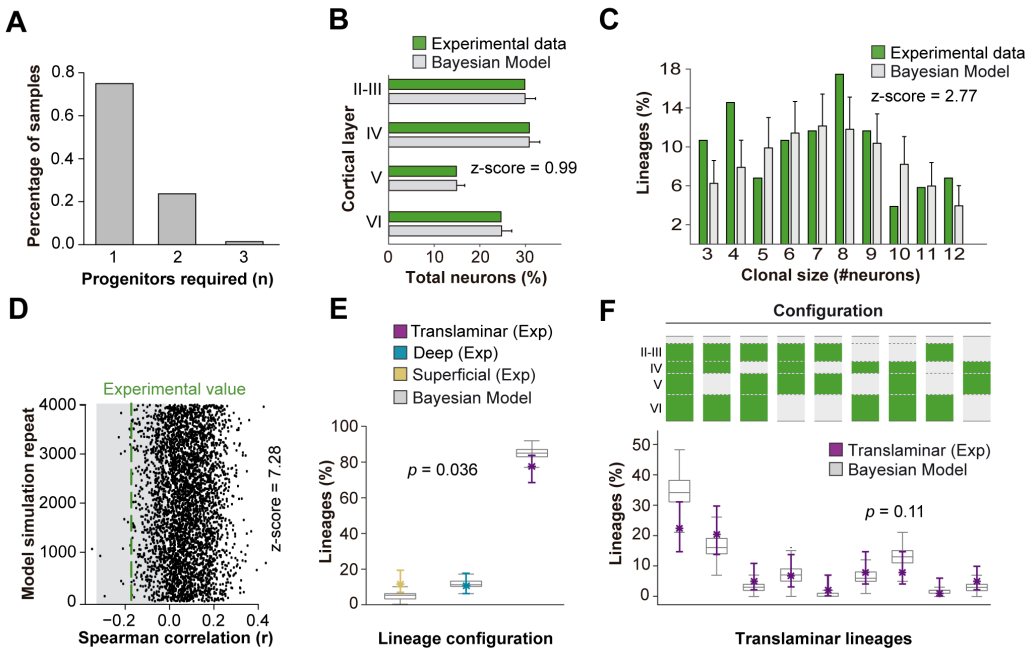

Fig 2.13. A stochastic model of cortical neurogenesis.
(**A**) Number of progenitor identities required to reproduce experimental lineage configurations inferred by Bayesian modeling. The *y* axis represents the fraction of simulations from a total of 4000 that demand a particular minimum number of progenitors. (**B**) Fraction of cells in each cortical layer (expressed as percentage of total) in experimental and modeled lineages. (**C**) Clonal size distribution in experimental and modeled lineages. (**D**) Spearman correlation (r) values for the fraction of superficial and deep layer neurons in modeled lineages. Each dot represents an r value for one simulation. The green line shows the experimental value; the shadow area around the experimental data represents a 95% confidence interval for the experimental value. (**E**) Fraction of translaminar, deep and superficial layer-restricted lineages found experimentally and predicted by the model (expressed as percentage of all modeled lineages within a single simulation). Grey boxes represent variability among 4000 simulations; colored stars and lines show experimental values and 95% confidence intervals for experimental values (p = 0.036, Chi-square test). (**F**) Relative frequency (expressed as percentage over all modeled translaminar lineages within a single simulation) of laminar configurations in experimental and modeled translaminar lineages. Grey boxes represent variability among 4000 simulations; colored stars and lines show experimental values and 95% confidence intervals for experimental values (p = 0.11, Chi-square test). Histograms represent mean ± standard deviation. Z-scores represent the distance between experimental and simulated datasets for each parameter, which is calculated as the difference between the averages of model and experimental data divided by the standard deviation within model simulations (see methods for details). n = 103 neurogenic lineages in the somatosensory cortex of 25 animals.

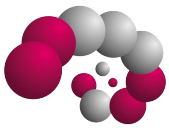

in S1. Model simulations with this number of lineages returned stable results, indicating that this number of lineages faithfully reflects population dynamics and minimises sampling effects to a reasonable extent. We reasoned that some lineage configurations observed in our experiments (such those containing cells exclusively in deep cortical layers) could derive from an early interruption of the developing lineage, reflecting an early terminal division, or a progenitor cell undergoing cell death after a few rounds of division. Since the genesis of such lineages might therefore not arise from specific developmental programmes, these configurations were also not taken into account for the inference of the stochastic rules governing this process. The Bayesian inference approach revealed that models using one or two progenitor types are sufficient to produce a diversity of lineage compositions as found in our experimental data (FIG 2.13 A,E,F). However, the approach failed to reproduce the anti-correlation in cell numbers between superficial and deep layers found experimentally (FIG 2.13D) and tended to underestimate the fractions of superficial and small lineages in our data set (FIG 2.13C,E). This suggests that while simple stochastic processes acting mostly on a single homogeneous population of VZ progenitor cells can originate a vast diversity of outcomes as observed in our experiments, some experimental observations may arise from additional developmental programmes and from features characteristic of the sequential process of neurogenesis.

A small number of progenitor identities underlies lineage diversity

Having established that the stochastic behaviour of a small number of progenitor types could in principle account for lineage diversity, we next explored

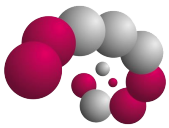

specifically how diversity can result from the sequential dynamics of stochastic neuron generation. To this end we simulated cortical progenitor behaviour using models based on four basic rules derived from experimental knowledge (FIG 2.14A and FIG 2.15A). First, in silico progenitors would generate neurons for different layers sequentially, following the observed inside-out pattern. Second, each in silico progenitor would have a set, randomly selected number of opportunities to generate neurons in each layer. Third, for any progenitor the decision to generate a neuron would be probabilistic, with cell generation probabilities varying by cortical layer but equal for all opportunities within the same layer. Thus, a progenitor type was defined by its specific combination of cell generation probabilities across layers. Fourth, to simulate the chances of premature terminal division and/or progenitor death, we introduced a probabilistic chance of lineage interruption at each opportunity for cell generation. In silico lineages generated using this model were then compared with the experimental lineages mapped in the primary somatosensory cortex (S1) of *Emx1-CreER^{T2};RCE* mice. We set cell generation probabilities in each layer to match the total laminar fractions of PCs (FIG 2.14B and FIG 2.15B), as well as the clonal size distribution (FIG 2.14C and FIG 2.15C) observed in those lineages.

In agreement with the Bayesian approach, we found that a stochastic model based on a single, equipotent VZ progenitor cell (Model 1), i.e., a single set of cell generation probabilities, was able to reproduce the majority of experimentally observed lineage features. Modelled lineages recapitulated the

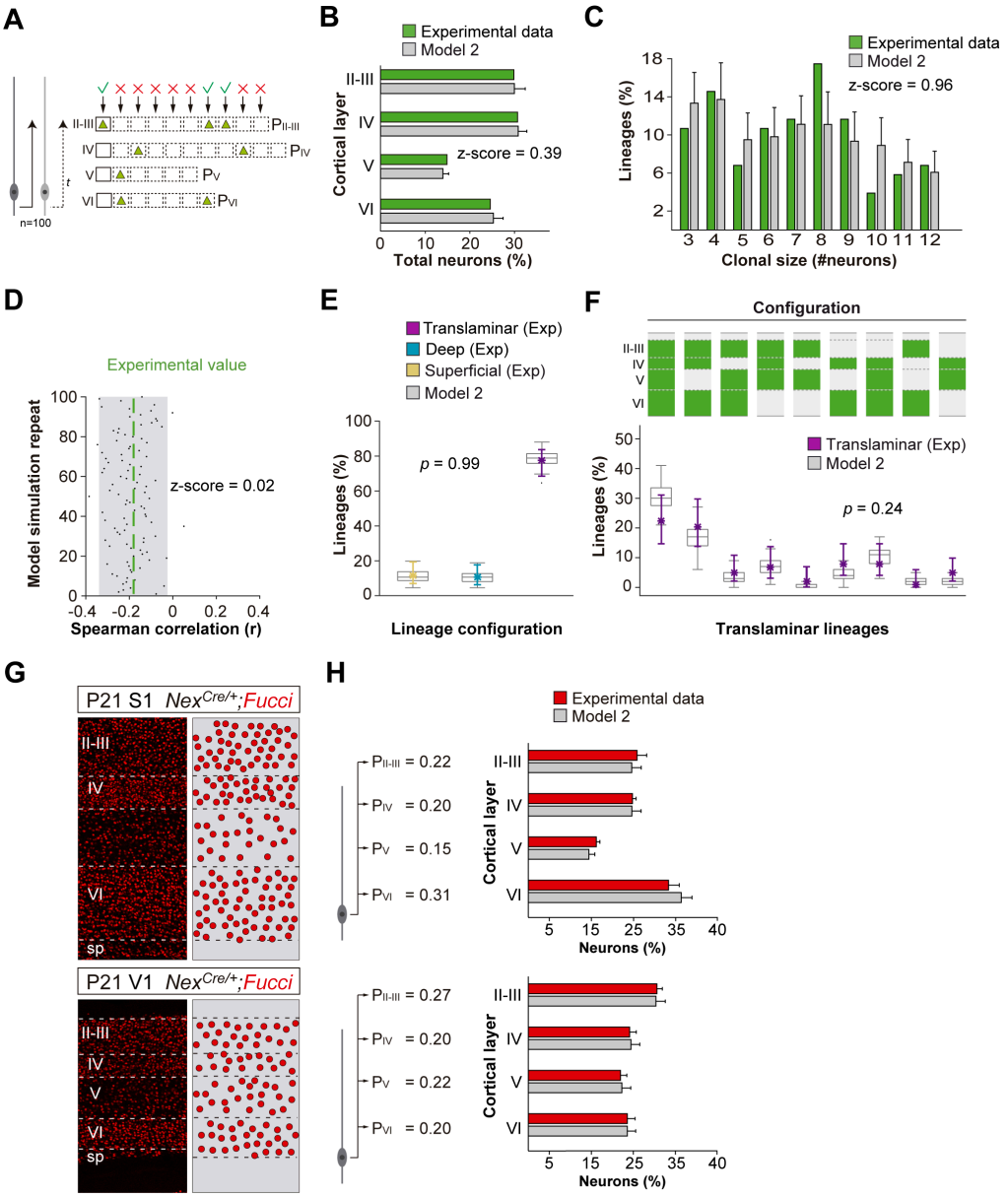

Fig 2.14. A small number of progenitor identities underlie lineage diversity.
(**A**) Schematic representation of a mathematical model of cortical neurogenesis in which two different progenitor identities are modeled (Model 2). Squares represent the maximum number of stochastic decisions performed by each progenitor for each cortical layer during *in silico* simulations. The odds of generating neurons for each chance are given by a probability value (P), which is unique for each layer and progenitor identity. The model runs 100 simulations with 100 progenitors. (**B**) Fraction of cells in each cortical layer (expressed as percentage of total) in experimental and modeled lineages. (**C**) Clonal size distribution in experimental and modeled lineages. (**D**) Spearman correlation (r) values for the fraction of superficial and deep layer neurons in modeled lineages. Each dot represents an r value for one simulation. The green line shows the experimental value; the shadow area around the experimental data represents a 95% confidence interval for the experimental value. (**E**) Fraction of translaminar, deep and superficial layer-restricted lineages found experimentally and predicted by the model (expressed as percentage of all modeled lineages within a single simulation). Grey boxes represent variability among 100 simulations; colored stars and lines show experimental values and 95% confidence intervals for experimental values (p = 0.99, Fisher's exact test).

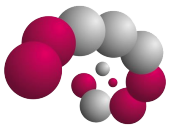

(**F**) Relative frequency (expressed as percentage over all modeled translaminar lineages within a single simulation) of laminar configurations in experimental and modeled translaminar lineages. Grey boxes represent variability among 100 simulations; colored stars and lines show experimental values and 95% confidence intervals for experimental values (p = 0.24, Chi-square test). (**G**) Coronal sections through the primary somatosensory (S1) and visual (V1) cortex of P21 NexCre/+;Fucci mice. The schemas on the right illustrate PC densities per layer. (**H**) Fraction of PCs per layer (expressed as percentage of total neurons) generated with two sets of laminar probability factors using Model 2 compared to the experimental data. Histograms represent mean ± standard deviation. Z-scores represent the distance between experimental and simulated datasets for each parameter, which is calculated as the difference between the averages of model and experimental data divided by the standard deviation within model simulations (see methods for details). n = 103 neurogenic lineages in the somatosensory cortex of 25 animals.

existence of restricted lineages as well as all observed laminar configurations of translaminar lineages (FIG 2.15E-F). However, this model generated lineages with an exaggerated anti-correlation in the number of cells in superficial versus deep layers (FIG 2.15D) and failed to reproduce the bimodal distribution of clonal sizes, underestimating the fraction of small lineages (those containing 3-4 cells). In addition, the fraction of lineages restricted to superficial layers, which largely contributes to the small lineage sizes, was also underestimated (FIG 2.15C,E). These results suggeste that the fraction of small superficial lineages is unlikely to arise from a single stochastic program common to all cortical progenitors.

We then generated a second model with two different sets of cell generation probabilities, defining two different progenitor populations (Model 2). In this model, the majority of progenitors belonged to a population generating the larger lineages, while a second, smaller population generated small progenies biased towards superficial layer PC fates (FIG 2.14A). We found that this model faithfully reproduced all the experimental features in our data: total laminar fractions (FIG 2.14B), bimodal distribution of clonal sizes (FIG 2.14C) and

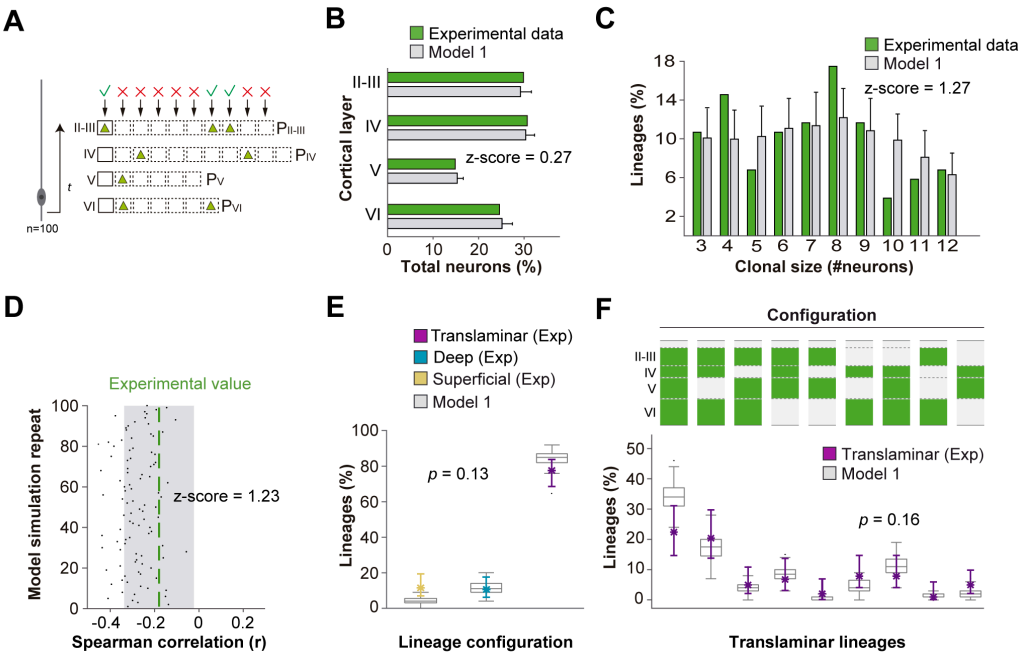

Fig. 2.15. Stochastic models considering single and multiple programmes corroborate Bayesian inference.

(**A**) Schematic representation of a mathematical model of cortical neurogenesis in which a unique progenitor identity is modeled (Model 1). Squares represent the maximum number of stochastic decisions performed by each progenitor for each cortical layer during *in silico* simulations. The odds of generating neurons for each chance are given by a probability value (P), which is unique for each layer and progenitor identity. The model runs 100 simulations with 100 progenitors. (**B**) Fraction of cells in each cortical layer (expressed as percentage of total) in experimental and modeled lineages. (**C**) Clonal size distribution in experimental and modeled lineages. (**D**) Spearman correlation (r) values for the fraction of superficial and deep layer neurons in modeled lineages. Each dot represents an r value for one simulation. The green line shows the experimental value; the shadow area around the experimental data represents a 95% confidence interval for the experimental value. (**E**) Fraction of translaminar, deep and superficial layer-restricted lineages found experimentally and predicted by the model (expressed as percentage of all modeled lineages within a single simulation). Grey boxes represent variability among 100 simulations; colored stars and lines show experimental values and 95% confidence intervals for experimental values (p = 0.13, Fisher's exact test). (**F**) Relative frequency (expressed as percentage over all modeled translaminar lineages within a single simulation) of laminar configurations in experimental and modeled translaminar lineages. Grey boxes represent variability among 100 simulations; colored stars and lines show experimental values and 95% confidence intervals for experimental values (p = 0.16, Chi-square test). Histograms represent mean ± standard deviation. Z-scores represent the distance between experimental and simulated datasets for each parameter, which is calculated as the difference between the averages of model and experimental data divided by the standard deviation within model simulations (see methods for details). n = 103 neurogenic lineages in the somatosensory cortex of 25 animals.

negative correlation in superficial versus deep layers (FIG 2.14D). In addition, the relative proportions of translaminar and laminar-restricted lineages were identical to those measured experimentally (FIG 2.14E). Finally, translaminar

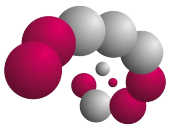

modeled lineages exhibited similar laminar configurations to the experimental lineages (FIG 2.14F). In sum, mathematical modelling suggests that a stochastic mechanism of cortical neurogenesis based on two independent progenitor cell populations best approximates the experimental data.

Finally, we explored whether the proposed stochastic model with two progenitor populations (Model 2) would be able to generate different ratios of layer-specific neurons under different circumstances (i.e., different cell generation probabilities), which would robustly account for the emergence of cytoarchitectonic differences across neocortical areas. To this end, we quantified the fraction of PCs in each layer of the primary somatosensory (S1) and visual (V1) cortices in *Nex-Cre;Fucci2* mice, in which all PCs in the neocortex are labeled with a nuclear fluorescent marker. As expected, we found marked differences in laminar cytoarchitecture between both regions (FIG 2.14G). Most importantly, layer IV and VI where relatively more dense in S1, while layer II/III was enlarged in V1. Remarkably, we found that subtle tuning of generation probabilities for both areas was sufficient to replicate the different laminar ratios *in silico* (FIG 2.14H). This suggests the stochastic mechanisms of neurogenesis described here would suffice to generate the diverse patterns of cytoarchitecture observed across neocortical areas.

3. DISCUSSION

Our results indicate that the output of individual progenitor cells in the developing mouse neocortex is much more heterogeneous than previously

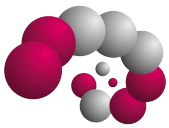

anticipated. Progenitor cells most frequently generate PCs for both deep and superficial layers of the neocortex, as suggested by previous studies. However, a sizeable fraction of those lineages lacks PCs in one or several layers. In addition, the heterogeneous output of cortical progenitor cells includes lineages in which PCs are restricted to either deep or superficial layers. Mathematical modelling suggests that this wide diversity of outputs is compatible with a stochastic model of cortical neurogenesis. Such model represents a robust and adaptable mechanism for the assembly of different neocortical cytoarchitectures.

Methodological considerations

Understanding how individual lineages contribute to the production and organisation of PCs is essential to articulate a coherent framework of cortical development. The analysis of the output of progenitor cells in the developing rodent cortex expands over three decades and has relied on four approaches: retroviral labelling (Luskin et al., 1988; Noctor et al., 2004; 2001; Price and Thurlow, 1998; Reid et al., 1995; Walsh and Cepko, 1995), mouse chimeras (Tan et al., 1998), MADM (Beattie et al., 2017; Gao et al., 2014) and genetic fate-mapping (Eckler et al., 2015; Franco et al., 2012; García-Moreno and Molnár, 2015; Guo et al., 2013; Kaplan et al., 2017). These studies often led to contradictory results, which has prevented the emergence of a consistent model. The prevalent view is that each progenitor cell in the developing pallium is multipotent and generates a cohort of PCs that populate all layers of the neocortex except layer I (Eckler et al., 2015; Gao et al., 2014; Guo et al., 2013; Kaplan et al., 2017), as originally conceived in the radial unit hypothesis (Rakic,

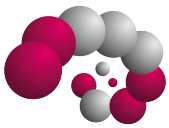

1988). In contrast, some authors have suggested that many cortical progenitor cells are fate-restricted to generate PCs that exclusively occupy deep or superficial layers of the neocortex (Franco et al., 2012; Franco and Müller, 2013; Gil-Sanz et al., 2015). Here, we have used three different methods (retroviral labelling, MADM and genetic fate-mapping) to investigate the clonal production of cortical neurons by capitalising on the synergy that emerges from the advantages of each individual approach. Our results indicate that this multi-modal approach is required to comprehensively capture the complex behaviour of progenitor cells in the developing cortex.

Retroviral labelling has two important limitations: it only labels hemi-lineages and is prone to silencing, which may prevent the identification of the entire progeny of a progenitor cell (Cepko et al., 2000). Conversely, retroviral labelling targets progenitor cells indiscriminately and, consequently, is not biased towards a particular genetic fate (Cepko et al., 2000), as is the case for genetic strategies. MADM, on the other hand, has the enormous advantage of identifying both sister cells resulting from a cell division. However, G2-X MADM events require progenitor cells to undergo cell division at the time of induction because it directly relies on Cre-dependent inter-chromosomal mitotic recombination (Zong et al., 2005). Our results revealed that MADM does not reliably label a small fraction of progenitor cells present in the pallial VZ at E12.5 that gives rise to cohorts of PCs exclusively located in superficial layers of the neocortex. These lineages were however observed in both retroviral labelling experiments and in genetic tracing experiments using the same genetic driver (*Emx1-CreER*^{T2}) as in

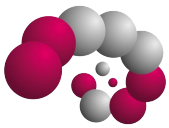

the MADM experiments, which strongly suggests that some Emx1+ progenitor cells producing exclusively superficial layer PCs in the developing cortex are not targeted by the MADM approach. We hypothesise that these progenitors might be quiescent or slow-dividing progenitors at this stage and become more active at later stages of development. Finally, although the use of genetic fate-mapping strategies (e.g., *Emx1-CreER^{T2};RCE*) is a powerful method to investigate cortical lineages, it has the important constraint of not being able to distinguish between symmetric proliferating and asymmetric neurogenic divisions. This hampers the analysis of clonal sizes, which can be otherwise accurately assessed with MADM except for the lineages that are not detected with this method.

Diversity of neocortical lineages

Previous clonal analysis based on MADM lineage tracing experiments led to the suggestion that individual progenitor cells in the pallial VZ produce a unitary output of approximately 8 excitatory neocortical neurons (Gao et al., 2014). However, since those studies failed to identify lineages with restricted laminar patterns (either deep or superficial layer restricted clones), they underestimated the fraction of lineages with relatively small clonal size. In contrast, our analysis of neurogenic lineages revealed a bimodal distribution of clonal sizes with defined peaks centered at approximately 4 and 8 cells, which largely corresponds to the contribution of laminar-restricted and translaminar lineages, respectively.

Previous studies have suggested that some neocortical progenitor cells generate laminar-restricted lineages of PCs (Franco et al., 2012; Gil-Sanz et al., 2015). In our experiments, approximately one in six cortical progenitor cells

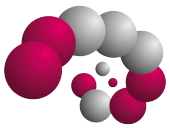

generate laminar-restricted lineages. The existence of lineages restricted to deep layers of the neocortex was observed with all three methods used in this study. Although some variation exists in the relative fraction of deep layer-restricted lineages observed with the different approaches, these differences lie within the expected experimental noise considering the relatively small number of lineages that belong to this category. In addition, both retroviral labelling and genetic fate-mapping experiments identified a fraction of cortical progenitor cells that generate PCs that exclusively populate the superficial layers of the neocortex. The discrepancy between the results of genetic fate-mapping and MADM experiments, in which the same mouse strain is used as the driver for recombination (*Emx1-CreER*^{T2}), suggests that these fate-restricted lineages arise from progenitor cells that are not actively dividing at E12.5. This hypothesis is consistent with the identification of a population of self-renewing progenitors with limited neurogenic potential during the earliest phases of corticogenesis (García-Moreno and Molnár, 2015). The existence of superficial layer-restricted cortical lineages is further supported by the identification of IPCs as early as E12.5 that generate superficial layer PCs (this study and Mihalas et al., 2016), when the majority of deep layer PCs are being generated. Since IPCs derive from VZ progenitor cells (Haubensak et al., 2004; Miyata, 2004; Noctor et al., 2004) and cortical neurogenesis begins at these stages in the mouse, this observation reinforces the idea that some progenitors are tuned to generate superficial layer PCs from early stages of corticogenesis.

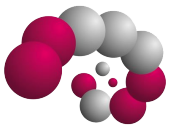

Our study also revealed that, independently of the laminar distribution, individual cortical progenitor cells generate lineages with very diverse combinations of PC types. Cortical progenitors are thought to undergo progressive changes in their competency to generate different layer-specific types of PCs (Desai and McConnell, 2000; Rakic, 1974). Consistent with this idea, our results reveal that most cortical progenitors generate diverse types of excitatory neurons. However, since many cortical progenitor cells fail to generate neurons for at least one layer of the neocortex, the majority of cortical lineages does not include the entire diversity of excitatory neurons. In other words, the fraction of individual cortical lineages that would be considered as "canonical" – i.e., containing all three main types of excitatory projection neurons (CCPN, SCPN and CThPN) – is significantly smaller than previously anticipated. Considering the variance in clonal size and lineage composition of neocortical lineages, our results indicate that cortical progenitor cells exhibit very heterogeneous patterns of neuronal generation and specification.

A stochastic model of cortical neurogenesis

Our results indicate that stochastic developmental programmes, in which cortical progenitors undergo a series of probability-based decisions for the generation of the different PC fates, are capable of generating the wide diversity of lineage configurations observed in our experiments. Therefore, in spite of the great diversity of configurations that exist among individual neocortical lineages, our results suggest that their genesis does not require a corresponding heterogeneity in VZ progenitors. The model proposed here is somewhat reminiscent of that

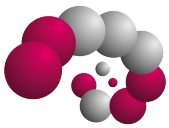

described for the developing rodent and zebrafish retina (Gomes et al., 2010; He et al., 2012). In line with our findings, stochastic mechanisms based on a single set of probability rules explain the genesis of most, but not all neuronal types in the mammalian retina (Gomes et al., 2010).

It is presently unclear whether laminar-restricted lineages arise from a pool of progenitor cells separate from those generating translaminar lineages or should simply be considered as extreme examples of the enormous diversity of lineage configurations uncovered by our study. The generation of lineages restricted to deep layers might be due to premature terminal division or death of the progenitor cell (Blaschke et al., 1996; Mihalas and Hevner, 2018), as considered in our models, but the existence of superficial layer-restricted lineages is more difficult to explain. Moreover, our mathematical model best reproduces the complex cytoarchitecture of the neocortex when two distinct progenitor cell identities are considered. Previous studies have identified morphological heterogeneity among pallial VZ progenitor cells (Gal, et al. 2006). However, there is limited evidence for important molecular differences among these cells (Mizutani et al., 2007; Pollen et al., 2014; Telley et al., 2016). In the absence of a definitive molecular signature, our results suggest that while a homogeneous population of progenitor cells following a common developmental program explains most of the observed outcomes, it fails to generate the fraction of small superficial lineages observed in the experimental dataset. The introduction of a second population of progenitor cells is required to reproduce these lineages. Although these findings might suggest the existence of a small

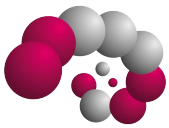

fraction of cortical progenitors tuned to preferentially generate superficial lineages, it should not be taken as a definitive proof of fate-restriction in cortical progenitors. In our model, replicating the experimental data does not require such progenitors to be restricted, but simply biased towards generating superficial fates.

Our study suggests that progenitor cells in different cortical areas are likely constrained by different probabilistic rules, which would contribute to the generation of the diverse cytoarchitectonic patterns found across the neocortex. How and when stochastic neurogenic decisions are made remains to be elucidated, but they likely depend on the influence of extrinsic and intrinsic signals on parameters such as cell cycle length, the asymmetric inheritance of cell components, the generation of dividing (IPCs) versus postmitotic progeny, and the membrane potential of progenitor cells (Haydar et al., 2003; Lange et al., 2009; Pilaz et al., 2009; Roccio et al., 2013; Vitali et al., 2018; Wang et al., 2009). Local signals in different neocortical areas would contribute to the tuning of progenitor cell behaviours to output different cytoarchitectures without the requirement of regional-specific progenitor populations. Consequently, this model allows great flexibility in the generation of heterogeneous cortical cytoarchitectures without the requirement of a large number of progenitor identities. The specification of a very small number of progenitor cells with competence to adapt their neurogenic behaviour to different probabilistic rules based on their location within the neocortical neuroepithelium represents the most parsimonious and robust mechanism for the generation of cortical circuitry.

RESULTS

CHAPTER II:

Mapping the origins of cortical interneuron diversity

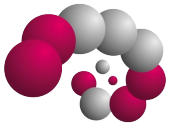

SUMMARY

The diverse types of inhibitory interneurons that populate the cerebral cortex originate in several regions of the embryonic subpallium. In these structures, progenitor cells divide intensely to generate postmitotic interneurons. Importantly, the mitotic behaviour of these progenitor cells, and their individual contribution to cortical neurogenesis remains largely unknown. Here, we investigated the mode of division of interneuron precursors in the MGE. Our results indicate that these progenitor cells generate remarkably complex lineages, undergoing several rounds of expansive divisions before generating postmitotic neurons. Also, we designed and tested a novel high-resolution labelling method for the faithful tracing of individual MGE progenitor outputs. This method eludes the caveats and limitations of previous high-resolution lineage tracing strategies, representing a useful tool for the future understanding of interneuron development.

1. INTRODUCTION

The mammalian cerebral cortex contains several types of inhibitory GABAergic INs that interconnect among themselves and with nearby PCs to form complex neuronal circuits. INs have their origin in multiple regions of the embryonic subpallium, from where they migrate long distances to reach their final position in the cerebral cortex (Anderson et al., 1997; De Carlos et al., 1996; Tamamaki et al., 1997). Despite decades of intense study, our current understanding of the developmental logic behind the generation of IN cell diversity remains

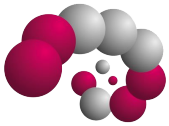

incomplete. For instance, the neurogenic behaviour of IN progenitor cells and their individual contribution to cortical neurogenesis have not yet been characterised in detail, in sharp contrast to the corresponding processes in the pallium.

Recent studies indicate that progenitor cells located in the MGE, the region of origin for PV and SST INs, are multipotent and often produce heterogeneous progenies containing different types of INs from both classes (Brown et al., 2011; Ciceri et al., 2013; Harwell et al., 2015; Mayer et al., 2015). However, the cellular and molecular mechanisms leading to the generation of these heterogeneous progenies remain largely unknown. In addition, whether IN progenies are instructed to migrate to specific cortical niches or disperse widely across different cortical territories remains a matter of intense debate (Garcia et al., 2016; Mayer et al., 2016; Sultan et al., 2016).

Two main reasons account for our limited understanding of the mechanisms regulating IN generation. First, the cell biology of IN generation has not been extensively studied. For example, it is currently unknown whether IN genesis follows highly stereotyped and organised patterns comparable to those governing PC birth in the cortex, or whether progenitor cells generating INs divide more promiscuously than in the cortex, generating complex ramified lineages as described in the LGE (Pilz et al., 2013). This uncertainty severely limits our understanding of the origin of IN diversity, since it complicates the interpretation of the neuronal output of subpallial progenitors. Second, the characterisation of single cell lineages, which has been crucial to discern the

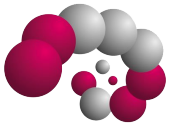

principles underlying the development of other brain structures (A Schmid, 1999; Bossing et al., 1996; Gao et al., 2013; Walsh and Cepko, 1995), has been particularly challenging for cortical INs. The enormous spatial dispersion of these cells precludes the use of many classical lineage-tracing technologies, typically based in spatial relationships, for their study. Instead, it demands the use of high-resolution methods for the unequivocal identification of lineage relationships.

Several high-resolution cell labelling strategies have been developed over the past decades for the analysis of neuronal progenies (Buckingham and Meilhac, 2011; Kretzschmar and Watt, 2012), largely based on two main principles, multicolour labelling and barcoding. Combinatorial multicolour labelling strategies are based on the simultaneous use of multiple fluorescent reporters in target cells. To achieve maximum resolution, most of these methods introduce multiple copies of the reporters into traced cells. Cells labelled this way are then meant to express a unique RGB-like colour tag, in which the number of copies of each reporter can be inferred from the fluorescent intensity in a particular wavelength. A number of approaches have been designed following this principle, using mouse genetics (Cai et al., 2013; Livet et al., 2007; Loulier et al., 2014; Snippert et al., 2010), viral vectors (Cai et al., 2013) or *in utero* electroporation (Garcia-Moreno et al., 2014; García-Marqués and López-Mascaraque, 2012; Loulier et al., 2014) to achieve the expression of reporter alleles in the desired cell populations. Although these methods have been postulated for the faithful identification of individual cells, they are not

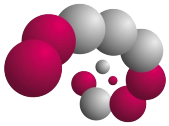

exempt of difficulties that preclude their use as trustable lineage-tracing strategies. Most importantly, the assumption of a linear relationship between fluorescent intensity and cell genomic content is extremely dangerous. Multiple factors modulate gene expression in a living cell, potentially leading to different expression profiles in cells with identical genetic content. Consequently, this could cause misinterpretations of lineage relationships among labelled cells, and therefore, question the use of these methods for such purposes.

Genetic barcoding strategies, on the other hand, are used to tag target cells with a unique genomic sequence, which is later utilised for their identification. These approaches use large genomic libraries containing an enormous amount of unique genetic sequences for the unequivocal reconstruction of lineage relationships among traced cells (Golden et al., 1995; McCarthy et al., 2001). Individual genetic tags, randomly selected from the entire library, are delivered into progenitor cells typically via low titer viral infections, so that the entire group of neurons derived from each targeted progenitor cell would inherit, and thus share, a common genetic tag distinctive of their lineage origin. Despite their extremely high resolution, these approaches have several technical caveats. Viral genomes are frequently silenced in mammalian cells (Cepko et al., 2000; Halliday and Cepko, 1992; McCarthy et al., 2001), potentially preventing the reconstruction of entire lineages. Moreover, genetic barcoding requires the recovery and analysis of the genomic content of targeted cells for the identification of lineage relationships, a remarkably inefficient process (Harwell et al., 2015; Mayer et al., 2015). In fact, most studies only manage to recover the

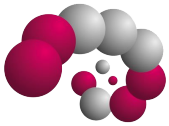

genome of a very small fraction of labelled cells, consequently leading to the reconstruction of incomplete lineages. These limitations have prevented a better understanding about the contribution of individual subpallial progenitors to the genesis of the cerebral cortex, reinforcing the need for novel lineage-tracing systems that ensure the faithful reconstruction of complete cell lineages.

In this study, we have characterised the mitotic patterns underlying the genesis of INs in the MGE. In addition, we have designed and tested a high-resolution lineage tracing system that avoids the caveats of previous strategies. This tool represents a novel powerful approach for the study of IN development.

2. RESULTS

Progenitor cell diversity in the MGE

The existence of different types of progenitor cells in the different subpallial sources that give rise to cortical INs, and their preferred division patterns, remain to be investigated. We focused on the MGE, a major source of cortical INs, to study the cellular logic of cortical IN generation. To test the existence of different morphotypes of progenitor cells in this structure, we performed short-term fate-mapping experiments using mouse genetics. To this end, we injected low doses of tamoxifen in *Nkx2-1-CreER^{T2};Ai9* pregnant females, which led to the sparse labelling of progenitor cells and early postmitotic INs in the embryonic MGE and POA. We performed tamoxifen injection at E11.5 to map progenitor cells during early neurogenic stages. Embryonic tissue was recovered for fixation 24 h later. In these experiments, immunostaining of Ki67 protein, a marker of cycling

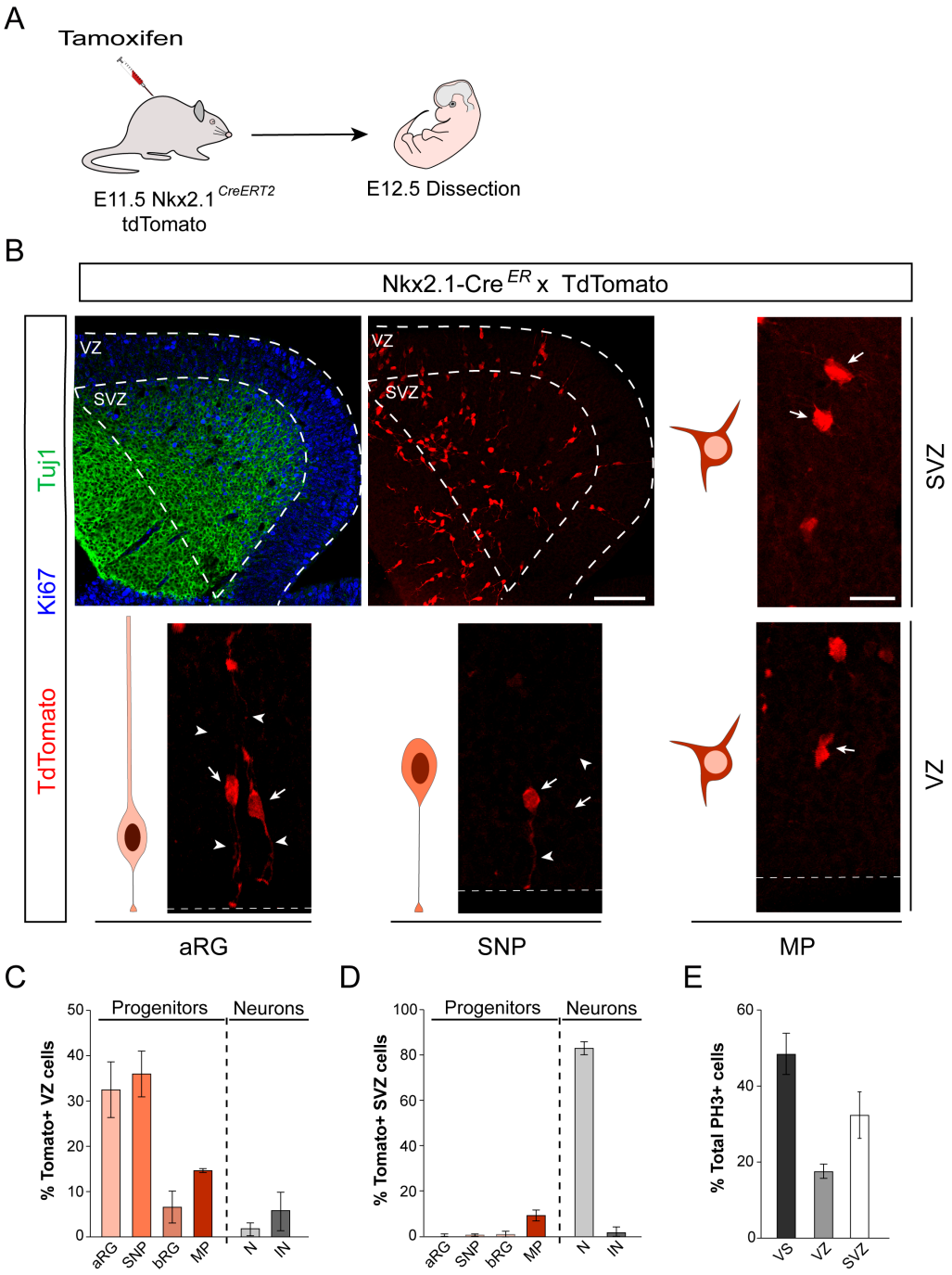

Figure 3.1. Progenitor cell diversity in the embryonic subpallium

(**A**) Experimental paradigm. (**B**) Coronal section of embryonic mouse MGE. *Top left*: Low magnification images of MGE germinal layers and the distribution of tdTomato+ cells among them. *Top right*: Schematics and example images of multipolar SVZ progenitor cells. *Bottom*: Schematics and example images of aRG, SNP and multipolar VZ progenitor cells. (**C**) Percentage of VZ cells identified as neurons or classified as the different morphotypes of progenitor cells. Data expressed as mean ± std. (**D**) Percentage of SVZ cells identified as neurons or classified as the different morphotypes of progenitor cells. Data expressed as mean ± std. (**E**) Percentage of PH3+ mitotic cells at the different germinal layers of the MGE. Data expressed as mean ± std. MGE, medial ganglionic eminence. VS, ventricular surface. VZ, ventricular zone. SVZ, subventricular zone. aRG, apical radial glia. SNP, short neural precursor. bRG, basal radial glia. MP, multipolar precursor. n = 4 brains (171 VZ and 264 SVZ progenitor cells). Scale bars 100µm and 25µm.

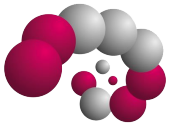

cells, was used to identify progenitor cells. The expression of tdTomato was used for their morphological classification into four different morphotypes, defined by the presence or absence of apical and/or basal processes (FIG 3.1A,B).

We observed that the population of apical progenitor cells located in the VZ exhibits several distinct morphologies, similarly to previous results in the LGE (Pilz et al., 2013). Remarkably, a large fraction of apical progenitors lacks basal processes and has the morphology described for SNPs in the developing cortex (FIG 3.1C). In contrast, basal progenitors in the SVZ were found to be mainly multipolar (FIG 3.1D). Finally, we also observed mitotic activity (i.e., cells labelled with a mitotic marker such phosphohistone-H3, PH3) in many VZ cells away from the apical surface (FIG 3.1E), corroborating previous results (Pilz et al., 2013). Taken together, our results indicate that progenitor cells in the MGE exhibit similar morphologies to those described in the LGE.

Mode of division of IN progenitor cells

To investigate the mode of division of MGE/POA progenitor cells, we performed short-term clonal labelling experiments in Nkx2-1 lineages using MADM (FIG 3.2 A). To this end, we induced MADM labelling at early neurogenic stages (E12.5, and E13.5) using single tamoxifen injections in *Nkx2-1-CreER^{T2};MADM* pregnant females, and recovered embryonic brains for fixation 24h later. We did not observe differences in the structure and size of MGE/POA lineages between these two ages (FIG 3.2 B), so both datasets were analysed together.

We focused on G2-X MADM segregation events, which result from the labelling of both daughter cells with different reporters (FIG 3.2C). We observed

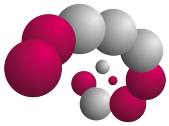

that the clonal size of these lineages was surprisingly large (FIG 3.2 B), with over 6 cells per lineage on average. This finding revealed that subpallial progenitors tend to divide quickly, generating relatively large interneuron clones within 24h. Clonal sizes of G2-X lineages ranged between 2 and 13 cells, which indicate that some MGE/POA progenitor cells may divide up to three times during that period. Consistently, both G2-X and G2-Z sub-lineages (defined as only one colour of the G2-X lineages and the complete G2-Z lineages) exhibit a wide range of different clonal sizes, with an average value of around 3 cells (FIG 3.2 B).

We classified the lineages in two main types: (i) sustained lineages contain at least one apical progenitor 24h after labelling, and therefore likely derive from a self-renewing stem cell. (ii) Exhausted lineages, lack a self-renewing apical progenitor cell, and exclusively contain neurons, multipolar IPCs, or a mixture of both, and likely represent the progeny of IPCs. These two lineage types were observed with similar frequencies (13/25 sustained, 12/25 exhausted) (FIG 3.2 D), which suggested that similar numbers of self-renewing and IPCs are present in the MGE. Surprisingly, we observed that the vast majority of exhausted lineages (75%, 9/12 lineages) contain more than 2 cells (FIG 3.2 E), and most of the present clonal sizes of four or more cells (FIG 3.2 F). This suggests that the mitotic behaviour of IPCs in the subpallium is remarkably different than in the pallium.

To test whether IPCs directly derived from self-renewing apical progenitors also exhibit this expansive behaviour, we then analysed the composition of

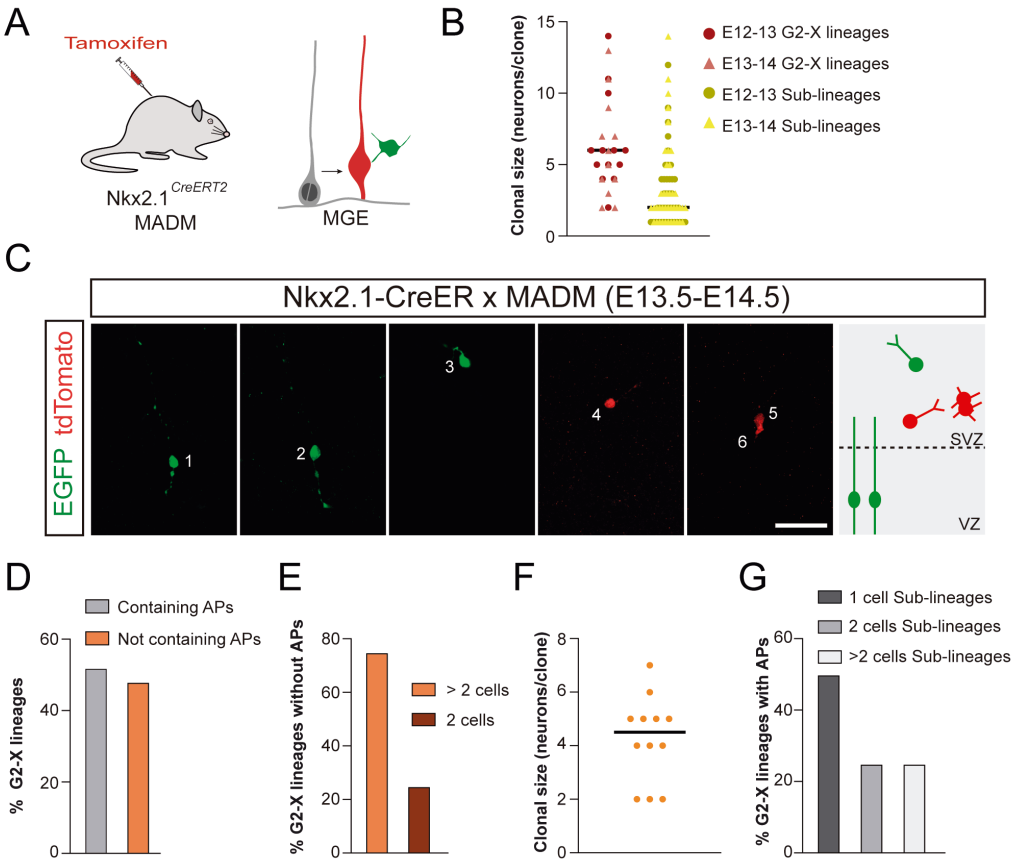

Figure 3.2. MGE progenitor cells generate complex expansive lineages
(**A**) Experimental paradigm. (**B**) Clonal size distribution (# neurons per lineage) of MGE/POA MADM labelled lineages and sub-lineages. Horizontal lines indicate median values. (**C**) Serial coronal sections of E14.5 Nkx2-1-CreERT2;MADM mice treated with tamoxifen at E13.5. The images show a example of a sustained lineage with an expansive red sub-lineage. (**D**) Percentage of G2-X lineages containing/not containing APs. (**E**) Percentage of G2-X exhausted lineages containing two or more cells. (**F**) Clobal size distribution (neurons per lineage) of exhausted lineages. Horizontal line indicates median value. (**G**) Percentage of G2-X sustained lineages with 1-cell, 2-cells or more than two cells sub-lineages. MGE, medial ganglionic eminence. AP, apical progenitor. SVZ, subventricular zone. VZ, ventricular zone. N = 25 lineages in 10 brains. Scale bar 25µm.

sustained lineages. In these lineages, the sub-lineage containing the apical progenitor cell would reflect the activity of this cell following the targeted division. Conversely, the other sub-lineage would reflect the progeny generated during the initial division that triggered the MADM labelling. Therefore, the study of the later sub-lineages can provide essential information about the mitotic patterns of apical progenitors and their immediate progenies. Intriguingly, only 25% (3/12) of total sustained lineages contained this type of sub-lineages with

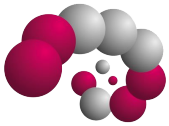

more than two cells (FIG 3.2 G). In contrast, half (6/12) of the observed sustained lineages only contained a single cell in these sub-lineages, indicating the generation of a neuron through direct neurogenesis (FIG 3.2 G). The remaining 25% of sustained lineages contained two cells in the sub-lineage lacking the apical progenitor (3/12) (FIG 3.2 G). Thus, although a large fraction (~ 75%) of MADM-targeted putative IPCs seem to generate large groups of cells, only half of the IPCs derived from self-renewing apical progenitor cells seem to follow this trend. Two alternative hypotheses may help to explain this apparent contradiction. First, lateral sub-lineages containing two cells may correspond to expansive sub-lineages composed by IPCs that only divided once within 24h, but would continue to divide in the future. In line with this idea, all two-cell sub-lineages were composed by cells with multipolar morphologies, possibly corresponding to classic SVZ IPCs. Second, a fraction of exhausted lineages may originate from a population of mitotically restricted IPCs that does not derive from self-renewing apical progenitors.

SVZ expansion of MGE lineages

The results of our clonal analysis suggest the existence of a population of IPCs that divide multiple times, thereby expanding nascent IN lineages. Whether these expansive IPCs reside in the VZ or the SVZ, however, remains unknown. To study the progression of MGE lineages in the different germinal layers, we used the FlashTag method (Govindan et al., 2018). FlashTag (FT) is based on the use of a fluorescent dye (carboxyfluorescein diacetate succinimidyl ester) that remains colourless in the extracellular space, and only becomes fluorescent after

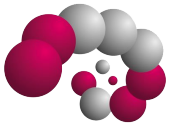

been enzymatically processed inside living cells. Thus, its delivery into the lateral ventricles of mouse embryonic brains via *in utero* injection results in the specific labelling of apical progenitors dividing at the ventricular surface, in contact with the cerebrospinal fluid. Labelled progenitors and their progenies retain the fluorescent labelling until it becomes diluted over a few rounds of division (FIG 3.3A). This allowed us to map the developmental trajectory of the progenies of MGE apical progenitors dividing in contact with the ventricular surface acutely at E12.5.

We analysed the result of FT labelling 3h, 6h, 14h, and 24h after injection, comparing lineage dynamics in the MGE and the pallium, where the cellular principles of PC generation are well understood. We observed that FT labelled cells remained in the VZ of the MGE and pallium at least 6h after labelling (FIG 3.3 B, C). A fraction of FT labelled cells was found in the SVZ 14h after labelling, which suggested that progenies of apical progenitors take between 6 to 14h to reach this germinal layer. Interestingly, the fraction of cells invading SVZ 14h after the labelling was larger in the MGE than in the pallium (FIG 3.3 C). Our results in the previous chapter indicate that at E12.5 about a third of cortical apical progenitors divide symmetrically at to generate two apical progenitors that remain at the VZ. Thus, the increased fraction of labelled cells in the SVZ of the MGE likely indicates that these symmetric divisions, if present, are less frequent in the subpallium. Consistently, only 1 out of 25 MADM lineages analysed in the previous experiment contain apical progenitors in both sub-lineages. Interestingly, we found that a minor fraction (~41%) of FT labelled SVZ cells in

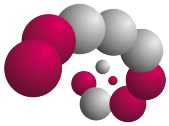

the pallium express the progenitor cell marker Ki67 (FIG 3.3D), while this fraction is much larger in the MGE (~72.5%). These results may reflect a preferential generation of INs through indirect neurogenesis, or the expansive division of the initial fraction of basal progenitors. Consistent with the larger number of basal progenitor cells in the MGE, the fraction of FT labelled cells observed in the SVZ increased remarkably 24h after the labelling. In contrast, this fraction is slightly reduced in the pallium, which indicates that some of the cells generated at the time of FT labelling left the SVZ to invade the cortical plate before being replenished by the next wave of VZ-derived cells. Since the speed of migration to the SVZ seems to be similar in both the pallium and the subpallium in light to our results, the increase in the number of SVZ cells in the MGE should arise from the expansion of basal progenitors. Finally, we found that the fraction of Ki67+ progenitor cells in the subpallial SVZ remains remarkably high (~52%) 24h after the FT labelling, which suggests that basal progenitors often divide generating other progenitor cells. Altogether, these results reveal that apical progenitors in the MGE generate basal IPCs that undergo multiple rounds of expansive divisions in the SVZ. However, a better understanding of these data will require the experimental estimation of cell cycle length in the MGE. This estimation has been previously made in the cerebral cortex, where apical progenitor cells divide in 11-13h at these stages (Calegari et al., 2005; Lange and Calegari 2010). This speed is remarkably reduced in cortical basal progenitors, whose take an around 26h to divide (Arai et al., 2011). This is consistent with the mostly stable fraction of SVZ progenitor cells observed in cortex in our FlashTag experiments. In the subpallium, these dynamics seem to

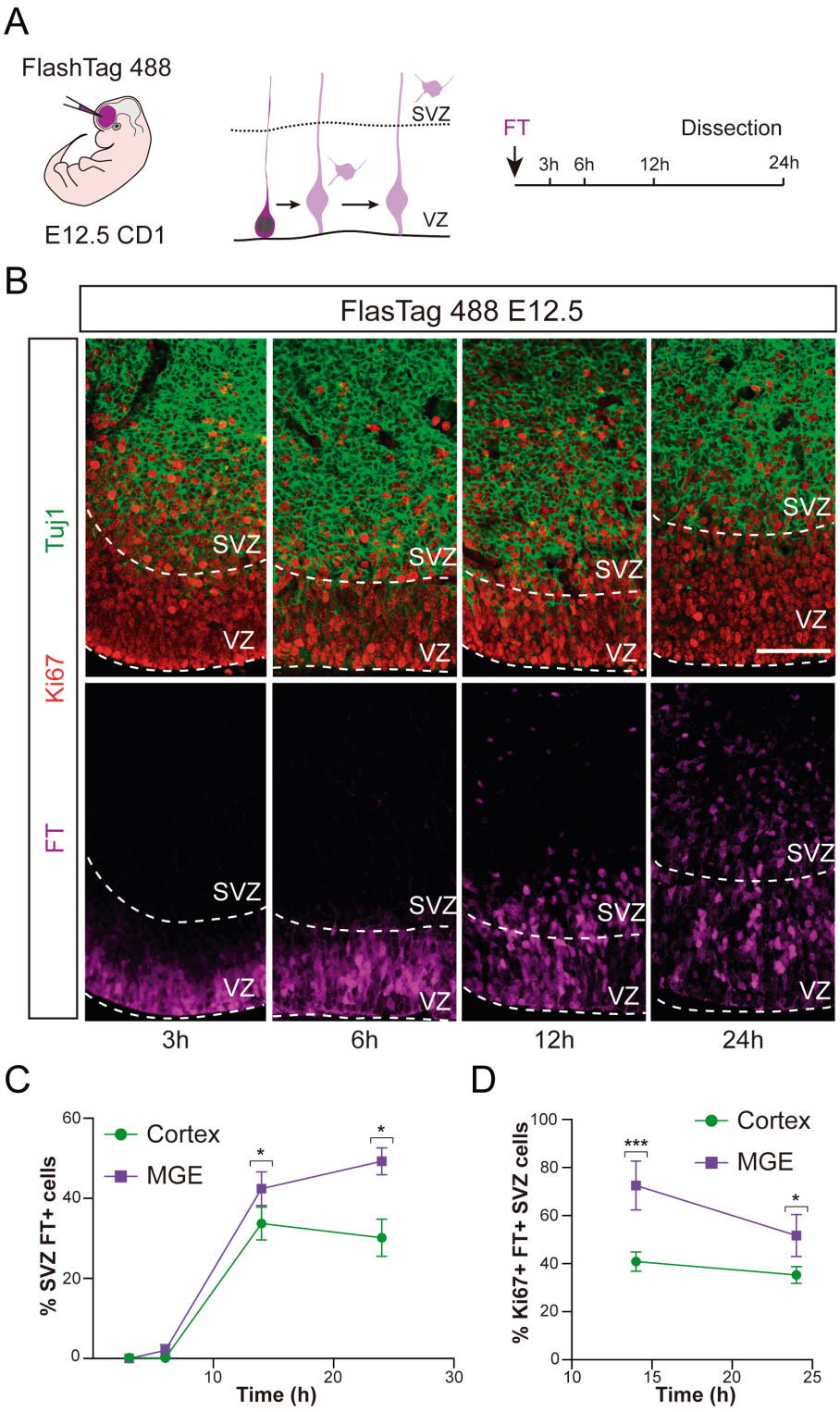

Figure 3.3. SVZ expansion of MGE lineages

(**A**) Experimental paradigm. (**B**) Coronal sections of embryonic mouse MGE 3h, 6h, 14h, and 24h after FT injection. (**C**) Quantification of the percentage of total FT labelled cells present at the SVZ. Data expressed as mean ± standard deviation (p-value = 0.0104 for 12h; p-value = 0.0372 for 24h, t-Student test). (**D**) Percentage of Ki67+ progenitor cells among FT labelled SVZ cells. Data expressed as mean ± standard deviation (p-value = 0.0023 for 12h; p-value = 0.0372 for 24h, t-Student test). MGE, medial ganglionic eminence. n = 3 brains (3h); 3 brains (6h); 4 brains (12h); 3 brains (24h). VZ, ventricular zone. SVZ, subventricular zone. FT, Flashtag. Scale bar 50μm.

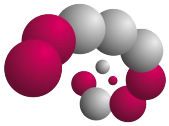

be remarkably different. Time lapse experiments in the LGE revealed that cell cycle length gets progressively reduced as lineages progress through apical, sub-apical and basal divisions (Pilz et al., 2013). Hence, apical progenitors in the LGE divide in approximately 25h at , and this duration reduces progressively, with basal progenitors dividing in only 12h. Further experiments investigating the speed of division of IN progenitor cells in the MGE both in VZ and SVZ, would be of great help to better understand the results presented in this section.

A novel strategy to map IN lineages: The *Binbow* system

Our capacity to reliably map the outcome of subpallial progenitors at single cell resolution is limited by currently available lineage-tracing methodologies. To overcome the caveats of previous methods, we designed a novel multicolour labelling strategy inspired in the *Brainbow* system (Livet et al., 2007). This system relies on the random expression of only one of four alternative reporters in two subcellular localisations in each cell, for a total of 16 colour/location possibilities. To this end, we engineered two Binary Brainbow-like (*Binbow*) cassettes that encode four alternative reporters destined for cytosolic (*cBinbow*) or nuclear (*nBinbow*) localisation, respectively. In these cassettes the four reporter genes are sequentially organised downstream of a common promoter sequence, so that the presence of each reporter prevents the expression of the next. In addition, the widespread expression of the first reporter is prevented in the absence of Cre by the presence of a stop cassette upstream of its coding sequence, consisting on a non-fluorescent variant of the PhiYFP protein (Cai et al., 2013). Two exclusive lox sites flank the coding sequences of each reporter

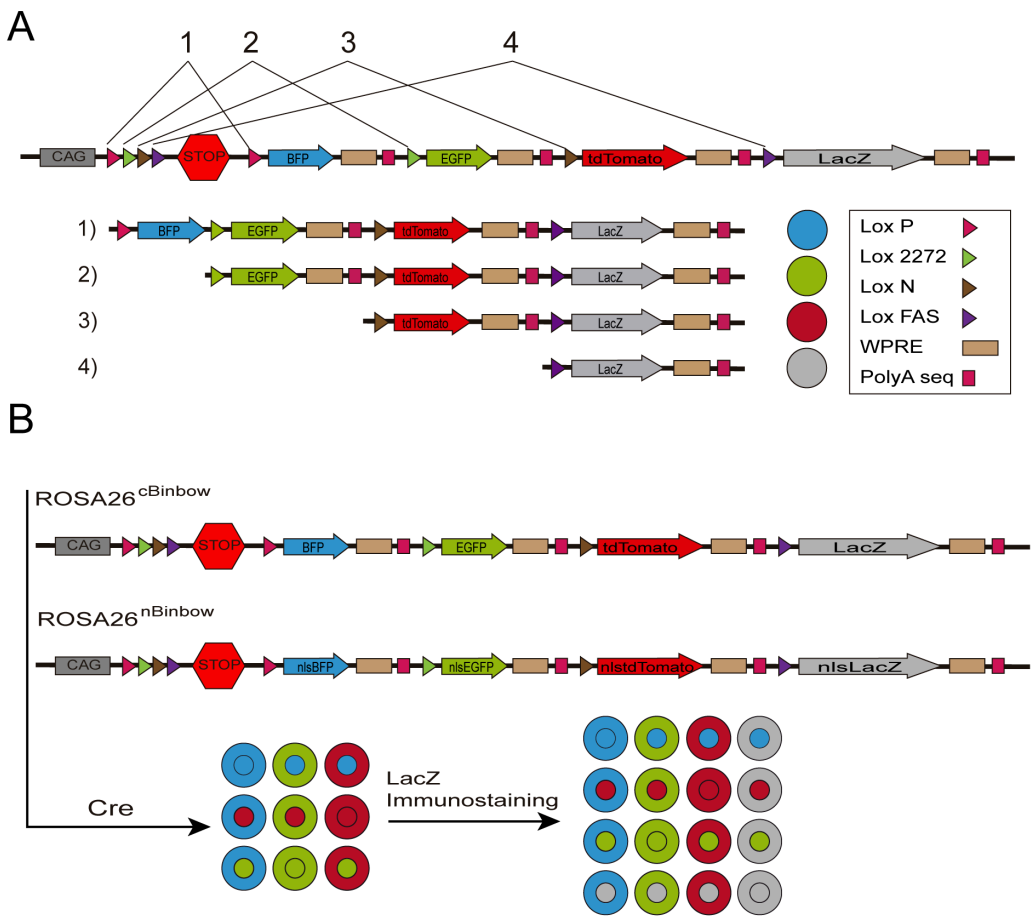

Figure 3.4. The *Binbow* system
(**A**) Schematic representation of the *Binbow* cassette. Coloured triangles represent different variants of lox site sequences. Cre-mediated recombination would lead to the stochastic rearrangement of the genetic cassette in one of our possible configurations, leading to the expression of a single reporter gene. Widespread expression of the first fluorescent protein is precluded by the existence of an upstream stop cassette. (**B**) Combined labelling with both *cBinbow* and *nBinbow* alleles tags target cells with a unique binary code, in which one of the four reporter genes is express in each subcellular localisation.

protein. Importantly, each pair of lox sites is capable to recombine with an exact reproduction of its own sequence, but not with the other lox variants. Thus, Cre-mediated recombination in this system randomly takes place between one of the lox pairs, leading to the final reorganisation of the *Binbow* cassette in one of four alternative configurations, and thus, the stochastic expression of one of the reporter genes (Fig 3.4A). Hence, in cells carrying both *nBinbow* and *cBinbow* alleles, Cre activity will lead to the random expression of one of the four

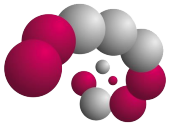

reporters in each subcellular localisation, consequently tagging the target cell with a distinctive combination from a sixteen-depth code (Fig 3.4B). If these cassettes were integrated in the genome of the cells, then progenies of cells labelled with these nuclear-cytosolic codes will inherit their distinctive colour code, therefore allowing the identification of lineage relationships.

A few technical details were considered in the engineering of this system, in other to conserve the flexibility to be used in a wide range of circumstances. For instance, our design of the *Binbow* system uses three fluorescent reporters and a non-fluorescent, *LacZ* reporter gene, to avoid automatically using all four light wavelength channels commonly used in fluorescent imaging. This last reporter could thus be detected via immunostaining, or ignored when needed, allowing the use of the corresponding channel for other purposes, at the expense of reducing the system resolution (Fig 3.4B). Also, given the size and complexity of *Binbow* cassettes, mouse genetics represents the easiest route for the introduction of the constructs into target cells. Therefore, once generated, these cassettes were introduced in early mouse embryos to generate the corresponding knock-in strains, whose combined use will lead to the desired combinatorial labelling.

Two main requirements should therefore be satisfied for the proper function of the *Binbow* strategy: (1) The introduction of four incompatible pairs of lox sites, and (2) the combination of four reporter genes distinguishable both in fluorescent spectra and immunohistochemical detection.

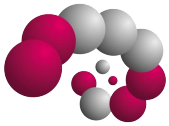

Identification of four incompatible lox sites

The use of different pairs of lox sites, incapable to recombine between each other, is critical for the correct function of the *Binbow* system, as described for the *Brainbow* one (Livet et al., 2007). We drew inspiration from the newest version of this cassette, *Brainbow* 3.2, to design our strategy. The *Brainbow* system uses three different pairs of lox sites that are unable to recombine among them: *LoxP*, *Lox2272* and *LoxN*. To identify a fourth pair of incompatible lox sequences, we designed a genetic strategy to test the recombination properties of different lox candidates (Langer et al., 2002; Lee and Saito, 1998; Siegel et al., 2001). To this end, we used a lox-test vector in which the expression of EGFP is induced after removal of an upstream stop cassette flanked by a pair of lox sites (Fig 3.5A). The compatibility of different lox variants was screened via introduction of different lox sites at the flanks of the stop cassette. For each pairing, the expression of EGFP following exposure to Cre recombinase activity would be indicative of successful recombination among these lox sites, and thus, reflect that the tested lox site is unsuitable for the *Binbow* constructs.

To test the compatibility of different lox pairs *in vitro*, we transfected lox-test constructs containing diverse combinations of lox sites in COS7 cell cultures. As expected, no fluorescent signal was detected in the absence of Cre recombinase; instead, the presence of the stop cassette was detected via immunostaining. In contrast, upon co-introduction with constitutive Cre expression vectors, green fluorescence was detected in some experiments, indicating that the tested sequences were compatible for recombination.

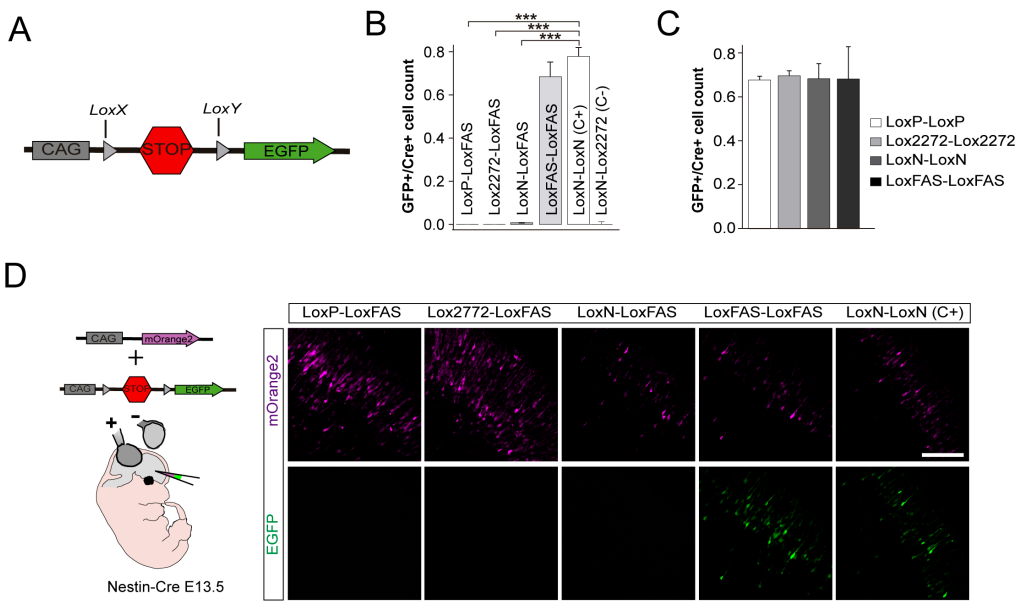

Figure 3.5. Identification of four incompatible pairs of lox sites
(**A**) Schematic representation of lox-test genetic construct. (**B**) Fraction of recombined (EGFP+) COS7 cells over total Cre+ transfected cells. Data expressed as mean ± standard deviation (p-value = 0.0028 for LoxP-LoxFAS pair; p-value = 0.005 for LoxN-LoxFAS pair; p-value = 0.0007 for Lox2272-LoxFAS pair; p-value = 0.2466 for LoxFAS-LoxFAS pair, t-Student test with Welch's correction). (**C**) Fraction of recombined (EGFP+) COS7 cells over total Cre+ transfected cells. Data expressed as mean ± standard deviation (p-value = 0.3102, one-way ANOVA). n = 3 cultures. (**D**) Lox compatibility *in vivo* test. Coronal sections of E18.5 Nestin-Cre mouse brains electroporated at E13.5. EGFP+ recombined cells can be exclusively detected in the LoxFAS-LoxFAS and the positive control experiments. Scale bar 100µm.

Remarkably, we found that a candidate lox sequence, named *LoxFAS,* was unable to recombine with any of the three sequences previously used in the *Brainbow* system (Fig 3.5B).

We next tested the recombination efficiency of each lox variant *in vitro*. For this purpose, we co-transfected Cre expression constructs and conditional vectors, in which the stop cassettes were flanked with homologous pairs of *LoxP*, *Lox2272*, *LoxN* and *LoxFAS* sites, into COS7 cell cultures. The recombination efficiency was estimated by the fraction of Cre expressing cells that also expressed EGFP. We found that the recombination efficiency of each of these lox

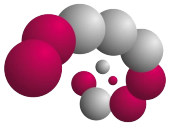

sites was similar (Fig 3.5C), further supporting *LoxFAS* as a viable candidate to be used in the *Binbow* constructs.

Finally, to better approximate the behaviour of Cre recombinase inside mouse neurons, we performed similar experiments *in vivo*. To this end, we introduced the lox-test cassettes into mouse PCs via *in utero* electroporation. In these experiments, constitutive vectors coding for the red fluorescent protein *mOrange2* were co-introduced with the lox-test cassettes to mark electroporated cells. These procedures were carried in *Nestin-Cre* embryos at E13.5 to target a large fraction of cortical progenitors. The results of these experiments corroborate those obtained *in vitro*, reinforcing the notion that *LoxFAS* efficiently recombines with its exact copy but it fails to do so with any of the other three lox sites used in *Brainbow 3.2* (Fig 3.5D). Taken together, these results indicate that the *LoxFAS* site efficiently mediates Cre recombination, while it is incompatible with the three sites previously used for similar purposes. Therefore, these conditions make it ideal for its inclusion in the *Binbow* system.

Alfredo Llorca took care of the design, construction, and test of both *nBinbow* and *cBinbow* cassettes. The generation of the corresponding knock-in mouse lines was carried by a specialised company (GenOway) under our direct supervision.

Combinatorial labelling with four distinguishable reporters

A second major challenge of the *Binbow* system is the use of four reporter genes with bright, non-overlapping fluorescent signal and minimum sequence

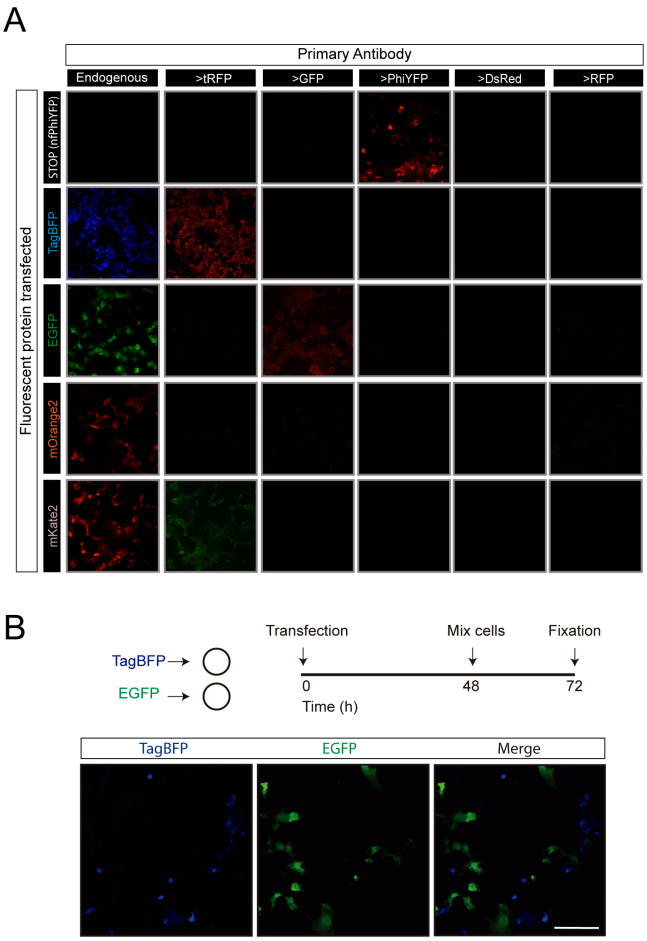

Figure 3.6. Selection of distinguishable reporters for combinatorial labelling
(**A**) *In vitro* test for fluorescent protein recognition with specific antibodies. Rows show the different fluorescent reporters independently transfected into COS7 cell cultures. Columns show specific antibodies used to recognise the fluorescent reporters (see methods for details). (**B**) *In vitro* test for fluorescent protein spectral separation. Scale bar 200µm.

homology, ensuring their independent recognition by specific antibodies. As discussed above, our design incorporates a non-fluorescent reporter (*LacZ*), which can be detected via immunostaining, to conserve some degree of flexibility in the detection of alternative proteins. Thus, a combination of three fluorescent proteins would fulfil the requirements of the *Binbow* system.

We first selected a number of candidate reporters following the criteria described above, and tested their recognition with specific antibodies. To this end, we transfected COS7 cell cultures with the different reporter candidates and used diverse antibodies for their immunodetection after fixation. Our results corroborated previous results (Cai et al., 2013), indicating that the blue fluorescent protein TagBFP is recognised by antibodies other than those used for

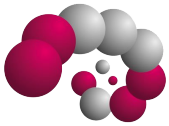

the detection of EGFP, tdTomato and mCherry (FIG 3.6A). Next, we tested our ability to faithfully segregate the fluorescent emission of TagBFP and EGFP, since these blue and green fluorescent proteins present minor overlaps in their fluorescent spectra. To this end, we transfected independent COS7 cultures with these proteins, and mixed both cultures following transfection (FIG 3.6B). Fluorescent imaging revealed minimum overlaps between the fluorescent spectra of these reporters, which allows the distinction of the two populations of cells under appropriate imaging conditions. Thus, our results indicate that the combined use of the fluorescent proteins TagBFP, EGFP and tdTomato, and the non-fluorescent reporter LacZ would provide a viable labelling code for mapping cell lineages.

Functional characterisation of *Binbow* cassettes

In light of these results, we generated two *Binbow* cassettes, in which the genes encoding the reporter proteins TagBFP, EGFP, tdTomato and LacZ are organised in sequence under the control of a general promoter, and respectively flanked by the lox variants *LoxP*, *Lox2272*, *LoxN* and *LoxFAS*. The main difference between the two cassettes consists of the subcellular localisation of the reporter genes, being cytosolic in one (*cBinbow*) and having a nuclear localisation signal fused to the reporter genes in the second, ensuring their confinement in the cell nucleus (*nBinbow*) (FIG 3.4A).

We next tested the function of the *Binbow* cassettes. To this end, we first transfected COS7 cells with *nBinbow* and *cBinbow* constructs (FIG 3.7A). As expected, no fluorescent signal was detected following transfection of the

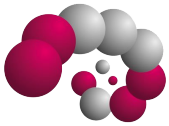

Binbow cassettes alone, although the presence of the stop cassette was detected via immunostaining. In contrast, all reporter genes were detected after co-transfection with a constitutive Cre expression vectors (FIG 3.7B). Notably, the vast majority of transfected cells exhibited the expression of all four reporters (FIG 3.7C), which reflected the promiscuous introduction of multiple plasmids in each transfected cell. We also observed that the number of cells expressing a unique reporter was similar for each reporter (FIG 3.7E). We next tested the expression of *Binbow* cassettes *in vivo* following *in utero* electroporation in the mouse embryonic cortex (FIG 3.7F). Consistent with the *in vitro* experiments, the expression of all four reporter genes was only detected when the *Binbow* cassettes were electroporated along with Cre expression vectors (FIG 3.7G). We found that most cells expressed all four different reporters (FIG 3.7H), and the fractions of cells exclusively expressing each reporter were comparable except for the first reporter, TagBFP, which seems to be expressed more frequently than the others (FIG 3.7J).

Stochastic recombination, leading to the expression of each reporter gene with similar probability, is critical for the proper function of the *Binbow* system. Thus, although the previous functional characterisation experiments showed approximately balanced expression of all four reporters, direct evidence of the relative frequency of each alternative recombination was required to ensure the correct function of our system. To estimate the expected frequency of each alternative recombination event, we induced Cre-mediated recombination of *Binbow* cassettes *in vitro*. In order to segregate recombinant clones, we

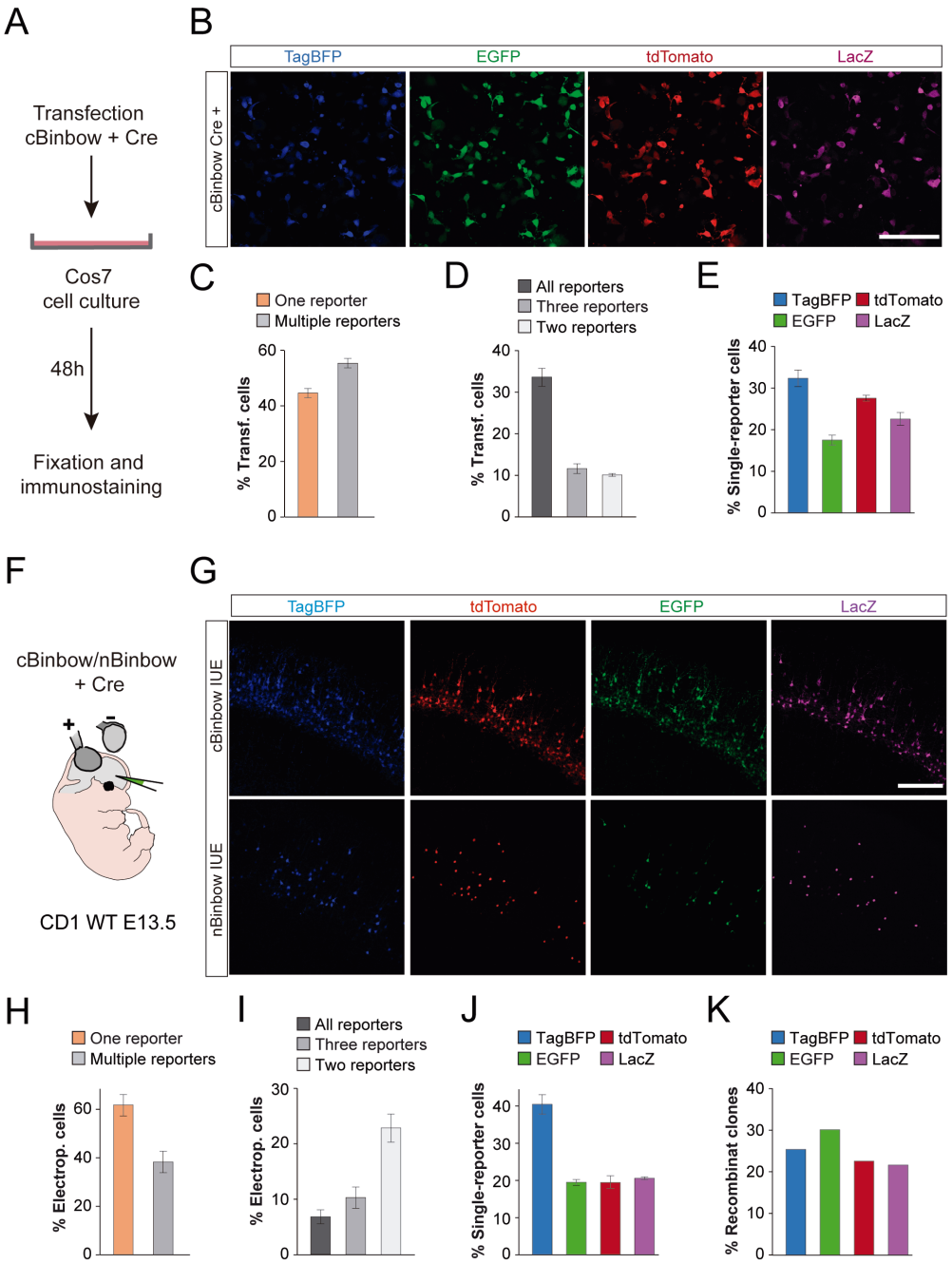

Figure 3.7. Functional characterisation of *Binbow* cassettes

(**A**) Experimental paradigm for *in vitro* characterisation of *Binbow* cassettes. (**B**) Example images of COS7 cultures transfected with *cBinbow* and constitutive Cre expressing plasmids. (**C**) Percentage of *nBinbow* transfected cells expressing one or multiple reporters. Data expressed as mean ± standard deviation. (**D**) Percentage of transfected cells expressing two, three or all reporters. Data expressed as mean ± standard deviation. (**E**) Percentage of cells expressing each reporter gene among transfected cells expressing only one reporter. Data expressed as mean ± standard deviation. (**F**) Experimental paradigm for *in vivo* characterisation of *Binbow* cassettes. (**G**) Coronal sections of E18.5 CD1 mouse brains electroporated at E13.5. Images show examples of neurons con-electroporated with *cBinbow* or *nBinbow* plasmids and constitutive Cre expressing vectors. (**H**) Percentage of *nBinbow* transfected cells expressing one or multiple reporters. Data expressed as mean ± standard deviation. (**I**) Percentage of transfected cells expressing two, three or all reporters. Data expressed as mean ± standard deviation.

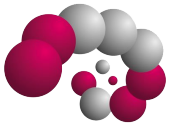

(**J**) Percentage of cells expressing each reporter gene among transfected cells expressing only one reporter. Data expressed as mean ± standard deviation. (**K**) Percentage of total recombinant clones observed in each possible configuration after in vitro recombination of *Binbow* vectors. N = 3 cultures (C-E); 3 brains (I, J); 100 colonies (K). Scale bars 200µm.

transformed the resulting plasmids in bacterial competent cells. These clones were then grown in bacterial cultures and recovered for analysis. Since the different recombinant variants arising from *Binbow* recombination should have different sizes, digestion with restriction endonucleases was used for their molecular profiling and their consequent assignment to a specific recombinant type. In these experiments, we recovered similar fractions of each possible configuration in over hundred recombinants quantified, indicating that the alternative recombination events occurred with similar probabilities (FIG 3.7K).

Altogether, these results indicate that *Binbow* cassettes functioned as expected both *in vitro* and *in vitro*, highlighting their potential use as a high-resolution lineage-tracing method. We then proceeded to generate both *cBinbow* and *nBinbow* mouse Knock-in strains.

3. DISCUSSION

Cellular logic of IN genesis

Understanding the cellular principles of IN generation in the embryonic subpallium is critical for our comprehension of IN development. In this study, we have characterised the diverse morphotypes of progenitor cells populating the MGE. Also, we have used a combination of clonal analysis and FT labelling of synchronously-dividing progenitor cell cohorts to study the mitotic patterns of these stem cells.

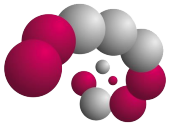

Two main types of progenitor cells have been described in the MGE; self-renewing progenitors undergo several rounds of cell division across different embryonic stages, sustaining the constant production of cortical INs. Intermediate progenitor cells divide a limited number of times, leading to the quick generation of postmitotic cells before getting exhausted. Self-renewing progenitors are thought to reside in the VZ exclusively, while IPCs seem to be present in different locations. In the cerebral cortex, for instance, SNPs are considered as apical IPCs residing in the VZ (Stancik et al., 2010; Tyler and Haydar, 2013), and this notion has been recently translated to the subpallium (Kelly et al., 2019). Multipolar SVZ progenitors are thought to behave as IPCs in both cortex and MGE, (Kelly et al., 2019; Miyata, 2004; Noctor et al., 2004). The most common view of neurogenesis in both regions considers that IPCs are typically generated by self-renewing apical progenitors.

Our results indicate that a large fraction of mitosis in the MGE/POA corresponds to IPC divisions, since their progenies did not include self-renewing apical progenitors. Surprisingly, most of these divisions were expansive, generating small groups of neurons typically larger than 2 cells. Thus, in sharp contrast with cortical IPCs, these cells seem to undergo several rounds of division before dividing terminally.

Intriguingly, IPCs derived from self-renewing apical progenitors only undergo expansive divisions in half of the cases. This contradiction raises the question about the origin of expansive IPCs. One possibility would be the existence of a population of expansive IPCs that do not originate from the self-

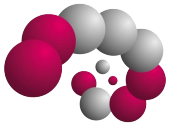

renewing apical progenitors. For instance, at the moment of MADM labelling, self-renewing apical progenitors in the MGE might share the VZ with a population of apical IPCs prone to undergo a few rounds of division, as described for SNPs in the cerebral cortex. In line with this idea, our morphological analysis of MGE progenitor cells identified a large fraction of apical MGE progenitors lacking basal processes, similar to the morphology of cortical SNPs. This view is, however, in disagreement with our FT labelling experiments. In such experiments, we observed a large fraction of VZ-derived basal progenitor cells dividing shortly after the invasion of the SVZ, and generating progenies that maintain their progenitor fate to a large extent. This suggests that these basal progenitors undergo multiple rounds of division before dividing terminally to generate postmitotic cells, further evidencing the existence of expansive divisions in the SVZ.

Alternatively, sub-lineages containing only two cells may correspond to expansive IPCs that only divided once before fixation, but were meat to do it again shortly. This view is further supported by previous data indicating that cell divisions in the LGE become faster as lineage progresses. In this structure, cell divisions in the VZ are slower, and become progressively faster in IPCs as the move towards the SVZ (Pilz et al., 2013). Further analysis of a larger numbers of MGE/POA lineages will help to clarify this point.

We also observed that self-renewing progenitor cells in the MGE seem to generate neurons through direct neurogenesis in 50% of their mitotic divisions. This finding seem to contrasts with our FT experiments, in which we observed a

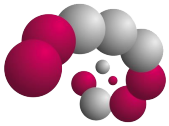

large proportion of Ki67+ progenitor cells (~72.5%) among total SVZ cells derived from apical progenitor divisions. However, these results are, to our view, compatible. The large clonal size of our MGE/POA MADM labelled lineages indicates that MGE progenitor cells may divide at least 3 times within 24h, suggesting a total cell cycle length of 8 to 10h. Thus, the initial population of IPCs generated via apical divisions could have replicated on their route towards the SVZ. Since, in light to our results, at least some of these divisions generate other IPCs, these divisions could have expanded the initial pool of IPCs, ultimately increasing the fraction of FT labelled progenitor cells in the SVZ.

Although these results seem to indicate that mitotic patterns underlying interneuron generation present clear differences with those observed in the dorsal pallium, they should be taken with caution. The number of MADM lineages analysed to date is still too small to be considered conclusive, and only further work will provide definitive evidence of the cellular logic underlying IN generation.

Lineage tracing in cortical INs

In the present study, we have designed and tested a novel multicolour lineage tracing system as a strategy to map the development of interneurons lineages. The *Binbow* system uses two complementary genomic cassettes that induce the stochastic expression of one of four alternative reporters in two subcellular localisations. The combined use of *cBinbow* and *nBinbow* cassettes thus leads to the ultimate labelling of targets cells with a unique colour code out of 16 different possibilities. Paired with the induction of Cre recombinase activity at

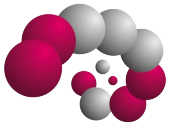

clonal levels, this system will represent a powerful tool for the identification of lineage relationships.

The proper function of this system relies on two key components of the *Binbow* construct: four incompatible lox site pairs and four distinguishable reporter genes. Our results indicate that the selected lox pairs are able to efficiently recombine with their exact copy, but not with any the other pairs in the system. We have also selected four reporter alleles which are distinguishable both in fluorescent spectra and via recognition with specific antibodies. Our design includes three fluorescent reporters, ensuring the compatibility of the *Binbow* system with *in vivo* applications, which rely in the detection of the endogenous fluorescence of the reporter. The fourth reporter consist in a *LacZ* cassette, which does no exhibit endogenous fluorescence, and thus, may either be detected via immunostaining or avoided when required. This gives us the opportunity to use the far-red wavelength channel for other purposes (i.e., detection of IN identity markers, birthdate analysis, etc.) at the expense of a reduced resolution of the system.

Our functional characterisation of *Binbow* cassettes indicates that the system exhibits all the desired features anticipated during its design. It functions as a Cre-inducible system, since no detectable fluorescent signal was observed in the absence of Cre recombinase activity. In addition, all four reporter genes are detected after Cre-mediated recombination both *in vitro* and *in vivo*. Finally, the four alternative recombination events happen with similar probability, ensuring the balanced expression of each combination of nuclear and cytosolic tags.

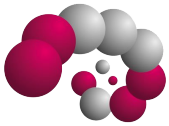

Although it lacks the extremely high resolution of multicolour RGB systems or genetic barcoding strategies, the *Binbow* system presents numerous advantages over previous lineage tracing methods, which make it ideal for such purposes. First, its genome-encoded nature ensures the detection of entire lineages, avoiding the risk of genome silencing inherently linked to viral strategies. Second, the detection of lineage relationships relies on the expression of a specific combination of reporter genes, circumventing the necessity to recover and map genome sequences into traced cells. This makes lineage reconstruction remarkably simple, and prevents the loss of a fraction of traced cells often linked to these procedures. Finally, one of the most important advantages of the *Binbow* system is its binary nature. In this system, the simple presence or absence of the reporter cassettes is used to identify their lineage relationships. Diverse RGB labelling systems, such as *Brainbow (*Can et al., 2013; Livet et al., 2007), *CloNe* (Garcia-Moreno et al., 2014), or *Startrack* (García-Marqués and López-Mascaraque, 2012) use the introduction of multiple fluorescent proteins in high copy number, providing a better resolution in terms of a larger number of possible outputs. However, the introduction of multiple copies of each protein may lead to potential misinterpretation of lineage relationships, making them less trustable for such purpose, as previously discussed. In contrast, the *Binbow* system does not require the measurement of fluorescent intensity in each channel, and hence circumvents the potential misinterpretation of lineage relationships that limits RGB systems.

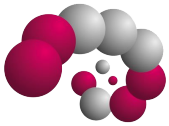

Despite evading most of these caveats, the *Binbow* system presents an obvious drawback in form of a limited (sixteen-depth) resolution. Such fact would, however, not limit the utility of this tool if the amount of starter cells traced were to be very small (i.e. of the order of units), so that the chances of sharing the code when not sharing lineage would be exceptionally reduced. Thus, this system would be an advantageous tool for lineage tracing when combined with a fine control of Cre activity, triggering the combinatorial labelling in a small amount of cell lineages. This would make the 16 colour code sufficient to faithfully recognise lineage relationships. Such control of Cre activity could be achieved in different ways, such as the injection of low doses of tamoxifen or the delivery of viral cassettes at very low titer, as described in the previous chapter.

In conclusion, while the resolution of the *Binbow* system is limited compared to other multicolour labelling systems, controlling the number of recombination events minimises this caveat. Under the appropriate circumstances, a 16-depth resolution code would suffice to reliably reconstruct mapped lineages, making it a simple, resolute, and reliable tool to map cell lineages *in vivo*.

DISCUSSION

The fascinating functions of the cerebral cortex emerge from complex cellular circuits composed by two main classes of neurons, excitatory pyramidal cells and inhibitory interneurons. The diverse neuronal fates that compose these groups arise from parallel developmental mechanisms that share fundamental principles but have different peculiarities. In this thesis, I have investigated the mechanisms underlying the generation of these two main classes of neocortical neurons. I have used multiple approaches to reliably map PC lineages from development to adult life. I have also developed a novel strategy to identify lineage relationships of cortical INs after migration to cortical territories, and studied the cellular principles of their genesis in the embryonic subpallium. In the following sections, I will discuss my main findings in the context of previous work.

Stochastic generation of PC diversity

The diverse PC fates that constitute the excitatory cell population of the adult cerebral cortex are known to arise from a population of radial glial progenitor cells in a temporally organised manner. However, the contribution of individual RGCs to the final composition of the cerebral cortex has been a matter of intense debate. Some studies observed that RGCs generate columnar progenies containing cells across the different cortical layers (Gao et al., 2014; Guo et al., 2013; Kaplan et al., 2017), while others detected progenies exclusively constituted by neurons with restricted laminar fates (Franco et al., 2012; García-Moreno and Molnár, 2015). These discrepancies have been previously attributed to technical limitations in the different approaches used to map the outcomes of single progenitor cells (Eckler et al., 2015; Gil-Sanz et al., 2015). In this study,

we used a combination of methods that, together, elude the limitations of individual approaches, providing a comprehensive picture of the developmental logic behind the generation of PC diversity in the murine developing cortex.

Our results indicate that the output of single RGCs is extremely heterogeneous in both the number of cells and the cell fates generated. Some lineages contained cells in all cellular layers of the neocortex, while others were constituted of diverse subsets of laminar fates, including a small fraction of lineages containing cells exclusively in superficial or deep cortical layers. These results are compatible with a stochastic framework of PC generation, in which RGCs develop through a temporal sequence of competence states with different probabilities of generating PCs during these temporal windows. Hence, despite sharing the basic molecular programmes, progenitor cells seem able of generating a wide diversity of variable and unpredictable outcomes, which are stochastic samples of the entire PC diversity. This works also follows previous studies that modeled cortical neurogenesis both at population and clonal level (Picco et al. 2018; Picco et al. 2019) and identified key parameters that could have strong effects in this process.

In our model, the probability to generate a given cell fate could reflect a number of different biological factors that can potentially impact in the neurogenic behaviour of individual progenitor cells.

First, the speed at which progenitor cells divide could be used to regulate the number of neurons produced during each competence window. For instance, a progenitor cell could divide relatively fast at early developmental windows and

then slow down its mitotic activity as development proceeds. This will generate a lineage enriched in deep (early born) layer neurons. The control of cell cycle speed may also be used to prevent cell division during the entire temporal window of a competence state, consequently eluding the generation of certain cell fates. Such regulatory mechanism, however, would demand a cell cycle-independent progression of the temporal sequence instructive of the cell fate. Supporting this view, recent studies have reported that temporal changes in gene expression experienced by cortical progenitors *in vitro* are indeed independent of cell division (Okamoto et al., 2016). In addition, progenitors that had their cell cycle arrested at early stages generate late PC fates when are allowed to divide at later stages, indicating that these cells are capable to progress in their temporal sequence despite the early blocking of mitosis. Studies measuring cell cycle duration in cortical progenitor cells are also consistent with this hypothesis. These studies have reported intriguing variations in the cell cycle length of cortical progenitors over the course of development. Overall, cell cycle is known to lengthen as development proceeds (Martynoga et al., 2005; Takahashi et al., 1995), a notion consistent with the idea that neurogenic progenitors have different cell cycle dynamics than proliferative progenitors (Calegari, 2005). These differences have also been described in studies comparing apical and basal progenitors in the murine cortex (Arai et al., 2011; Salomoni and Calegari, 2010). Such changes in cell cycle length, however, have exclusively been measured at population levels. Thus, at this point it is impossible to distinguish whether such changes should be attributed to synchronic changes affecting the entire population of cortical progenitor cells or to a large variation of cell cycle

speeds among individual progenitor cells. The later scenario would support the fine regulation of the mitotic kinetics of individual progenitor cells, a powerful mechanism to instruct their final output. Remarkably, this precise control of cell cycle kinetics has been previously related to the generation of region-specific rates of PCs (Dehay and Kennedy, 2007).

Second, the mode of division used by progenitor cells during each competence window may also impact the final composition of the lineage. Hence, RGCs could generate different IPC/neuron ratios during different temporal windows, evoking the generation of unbalanced fractions of the different PC fates in the nascent lineage.

Third, the temporal length of each competence window could also be subject of variation among individual progenitor cells, consequently increasing or reducing the likelihood of producing cells of the corresponding fates. *Drosophila* embryonic NBs represent a good example of this type of regulatory logic. Although based in shared molecular principles, temporal progression of different NBs seems able to deviate from the canonical pathway. Remarkable changes in the length of the different expression windows, even omitting the expression of some temporal TFs in certain cases, have been described (Doe, 2017). Interestingly, our MADM dataset showed that individual progenitor cells labelled at the onset of neurogenesis generate different cell fates in parallel divisions. Progenitor divisions at E12.5 generated layer VI neurons in most lineages, but a fraction of synchronous mitosis gave rise to layer V PCs. This reflects a certain degree of asynchrony in RGCs, consistent with previous data

(Magrinelli et al., 2018). This observation further supports the notion that differentially regulated temporal dynamics coexist among progenitor cells in the mammalian cortex.

Importantly, the potential of these different mechanisms to regulate the output of individual progenitor cells is likely to be additive. These regulatory strategies could be, and probably are, used in combination for a sophisticated and robust control of cortical neurogenesis, providing great flexibility to the neurogenic behaviour of individual progenitor cells.

Several lines of evidence suggest that fate specification in the cerebral cortex initially relies on molecular programmes intrinsically encoded in RGCs (Gaspard et al., 2008; Shen et al., 2006a), but receptive to be regulated by external influences (Desai and McConnell, 2000; Oberst et al., 2019; Okamoto et al., 2016). Cortical progenitors are thought to be exposed to a complex code of extrinsic signals, acting as potential regulators of their neurogenic behaviour (Reillo et al., 2017). This is highlighted by recent reports indicating that nascent cortical neurons acquire more 'extroverted' fates as neurogenesis proceeds, being progressively more sensitive to the surrounding environment (Telley et al., 2018). This continuous dialog between internal programmes and external signals is likely to influence fate specification in the developing cortex, potentially regulating RGC cell cycle kinetics, mode of division, and temporal progression, and therefore, ultimately controlling their neuronal output.

Diffusive signals of diverse nature could play important roles in the regulation of cortical progenitor cell behaviour. Indeed, the location of RGCs and

their extension of apical processes in contact with the ventricular surface places them in a privileged position to receive influences from the cerebrospinal fluid, which is known to contain diverse regulatory cues (Borrell et al., 2012; Lehtinen and Walsh, 2011; Lehtinen et al., 2011). Also, the basal process of these stem cells seems to exhibit multiple varicosities and short ramifications along their vertical extension (Rakic, 1973; Sidman and Rakic, 1972), a feature that has been previously related to the detection of environmental signals (Errede et al., 2014). Diverse cell populations can source the aforementioned signals. Cajal-Retzius cells, for example, are well known for their secretory role in cortical neurogenesis, regulating the radial migration of PC via Reelin signalling (Caviness, 1982; Rice and Curran, 1999). Similar roles of this transient cell population in the regulation of other aspects of neurogenesis are thus imaginable. In addition, it is conceivable that RGCs may generate paracrine signalling, regulating the activity of surrounding progenitors. Finally, the nascent progeny has been reported to provide feedback signalling onto their progenitor cells (Anton et al., 1997; Seuntjens et al., 2009), potentially regulating their output to control the balance of neuronal fates. This kind of feedback control of progenitor performance has been previously described in other neural systems, like the mammalian retina (Cepko, 1999).

The secretion of diffusive signals, however, is only one of several possible paths mediating progenitor-progeny interactions. Newly generated PCs in the developing cortex migrate radially following the basal processes of RGCs, a mechanism that implies an intimate contact between these cells. Consequently,

potential interactions through cell adhesion-mediated signalling could be taking place during this process, representing an alternative route through which postmitotic neurons could influence the performance of their stem cells. Consistently, contact-mediated Notch-Delta signalling from both PCs and IPCs onto RGCs is known to be necessary for the maintenance of RGC stem cell fate (Nelson et al., 2013; Yoon et al., 2008). Interestingly, the normal temporal progression of RGCs seems to be compromised in culture conditions that prevent physical contacts with other progenitors and their nascent progenies (Okamoto et al., 2016), which suggests a regulatory role for these contacts in controlling temporal patterning and fate specification in the cerebral cortex.

Finally, activity dependent mechanisms have also been proposed to participate in the regulation of cortical neurogenesis. Thalamic afferents are known to influence cell cycle kinetics in RGCs, consequently tuning their neuronal output, and perhaps, controlling the appearance of the cytoarchitectonic differences that define cortical areas. In addition, the neurotransmitters glutamate and GABA have been shown to severely influence the proliferative dynamics of cortical progenitors *in vitro* (LoTurco et al., 1995), which suggests a possible role of both excitatory and inhibitory neurotransmission in controlling the performance of cortical progenitors. Such mechanisms could work via juxtaposed delivery of neurotransmitters onto RGC fibres or cell bodies, or through volumetric transmission of these signals.

The translation of environmental signals to internal changes in progenitor cell states can follow diverse routes, from the activation of classic molecular

pathways in response to external cues to more sophisticated mechanisms involving electric signals. For instance, recent reports indicate that some classical signalling molecules are able to modulate the generation of calcium waves at the basal process of RGCs (Rash et al., 2016), which seems to propagate across their cell body, ultimately regulating the genesis of PCs (Weissman et al., 2004). In addition, the membrane potential of RGCs has been recently described to experience changes during the course of development, changes that seem to influence the signalling of classic diffusive signals, such as Wnt, and have been linked to the temporal progression of these cells (Oberst et al., 2019; Vitali et al., 2018).

In sum, cortical progenitors seem to be exposed to an exquisitely sophisticated code of intrinsic and extrinsic signals regulating neurogenesis. The interaction of these signals should be capable of fine-tuning cell cycle kinetics, mode of division, and temporal progression of individual RGCs. Therefore, the ultimate control of RGC output would be performed through probabilistic, rather than invariant rules, as supported by our results based on the analysis of individual lineages. The broad, population-level regulation of these probabilities would ensure the collective generation of balanced ratios of cell identities, while allowing progenitor cells to exhibit flexible neurogenic fates, as observed in our experiments.

The use of developmental regulatory mechanisms subjected to stochastic rules provides multiple benefits in the construction of biological machineries (Johnston and Desplan, 2010). A major advantage, for instance, is its flexibility,

allowing progenitor cells to adapt their output in response to different circumstances. Such flexibility also endows the system with an important degree of robustness, since dysfunction or even loss of a group of progenitor cells can be rescued via modulation of the general population, ensuring the structural integrity of the nascent organ. In addition, I propose that such flexibility can be used to regulate the assembly of the very diverse cytoarchitectures that exist in different regions of the cerebral cortex. The generation of regional-specific ratios of different PC fates could be achieved through the local control of progenitor cell behaviours, rather than by establishing region-specific progenitor populations instructed by distinct intrinsic programmes. Our *in silico* models support this hypothesis. Hence, fine tuning of the probability values instructing progenitor neurogenic behaviours lead to the generation of very different ratios of laminar fates, easily replicating those observed in different regions of the cerebral cortex. In agreement with this idea, lineages located in different cortical regions often exhibit differences in their composition, thereby reflecting the particular cellular architecture of that region. For example, lineages lacking layer IV were especially frequent in motor, cingulate, and retrosplenial cortices (data not shown), which are known to have very few neurons in such layer. Unfortunately, the quantity of linages mapped in our study, although high for the standards of clonal analyses, is insufficient to provide conclusive evidence of regional differences in lineage composition, especially in the smaller areas where less lineages were found.

It is currently well established that the delineation of the various cortical regions that exist in the adult cortex depends on spatial patterning cues during early development (Greig et al., 2013). However, at neurogenic stages, little evidence for regional heterogeneity in the molecular signatures of RGCs has been provided (Pollen et al., 2015; 2014; Telley et al., 2016), suggesting that a molecularly homogeneous population of RGCs could account for the genesis of different cortical areas. Such early cues, could mediate the regulation of the diverse intrinsic and extrinsic factors that take part in the complex regulatory logic discussed above, representing an interesting model in which the early spatial patterning participates in the posterior modulation of progenitors temporal progression.

In summary, our study describes how relatively simple developmental mechanisms, coupled with sophisticated regulatory logics, can endow cortical progenitor cells with the required flexibility to behave in remarkably different ways. This would make them capable of building very diverse cytoarchitectures. Despite their novelty, these findings should not catch us by surprise. Biology, just like language or music, seems to excel in the use of very simple principles to generate extremely complex and diverse machineries. The genetic code, for instance, illustrates this outstanding ability. In my view, we are just before another great example of this universal biological property, through which nature seems to exhibit its most elegant signature.

Development of IN lineages

Despite our growing understanding of IN diversity, development and function (Lim et al., 2018a), the cellular principles regulating the generation of INs in the developing subpallium remain surprisingly obscure, precluding an complete notion of the developmental origins of IN diversity. In this thesis, I describe a very distinctive mitotic behaviour for progenitor cells in the MGE, with a sizeable fraction of them dividing quickly several times before undergoing an early terminal division. This would lead to the synchronous generation of small groups or "bursts" of INs within a few hours. This mode of neurogenesis may explain some of the apparently contradictory results found in previous studies that, in spite of severe technical limitations, ventured to describe the cellular composition and spatial distribution of individual IN lineages using different experimental strategies (Brown et al., 2011; Ciceri et al., 2013; Harwell et al., 2015; Mayer et al., 2015).

Progenies of putative single MGE/POA progenitor cells labelled with reporter retroviruses were found to organise into small (4-6 cells), spatially-segregated clusters in the adult brain (Brown et al., 2011; Ciceri et al., 2013). These findings led to the suggestion that IN migration and final allocation in the developing cortex was somehow encoded in the progenitor cells, and thus common to the entire lineage. However, later studies using retroviral-mediated genetic barcoding in cortical INs concluded that lineage-related cells may disperse widely among cortical regions, even crossing large anatomical

boundaries (e.g., basal ganglia and neocortex) in a minority of cases (Harwell et al., 2015; Mayer et al., 2015).

In light of our observations regarding the cell biology of IN generation, these results may not be completely irreconcilable. A conciliated view of these results could consider that apical progenitor cells in the MGE generate sequential waves of intermediate progenitors that subsequently expand over a few divisions, as observed in the LGE (Pilz et al., 2013). This will lead to the generation of synchronous cohorts of INs. Such cohorts would therefore share lineage relationships and spatiotemporal origin, being also exposed to a common environment. Given these premises, it is therefore not hard to imagine that their shared origin would influence their coordinated migratory behaviour and colonisation of adjacent cortical regions. In this case, the nature of local clusters might not be completely clonal, but instead arise from multiple spatially-related progenitors as previously suggested (Ciceri et al., 2013). Subsequent cohorts, potentially containing different cell fates, would then migrate to different cortical regions. In line with this idea, other germinal regions of the mammalian subpallium seem to follow a similar logic. LGE progenitors, for instance, have been proposed to generate different striatal cell fates through sequential waves of IPCs (Kelly et al., 2018).

In the proposed scenario, the apparent contradictions between the two datasets could simply be explained by the technical limitations of each of the experimental approaches used. Classic retroviral fate-mapping lacks the required resolution to reliably identify unique lineage relationships, since labelling

systematically includes more than a single apical progenitor cell. On the other hand, the recovery of the viral genome contained in traced cells is extremely inefficient in genetic barcoding experiments, which leads to the incomplete reconstruction of IN lineages. The spatial clusters identified with reporter retroviruses could reflect IPC-derived cohorts, and thus, multiple spatial clusters located distantly could indeed derive from common progenitor cells. Consistent with this view, spatial clusters of cortical INs tend to be composed of INs with shared birthdates (Ciceri et al., 2013). Distant sister neurons, in contrast, would correspond to different temporal cohorts.

This model is only one of several possible interpretations that could conciliate these data, and further studies on this matter will be required to fully understand this aspect of IN development. Such studies would however be primarily limited by our knowledge about the cellular dynamics of IN neurogenesis, and our capacity to reliably map the cellular components of IN lineages and their spatial dispersion. It is here were additional studies on the dynamics of IN neurogenesis, together with the introduction of novel high-resolution lineage mapping technologies, such as the *Binbow* system described in this thesis, will be indispensable.

Fate and freedom in cortical neurogenesis: An integrated view of PC and IN fate-specification

The study of the cellular mechanisms for the genesis of both excitatory and inhibitory neurons carried in this thesis has revealed that the development of

these two large classes of neurons shares common principles, but also exhibits some important differences that likely reflect their functional specialisation.

The specification of both classes of neurons commences with the segregation of progenitor cells into several spatial domains, defined by the expression of certain combinations of TFs. In the dorsal pallium, these early spatial patterning events delineate the presumptive "protomap" that will lead to the appearance of distinct functional regions of the mature cortex, typically with unique cytoarchitectonic patterns (Greig et al., 2013). In the subpallium, patterning events delineate the various structures that generate cortical INs (Xu et al., 2010), and perhaps further regionalise them into smaller domains with specialised neurogenic capabilities (Flames et al., 2007; Fogarty et al., 2007; He et al., 2016; Torigoe et al., 2016). One important difference between these two processes is that while cortical RGCs in the different presumptive areas seem to retain the capacity to generate all cardinal classes of excitatory pyramidal cells, such capacity seems to be segregated in subpallial progenitors. Hence, IN progenitors in different subpallial structures are known to exclusively produce certain subclasses of INs (Butt et al., 2005; Xu, 2004). In contrast, our lineage tracing data corroborates the idea that individual RGCs are able to generate a large diversity of excitatory PCs.

Several reasons could explain this divergence of developmental strategies. For instance, the molecular profile of different IN subclasses might be significantly less similar than those of different PC. Thus, they may require more specific, and thus segregated, developmental programmes for their specification.

Cardinal subclasses of PCs, in contrast, might share the bulk of their molecular signatures, and thus could be specified via remarkably similar developmental programmes. Such programmes could therefore be easily be triggered by the same progenitor cells. In line with this idea, although the adult transcriptomic diversity of excitatory PCs is remarkably large (Tasic et al., 2018; 2016), the morphological and physiological properties of PCs are known to be less variable than those exhibited by the different types of INs (DeFelipe et al., 2013). This suggests that the earliest steps in their differentiation route might be similar in the different PC types, using a few selector genes to trigger the molecular pathways that establish their core molecular identities. Further downstream mechanisms taking place in postmitotic cells could then be responsible for their precise differentiation into region-specific projection subtypes. Alternatively, these differences might be understood as a consequence of the developmental history of each class of neurons. PCs are born close to their adult location, whereas INs migrate long distances to reach their final destination. Cortical computation requires the collective action of diverse types of PCs across the different regions of the cerebral cortex. Therefore, the spatial segregation in the origin of these different types would have imposed major constrains in cortical development. One can imagine a scenario where spatial patterning is the primary mechanism specifying different pools of progenitor cells restricted for the generation of certain types of excitatory neurons. In such scenario, PCs would be forced to migrate tangentially from their place of origin, in order to invade the different cortical areas, significantly increasing the complexity of the process. Thus, the specification of the diverse PC identities via temporal patterning

mechanisms seems the most parsimonious strategy for the genesis of these cells, allowing them to remain close to their place of birth. Cortical INs, in contrast, are condemned to migrate tangentially given their subpallial origin. Thus, the spatial segregation in the origin of different classes represents a cheap luxury for them, and would not further complicate their development.

After the initial patterning events, most progenitor cells generating both excitatory PCs and INs seem to retain a multipotent fate, being capable of producing diverse neuronal types. Our findings regarding the development of excitatory PC lineages are, to some extent, compatible with the classic paradigm. In this paradigm the different types of PCs are established via temporal specification, using a mechanism similar to the molecular clocks described for *Drosophila* NBs (Doe, 2017; Pearson and Doe, 2004) This process would, however, be controlled by stochastic regulatory rules. Consistent with this view, the outcome of RGCs in the developing cortex often contains cells of different fates. IPCs, in contrast, exhibit a more restricted potential, typically generating cells confined to one or two adjacent layers. Whether similar mechanisms account for the generation of IN fates remains unexplored. The small number of clonal studies available suggests however that at least some MGE/POA progenitors are capable of generating both PV and SST interneurons. Hence exhibiting a multipotent fate similar to their pallial counterparts (Harwell et al., 2015; Mayer et al., 2015). Nevertheless, since these studies likely map incomplete lineages due to the limitations discussed above, the neurogenic potential of IN progenitors may have been underestimated. The diverse temporal

biases described for the origin of different IN types (Inan et al., 2012; Miyoshi et al., 2007; Taniguchi et al., 2013) suggest that this multipotent fate may also be achieved via temporal patterning mechanisms similar to those observed in the cerebral cortex. However, in light of our results, the temporal regulation of IN fate specification is likely far more complex than the corresponding processes in the pallium. For example, the MGE exhibits very complex mitotic patterns, with a large fraction of progenitor cells undergoing expansive divisions that lead to the quick exhaustion of the lineage. It is therefore difficult to predict at which stage of this ramified pattern of division the temporal sequence may reside. One possibility could be a stochastic mechanism governing both the mode of division and the fates of the nascent progenies, as described in the fish and mammalian retina (Gomes et al., 2010; He et al., 2012). Alternatively, if these expansive divisions take place in IPCs arising from a population of self-renewing progenitors, the temporal progression could occur in those cells. IPCs would then act as an expansive step with restricted potential imposed by the general temporal progression, as observed in the cerebral cortex. Finally, nested temporal progressions could take place in self-renewing and intermediated progenitor cells, mirroring the temporal patterning mechanisms described for *Drosophila* type II NBs (Bayraktar and Doe, 2014). In any case, much work is needed to reach an understanding of the mechanisms regulating the genesis of INs comparable to our current notion of PC generation.

Notwithstanding the evidence of multipotent fate in neural progenitor cells, a number of recent studies postulated the existence of fate-restricted populations

of progenitor cells in both pallium and subpallium, a view that has found strong resistance in the scientific community. Our experiments revealed a small but relevant fraction of cortical progenitor cells that generate laminar-restricted lineages, consistent with previously reported findings. Fate-mapping experiments in *Cux2*-expressing RGCs in the dorsal pallium revealed a strong tendency of those cells to generate a dominant fraction of superficial layer neuronal fates (Franco et al., 2012), which led to the conclusion that *Cux2*+ progenitor cells are committed to the exclusive generation of superficial layer PCs. This notion was further strengthen by similar findings using a different strategy (García-Moreno and Molnár, 2015). Interestingly, a similar conclusion has been reached for subpallial progenitor cells. Although MGE-derived INs are known to be generated in an inside-out pattern (Miyoshi et al., 2007; Sultan et al., 2018), INs destined to occupy deep or superficial cortical layers seem to arise from different progenitor pools (Ciceri et al., 2013). In addition, recent studies propose that two different populations of MGE progenitor cells preferentially generate SST or PV INs (Petros et al., 2015). These findings are however a matter of current debate, since definitive evidence of fate-restriction in any of these two systems has yet to be provided. For instance, the increased ratios of superficial layer neuronal fates produced by the putative fate-restricted *Cux2*-expressing progenitor cells are insufficient evidence of fate-restriction. Indeed, later clonal studies in *Cux2*+ RGCs revealed an enrichment in the production of superficial layer neuronal identities, but these clones often contained a fraction of deep layer neurons (Eckler et al., 2015; Gil-Sanz et al., 2015). This observation suggests a preferential generation of superficial neurons, rather than an absolute fate-

restriction, in these progenitor cells. Our mathematical modelling supports this notion, since the inclusion of multipotent progenitors tuned to preferentially generate superficial neurons, is sufficient to generate the fraction of superficially restricted lineages observed in our experiments. Thus, while the coexistence of parallel developmental programmes is possible and even likely in light of our results, such programmes would not necessarily imply a restriction, but rather a tuning of the preferential generation of certain cell fates, while progenitor cells retain their multipotent fate. Such paradigm would, moreover, be strongly consistent with the observations regarding *Cux2*+ RGC fate-mapping experiments.

Although less controversial, the laminar restriction of MGE lineages, and the existence of differentiated progenitor pools for the genesis of SST and PV cells should also be put in context. Our short-term analysis of lineage development in this structure indicates that IN lineages might reflect a complex mixture of events, and clonal labelling may occur at different points of the ramified lineage. For instance, the observed lineages could reflect the output of fate-restricted expansive IPCs derived from multipotent self-renewing progenitors, as discussed above. Whether the segregation of cell fates occurs at the start of the lineage or at any of the different branching points remains to be unravelled and should be the subject of further research.

These discrepancies in developmental strategies used by PCs and INs should also be considered in the context of mechanisms that are beyond the scope of this thesis. For instance, a large number of cortical INs undergo

programmed cell death during the first two postnatal weeks in mice (Southwell et al., 2012; Wong et al., 2018), a mechanism thought to ensure the final balance of neuronal types in cortical circuits. PCs, on the other hand, seem to be less influenced by this process, with a significantly smaller fraction of them undergoing programmed cell death. This fact highlights the importance of a fine control in the generation of different PCs in balanced ratios, since these numbers will not undergo an extensive correction via cell death. This justifies the existence of robust mechanisms for the generation of cell fates and their regulation under stochastic and flexible logics. INs on the other hand, seem to enjoy a higher degree of freedom in the mechanisms underlying their origin and sculpt their final numbers via programmed cell death. Thus, while the existence of highly stereotyped and organised patterns for the genesis of IN diversity remains to be investigated, they might not be strictly necessary for their successful development and function. The discovery of heterogeneous patterns of division in IN progenitors might reflect this freedom.

In conclusion, the development of excitatory and inhibitory neurons in the cerebral cortex exhibits remarkable differences that, under appropriate interpretation, may provide interesting links between neuronal development, physiology and function. This emphasises the importance of a deep understanding of brain development for the comprehension of adult brain function.

REFERENCES

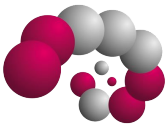

A Schmid, A., Chiba, A., Doe, C. 1999. Clonal analysis of Drosophila embryonic neuroblasts: neural cell types, axon projections and muscle targets. Development 126, 4653-4686.

Alcamo, E.A., Chirivella, L., Dautzenberg, M., Dobreva, G., Fariñas, I., Grosschedl, R., McConnell, S.K., 2008. Satb2 Regulates Callosal Projection Neuron Identity in the Developing Cerebral Cortex. Neuron 57, 364–377. doi:10.1016/j.neuron.2007.12.012

Alexiades, M.R., Cepko, C. 1996. Quantitative Analysis of Proliferation and Cell Cycle Length During Development of the Rat Retina. Developmental Dynamics 205, 293-307. doi: 10.1002/(SICI)1097-0177(199603)205:3<293::AID-AJA9>3.0.CO;2-D

Allan, D.W., Thor, S. 2015. Transcriptional selectors, masters, and combinatorial codes: regulatory principles of neural subtype specification. WIREs Dev Biol 4, 505–528. doi:10.1002/wdev.191

Alvarez, F.J., Jonas, P.C., Sapir, T., Hartley, R., Berrocal, M.C., Geiman, E.J., Todd, A.J., Goulding, M. 2005. Postnatal phenotype and localization of spinal cord V1 derived interneurons. J. Comp. Neurol. 493, 177–192. doi: 10.1002/cne.20711

Anderson, S.A., Eisenstat, D.D., Rubenstein, J.L.R. 1997. Interneuron Migration from Basal Forebrain to Neocortex: Dependence on Dlx Genes. Science 278, 474–476. doi: 10.1126/science.278.5337.474

Anton, E.S., Marchionni, M.A., Lee, K.-F., Rakic, P. 1997. Role of GGF/neuregulin signaling in interactions between migrating neurons and radial glia in the developing cerebral cortex. Development 124, 3501–3510.

Arai, Y., Pulvers, J.N., Haffner, C., Schilling, B., Nüsslein, I., Calegari, F., Huttner, W.B. 2011. Neural stem and progenitor cells shorten S-phase on commitment to neuron production. Nat Commun 2, 154–12. doi:10.1038/ncomms1155

Arlotta, P., Molyneaux, B.J., Chen, J., Inoue, J., Kominami, R., Macklis, J.D. 2005. Neuronal Subtype-Specific Genes that Control Corticospinal Motor Neuron Development In Vivo. Neuron 45, 207–221. doi:10.1016/j.neuron.2004.12.036

Armentano, M., Chou, S. J., Srubek Tomassy, G., Leingärtner, A., O'Leary, D.D.M., Studer, M. 2007. COUP-TFI regulates the balance of cortical patterning between frontal/motor and sensory areas. Nat. Neurosci. 10, 1277–1286. doi:10.1038/nn1958

Arshad A., Vose LR., Vinukonda G., Hu F., Yoshikawa K., Csiszar A., et al. 2016. Extended Production of Cortical Interneurons into the Third Trimester of Human Gestation. Cereb Cortex 26, 2242–56. doi:10.1093/cercor/bhv074

Azzarelli, R., Hardwick, L.J.A., Philpott, A. 2015. Emergence of neuronal diversity from patterning of telencephalic progenitors. WIREs Dev Biol 4,

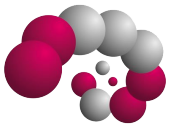

197–214. doi:10.1002/wdev.174

Balaskas, N., Ribeiro, A., Panovska, J., Dessaud, E., Sasai, N., Page, K.M., Briscoe, J., Ribes, V. 2012. Gene Regulatory Logic for Reading the Sonic Hedgehog Signaling Gradient in the Vertebrate Neural Tube. Cell 148, 273–284. doi:10.1016/j.cell.2011.10.047

Baumgardt, M., Karlsson, D., Salmani, B.Y., Bivik, C., MacDonald, R.B., Gunnar, E., Thor, S. 2014. Global Programmed Switch in Neural Daughter Cell Proliferation Mode Triggered by a Temporal Gene Cascade. Developmental Cell 30, 192–208. doi:10.1016/j.devcel.2014.06.021

Baumgardt, M., Karlsson, D., Terriente, J., DIaz-Benjumea, F.J., Thor, S. 2009. Neuronal Subtype Specification within a Lineage by Opposing Temporal Feed-Forward Loops. Cell 139, 969–982. doi:10.1016/j.cell.2009.10.032

Baumgardt, M., Miguel-Aliaga, I., Karlsson, D., Ekman, H., Thor, S. 2007. Specification of Neuronal Identities by Feedforward Combinatorial Coding. PLoS Biol 5, 37–14. doi:10.1371/journal.pbio.0050037

Baye, L.M., Link, B.A. 2008. Nuclear migration during retinal development. Brain Research 1192, 29–36. doi:10.1016/j.brainres.2007.05.021

Baye, L.M., Link, B.A. 2007. Interkinetic Nuclear Migration and the Selection of Neurogenic Cell Divisions during Vertebrate Retinogenesis. J Neuronsci 27, 10143–10152. doi:10.1523/JNEUROSCI.2754-07.2007

Bayraktar, O.A., Doe, C.Q. 2014. Combinatorial temporal patterning in progenitors expands neural diversity. Nature 498, 449–455. doi:10.1038/nature12266

Beattie, R., Postiglione, M.P., Burnett, L.E., Laukoter, S., Streicher, C., Pauler, F.M., Xiao, G., Klezovitch, O., Vasioukhin, V., Ghashghaei, T.H., Hippenmeyer, S. 2017. Mosaic Analysis with Double Markers Reveals Distinct Sequential Functions of Lgl1 in Neural Stem Cells. Neuron 94, 517–533.e3. doi:10.1016/j.neuron.2017.04.012

Bedogni, F., Hodge, R.D., Elsen, G.E., Daza, R.A., Beyer, R.P., Bammler, T.K., Rubenstein, J.L.R., Hevner, R.F. 2010. Tbr1 regulates regional and laminar identity of postmitotic neurons in developing neocortex. Proc Natl Acad Sci U S A 107, 13129-13134. doi:10.1073/pnas.1002285107/-/DCSupplemental/pnas.201002285SI.pdf

Bel-Vialar, S., Itasaki, N., Krumlauf, R. 2002. Initiating Hox gene expression: in the early chick neural tube differential sensitivity to FGF and RA signaling subdivides the HoxB genes in two distinct groups. Development 129, 5103-5115.

Belecky-Adams, T., Cook, B., Alder, R. 1996. Correlations between Terminal Mitosis and Differentiated Fate of Retinal Precursor Cells in Vivo and in Vitro: Analysis with the “Window-Labeling” Technique. Developmental Biology. 178, 304-315. doi:10.1006/dbio.1996.0220

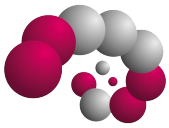

Belliveau, M.J., Young, T.L., Cepko, C.L. 2000. Late Retinal Progenitor Cells Show Intrinsic Limitations in the Production of Cell Types and the Kinetics of Opsin Synthesis. The J Neuronsci. 20(6), 2247-2254. doi: 10.1523/JNEUROSCI.20-06-02247.2000

Bello, B.C., Izergina, N., Caussinus, E., Reichert, H., 2008. Amplification of neural stem cell proliferation by intermediate progenitor cells in Drosophila brain development. Neural Dev 3, 5–18. doi:10.1186/1749-8104-3-5

Benito-Sipos, J., Estacio-Gomez, A., Moris-Sanz, M., Baumgardt, M., Thor, S., Diaz-Benjumea, F.J. 2010. A genetic cascade involving klumpfuss, nab and castor specifies the abdominal leucokinergic neurons in the Drosophila CNS. Development 137, 3327–3336. doi:10.1242/dev.052233

Benito-Sipos, J., Ulvklo, C., Gabilondo, H., Baumgardt, M., Angel, A., Torroja, L., Thor, S. 2011. Seven up acts as a temporal factor during two different stages of neuroblast 5-6 development. Development 138, 5311–5320. doi: 10.1242/dev.070946

Berggren, K., McCaffery, P., Drager, U., Forehand, C. J. 1999. Differential Distribution of Retinoic Acid Synthesis in the Chicken Embryo as Determined by Immunolocalization of the Retinoic Acid Synthetic Enzyme, RALDH-2. Developmental Biology. 210, 288-304. doi: 10.1006/dbio.1999.9286

Bielle, F., Griveau, A., Narboux-Nême, N., Vigneau, S., Sigrist, M., Arber, S., Wassef, M., Pierani, A. 2005. Multiple origins of Cajal-Retzius cells at the borders of the developing pallium. Nat. Neurosci. 8, 1002–1012. doi: 10.1038/nn1511

Bikoff, J.B., Gabitto, M.I., Rivard, A.F., Drobac, E., Machado, T.A., Miri, A., Brenner-Morton, S., Famojure, E., Diaz, C., Alvarez, F.J., Mentis, G.Z., Jessell, T.M. 2016. Spinal Inhibitory Interneuron Diversity Delineates Variant Motor Microcircuits. Cell 165, 207–219. doi:10.1016/j.cell.2016.01.027

Bishop, K.M., Goudreau, G., O'Leary, D.D.M. 2000. Regulation of Area Identity in the Mammalian Neocortex by Emx2 and Pax6. Science 288, 344-349. doi: 10.1126/science.288.5464.344

Blackshaw, S., Harpavat, S., Trimarchi, J., Cai, L., Huang, H., Kuo, W.P., Weber, G., Lee, K., Fraioli, R.E., Cho, S.-H., Yung, R., Asch, E., Ohno-Machado, L., Wong, W.H., Cepko, C. 2004. Genomic Analysis of Mouse Retinal Development. PLoS Biol 2, e247–21. doi:10.1371/journal.pbio.0020247

Blanquie, O., Yang, J.-W., Kilb, W., Sharopov, S., Sinning, A., Luhmann, H.J. 2017. Electrical activity controls area-specific expression of neuronal apoptosis in the mouse developing cerebral cortex. eLife 217;6, e27696. doi: 10.7554/eLife.27696.001

Blaschke, A.J., Staley, K., Chun, J. 1996. Widespread programmed cell death in proliferative and postmitotic regions of the fetal cerebral cortex.

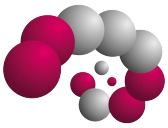

Development 122, 1165-1174.

Boone, J.Q., Doe, C.Q. 2008. Identification of Drosophila type II neuroblast lineages containing transit amplifying ganglion mother cells. Devel Neurobio 68, 1185–1195. doi:10.1002/dneu.20648

Borrell, V., Cárdenas, A., Ciceri, G., Galcerán, J., Flames, N., Pla, R., Nóbrega-Pereira, S., García-Frigola, C., Peregrín, S., Zhao, Z., Le Ma, Tessier-Lavigne, M., Marín, O. 2012. Slit/Robo Signaling Modulates the Proliferation of Central Nervous System Progenitors. Neuron 76, 338–352. doi:10.1016/j.neuron.2012.08.003

Bortone, D.S., Olsen, S.R., Scanziani, M. 2014. Translaminar Inhibitory Cells Recruited by Layer 6 Corticothalamic Neurons Suppress Visual Cortex. Neuron 82, 474–485. doi:10.1016/j.neuron.2014.02.021

Bossing, T., Udolph, G., Doe, C.Q., Technau, G. 1996. The Embryonic Central Nervous System Lineages of Drosophila melanogaster. Developmental Biology 179, 41-64. doi:10.1006/dbio.1996.0240

Briscoe, J., Pierani, A., Jessell, T.M. 2000. A Homeodomain Protein Code Specifies Progenitor Cell Identity and Neuronal Fate in the Ventral Neural Tube. Cell 101, 435-445. doi:10.1016/s0092-8674(00)80853-3

Briscoe, J., Sussel, L., Serup, P., Hartigan-OConnor, D., Jessell, T.M., Rubenstein, J.L.R., Ericson, J. 1999. Homeobox gene Nkx2.2 and specification of neuronal identity by graded Sonic hedgehog signalling. Nature 398, 622-626. doi:10.1038/19315

Britanova, O., de Juan Romero, C., Cheung, A., Kwan, K.Y., Schwark, M., Gyorgy, A., Vogel, T., Akopov, S., Mitkovski, M., Agoston, D., Sestan, N., Molnár, Z., Tarabykin, V. 2008. Satb2 Is a Postmitotic Determinant for Upper-Layer Neuron Specification in the Neocortex. Neuron 57, 378–392. doi:10.1016/j.neuron.2007.12.028

Brodmann, K., Garey, L.J., 1909. Brodmann's Localisation in the Cerebral Cortex: the principles of comparative localisation in the cerebral cortex based on cytoarchitectonics 1–307.

Brown, K.N., Chen, S., Han, Z., Lu, C.H., Tan, X., Zhang, X.J., Ding, L., Lopez-Cruz, A., Saur, D., Anderson, S.A., Huang, K., Shi, S.H. 2011. Clonal Production and Organization of Inhibitory Interneurons in the Neocortex. Science 334, 480–486. doi:10.1126/science.1208884

Brzezinski, J.A., Kim, E.J., Johnson, J.E., Reh, T.A. 2011. Ascl1 expression defines a subpopulation of lineage-restricted progenitors in the mammalian retina. Development 138, 3519–3531. doi:10.1242/dev.064006

Buckingham, M.E., Meilhac, S.M. 2011. Tracing Cells for Tracking Cell Lineage and Clonal Behavior. Developmental Cell 21, 394–409. doi:10.1016/j.devcel.2011.07.019

Butt, S.J.B., Fuccillo, M., Nery, S., Noctor, S., Kriegstein, A., Corbin, J.G.,

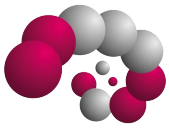

Fishell, G. 2005. The Temporal and Spatial Origins of Cortical Interneurons Predict Their Physiological Subtype. Neuron, 48, 591–604. doi:10.1016/j.neuron.2005.09.034

Cai, D., Cohen, K.B., Luo, T., Lichtman, J.W., Sanes, J.R. 2013. Improved tools for the Brainbow toolbox. Nat Meth 10, 540–547. doi:10.1038/nmeth.2450

Calegari, F. 2005. Selective Lengthening of the Cell Cycle in the Neurogenic Subpopulation of Neural Progenitor Cells during Mouse Brain Development. J Neuronsci 25, 6533–6538. doi:10.1523/JNEUROSCI.0778-05.2005

Carpenter, E.M. 2002. Hox Genes and Spinal Cord Development. Dev Neurosci 24, 24-34. doi:10.1159/000064943

Caviness, V.S., 1982. Neocortical Histogenesis in Normal and Reeler Mice: A Developmental Study Based Upon [3H]Thymidine Autoradiography. Developmental Brain Research 4, 293-302. doi: 10.1016/0165-3806(82)90141-9

Cayouette, M., Barres, B.A., Raff, M. 2003. Importance of Intrinsic Mechanisms in Report Cell Fate Decisions in the Developing Rat Retina. Neuron 40, 897-904. doi:10.1016/s0896-6273(03)00756-6

Cepko, C.L., Austin, C.P., Yang, X., Alexiades, M., Ezzedine, D. 1996. Cell fate determination in the vertebrate. Proc Natl Acad Sci U S A 93, 589-595. doi: 10.1016/j.tins.2012.05.004

Cepko, C., Ryder, E., Austin, C., Golden, J., Fields-Berry, S.C., Lin, J. 2000. Lineage Analysis with Retroviral Vectors. Methods in enzymology 327, 118-145. doi: 10.1016/s0076-6879(00)27272-8

Belliveau, M. J., Cepko, C. 1999. Extrinsic and intrinsic factors control the genesis of amacrine and cone cells in the rat retina. Development 126, 555-566.

Chen, B., Schaevitz, L.R., McConnell, S.K. 2005. Fezl regulates the differentiation and axon targeting of layer 5 subcortical projection neurons in cerebral cortex. Proc Natl Acad Sci U S A 102, 17184-17189. doi:10.1073/pnas.0508732102

Chen, J. G., Rašin, M.-R., Kwan, K.Y., Sestan, N. 2005. Zfp312 is required for subcortical axonal projections and dendritic morphology of deep-layer pyramidal neurons of the cerebral cortex. Proc Natl Acad Sci U S A 102, 17792-17797. doi: 10.1073/pnas.0509032102

Ciceri, G., Dehorter, N., Sols, I., Josh Huang, Z., Maravall, M., Marín, O. 2013. Lineage-specific laminar organization of cortical GABAergic interneurons. Nat. Neurosci 16, 1199-1210. doi:10.1038/,DanaInfo=www.nature.com+nn.3485

Cleary, M.D., Doe, C.Q. 2006. Regulation of neuroblast competence: multiple temporal identity factors specify distinct neuronal fates within a single early competence window. Genes & Development 20, 429-434. doi: 10.1101/gad.

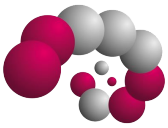

1382206

Clowry GJ. 2015. An enhanced role and expanded developmental origins for gamma-aminobutyric acidergic interneurons in the human cerebral cortex. J Anat. 227, 384–93. doi:10.1111/joa.12198

Crossley, P.H., Martin, G.R. 1995. The mouse Fgf8 gene encodes a family of polypeptides and is expressed in regions that direct outgrowth and patterning in the developing embryo. Development 121, 439-451.

Dasen, J.S., Liu, J.-P., Jessell, T.M. 2003. Motor neuron columnar fate imposed by sequential phases of Hox-c activity. Nature 425, 926-933. doi: https://doi.org/10.1038/nature02051

De Carlos, J.A., López-Mascaraque, L., and Valverde, F. 1996. Dynamics of cell migration from the lateral ganglionic eminence in the rat. J. Neurosci. *16*, 6146–6156. doi: 10.1523/jneurosci.16-19-06146.1996

De la Huerta, I., Kim, I.J., Voinescu, P.E., Sanes, J.R. 2012. Direction-selective retinal ganglion cells arise from molecularly specified multipotential progenitors. Proc Natl Acad Sci U S A 109, 17663-17668. doi:10.1073/pnas.1215806109

De Marco García, N.V., Karayannis, T., Fishell, G. 2012. Neuronal activity is required for the development of specific cortical interneuron subtypes. Nature 472, 351–355. doi:10.1038/nature09865

De Marco García, N.V., Karayannis, T., Fishell, G., 2011. Neuronal activity is required for the development of specific cortical interneuron subtypes. Nature 472, 351–355. doi:10.1038/nature09865

DeFelipe, J., López-Cruz, P.L., Benavides-Piccione, R., Bielza, C., Larrañaga, P., Anderson, S., Burkhalter, A., Cauli, B., Fairén, A., Feldmeyer, D., Fishell, G., Fitzpatrick, D., Freund, T.F., González-Burgos, G., Hestrin, S., Hill, S., Hof, P.R., Huang, J., Jones, E.G., Kawaguchi, Y., Kisvárday, Z., Kubota, Y., Lewis, D.A., Marín, O., Markram, H., McBain, C.J., Meyer, H.S., Monyer, H., Nelson, S.B., Rockland, K., Rossier, J., Rubenstein, J.L.R., Rudy, B., Scanziani, M., Shepherd, G.M., Sherwood, C.C., Staiger, J.F., Tamás, G., Thomson, A., Wang, Y., Yuste, R., Ascoli, G.A. 2013. New insights into the classification and nomenclature of cortical GABAergic interneurons. Nat Rev Neurosci 14, 1–15. doi:10.1038/nrn3444

Dehay, C., Kennedy, H. 2007. Cell-cycle control and cortical development. Nat Rev Neurosci 8, 438–450. doi:10.1038/nrn2097

Dehorter, N., Ciceri, G., Bartolini, G., Lim, L., del Pino, I., Marín, O. 2015. Tuning of fast-spiking interneuron properties by an activity-dependent transcriptional switch. Science 349, 1216–1220. doi:10.1126/science.aab3415

Dehorter, N., Marichal, N., Marín, O., Berninger, B. 2017. Tuning neural circuits by turning the interneuron knob. Current Opinion in Neurobiology 42, 144–151. doi:10.1016/j.conb.2016.12.009

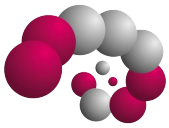

Del Corral, R.D., Storey, K.G. 2004. Opposing FGF and retinoid pathways: a signalling switch that controls differentiation and patterning onset in the extending vertebrate body axis. Bioessays 26, 857–869. doi:10.1002/bies.20080

Desai, A.R.,McConnell, K.S. 2000. Progressive restriction in fate potential by neural progenitors during cerebral cortical development. Development 127, 2863-2872.

Doe, C.Q., 2017. Temporal Patterning in the DrosophilaCNS. Annu. Rev. Cell Dev. Biol. 33, 219–240. doi:10.1146/annurev-cellbio-111315-125210

Doe, C.Q., Technau, G. 1993. Identification and cell lineage of individual neural precursors in the Drosophila CNS. Trends in Neurosciences 16, 510-514. doi: 10.1016/0166-2236(93)90195-R

Douglas, R.J., Martin, K.A.C. 2004. Neuronal circuits of the neocortex. Annu. Rev. Neurosci. 27, 419–451. doi:10.1146/annurev.neuro.27.070203.144152

Eckler, M.J., Nguyen, T.D., McKenna, W.L., Ben L Fastow, Guo, C., Rubenstein, J.L.R., Chen, B. 2015. Cux2-Positive Radial Glial Cells Generate Diverse Subtypes of Neocortical Projection Neurons and Macroglia. Neuron 86, 1100–1108. doi:10.1016/j.neuron.2015.04.020

Elliott, J., Jolicoeur, C., Ramamurthy, V., Cayouette, M. 2008. Ikaros Confers Early Temporal Competence to Mouse Retinal Progenitor Cells. Neuron 60, 26–39. doi:10.1016/j.neuron.2008.08.008

Emerson, M.M., Surzenko, N., Goetz, J.J., Trimarchi, J., Cepko, C. 2013. Otx2 and Onecut1 Promote the Fates of Cone Photoreceptors and Horizontal Cells and Repress Rod Photoreceptors. Developmental Cell 26, 59–72. doi: 10.1016/j.devcel.2013.06.005

Engelhardt, von, J., Khrulev, S., Eliava, M., Wahlster, S., Monyer, H. 2011. 5-HT3A Receptor-Bearing White Matter Interstitial GABAergic Interneurons Are Functionally Integrated into Cortical and Subcortical Networks. J Neuronsci 31, 16844–16854. doi:10.1523/JNEUROSCI.0310-11.2011

Englund, C., Fink, A., Lau, C., Pham, D., Daza, R.A.M., Bulfone, A., Kowalczyk, T., Hevner, R.F. 2005. Pax6, Tbr2, and Tbr1 are expressed sequentially by radial glia, intermediate progenitor cells, and postmitotic neurons in developing neocortex. J Neuronsci 25, 247–251. doi:10.1523/JNEUROSCI.2899-04.2005

Ericson, J., Briscoe, J., Rashbass, P., van Heyningen, V., Jessell, T.M. 1997a. Graded Sonic Hedgehog Signaling and the Specification of Cell Fate in the Ventral Neural Tube. Cold Spring Harbor Symp Quant Biol 62, 451-466. doi: 10.1101/SQB.1997.062.01.053

Ericson, J., Morton, S., Kawakami, A., Roelink, H., Jessell, T.M. 1996. Two Critical Periods of Sonic Hedgehog Signaling Required for the Specification of Motor Neuron Identity. Cell 87, 661-673. doi: 10.1016/s0092-8674(00)81386-0

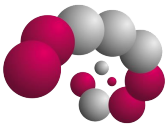

Ericson, J., Rashbass, P., Schedl, A., Brenner-Morton, S., Kawakami, A., van Heyningen, V., Jessell, T.M., Briscoe, J. 1997b. Pax6 Controls Progenitor Cell Identity and Neuronal Fate in Response to Graded Shh Signaling. Cell 90, 169-180. doi: 10.1016/s0092-8674(00)80323-2

Errede, M., Girolano, F., Rizzi, M., Bertossi, M., Roncali, L., Virgintino, D. 2014. The contribution of CXCL12-expressing radial glia cells to neuro-vascular patterning during human cerebral cortex development. Frontiers in Neuroscience 8, 1–11. doi:10.3389/fnins.2014.00324

Fairén, A., Cobas, A., Fonseca, M. 1986. Times of Generation of Glutamic Acid Decarboxylase Immunoreactive Neurons in Mouse Somatosensory Cortex. J Comp Neurol 251, 67-83. doi: 10.1002/cne.902510105

Fernald, R.D. 2006. Casting a Genetic Light on the Evolution of Eyes. Science 313, 1914–1918. doi:10.1126/science.1127889

Fietz, S.A., Kelava, I., Vogt, J., Wilsch-Bräuninger, M., Stenzel, D., Fish, J.L., Corbeil, D., Riehn, A., Distler, W., Nitsch, R., Huttner, W.B. 2010. OSVZ progenitors of human and ferret neocortex are epithelial-like and expand by integrin signaling. Nat. Neurosci 13, 690–699. doi:10.1038/nn.2553

Flames, N., Pla, R., Gelman, D.M., Rubenstein, J.L.R., Puelles, L., Marin, O. 2007. Delineation of Multiple Subpallial Progenitor Domains by the Combinatorial Expression of Transcriptional Codes. J Neuronsci 27, 9682–9695. doi:10.1523/JNEUROSCI.2750-07.2007

Fogarty, M., Grist, M., Gelman, D., Marin, O., Pachnis, V., Kessaris, N. 2007. Spatial Genetic Patterning of the Embryonic Neuroepithelium Generates GABAergic Interneuron Diversity in the Adult Cortex. J Neuronsci 27, 10935–10946. doi:10.1523/JNEUROSCI.1629-07.2007

Franco, S.J., Gil-Sanz, C., Martinez-Garay, I., Espinosa, A., Harkins-Perry, S.R., Ramos, C., Muller, U. 2012. Fate-Restricted Neural Progenitors in the Mammalian Cerebral Cortex. Science 337, 746–749. doi:10.1126/science.1223616

Franco, S.J., Müller, U., 2013. Shaping Our Minds: Stem and Progenitor Cell Diversity in the Mammalian Neocortex. Neuron 77, 19–34. doi:10.1016/j.neuron.2012.12.022

Frazer, S., Prados, J., Niquille, M., Cadilhac, C., Markopoulos, F., Gomez, L., Tomasello, U., Telley, L., Holtmaat, A., Jabaudon, D., Dayer, A. 2017. Transcriptomic and anatomic parcellation of 5-HT3AR expressing cortical interneuron subtypes revealed by single-cell RNA sequencing. Nat Commun 8, 1–12. doi:10.1038/ncomms14219

Gal, J.S., Morozov, Y.M., Ayoub, A.E., Chatterjee, M., Rakic, P., Haydar, T.F. 2006. Molecular and Morphological Heterogeneity of Neural Precursors in the Mouse Neocortical Proliferative Zones. J Neuronsci 26, 1045–1056. doi:10.1523/JNEUROSCI.4499-05.2006

Gao, P., Postiglione, M.P., Krieger, T.G., Hernandez, L., Wang, C., Han, Z.,

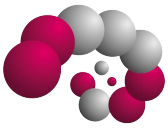

Streicher, C., Papusheva, E., Insolera, R., Chugh, K., Kodish, O., Huang, K., Simons, B.D., Luo, L., Hippenmeyer, S., Shi, S.-H. 2014. Deterministic progenitor behavior and unitary production of neurons in the neocortex. Cell 159, 775–788. doi:10.1016/j.cell.2014.10.027

Gao, P., Sultan, K.T., Zhang, X.J., Shi, S.H. 2013. Lineage-dependent circuit assembly in the neocortex. Development 140, 2645–2655. doi:10.1242/dev.087668

Garcia, M.T., Mazzola, E., Harwell, C.C. 2016. Lineage Relationships Do Not Drive MGE/PoA- Derived Interneuron Clustering in the Brain. Neuron 92, 52–58. doi:10.1016/j.neuron.2016.09.034

Garcia-Moreno, F., Vasistha, N.A., Begbie, J., Molnar, Z. 2014. CLoNe is a new method to target single progenitors and study their progeny in mouse and chick. Development 141, 1589–1598. doi:10.1242/dev.105254

García-Marqués, J., López-Mascaraque, L. 2012. Clonal Identity Determines Astrocyte Cortical Heterogeneity. Cerebral Cortex 23, 1463–1472. doi:10.1093/cercor/bhs134

García-Moreno, F., Molnár, Z. 2015. Subset of early radial glial progenitors that contribute to the development of callosal neurons is absent from avian brain. Proc Natl Acad Sci U S A 112, E5058–E5067. doi:10.1073/pnas.1506377112

Garel, S., Huffman, K.J., Rubenstein, J.L.R. 2003. Molecular regionalization of the neocortex is disrupted in Fgf8 hypomorphic mutants. Development 130, 1903–1914. doi:10.1242/dev.00416

Gaspard, N., Bouschet, T., Hourez, R., Dimidschstein, J., Naeije, G., van den Ameele, J., Espuny-Camacho, I., Herpoel, A., Passante, L., Schiffmann, S.N., Gaillard, A., Vanderhaeghen, P. 2008. An intrinsic mechanism of corticogenesis from embryonic stem cells. Nature 455, 351–357. doi:10.1038/nature07287

Gelman, D.M., Marín, O. 2010. Generation of interneuron diversity in the mouse cerebral cortex. European J Neuronsci 31, 2136–2141. doi:10.1111/j.1460-9568.2010.07267.x

Gelman, D.M., Martini, F.J., Nobrega-Pereira, S., Pierani, A., Kessaris, N., Marin, O. 2009. The Embryonic Preoptic Area Is a Novel Source of Cortical GABAergic Interneurons. J Neuronsci 29, 9380–9389. doi:10.1523/JNEUROSCI.0604-09.2009

Gil-Sanz, C., Espinosa, A., Fregoso, S.P., Bluske, K.K., Cunningham, C.L., Martinez-Garay, I., Zeng, H., Franco, S.J., Müller, U. 2015. Lineage Tracing Using Cux2-Cre and Cux2-CreERT2 Mice. Neuron, 86, 1091–1099. doi:10.1016/j.neuron.2015.04.019

Glickstein, S.B., Monaghan, J.A., Koeller, H.B., Jones, T.K., Ross, M.E. 2009. Cyclin D2 Is Critical for Intermediate Progenitor Cell Proliferation in the Embryonic Cortex. J Neuronsci 29, 9614–9624. doi:10.1523/JNEUROSCI.2284-09.2009

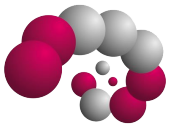

Glickstein, S.B., Moore, H., Slowinska, B., Racchumi, J., Suh, M., Chuhma, N., Ross, M.E. 2007. Selective cortical interneuron and GABA deficits in cyclin D2-null mice. Development 134, 4083–4093. doi:10.1242/dev.008524

Godinho, L., Williams, P.R., Claassen, Y., Provost, E., Leach, S.D., Kamermans, M., Wong, R.O.L., 2007. Nonapical Symmetric Divisions Underlie Horizontal Cell Layer Formation in the Developing Retina In Vivo. Neuron 56, 597–603. doi:10.1016/j.neuron.2007.09.036

Goebbels, S., Bormuth, I., Bode, U., Hermanson, O., Schwab, M.H., Nave, K.-A. 2006. Genetic targeting of principal neurons in neocortex and hippocampus of NEX-Cre mice. Genesis 44, 611–621. doi:10.1002/dvg.20256

Golden, J.A., Fields-Berry, S.C., Cepko, C.L. 1995. Construction and characterization of a highly complex retroviral library for lineage analysis. Proc Natl Acad Sci U S A 92, 5704-5708. doi:10.1073/pnas.92.12.5704

Gomes, F.L.A.F., Zhang, G., Carbonell, F., Correa, J.A., Harris, W.A., Simons, B.D., Cayouette, M. 2010. Reconstruction of rat retinal progenitor cell lineages in vitro reveals a surprising degree of stochasticity in cell fate decisions. Development 138, 227–235. doi:10.1242/dev.059683

Götz, M., Huttner, W.B. 2005. The cell biology of neurogenesis. Nat Rev Mol Cell Biol 6, 777–788. doi:10.1038/nrm1739

Götz, M., Stoykova, A., Gruss, P. 1998. Pax6 Controls Radial Glia Differentiation in the Cerebral Cortex. Neuron 21, 1031-1044. doi: 10.1016/s0896-6273(00)80621-2

Govindan, S., Oberst, P., Jabaudon, D. 2018. In vivo pulse labeling of isochronic cohorts of cells in the central nervous system using FlashTag. Nat Protoc 13, 2297–2311. doi:10.1038/s41596-018-0038-1

Greig, L.C., Woodworth, M.B., Galazo, M.J., Padmanabhan, H., Macklis, J.D. 2013. Molecular logic of neocortical projection neuron specification, development and diversity. Nat Rev Neurosci 14, 755–769. doi:10.1038/nrn3586

Grosskortenhaus, R., Robinson K.J., Doe, C. 2006. Pdm and Castor specify late-born motor neuron identity in the NB7-1 lineage. Genes & Development 20, 2618–2627. doi:10.1101/gad.1445306

Grosskortenhaus, R., Pearson, B.J., Marusich, A., Doe, C.Q. 2005. Regulation of Temporal Identity Transitions in Drosophila Neuroblasts. Developmental Cell 8, 193–202. doi:10.1016/j.devcel.2004.11.019

Guillemot, F., Joyner, A. 1993. Dynamic expression of the murine *Achaete-Scute* homologe *Mash-1* in the developing nervous system. Mech Dev 42, 171-185. doi: 10.1016/0925-4773(93)90006-j

Guo, C., Eckler, M.J., McKenna, W.L., McKinsey, G.L., Rubenstein, J.L.R., Chen, B. 2013. Fezf2 expression identifies a multipotent progenitor for neocortical projection neurons, astrocytes, and oligodendrocytes. Neuron 80,

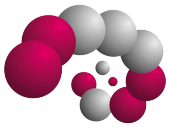

1167–1174. doi:10.1016/j.neuron.2013.09.037

Hafler, B.P., Surzenko, N., Beier, K.T., Punzo, C., Trimarchi, J.M., Kong, J.H., Cepko, C.L. 2012. Transcription factor Olig2 defines subpopulations of retinal progenitor cells biased toward specific cell fates. Proc Natl Acad Sci U S A 109, 7882-7887. doi:10.1073/pnas.1203138109

Halliday, A.L., Cepko, C.L. 1992. Generation and Migration of Cells in the Developing Striatum. Neuron 9, 15-26. doi:10.1016/0896-6273(92)90216-Z

Hamasaki, T., Leingärtner, A., Ringstedt, T., O'Leary, D.D.M. 2004. EMX2 Regulates Sizes and Positioning of the Primary Sensory and Motor Areas in Neocortex by Direct Specification of Cortical Progenitors. Neuron 43, 359–372. doi:10.1016/j.neuron.2004.07.016

Han, W., Kwan, K.Y., Shim, S., Lam, M.M.S., Shin, Y., Xu, X., Zhu, Y., Li, M., Sestan, N. 2011. TBR1 directly represses Fezf2 to control the laminar origin and development of the corticospinal tract. Proc Natl Acad Sci U S A 108, 3041-3046. doi:10.1073/pnas.1016723108

Hansen, D.V., Lui, J.H., Flandin, P., Yoshikawa, K., Rubenstein, J.L., Alvarez-Buylla, A., Kriegstein, A.R. 2013. Non-epithelial stem cells and cortical interneuron production in the human ganglionic eminences. Nature Publishing Group 16, 1576–1587. doi:10.1038/nn.3541

Hansen, D.V., Lui, J.H., Parker, P.R.L., Kriegstein, A.R. 2010. Neurogenic radial glia in the outer subventricular zone of human neocortex. Nature 464, 554–561. doi:10.1038/nature08845

Harb, K., Magrinelli, E., Nicolas, C.S., Lukianets, N., Frangeul, L., Pietri, M., Sun, T., Sandoz, G., Grammont, F., Jabaudon, D., Studer, M., Alfano, C. 2016. Area-specific development of distinct projection neuron subclasses is regulated by postnatal epigenetic modifications. eLife 5, e09531. doi: 10.7554/eLife.09531

Harris, J.A., Mihalas, S., Hirokawa, K.E., Whitesell, J.D., Knox, J., Bernard, A., Bohn, P., Caldejon, S., Casal, L., Cho, A., Feng, D., Gaudreault, N., Graddis, N., Groblewski, P.A., Henry, A., Ho, A., Howard, R., Kuan, L., Lecoq, J., Luviano, J., McConoghy, S., Mortrud, M., Naeemi, M., Ng, L., Oh, S.W., Ouellette, B., Sorensen, S., Wakeman, W., Wang, Q., Williford, A., Phillips, J., Koch, C., Zeng, H. 2019. Hierarchical organization of cortical and thalamic connectivity. Nature 575, 195-202. doi:10.1038/s41586-019-1716-z

Harwell, C.C., Fuentealba, L.C., Gonzalez-Cerrillo, A., Parker, P.R.L., Gertz, C.C., Mazzola, E., Garcia, M.T., Alvarez-Buylla, A., Cepko, C.L., Kriegstein, A.R. 2015. Wide Dispersion and Diversity of Clonally Related Inhibitory Interneurons. Neuron 87, 1–10. doi:10.1016/j.neuron.2015.07.030

Haubensak, W., Attardo, A., Denk, W., Huttner, W.B. 2004. Neurons arise in the basal neuroepithelium of the early mammalian telencephalon: A major site of neurogenesis. Proc Natl Acad Sci U S A 101, 3196-3201. doi:10.1073/pnas.0308600100

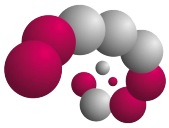

Haydar, T.F., Eugenius Ang, J., Rakic, P. 2003. Mitotic spindle rotation and mode of cell division in the developing telencephalon. Proc Natl Acad Sci U S A 100, 2890-2895. doi:10.1073/pnas.0437969100

He, J., Zhang, G., Almeida, A.D., Cayouette, M., Simons, B.D., Harris, W.A., 2012. How Variable Clones Build an Invariant Retina. Neuron 75, 786–798. doi:10.1016/j.neuron.2012.06.033

He, M., Tucciarone, J., Lee, S., Nigro, M.J., Kim, Y., Levine, J.M., Kelly, S.M., Krugikov, I., Wu, P., Chen, Y., Gong, L., Hou, Y., Osten, P., Rudy, B., Huang, Z.J. 2016. Strategies and Tools for Combinatorial Targeting of GABAergic Neurons in Mouse Cerebral Cortex. Neuron 91, 1–17. doi:10.1016/j.neuron.2016.08.021

Heins, N., Malatesta, P., Cecconi, F., Nakafuku, M., Tucker, K.L., Hack, M.A., Chapouton, P., Barde, Y.-A., Götz, M. 2002. Glial cells generate neurons: the role of the transcription factor Pax6. Nat. Neurosci. 5, 308–315. doi:10.1038/nn828

Hébert, J.M., Fishell, Gord. 2008. The genetics of early telencephalon patterning: some assembly required. Nat Rev Neurosci 9, 678–685. doi:10.1038/nrn2463

Hilscher, M.M., Leão, R.N., Edwards, S.J., Leão, K.E., Kullander, K., 2017. Chrna2-Martinotti Cells Synchronize Layer 5 Type A Pyramidal Cells via Rebound Excitation. PLoS Biol 15, 2–26. doi:10.1371/journal.pbio.2001392

Hippenmeyer, S., Youn, Y.H., Moon, H.M., Miyamichi, K., Zong, H., Wynshaw-Boris, A., Luo, L. 2010. Genetic Mosaic Dissection of Lis1 and Ndel1 in Neuronal Migration. Neuron 68, 695–709. doi:10.1016/j.neuron.2010.09.027

Holt, C.E., Bertsch, T.W., Ellis, H.M., Harris, W.A. 1988. Cellular Determination in the Xenopus Retina Is Independent of Lineage and Birth Date. Neuron 1, 15-26. doi:10.1016/0896-6273(88)90205-x

Horton, J.C., Adams, D.L. 2005. The cortical column: a structure without a function. Philosophical Transactions of the Royal Society B: Biological Sciences 360, 837–862. doi:10.1098/rstb.2005.1623

Hu, H., Gan, J., Jonas, P. 2014. Fast-spiking, parvalbumin+ GABAergic interneurons: From cellular design to microcircuit function. Science 345, 1255263–1255263. doi:10.1126/science.1255263

Hubel, D.H., Wiesel, T.N., 1969. Anatomical Demonstration of Columns in the Monkey Striate. Nature 221, 747-750. doi:10.1038/221747a0

Hubel, D.H., Wiesel, T.N. 1968. Receptive fields and functional architecture of monkey striate cortex. J Physiol 195, 215-243. doi: 10.1113/jphysiol.1968.sp008455

Hubel, D.H., Wiesel, T.N., 1963. Shape and arragement of colums in cat's striate cortex. J Physiol 165, 559-568. doi:10.1113/jphysiol.1963.sp007079

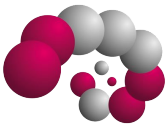

Inan, M., Welagen, J., Anderson, S.A. 2012. Spatial and Temporal Bias in the Mitotic Origins of Somatostatin- and Parvalbumin-Expressing Interneuron Subgroups and the Chandelier Subtype in the Medial Ganglionic Eminence. Cerebral Cortex 22, 820–827. doi:10.1093/cercor/bhr148

Isshiki, T., Pearson, B.J., Holbrook, S., Doe, C.Q. 2001. Drosophila Neuroblasts Sequentially Express Transcription Factors which Specify the Temporal Identity of Their Neuronal Progeny. Cell 106, 511-521. doi:10.1016/S0092-8674(01)00465-2

Ito, M., Masuda, N., Shinomiya, K., Endo, K., Ito, K. 2013. Systematic Analysis of Neural Projections Reveals Clonal Composition of the Drosophila Brain. Current Biology 23, 644–655. doi:10.1016/j.cub.2013.03.015

Jabaudon, D. 2017. Fate and freedom in developing neocortical circuits. Nat Commun 8, 1–9. doi:10.1038/ncomms16042

Jasoni, C., Reh, T. 1996. Temporal and Spatial Pattern of *MASH-1* Expression in Developing Rat Retina Demostrates Progenitor Cell Heterogeneity. J Comp Neurol 369, 319-327. doi: 10.1002/(SICI)1096-9861(19960527)369:2<319::AID-CNE11>3.0.CO;2-C

Jensen, A.M., Raff, M.C. 1997. Continuous Observation of Multipotential Retinal Progenitor Cells in Clonal Density Culture. Dev Biol 188, 267-279. doi:10.1006/dbio.1997.8645

Jessell, T.M., 2000. Neuronal Specification in the Spinal Cord: Inductive Signals and Transcriptonal Codes. Nat Rev Genet. 1, 20-29. doi:10.1038/35049541

Jiang, X., Shen, S., Cadwell, C.R., Berens, P., Sinz, F., Ecker, A.S., Patel, S., Tolias, A.S. 2015. Principles of connectivity among morphologically defined cell types in adult neocortex. Science 350, 9462–9462. doi:10.1126/science.aac9462

Johnston, R.J., Jr., Desplan, C. 2010. Stochastic Mechanisms of Cell Fate Specification that Yield Random or Robust Outcomes. Annu. Rev. Cell Dev. Biol. 26, 689–719. doi:10.1146/annurev-cellbio-100109-104113

Kaplan, E.S., Ramos-Laguna, K.A., Mihalas, A.B., Daza, R.A.M., Hevner, R.F. 2017. Neocortical Sox9+ radial glia generate glutamatergic neurons for all layers, but lack discernible evidence of early laminar fate restriction. Neural Dev 12, 1–10. doi:10.1186/s13064-017-0091-4

Kawaguchi, Y., Kubota, Y. 1998. Neurochemical Features and Synaptic Connections of Large Physiologically-Identified GABAergic Cells in the Rat Frontal Cortex. Neuroscience 85, 677-701. doi:10.1016/s0306-4522(97)00685-4

Kelly, S.M., Raudales, R., He, M., Lee, J.H., Kim, Y., Gibb, L.G., Wu, P., Matho, K., Osten, P., Graybiel, A.M., Huang, Z.J. 2018. Radial Glial Lineage Progression and Differential Intermediate Progenitor Amplification Underlie Striatal Compartments and Circuit Organization. Neuron 99, 345–361. doi:10.1016/j.neuron.2018.06.021

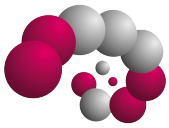

Kelly, S.M., Raudales, R., Moissidis, M., Kim, G., Huang, Z.J. 2019. Multipotent radial glia progenitors and fate-restricted intermediate progenitors sequentially generate diverse cortical interneuron types. bioRxiv. doi: 10.1101/735019

Kepecs, A., Fishell, Gordon 2014. Interneuron cell types are fit to function. Nature 505, 318–326. doi:10.1038/nature12983

Kessaris, N., Fogarty, M., Iannarelli, P., Grist, M., Wegner, M., Richardson, W.D. 2006. Competing waves of oligodendrocytes in the forebrain and postnatal elimination of an embryonic lineage. Nat. Neurosci. 9, 173–179. doi: 10.1038/nn1620

Kmita, M., Duboule, D. 2003. Organizing Axes in Time and Space; 25 Years of Colinear Tinkering. Science 301, 331-333. doi:10.1126/science.1085753

Kohwi, M., Doe, C.Q. 2013. Temporal fate specification and neural progenitor competence during development. Nat Rev Neurosci 14, 823–838. doi: 10.1038/nrn3618

Kretzschmar, K., Watt, F.M. 2012. Lineage Tracing. Cell 148, 33–45. doi: 10.1016/j.cell.2012.01.002

Kriegstein, A.R., Götz, M. 2003. Radial glia diversity: A matter of cell fate. Glia 43, 37–43. doi:10.1002/glia.10250

Lange, C., Huttner, W.B., Calegari, F. 2009. Cdk4/CyclinD1 Overexpression in Neural Stem Cells Shortens G1, Delays Neurogenesis, and Promotes the Generation and Expansion of Basal Progenitors. Cell Stem Cell 5, 320–331. doi:10.1016/j.stem.2009.05.026

Lange, C., and Calegari, F. 2014. Cdks and cyclins link G 1length and differentiation of embryonic, neural and hematopoietic stem cells. Cell Cycle *9*, 1893–1900. doi: 10.4161/cc.9.10.11598

Langer, S.J., Ghafoori, P., Byrd, M., Leinwand, L. 2002. A genetic screen identifies novel non-compatible loxP sites. Nucleic Acid Res 30, 3067-3077.

Lavdas, A.A., Grigoriou, M., Pachnis, V., Parnavelas, J.G. 1999. The Medial Ganglionic Eminence Gives Rise to a Population of Early Neurons in the Developing Cerebral Cortex. J Neurosci 99, 7881-7888. doi:10.1523/JNEUROSCI.19-18-07881.1999

Lee, G., Saito, I. 1998. Role of nucleotide sequences of loxP spacer region in Cre-mediated recombination. Gene 216, 55-65. doi:10.1016/s0378-1119(98)00325-4

Lee, S., Hjerling-Leffler, J., Zagha, E., Fishell, G., Rudy, B. 2010. The Largest Group of Superficial Neocortical GABAergic Interneurons Expresses Ionotropic Serotonin Receptors. J Neurosci 30, 16796–16808. doi:10.1523/JNEUROSCI.1869-10.2010

Lehtinen, M.K., Walsh, C.A. 2011. Neurogenesis at the Brain–Cerebrospinal

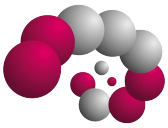

Fluid Interface. Annu. Rev. Cell Dev. Biol. 27, 653–679. doi:10.1146/annurev-cellbio-092910-154026

Lehtinen, M.K., Zappaterra, M.W., Chen, X., Yang, Y.J., Hill, A.D., Lun, M., Maynard, T., Gonzalez, D., Kim, S., Ye, P., D'Ercole, A.J., Wong, E.T., LaMantia, A.S., Walsh, C.A. 2011. The Cerebrospinal Fluid Provides a Proliferative Niche for Neural Progenitor Cells. Neuron 69, 893–905. doi:10.1016/j.neuron.2011.01.023

Leone, D.P., Heavner, W.E., Ferenczi, E.A., Dobreva, G., Huguenard, J.R., Grosschedl, R., McConnell, S.K. 2015. Satb2 Regulates the Differentiation of Both Callosal and Subcerebral Projection Neurons in the Developing Cerebral Cortex. Cereb. Cortex 25, 3406–3419. doi:10.1093/cercor/bhu156

Leone, D.P., Srinivasan, K., Chen, B., Alcamo, E., McConnell, S.K. 2008. The determination of projection neuron identity in the developing cerebral cortex. Current Opinion in Neurobiology 18, 28–35. doi:10.1016/j.conb.2008.05.006

Lim, L., Mi, D., Llorca, A., Marín, O., 2018a. Development and Functional Diversification of Cortical Interneurons. Neuron 100, 294–313. doi:10.1016/j.neuron.2018.10.009

Lim, L., Pakan, J.M.P., Selten, M.M., Marques-Smith, A.X., Llorca, A., Bae, S.E., Rochefort, N.L., Marín, O. 2018b. Optimization of interneuron function by direct coupling of cell migration and axonal targeting. Nat Neurosci 21, 1–18. doi:10.1038/s41593-018-0162-9

Liu, J.-P., Laufer, E., Jessell, T.M. 2001. Assigning the Positional Identity of Spinal Motor Neurons: Rostrocaudal Patterning of Hox-c Expression by FGFs, Gdf11, and Retinoids. Neuron 32, 997-1012. doi:10.1016/s0896-6273(01)00544-x

Livesey, F.J., Cepko, C.L. 2001.Vertebrate neural cell-fate determination: Lessons from the retina. Nat Rev Neuorsci 2, 109-118. doi:10.1038/35053522

Livet, J., Weissman, T.A., Kang, H., Draft, R.W., Lu, J., Bennis, R.A., Sanes, J.R., Lichtman, J.W. 2007. Transgenic strategies for combinatorial expression of fluorescent proteins in the nervous system. Nature 450, 56–62. doi:10.1038/nature06293

Lodato, S., Arlotta, P. 2015. Generating Neuronal Diversity in the Mammalian Cerebral Cortex. Annu Rev Cell Dev Bio 31, 699–720. doi:10.1146/annurev-cellbio-100814-125353

Lodato, S., Rouaux, C., Quast, K.B., Jantrachotechatchawan, C., Studer, M., Hensch, T.K., Arlotta, P. 2011. Excitatory Projection Neuron Subtypes Control the Distribution of Local Inhibitory Interneurons in the Cerebral Cortex. Neuron 69, 763–779. doi:10.1016/j.neuron.2011.01.015

LoTurco, J.J., Owens, D.F., Heath, M.J.S., Davis, M.B.E., Kriegstein, A.R. 1995. GABA and glutamate depolarize cortical progenitor cells and inhibit DNA

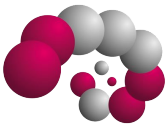

synthesis. Neuron 15, 1287–1298. doi:10.1016/0896-6273(95)90008-X

Loulier, K., Barry, R., Mahou, P., Le Franc, Y., Supatto, W., Matho, K.S., Ieng, S., Fouquet, S., Dupin, E., Benosman, R., Chédotal, A., Beaurepaire, E., Morin, X., Livet, J. 2014. Multiplex Cell and Lineage Tracking with Combinatorial Labels. Neuron 81, 505–520. doi:10.1016/j.neuron.2013.12.016

Lui, J.H., Hansen, D.V., Kriegstein, A.R. 2011. Development and Evolution of the Human Neocortex. Cell 146, 18–36. doi:10.1016/j.cell.2011.06.030

Lundgren, S.E., Callahan, C.A., Thor, S., Thomas, J.B. 1995. Control of neuronal pathway selection by the Drosophila LIM homeodomain gene apterous. Development 121, 1769-1773.

Luskin, M.B., Pearlman, A.L., Sanes, J.R. 1988. Cell lineage in the Cerebral Cortex of the Mouse Studied In Vivo and In Vitro with a Recombinant Retrovirus. Neuron 1, 635-647. doi: 10.1016/0896-6273(88)90163-8

Ma, T., Wang, C., Wang, L., Zhou, X., Tian, M., Zhang, Q., Zhang, Y., Li, J., Liu, Z., Cai, Y., Liu, F., You, Y., Chen, C., Campbell, K., Song, H., Ma, L., Rubenstein, J.L., Yang, Z. 2013. Subcortical origins of human and monkey neocortical interneurons. Nat Neurosci 16, 1588–1597. doi:10.1038/nn.3536

Madisen, L., Zwingman, T.A., Sunkin, S.M., Oh, S.W., Zariwala, H.A., Gu, H., Ng, L.L., Palmiter, R.D., Hawrylycz, M.J., Jones, A.R., Lein, E.S., Zeng, H. 2009. A robust and high-throughput Cre reporting and characterization system for the whole mouse brain. Nat Neurosci 13, 133–140. doi:10.1038/nn.2467

Magrinelli, E., Wagener, R.J., Jabaudon, D. 2018. Simultaneous production of diverse neuronal subtypes during early corticogenesis. bioRxiv. doi: 10.1101/369678

Mahmood, R., Kiefer, P., Guthire, S., Dickson, C., Mason, I. 1995. Multiple roles for FGF-3 during cranial neural development in the chicken. Development 121, 1399-1410.

Malatesta P., Hartfuss, E., Götz, M. 2000. Isolation of radial glial cells by fluorescent-activated cell sorting reveals a neuronal lineage. Development 127, 5253-5263.

Marin, O., Valiente, M., Ge, X., Tsai, L.H. 2010. Guiding Neuronal Cell Migrations. Cold Spring Harb Perspect Biol 2, a001834. doi:10.1101/cshperspect.a001834

Marín, O., Müller, U. 2014. Lineage origins of GABAergic versus glutamatergic neurons in the neocortex. Current Opinion in Neurobiology 26, 132–141. doi:10.1016/j.conb.2014.01.015

Marín, O., Rubenstein, J.L.R. 2001. A long, remarkable journey: Tangential migration in the thelencephalon. Nat Rev Neurosci 2, 780-790. doi: 10.1038/35097509

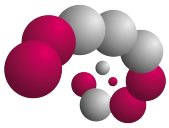

Martinez-Morales, J.-R., Del Bene, F., Nica, G., Hammerschmidt, M., Bovolenta, P., Wittbrodt, J. 2005. Differentiation of the Vertebrate Retina Is Coordinated by an FGF Signaling Center. Dev Cell 8, 565–574. doi:10.1016/j.devcel.2005.01.022

Martynoga, B., Morrison, H., Price, D.J., Mason, J.O. 2005. Foxg1 is required for specification of ventral telencephalon and region-specific regulation of dorsal telencephalic precursor proliferation and apoptosis. Developmental Biology 283, 113–127. doi:10.1016/j.ydbio.2005.04.005

Masland, R.H., 2012. The Neuronal Organization of the Retina. Neuron 76, 266–280. doi:10.1016/j.neuron.2012.10.002

Maximiliano José, N., Hashikawa, Y., Rudy, B. 2018. Diversity and connectivity of layer 5 somatostatin-expressing interneurons in the mouse barrel cortex. J Neurosci 38, 1622-1633. doi:10.1523/JNEUROSCI.2415-17.2017

Mayer, C., Bandler, R.C., Fishell, G. 2016. Lineage Is a Poor Predictor of Interneuron Positioning within the Forebrain. Neuron 92, 45–51. doi:10.1016/j.neuron.2016.09.035

Mayer, C., Hafemeister, C., Bandler, R.C., Machold, R., Brito, R.B., Jaglin, X., Allaway, K., Butler, A., Fishell, G., Satija, R. 2018. Developmental diversification of cortical inhibitory interneurons. Nature 555, 457–462. doi:10.1038/nature25999

Mayer, C., Jaglin, X.H., Cobbs, L.V., Bandler, R.C., Streicher, C., Cepko, C.L., Hippenmeyer, S., Fishell, G. 2015. Clonally Related Forebrain Interneurons Disperse Broadly across Both Functional Areas and Structural Boundaries. Neuron 87, 1–11. doi:10.1016/j.neuron.2015.07.011

McCarthy, M., Turnbull, D.H., Walsh, C.A., Fishell, G. 2001. Telencephalic Neural Progenitors Appear To Be Restricted to Regional and Glial Fates before the Onset of Neurogenesis. J Neuronsci 21, 6772-6781. doi:10.1523/JNEUROSCI.21-17-06772.2001

McKenna, W.L., Betancourt, J., Larkin, K.A., Abrams, B., Guo, C., Rubenstein, J.L.R., Chen, B. 2011. Tbr1 and Fezf2 Regulate Alternate Corticofugal Neuronal Identities during Neocortical Development. J Neuronsci 31, 549–564. doi:10.1523/JNEUROSCI.4131-10.2011

Mettler, U. 2006. Timing of identity: spatiotemporal regulation of hunchback in neuroblast lineages of Drosophila by Seven-up and Prospero. Development 133, 429–437. doi:10.1242/dev.02229

Mi, D., Li, Z., Lim, L., Li, M., Moissidis, M., Yang, Y., Gao, T., Hu, T.X., Pratt, T., Price, D.J., Sestan, N., Marín, O. 2018. Early emergence of cortical interneuron diversity in the mouse embryo. Science 360, 81-85. doi:10.1126/science.aar6821

Mihalas, A.B., Elsen, G.E., Bedogni, F., Daza, R.A.M., Ramos-Laguna, K.A., Arnold, S.J., Hevner, R.F. 2016. Intermediate Progenitor Cohorts Differentially Generate Cortical Layers and Require Tbr2 for Timely

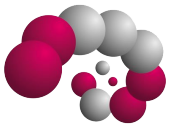

Acquisition of Neuronal Subtype Identity. CellReports 16, 92–105. doi: 10.1016/j.celrep.2016.05.072

Mihalas, A.B., Hevner, R.F. 2018. Clonal analysis reveals laminar fate multipotency and daughter cell apoptosis of mouse cortical intermediate progenitors. Development 145, dev164335–7. doi:10.1242/dev.164335

Miyata, T., 2004. Asymmetric production of surface-dividing and non-surface-dividing cortical progenitor cells. Development 131, 3133–3145. doi: 10.1242/dev.01173

Miyata, T., Kawaguchi, A., Okano, H., Ogawa, M., 2001. Asymmetric Inheritance of Radial Glial Fibers by Cortical Neurons. Neuron 31, 727-741. doi:10.1016/s0896-6273(01)00420-2

Miyoshi, G., Butt, S.J.B., Takebayashi, H., Fishell, G. 2007. Physiologically Distinct Temporal Cohorts of Cortical Interneurons Arise from Telencephalic Olig2-Expressing Precursors. J Neuronsci 27, 7786–7798. doi:10.1523/ JNEUROSCI.1807-07.2007

Miyoshi, G., Hjerling-Leffler, J., Karayannis, T., Sousa, V.H., Butt, S.J.B., Battiste, J., Johnson, J.E., Machold, R.P., Fishell, G. 2010. Genetic Fate Mapping Reveals That the Caudal Ganglionic Eminence Produces a Large and Diverse Population of Superficial Cortical Interneurons. J Neuronsci 30, 1582–1594. doi:10.1523/JNEUROSCI.4515-09.2010

Mizutani, K.-I., Yoon, K., Dang, L., Tokunaga, A., Gaiano, N. 2007. Differential Notch signalling distinguishes neural stem cells from intermediate progenitors. Nature 449, 351–355. doi:10.1038/nature06090

Molnár Z., Métin C., Stoykova A., Tarabykin V., Price DJ., Francis F., Meyer, G., Dehay, C., Kennedy H. 2006. Comparative aspects of cerebral cortical development. Eur J Neurosci.;23(4),921–34. doi:10.1111/j. 1460-9568.2006.04611

Molyneaux, B.J., Arlotta, P., Hirata, T., Hibi, M., Macklis, J.D. 2005. Fezl Is Required for the Birth and Specification of Corticospinal Motor Neurons. Neuron 47, 817–831. doi:10.1016/j.neuron.2005.08.030

Molyneaux, B.J., Arlotta, P., Menezes, J.R.L., Macklis, J.D. 2007. Neuronal subtype specification in the cerebral cortex. Nat Rev Neurosci 8, 427–437. doi:10.1038/nrn2151

Molyneaux, B.J., Goff, L.A., Brettler, A.C., Chen, H.-H., Brown, J.R., Hrvatin, S., Rinn, J.L., Arlotta, P. 2015. DeCoN: Genome-wide Analysis of In Vivo Transcriptional Dynamics during Pyramidal Neuron Fate Selection in Neocortex. Neuron 85, 275–288. doi:10.1016/j.neuron.2014.12.024

Mort, R.L., Ford, M.J., Sakaue-Sawano, A., Lindstrom, N.O., Casadio, A., Douglas, A.T., Keighren, M.A., Hohenstein, P., Miyawaki, A., Jackson, I.J. 2014. Fucci2a:A bicistronic cell cycle reporter that allows Cre mediated tissue specific expression in mice. Cell Cycle 13, 2681–2696. doi: 10.4161/15384101.2015.945381

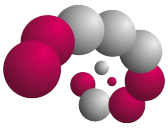

Mountcastle, V.B. 1997. The columnar organization of the neocortex. Brain 120, 701-722. doi: 10.1093/brain/120.4.701

Muzio, L., Di Benedetto, B., Stoykova, A., Boncinelli, E., Gruss, P., Mallamaci, A. 2002. Emx2 and Pax6 Control Regionalization of the Pre-neuronogenic Cortical Primordium. Cerebral Cortex 12, 129–139. doi:10.1093/cercor/12.2.129

Nakamura, K., Harada, C., Namekata, K., Harada, T. 2006. Expression of olig2 in retinal progenitor cells. Dev Neurosci 17, 345-349. doi: 10.1097/01.wnr.0000203352.44998.6b

Nakashima, M., Toyono, T., Akamine, A., Joyner, A. 1999. Expression of growth/differentiation factor 11, a new member of the BMP/ TGFb superfamily during mouse embryogenesis. Mech Dev 80, 185-189. doi: 10.1016/s0925-4773(98)00205-6

Nelson, B.R., Hodge, R.D., Bedogni, F., Hevner, R.F. 2013. Dynamic Interactions between Intermediate Neurogenic Progenitors and Radial Glia in Embryonic Mouse Neocortex: Potential Role in Dll1-Notch Signaling. J Neuronsci 33, 9122–9139. doi:10.1523/JNEUROSCI.0791-13.2013

Nery, S., Fishell, G., Corbin, J.G. 2002. The caudal ganglionic eminence is a source of distinct cortical and subcortical cell populations. Nat. Neurosci. 5, 1279–1287. doi:10.1038/nn971

Neumann, C.J., Nuesselein-Volhard, C. 2000. Patterning of the Zebrafish Retina by a Wave of Sonic Hedgehog Activity. Science 289, 2137-2139. doi: 10.1126/science.289.5487.2137

Niederreither, K., McCaffery, P., Dräger, U.C., Chambon, P., Dollé, P. 1997. Restricted expression and retinoic acid-induced downregulation of the retinaldehyde dehydrogenase type 2 (RALDH-2) gene during mouse development. Mech Dev 62, 67-78. doi:10.1016/s0925-4773(96)00653-3

Niquille, M., Limoni, G., Markopoulos, F., Cadilhac, C., Prados, J., Holtmaat, A., Dayer, A. 2018. Neurogliaform cortical interneurons derive from cells in the preoptic area. eLife 2018;7, 1–24. doi:10.7554/eLife.32017.001

Niswander, L., Martin, G.R. 1992. expression during gastrulation, myogenesis, limb and tooth development in the mouse. Development 114, 755-768.

Nobrega-Pereira, S., Gelman, D., Bartolini, G., Pla, R., Pierani, A., Marin, O. 2010. Origin and Molecular Specification of Globus Pallidus Neurons. J Neuronsci 30, 2824–2834. doi:10.1523/JNEUROSCI.4023-09.2010

Noctor, S.C., Flint, A.C., Weissman, T.A., Dammerman, R.S., Kriegstein, A.R. 2001. Neurons derived from radial glial cells establish radial units in neocortex. Nature 408, 714-720. doi:10.1038/35055553

Noctor, S.C., Martínez-Cerdeño, V., Ivic, L., Kriegstein, A.R. 2004. Cortical neurons arise in symmetric and asymmetric division zones and migrate through specific phases. Nat. Neurosci. 7, 136–144. doi:10.1038/nn1172

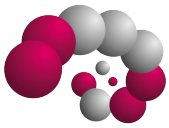

Oberst, P., Agirman, G., Jabaudon, D. 2019. Principles of progenitor temporal patterning in the developing invertebrate and vertebrate nervous system. Current Opinion in Neurobiology 56, 185–193. doi:10.1016/j.conb.2019.03.004

Oberst, P., Fievre, S., Baumann, N., Concetti, C., Jabaudon, D. 2019. Temporal plasticity of apical progenitors in the developing mouse neocortex. Nature 573, 370-374. doi:10.1038/s41586-019-1515-6

Okamoto, M., Miyata, T., Konno, D., Ueda, H.R., Kasukawa, T., Hashimoto, M., Matsuzaki, F., Kawaguchi, A. 2016. Cell-cycle-independent transitions in temporal identity of mammalian neural progenitor cells. Nat Commun 7:11349. doi:10.1038/ncomms11349

Oláh, S., Komlósi, G., Szabadics, J., Varga, C., Tóth, É., Barzó, P., Tamás, G. 2007. Output of neurogliaform cells to various neuron types in the human and rat cerebral cortex. Front Neural Circuits 1, 1–7. doi:10.3389/neuro.04/004.2007

Pearson, B.J., Doe, C.Q. 2004. Specification of temporal identity in the developing nervous system. Annu. Rev. Cell Dev. Biol. 20, 619–647. doi:10.1146/annurev.cellbio.19.111301.115142

Pearson, B.J., Doe, C.Q. 2003. Regulation of neuroblast competence in Drosophila. Nature 425, 620–624. doi:10.1038/nature02024

Petros, T.J., Bultje, R.S., Ross, M.E., Fishell, G., Anderson, S.A. 2015. Apical versus Basal Neurogenesis Directs Cortical Interneuron Subclass Fate. Cell Rep 13, 1090–1095. doi:10.1016/j.celrep.2015.09.079

Pfeffer, C.K., Xue, M., He, M., Huang, Z.J., Scanziani, M. 2013. Inhibition of inhibition in visual cortex: the logic of connections between molecularly distinct interneurons. Nat Neurosci 16, 1068–1076. doi:10.1038/nn.3446

Picco, N., García-Moreno, F., Maini, P.K., Woolley, T.E., and Molnár, Z. 2018. Mathematical modeling of cortical neurogenesis reveals that the founder population does not necessarily scale with neurogenic output. Cereb Cortex 28, 2540–2550.

Picco, N., Hippenmeyer, S., Rodarte, J., Streicher, C., Molnár, Z., Maini, P.K., and Woolley, T.E. 2019. A mathematical insight into cell labelling experiments for clonal analysis. J Anat. 235, 687–696.

Pierani, A., Brenner-Morton, S., Chiang, C., Jessell, T.M. 1999. A Sonic Hedgehog–Independent, Retinoid-Activated Pathway of Neurogenesis in the Ventral Spinal Cord. Cell 97, 903-915. doi:10.1016/s0092-8674(00)80802-8

Pilaz, L.J., Patti, D., Marcy, G., Oillier, E., Pfister, S., Douglas, R.J., Betizeau, M., Gautier, E., Cortay, V., Doerflinger, N., Kennedy, H., Dehay, C. 2009. Forced G1-phase reduction alters mode of division, neuron number, and laminar phenotype in the cerebral cortex. Proc Natl Acad Sci U S A 106, 21924-21929. doi:10.1073/pnas.0909894106

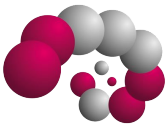

Pilz, G.A., Shitamukai, A., Reillo, I., Pacary, E., Schwausch, J., Stahl, R., Ninkovic, J., Snippert, H.J., Clevers, H., Godinho, L., Guillemot, F., Borrell, V., Matsuzaki, F., Götz M. 2013. Amplification of progenitors in the mammalian telencephalon includes a new radial glial cell type. Nat Commun 4:2125. doi:10.1038/ncomms3125

Pimeisl, I.M., Tanriver, Y., Daza, R.A., Vauti, F., Hevner, R.F., Arnold, H.-H., Arnold, S.J. 2013. Generation and characterization of a tamoxifen-inducible Eomes CreERmouse line. Genesis 51, 725–733. doi:10.1002/dvg.22417

Pla, R., Borrell, V., Flames, N., Marín, O. 2006. Layer acquisition by cortical GABAergic interneurons is independent of Reelin signaling. J Neurosci 26, 6924–6934. doi:10.1523/JNEUROSCI.0245-06.2006

Placzek, M., 1995. The role of the notochord and floor plate in inductive interactions. Curr Opin Genet Dev 5, 499-506. doi: 10.1016/0959-437x(95)90055-l

Pollen, A.A., Nowakowski, T.J., Chen, J., Retallack, H., Sandoval-Espinosa, C., Nicholas, C.R., Shuga, J., Liu, S.J., Oldham, M.C., Diaz, A., Lim, D.A., Leyrat, A.A., West, J.A., Kriegstein, A.R. 2015. Molecular Identity of Human Outer Radial Glia during Cortical Development. Cell 163, 55–67. doi:10.1016/j.cell.2015.09.004

Pollen, A.A., Nowakowski, T.J., Shuga, J., Wang, X., Leyrat, A.A., Lui, J.H., Li, N., Szpankowski, L., Fowler, B., Chen, P., Ramalingam, N., Sun, G., Thu, M., Norris, M., Lebofsky, R., Toppani, D., Kemp, D.W., Wong, M., Clerkson, B., Jones, B.N., Wu, S., Knutsson, L., Alvarado, B., Wang, J., Weaver, L.S., May, A.P., Jones, R.C., Unger, M.A., Kriegstein, A.R., West, J.A.A. 2014. Low-coverage single-cell mRNA sequencing reveals cellular heterogeneity and activated signaling pathways in developing cerebral cortex. Nat Biotech 32, 1053-1061. doi:10.1038/nbt.2967

Pontious, A., Kowalczyk, T., Englund, C., Hevner, R.F. 2008. Role of Intermediate Progenitor Cells in Cerebral Cortex Development. Dev Neurosci 30, 24–32. doi:10.1159/000109848

Price, J., Thurlow, L. 1998. Cell lineage in the rat cerebral cortex: a study using retroviral-mediated gene transfer. Development 104, 473-482.

Prönneke, A., Scheuer, B., Wagener, R.J., Möck, M., Witte, M., Staiger, J.F., 2015. Characterizing VIP Neurons in the Barrel Cortex of VIPcre/tdTomato Mice Reveals Layer-Specific Differences. Cerebral Cortex 25, 4854-4868. doi:10.1093/cercor/bhv202

Rakic, P., Bourgeois, J.P., and Goldman-Rakic, P.S. 1994. Synaptic development of the cerebral cortex: implications for learning, memory, and mental illness. Prog. Brain Res.102, 227-243.

Rakic, P. 1988. Specification of Cerebral Cortical Areas. Science 241, 170-176. doi:10.1126/science.3291116

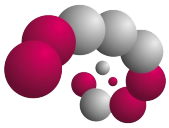

Rakic, P. 1974. Neurons in Rhesus Monkey Visual Cortex Systematic Relation between Time of Origin and Eventual Disposition. Science 83, 425-427. doi: 10.1126/science.183.4123.425

Rakic, P. 1973. Mode of Cell Migration to the Superficial Layers of Fetal Monkey Neocortex. J Comp Neurol 145, 61-68. doi:10.1002/cne.901450105

Rallu, M., Corbin, J.G., Fishell, G. 2002. Parsing the prosencephalon. Nat Rev Neurosci 3, 943–951. doi:10.1038/nrn989

Rapaport, D.H., Wong, L.L., Wood, E.D., Yasumura, D., LaVail, M.M. 2004. Timing and topography of cell genesis in the rat retina. J. Comp. Neurol. 474, 304–324. doi:10.1002/cne.20134

Rash, B.G., Ackman, J.B., Rakic, P. 2016. Bidirectional radial Ca 2+activity regulates neurogenesis and migration during early cortical column formation. Sci. Adv. 2,:e1501733. doi:10.1126/sciadv.1501733

Reh, T.A., Kljavin, J. 1989. Age of Differentiation Determines Rat Retinal Germinal Cell Phenotype: Induction of Differentiation by Dissociation. J Neurosci 9, 4179-4189. doi:10.1523/JNEUROSCI.09-12-04179

Reid, C.B., Liang, I., Walsh, C.A. 1995. Systematic Widespread Clonal Organization in Cerebral Cortex. Neuron 15, 299-310. doi: 10.1016/0896-6273(95)90035-7

Reillo, I., de Juan Romero, C., Cárdenas, A., Clascá, F., Martínez-Martinez, M.Á., Borrell, V. 2017. A Complex Code of Extrinsic Influences on Cortical Progenitor Cells of Higher Mammals. Cereb. Cortex 27, 4586–4606. doi: 10.1093/cercor/bhx171

Reillo, I., de Juan Romero, C., García-Cabezas, M.Á., Borrell, V. 2010. A Role for Intermediate Radial Glia in the Tangential Expansion of the Mammalian Cerebral Cortex. Cerebral Cortex 21, 1674–1694. doi:10.1093/cercor/bhq238

Ren, Q., Yang, C.-P., Liu, Z., Sugino, K., Mok, K., He, Y., Ito, M., Nern, A., Otsuna, H., Lee, T., 2017. Stem Cell-Intrinsic, Seven-up-Triggered Temporal Factor Gradients Diversify Intermediate Neural Progenitors. Current Biology 27, 1303–1313. doi:10.1016/j.cub.2017.03.047

Rice, D.S., Curran, T. 1999. Mutant mice with scrambled brains: understanding the signaling pathways that control cell positioning in the CNS. Genes Dev 13, 2758-2773. doi:10.1101/gad.13.21.2758

Riese, J., Zeller, R., Dono, R. 1995. Nucleo-cytoplasmic translocation and secretion of fibroblast growth factor-2 during avian gastrulation. Mech Dev 49, 13-22. doi: 0.1016/0925-4773(94)00296-y

Roccio, M., Schmitter, D., Knobloch, M., Okawa, Y., Sage, D., Lutolf, M.P. 2013. Predicting stem cell fate changes by differential cell cycle progression patterns. Development 140, 459–470. doi:10.1242/dev.086215

Roelink, H., Porter, J.A., Chiang, C., Tanabe, Y., Chang, D.T., Beachy, P.A.,

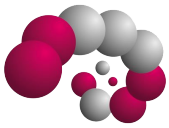

Jessell, T.M. 1995. Floor Plate and Motor Neuron Induction by Different Concentrations of the Amino-Terminal Cleavage Product of Sonic Hedgehog Autoproteolysis. Cell 81, 445-456. doi:10.1016/0092-8674(95)90397-6

Rymar, V.V., Sadikot, A.F. 2007. Laminar fate of cortical GABAergic interneurons is dependent on both birthdate and phenotype. J. Comp. Neurol. 501, 369–380. doi:10.1002/cne.21250

Salomoni, P., Calegari, F. 2010. Cell cycle control of mammalian neural stem cells: putting a speed limit on G1. Trends Cell Biol. 20, 233–243. doi: 10.1016/j.tcb.2010.01.006

Sapir, T., Geiman, E.J., Wang, Z., Velasquez, T., Mitsui, S., Yoshihara, Y., Frank, E., Alvarez, F.J., Goulding, M. 2004. Pax6 and engrailed 1 regulate two distinct aspects of renshaw cell development. J. Neurosci. 24, 1255–1264. doi:10.1523/JNEUROSCI.3187-03.2004

Schuman, B., Machold, R., Hashikawa, Y., Fuzik, J., Fishell, G., Rudy, B. 2018. Four unique interneuron populations reside in neocortical layer 1. J Neuronsci 39, 125-139. doi:10.1523/JNEUROSCI.1613-18.2018

Schwab, M.H., Bartholomae, A., Heimrich, B., Feldmeyer, D., Druffel-Augustin, S., Goebbels, S., Naya, F.J., Zhao, S., Frotscher, M., Tsai, M.-J., Nave, K.-A. 2000. Neuronal Basic Helix-Loop-Helix Proteins (NEX and BETA2/Neuro D) Regulate Terminal Granule Cell Differentiation in the Hippocampus J Neurosci 20, 3714-3724. doi:10.1523/JNEUROSCI.20-10-03714.2000

Seuntjens, E., Nityanandam, A., Miquelajauregui, A., Debruyn, J., Stryjewska, A., Goebbels, S., Nave, K.-A., Huylebroeck, D., Tarabykin, V. 2009. Sip1 regulates sequential fate decisions by feedback signaling from postmitotic neurons to progenitors. Nat. Neurosci. 12, 1373–1380. doi:10.1038/nn.2409

Shah, V., Drill, E., Lance-Jones, C. 2004. Ectopic expression of Hoxd10 in thoracic spinal segments induces motoneurons with a lumbosacral molecular profile and axon projections to the limb. Dev. Dyn. 231, 43–56. doi:10.1002/dvdy.20103

Shen, Q., Wang, Y., Dimos, J.T., Fasano, C.A., Phoenix, T.N., Lemischka, I.R., Ivanova, N.B., Stifani, S., Morrisey, E.E., Temple, S. 2006a. The timing of cortical neurogenesis is encoded within lineages of individual progenitor cells. Nat. Neurosci. 9, 743–751. doi:10.1038/nn1694

Sidman, R., Rakic, P. 1972. Neuronal migration, with special reference to developing human brain: A review. Brain Res 62, 1–35. doi: 10.1016/0006-8993(73)90617-3

Siegel, R.W., Jain, R., Bradbury, A. 2001. Using an in vivo phagemid system to identify non-compatible loxP sequences. FEBS Lett 505, 467-473. doi: 10.1016/s0014-5793(01)02806-x

Skeath, J.B., Thor, S. 2003. Genetic control of Drosophila nerve cord development. Current Opinion in Neurobiology 13, 8–15. doi:10.1016/S0959-4388(03)00007-2

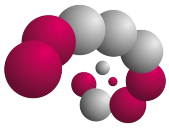

Smart, I.H.M., Dehay, C., Giroud, P., Berland, M., Kennedy, H. 2007. Unique Morphological Features of the Proliferative Zones and Postmitotic Compartments of the Neural Epithelium Giving Rise to Striate and Extrastriate Cortex in the Monkey. Cerebral Cortex 12, 37-53. doi: 10.1093/cercor/12.1.37

Snippert, H.J., van der Flier, L.G., Sato, T., van Es, J.H., van den Born, M., Kroon-Veenboer, C., Barker, N., Klein, A.M., van Rheenen, J., Simons, B.D., Clevers, H. 2010. Intestinal Crypt Homeostasis Results from Neutral Competition between Symmetrically Dividing Lgr5 Stem Cells. Cell 143, 134–144. doi:10.1016/j.cell.2010.09.016

Somogyi, P., Freund, T.F., Cowey, A. 1982. The Axo-Axonic Interneuron In The Cerebral Cortex Of The Rat, Cat and Monkey. Neuroscience 7, 2577-2607. doi:0.1016/0306-4522(82)90086-0

Sousa, V.H., Miyoshi, G., Hjerling-Leffler, J., Karayannis, T., Fishell, G. 2009. Characterization of Nkx6-2-Derived Neocortical Interneuron Lineages. Cerebral Cortex 19, i1–i10. doi:10.1093/cercor/bhp038

Southwell, D.G., Paredes, M.F., Galvao, R.P., Jones, D.L., Froemke, R.C., Sebe, J.Y., Alfaro-Cervello, C., Tang, Y., Garcia-Verdugo, J.M., Rubenstein, J.L., Baraban, S.C., Alvarez-Buylla, A. 2012. Intrinsically determined cell death of developing cortical interneurons. Nature 490, 109-113. doi:10.1038/nature11523

Stancik, E.K., Navarro-Quiroga, I., Sellke, R., Haydar, T.F. 2010. Heterogeneity in ventricular zone neural precursors contributes to neuronal fate diversity in the postnatal neocortex. 30, 7028–7036. doi:10.1523/JNEUROSCI.6131-09.2010

Stratmann, J., Ganilondo, H., Benito-Sipos, J., Tor, S. 2016. Neuronal cell fate diversification controlled by sub-temporal action of Kruppel. eLife 2016;5:e19311. doi:10.7554/eLife.19311.001

Sultan, K.T., Han, Z., Zhang, X.-J., Xianyu, A., Li, Z., Huang, K., Shi, S.-H., 2016. Clonally Related GABAergic Interneurons Do Not Randomly Disperse but Frequently Form Local Clusters in the Forebrain. Neuron 92, 31–44. doi:10.1016/j.neuron.2016.09.033

Sultan, K.T., Liu, W.A., Li, Z.-L., Shen, Z., Li, Z., Zhang, X.-J., Dean, O., Ma, J., Shi, S.-H. 2018. Progressive divisions of multipotent neural progenitors generate late-born chandelier cells in the neocortex. Nat Commun 9, 1–15. doi:10.1038/s41467-018-07055-7

Suzuki, S.C., Bleckert, A., Williams, P.R., Takechi, M., Kawamura, S., Wong, R.O.L. 2013. Cone photoreceptor types in zebrafish are generated by symmetric terminal divisions of dedicated precursors. Proc Natl Acad Sci U S A 110, 15109-15114. doi:10.1073/pnas.1303551110

Sùper, H., Uylings, H.B.M. 2001. The Early Differentiation of the Neocortex: a Hypothesis on Neocortical Evolution. Cereb Cortex 11, 1101–1109. doi:

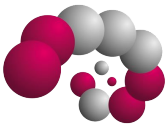

10.1093/cercor/11.12.1101

Sweeney, L.B., Bikoff, J.B., Gabitto, M.I., Brenner-Morton, S., Baek, M., Yang, J.H., Tabak, E.G., Dasen, J.S., Kintner, C.R., Jessell, T.M. 2018. Origin and Segmental Diversity of Spinal Inhibitory Interneurons. Neuron 97, 341–355.e3. doi:10.1016/j.neuron.2017.12.029

Syed, M.H., Doe, C.Q. 2017. Steroid hormone induction of temporal gene expression in Drosophila brain neuroblasts generates neuronal and glial diversity. eLife 2017,6:e26287. doi:10.7554/eLife.26287.001

Novotny, T., Eiselt, R., Urban J. 2002. Hunchback is required for the specification of the early sublineage of neuroblast 7-3 in the Drosophila central nervous system. Development 129, 1027-1036.

Takahashi, T., Nowakowski, T.J., Caviness, V.S. 1995. The Cell Cycle of the Pseudostratified Ventricular Epithelium of the Embryonic Murine Cerebral Wall. J Neurosci 15, 6046-6057. doi: 10.1523/JNEUROSCI.15-09-06046.1995

Tamamaki, N., Fujimori, K.E., Takauji, R. 1997. Origin and Route of Tangentially Migrating Neurons in the Developing Neocortical Intermediate Zone. J Neurosci 17, 8313-8323. doi:10.1523/JNEUROSCI.17-21-08313.1997

Tan, S.S., Kalloniatis, M., Sturm, K., Tam, P.P.L., Reese, B.E., Faulkner-Jones, B. 1998. Separate Progenitors for Radial and Tangential Cell Dispersion during Development of the Cerebral Neocortex. Neuron 21, 295-304. doi: 10.1016/s0896-6273(00)80539-5

Taniguchi, H., He, M., Wu, P., Kim, S., Paik, R., Sugino, K., Kvitsani, D., Fu, Y., Lu, J., Lin, Y., Miyoshi, G., Shima, Y., Fishell, G., Nelson, S.B., Huang, Z.J. 2011. A Resource of Cre Driver Lines for Genetic Targeting of GABAergic Neurons in Cerebral Cortex 71, 995–1013. doi:10.1016/j.neuron.2011.07.026

Taniguchi, H., Lu, J., Huang, Z.J. 2013. The Spatial and Temporal Origin of Chandelier Cells in Mouse Neocortex. Science 339, 67–70. doi:10.1126/science.1228246

Tasic, B., Menon, V., Nguyen, T.N., Kim, T.K., Jarsky, T., Yao, Z., Levi, B., Gray, L.T., Sorensen, S.A., Dolbeare, T., Bertagnolli, D., Goldy, J., Shapovalova, N., Parry, S., Lee, C., Smith, K., Bernard, A., Madisen, L., Sunkin, S.M., Hawrylycz, M., Koch, C., Zeng, H. 2016. Adult mouse cortical cell taxonomy revealed by single cell transcriptomics. Nat. Neurosci 19, 335-346. doi:10.1038/nn.4216

Tasic, B., Yao, Z., Graybuck, L.T., Smith, K.A., Nguyen, T.N., Bertagnolli, D., Goldy, J., Garren, E., Economo, M.N., Viswanathan, S., Penn, O., Bakken, T., Menon, V., Miller, J., Fong, O., Hirokawa, K.E., Lathia, K., Rimorin, C., Tieu, M., Larsen, R., Casper, T., Barkan, E., Kroll, M., Parry, S., Shapovalova, N.V., Hirschstein, D., Pendergraft, J., Sullivan, H.A., Kim, T.K., Szafer, A., Dee, N., Groblewski, P., Wickersham, I., Cetin, A., Harris,

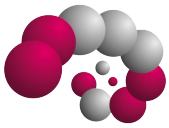

J.A., Levi, B.P., Sunkin, S.M., Madisen, L., Daigle, T.L., Looger, L., Bernard, A., Phillips, J., Lein, E., Hawrylycz, M., Svoboda, K., Jones, A.R., Koch, C., Zeng, H. 2018. Shared and distinct transcriptomic cell types across neocortical areas. Nature 563, 72-78. doi:10.1038/s41586-018-0654-5

Taverna, E., Götz, M., Huttner, W.B. 2014. The Cell Biology of Neurogenesis: Toward an Understanding of the Development and Evolution of the Neocortex 30, 465–502. doi:10.1146/annurev-cellbio-101011-155801

Telley, L., Agirman, G., Prados, J., Fievre, S., Oberst, P., Vitali, I., Nguyen, L., Dayer, A., Jabaudon, D. 2018. Single-cell transcriptional dynamics and origins of neuronal diversity in the developing mouse neocortex. bioRxiv. doi:10.1101/409458

Telley, L., Govindan, S., Prados, J., Stevant, I., Nef, S., Dermitzakis, E., Dayer, A., Jabaudon, D. 2016. Sequential transcriptional waves direct the differentiation of newborn neurons in the mouse neocortex. Science 351, 1443-1446. doi:10.1126/science.aad8361

Thomson, A.M., Bannister, A.P., 2003. Interlaminar Connections in the Neocortex. Cereb Cortex 13, 5-14. doi:10.1093/cercor/13.1.5

Thor, S., Thomas, J.B. 1997. The Drosophila *islet* Gene Governs Axon Pathfiding and Neurotransmitter Identity. Neuron 18, 397-409. doi:10.1016/s0896-6273(00)81241-6

Torigoe, M., Yamauchi, K., Kimura, T., Uemura, Y., Murakami, F. 2016. Evidence That the Laminar Fate of LGE/CGE-Derived Neocortical Interneurons Is Dependent on Their Progenitor Domains. J Neuronsci 36, 2044–2056. doi:10.1523/JNEUROSCI.3550-15.2016

Toyoda, R., Assimacopoulos, S., Wilcoxon, J., Taylor, A., Feldman, P., Suzuki-Hirano, A., Shimogori, T., Grove, E.A. 2010. FGF8 acts as a classic diffusible morphogen to pattern the neocortex. Development 137, 3439–3448. doi:10.1242/dev.055392

Tran, K.D., Doe, C.Q. 2008. Pdm and Castor close successive temporal identity windows in the NB3-1 lineage. Development 135, 3491–3499. doi:10.1242/dev.024349

Tremblay, R., Lee, S., Rudy, B. 2016. GABAergic Interneurons in the Neocortex: From Cellular Properties to Circuits. Neuron 91, 260–292. doi:10.1016/j.neuron.2016.06.033

Trimarchi, J.M., Stadler, M.B., Cepko, C.L. 2008. Individual Retinal Progenitor Cells Display Extensive Heterogeneity of Gene Expression. PLoS ONE 3, e1588. doi:10.1371/journal.pone.0001588

Tsuji, T., Hasegawa, E., Isshiki, T. 2008. Neuroblast entry into quiescence is regulated intrinsically by the combined action of spatial Hox proteins and temporal identity factors. Development 135, 3859–3869. doi:10.1242/dev.025189

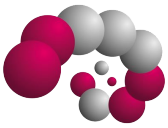

Turner, D.L., Snyder, E.Y., Cepko, C.L. 1990. Lineage-Independent Determination of Cell Type in the Embryonic Mouse Retina. Neuron 4, 833-845. doi:10.1016/0896-6273(90)90136-4

Tyler, W.A., Haydar, T.F. 2013. Multiplex Genetic Fate Mapping Reveals a Novel Route of Neocortical Neurogenesis, Which Is Altered in the Ts65Dn Mouse Model of Down Syndrome. J Neuronsci 33, 5106–5119. doi:10.1523/JNEUROSCI.5380-12.2013

Valcanis, H., Tan, S.-S. 2003. Layer Specification of Transplanted Interneurons in Developing Mouse Neocortex. J Neurosci 23, 5113-5122. doi:10.1523/JNEUROSCI.23-12-05113.2003

Vasistha, N.A., García-Moreno, F., Arora, S., Cheung, A.F.P., Arnold, S.J., Robertson, E.J., and Molnár, Z. 2015. Cortical and Clonal Contribution of Tbr2 Expressing Progenitors in the Developing Mouse Brain. Cereb Cortex 25, 290-302. doi: 10.1093/cercor/bhu125

Vitali, I., Fievre, S., Telley, L., Oberst, P., Bariselli, S., Frangeul, L., Baumann, N., McMahon, J.J., Klingler, E., Bocchi, R., Kiss, J.Z., Bellone, C., Silver, D.L., Jabaudon, D. 2018. Progenitor Hyperpolarization Regulates the Sequential Generation of Neuronal Subtypes in the Developing Neocortex. Cell 174, 1264–1276.e15. doi:10.1016/j.cell.2018.06.036

Walsh, C.A., Cepko, C.L. 1995. Clonally Related Cortical Cells Show Several Migration Patterns. Science 241, 1342-1345. doi:10.1126/science.3137660

Wamsley, B., Fishell, Gord. 2017. Genetic and activity-dependent mechanisms underlying interneuron diversity. Nat Rev Neurosci 18, 299–309. doi:10.1038/nrn.2017.30

Wang, X., Tsai, J.W., Imai, J.H., Lian, W.-N., Vallee, R.B., Shi, S.-H. 2009. Asymmetric centrosome inheritance maintains neural progenitors in the neocortex. Nature 461, 947–955. doi:10.1038/nature08435

Wang, X., Tsai, J.W., LaMonica, B., Kriegstein, A.R. 2011. A new subtype of progenitor cell in the mouse embryonic neocortex. Nat Neurosci 14, 555–561. doi:10.1038/nn.2807

Wang, Y., Toledo-Rodriguez, M., Gupta, A., Wu, C., Silberberg, G., Luo, J., Markram, H. 2004. Anatomical, physiological and molecular properties of Martinotti cells in the somatosensory cortex of the juvenile rat. J Physiol 561, 65–90. doi:10.1113/jphysiol.2004.073353

Wang, Y., Ye, M., Kuang, X., Li, Y., Hu, S. 2018. A simplified morphological classification scheme for pyramidal cells in six layers of primary somatosensory cortex of juvenile rats. IBRO Reports 5, 74–90. doi:10.1016/j.ibror.2018.10.001

Weissman, T.A., Riquelme, P.A., Ivic, L., Flint, A.C., Kriegstein, A.R. 2004. Calcium Waves Propagate through Radial Glial Cells and Modulate Proliferation in the Developing Neocortex. Neuron 43, 647–661. doi:10.1016/j.neuron.2004.08.015

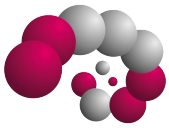

Weits, R., Fraser, S.E. 1988. Multipotent Precursos Can Give Rise to All Major Cell Types of the Frog Retina. Science 239, 1142-1145. doi:10.1126/science.2449732

Wolfram, V., Southall, T.D., Gunay, C., Prinz, A.A., Brand, A.H., Baines, R.A., 2014. The Transcription Factors Islet and Lim3 Combinatorially Regulate Ion Channel Gene Expression. J Neuronsci 34, 2538–2543. doi:10.1523/JNEUROSCI.4511-13.2014

Wonders, C.P., Anderson, S.A. 2006. The origin and specification of cortical interneurons. Nat Rev Neurosci 7, 687–696. doi:10.1038/nrn1954

Wonders, C.P., Taylor, L., Welagen, J., Mbata, I.C., Xiang, J.Z., Anderson, S.A. 2008. A spatial bias for the origins of interneuron subgroups within the medial ganglionic eminence. Developmental Biology 314, 127–136. doi:10.1016/j.ydbio.2007.11.018

Wong, F.K., Bercsenyi, K., Sreenivasan, V., Portalés, A., Fernández-Otero, M., Marín, O. 2018. Pyramidal cell regulation of interneuron survival sculpts cortical networks. Nature 557, 668–673. doi:10.1038/s41586-018-0139-6

Wong, L.L., Rapaport, D.H. 2009. Defining retinal progenitor cell competence in Xenopus laevis by clonal analysis. Development 136, 1707–1715. doi:10.1242/dev.027607

Woodworth, M.B., Greig, L.C., Liu, K.X., Ippolito, G.C., Tucker, H.O., Macklis, J.D. 2016. Ctip1 Regulates the Balance between Specification of Distinct Projection Neuron Subtypes in Deep Cortical Layers. CellReports 15, 999–1012. doi:10.1016/j.celrep.2016.03.064

Xu, H., Jeong, H.-Y., Tremblay, R., Rudy, B. 2013. Neocortical Somatostatin-Expressing GABAergic Interneurons Disinhibit the Thalamorecipient Layer 4. Neuron 77, 155–167. doi:10.1016/j.neuron.2012.11.004

Xu, Q. 2004. Origins of Cortical Interneuron Subtypes. J Neuronsci 24, 2612–2622. doi:10.1523/JNEUROSCI.5667-03.2004

Xu, Q., Guo, L., Moore, H., Waclaw, R.R., Campbell, K., Anderson, S.A. 2010. Sonic Hedgehog Signaling Confers Ventral Telencephalic Progenitors with Distinct Cortical Interneuron Fates. Neuron 65, 328–340. doi:10.1016/j.neuron.2010.01.004

Xu, Q., Tam, M., Anderson, S.A. 2008. Fate mapping Nkx2.1-lineage cells in the mouse telencephalon. J. Comp. Neurol. 506, 16–29. doi:10.1002/cne.21529

Yoon, K.J., Koo, B.K., Im, S.K., Jeong, H.W., Ghim, J., Kwon, M.C., Moon, J.S., Miyata, T., Kong, Y.Y. 2008. Mind Bomb 1-Expressing Intermediate Progenitors Generate Notch Signaling to Maintain Radial Glial Cells. Neuron 58, 519–531. doi:10.1016/j.neuron.2008.03.018

Young, R.W. 1985. Cell Differentiation in the Retina of the Mouse. Anat Rec 212, 199-205. doi:10.1002/ar.1092120215

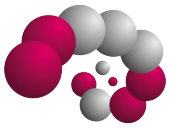

Zecevic, N., Chen, Y., Filipovic, R. 2005. Contributions of cortical subventricular zone to the development of the human cerebral cortex. J. Comp. Neurol. 491, 109–122. doi:10.1002/cne.20714

Zembrzycki, A., Griesel, G., Stoykova, A., Mansouri, A. 2007. Genetic interplay between the transcription factors Sp8 and Emx2 in the patterning of the forebrain. Neural Dev 2, 8–18. doi:10.1186/1749-8104-2-8

Zong, H., Espinosa, J.S., Su, H.H., Muzumdar, M.D., Luo, L. 2005. Mosaic Analysis with Double Markers in Mice. Cell 121, 479–492. doi:10.1016/j.cell.2005.02.012

APPENDIX

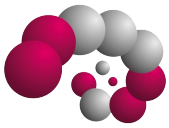

Table 1. Summary of data and statistical analyses for Results: Chaper I

Figure 2.1	Measurement	Values	N	Statistical	P value
Figure 2.1D	Number of neurons per lineage (Top:mean ± SEM Bottom: median ± IC distance)	E9.5: 199.23 ± 28.83; E10.5: 59.62 ± 8.02; E11.5: 13.04 ± 0.94; E12.5: 6.14 ± 0.27; E14.5: 2.84 ± 0.17 E9.5: 219 ± 178; E10.5: 46 ± 51.5; E11.5: 11 ± 26; E12.5: 5 ± 11; E14.5: 3 ± 2	[Clones] E9.5, n = 13; E10.5, n = 21; E11.5, n = 51; E12.5, n = 73; E14.5, n = 32; [Brains] E9.5, n = 4; E10.5, n = 3; E11.5, n = 5; E12.5, n = 7; E14.5, n = 3		
Figure 2.1E	Fraction of one cell, two cells, and three or more cell lineages (percentage over total)	One cell: E9.5: 0%; E10.5: 0%; E11.5: 18.75%; E12.5: 39.15%	[Clones] E9.5, *n* = 13; E10.5, *n* = 21; E11.5, *n* = 64; E12.5, n = 166; [Brains] E9.5, n = 4; E10.5, n = 3; E11.5, n = 5; E12.5, n = 7;		
		Two cells: E9.5: 0%; E10.5: 0%; E11.5: 1.56%; E12.5: 16.46%	[Clones] E9.5, n = 13; E10.5, n = 21; E11.5, *n* = 64; E12.5, n = 166; [Brains] E9.5, n = 4; E10.5, n = 3; E11.5, n = 5; E12.5, n = 7		
		Three or more cells: E9.5: 100%; E10.5: 100%; E11.5: 79.69%; E12.5: 44.39%;	[Clones] E9.5, n = 13; E10.5, *n* = 21; E11.5, *n* = 64; E12.5, n = 166; [Brains] E9.5, n = 4; E10.5, n = 3; E11.5, n = 5; E12.5, n = 7		
Figure 2.2	Measurement	Values	N	Statistical	P value
Figure 2.2B	Fraction of lineages with one or two reporters (percentage over total)	One: 95.83%; Two: 4.17%	[Clones]: n = 296 [Brains]: n = 19		
Figure 2.3	Measurement	Values	N	Statistical	P value
Figure 2.3E	Fraction of translaminar, deep, and superficial lineages (precentage over total)	Translaminar: 63.01%; Deep: 15.07%; Superficial: 21.92%	[Clones]: n = 73 [Brains]: n = 7		
	Number of neurons per lineage (Top:mean ± SEM Bottom: median ± IC distance)	Translaminar: 6.96 ± 2.38; Deep: 4.45 ± 0.93; Superficial: 4.94 ± 1.24% Translaminar: 6 ± 4; Deep: 5 ± 1; Superficial: 5 ± 2%	[Clones]: n = 73 [Brains]: n = 7		
Figure 2.3I	Fraction of translaminar, deep, and superficial lineages (precentage over total)	Translaminar: 6.67%; Deep: 80%; Superficial: 13.33%	[Clones]: n = 30 [Brains]: n = 7		
Figure 2.3M	Fraction of lineages per cortical layer (precentage over total)	Layer II/III: 4.76%; Layer IV: 19.05%; Layer V: 17.46%; Layer VI: 58.73%	[Clones]: n = 63 [Brains]: n = 7		
Figure 2.4	Measurement	Values	N	Statistical	P value
Figure 2.4D	Fraction of translaminar, deep, and superficial lineages (precentage over total)	Translaminar: 2.78%; Deep: 56.94%; Superficial: 40.28%	[Clones]: n = 72 [Brains]: n = 12		
Figure 2.5	Measurement	Values	N	Statistical	P value
Figure 2.5D	Fraction of translaminar, deep, and superficial lineages (precentage over total)	Translaminar: 91.05%; Deep: 6.6%; Superficial: 1.89%	[Clones]: n = 106 [Brains]: n = 28		
	Number of neurons per lineage (Top:mean ± SEM Bottom: median ± IC distance)	Translaminar: 8.05 ± 2.83; Deep: 4.00 ± 1.00 Translaminar: 8 ± 3; Deep: 4 ± 1	[Clones]: n = 106 [Brains]: n = 28		
Figure 2.6	Measurement	Values	N	Statistical	P value
Figure 2.6D	Fraction of translaminar, deep, and superficial hemilineages (precentage over total)	Translaminar: 80.71%; Deep: 7.11%; Superficial: 12.18%	[Clones]: n = 106 [Brains]: n = 28		
Figure 2.7	Measurement	Values	N	Statistical	P value
Figure 2.7E	Fraction of translaminar, deep, and superficial lineages (precentage over total)	Translaminar: 75.38%; Deep: 13.46%; Superficial: 11.15%	[Clones]: n = 260 [Brains]: n = 25		
	Number of neurons per lineage (Top:mean ± SEM Bottom: median ± IC distance)	Translaminar: 7.22 ± 2.37; Deep: 3.77 ± 1.29; Superficial: 4.90 ± 1.82 Translaminar: 7 ± 4; Deep: 3 ± 1; Superficial: 4 ± 2.5	[Clones]: n = 260 [Brains]: n = 25		
Figure 2.8	Measurement	Values	N	Statistical	P value
Figure 2.8E	Fraction of lineages containing 3 to 12 cells (percentage over total)	Translaminar: [3]: 3.46%; [4]: 8.08%; [5]: 8.85%; [6]: 9.23%; [7]: 11.54%; [8]: 11.54%; [9]: 8.85%; [10]: 6.15%; [11]: 4.62%; [12]: 3.08%; Deep: [3]: 8.08%; [4]: 3.08%; [5]:1.15%; [7]: 0.77%; [8]: 0.38%; Superficial: [3]: 2.69; [4]: 3.85%; [5]: 0.77%; [6]: 1.54%; [7]: 0.77%; [8]: 1.15%; [9]: 0.38%	[Clones]: n = 260 [Brains]: n = 25		

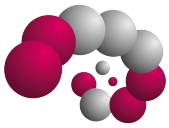

Figure 2.8F	Fraction of lineages in each configuration (percentage over total)	[II/III]: 1.92%; [IV]: 1.54%; [II/III-IV]: 7.69%; [V]: 1.54%; [VI]: 5.77%; [V-VI]: 6.15%; [II/III to VI]: 22.69%; [II/III-IV-VI]: 14.62%; [II/III-V-VI]: 10.38%; [II/III to V]: 7.31%; [II/III-V]: 5.38%; [IV-VI]: 4.62%; [IV to VI]: 3.85%; [II/III-VI]: 3.46%; [IV-V]: 3.08%	[Clones]: n = 260 [Brains]: n = 25		
Figure 2.8G	Number of lineages in each combination(total number)	[y-x] // [2-2]: 2; [2-3]: 1; [2-4]: 1; [3-3]: 3; [3-5]: 1; [3-6]: 1; [3-8]: 2; [4-2]: 3; [4-3]: 3; [4-4]: 3; [4-5]: 3; [4-6]: 1; [5-2]: 4; [5-3]: 3; [5-4]: 2; [5-5]: 3; [6-2]: 3; [6-3]: 2; [6-4]: 3; [6-5]: 4; [7-3]: 3; [7-4]: 2; [8-3]: 1; [8-4]: 1; [9-3]: 1; [10-2]: 1	[Clones]: n = 57 [Brains]: n = 25		
Figure 2.8H	Fraction of lineages containing each sutype combination (precentage over total all-layer lineages)	[CCPN]: 23.08%; [CCPN; L5SCPN]: 7.69%; [CCPN; L6CThPN]: 11.54%; [CCPN; L5HPN]: 11.54%; [CCPN; L5HPN; L6CThPN]: 15.38%; [CCPN; L5SCPN; L5HPN]: 7.69%; [CCPN; L5SCPN; L6CThPN]: 15.38%; [CCPN; L5SCPN; L5HPN; L6CThPN]: 7.69%	[Clones]: n = 26 [Brains]: n = 25		
Figure 2.9	Measurement	Values	N	Statistical	P value
Figure 2.9D	Fraction of lineages containing 3 to 12 cells (percentage over total)	Translaminar, [4]: 5.48%; [5]: 19.18%; [6]: 9.59%; [7]: 4.11%; [8]: 6.85%; [9]: 9.59%; [10]: 2.74%; [11]: 2.74%; [12]: 1.37%; [14]: 1.37%; Deep, [3]: 2.74%; [4]: 4.12%; [5]: 6.85%; [6]: 1.37%; Superficial, [3]: 2.74; [4]: 5.48%; [5]: 6.85%; [6]:4.11%; [7]: 2.74	[Clones]: n = 73 [Brains]: n = 7		
Figure 2.9E	Fraction of lineages in each configuration (percentage over total)	[IV]: 8.22%; [II/III-IV]: 13.7%; [V]: 1.37%; [VI]: 10.96%; [V-VI]: 2.74%; [II/III to VI]: 16.44%; [II/III-IV-VI]: 24.66%; [II/III to V]: 10.96%; [IV-VI]: 4.11%; [IV to VI]: 5.48%; [IV-V]: 1.37%	[Clones]: n = 73 [Brains]: n = 7		
Figure 2.9I	Fraction of lineages containing 3 to 12 cells (percentage over total)	Translaminar, [3]: 0.94%; [4]: 4.72%; [5]: 9.43%; [6]:12.26%; [7]: 14.15%; [8]: 17.92%; [9]: 12.26%; [10]: 3.77%; [11]: 5.66%; [12]: 5.66%; [13]: 0.94%; [14]: 0.94%; [15]: 1.89%; [21]: 0.94%; Deep, [3]: 1.89%; [4]: 3.77%; [6]: 0.94%; Superficial, [6]: 1.89%	[Clones]: n = 106 [Brains]: n = 28		
Figure 2.9J	Fraction of lineages in each configuration (percentage over total)	[II/III-IV]: 1.89%; [VI]: 6.6%; [II/III to VI]: 44.34%; [II/III-IV-VI]: 21.70%; [II/III-V-VI]: 1.89%; [II/III to V]: 9.43%; [IV-VI]: 3.77%; [IV to VI]: 9.43%; [IV-V]: 0.94%	[Clones]: n = 106 [Brains]: n = 28		
Figure 2.10	Measurement	Values	N	Statistical	P value
Figure 2.10C	Fraction of cells expressing Tle4 (mean % ± Std)	C+/S-: [Tle4+]: 77.43 ± 12.46%; [Tle4-]: 22.57 ± 12.46; C-/S+: [Tle4+]: 10.19 ± 7.20%; [Tle4-]: 89.81 ± 7.20%; C-/S-: [Tle4+]: 22.39 ± 3.38%; [Tle4-]: 77.61 ± 3.38%; C+/S+: [Tle4+]: 58.21 ± 1.33%; [Tle4-]: 41.79 ± 1.33	[Cells]: n = 1123 [Brains]: n = 2		
Figure 2.11		Values	N	Statistical	P value
Figure 2.11B	Number of neurons per lineage (mean ± Std)	[P21] : 6.51± 2.56; [P2]: 6.97 ± 2.76	P21, [Clones]: n = 260; [Brains]: n = 25; P2, [Clones]: n = 110; [Brains]: n = 10	Mann-Whitney test	p = 0.1501
Figure 2.11C	Fraction of lineages containing 3 to 12 cells (percentage over total)	P21: [3]: 14.23%; [4]: 15.00%; [5]: 10.77%; [6]: 10.77%; [7]: 13.08%; [8]: 13.08%; [9]: 9.23%; [10]: 6.15%; [11]: 4.62%; [12]: 3.08%; P2: [3]: 17.27%; [4]: 5.45%; [5]: 8.18%; [6]: 13.63%; [7]: 14.55%; [8]: 8.18%; [9]: 12.72%; [10]: 7.27%; [11]: 6.36%; [12]: 6.36%	P21, [Clones]: n = 260; [Brains]: n = 25; P2, [Clones]: n = 110; [Brains]: n = 10	Chi-square test	p = 0.1653
Figure 2.11D	Fraction of translaminar, deep, and superficial lineages (precentage over total)	P21, Translaminar: 75.38%; Deep: 13.46%; Superficial: 11.15%; P2, Translaminar: 83.63%; Deep: 7.27%; Superficial: 9.09%	P21, [Clones]: n = 260; [Brains]: n = 25; P2, [Clones]: n = 110; [Brains]: n = 10	Fisher's exact test	p = 0.1127
Figure 2.11E	Fraction of lineages in each configuration (percentage over total)	P21: [II/III_&_IV to VI]: 36.78%; [II/III_&_IV-VI]: 22.99%; [II/III_&_IV to V]: 15.71%; P2: [II/III_&_IV to VI]: 47.27%; [II/III_&_IV-VI]: 15.45%; [II/III_&_IV to V]: 20.91%	P21, [Clones]: n = 260; [Brains]: n = 25; P2, [Clones]: n = 110; [Brains]: n = 10	Chi-square test	p = 0.0994
Figure 2.12	Measurement	Values	N	Statistical	P value
Figure 2.12A	Fraction of cells per layer (percentage over total & mean percentage ± Std)	Experimental data, [II/III]: 29.86%; [IV]: 30.69%; [V]: 14.86%; [VI]: 24.58%; Permuted, [II/III]: 29.86 ± 0%; [IV]: 30.69 ± 0%; [V]: 14.86 ± 0%; [VI]: 24.58 ± 0%	Experimental, [Clones]: n = 103; [Brains]: n = 25; Permuted, [Clones]: n = 103		
Figure 2.12B	Fraction of lineages containing 3 to 12 cells (percentage over total & mean percentage ± Std)	Experimental data, [3]: 10.68%; [4]: 14.56%; [5]: 6.80%; [6]: 10.68%; [7]: 11.65%; [8]: 17.48%; [9]: 11.65%; [10]: 3.88%; [11]: 5.83%; [12]: 6.80%; Permuted, [3]: 10.68 ± 0%; [4]: 14.56 ± 0%; [5]: 6.80 ± 0%; [6]: 10.68 ± 0%; [7]: 11.65 ± 0%; [8]: 17.48 ± 0%; [9]: 11.65 ± 0%; [10]: 3.88 ± 0%; [11]: 5.83 ± 0%; [12]: 6.80 ± 0%	Experimental, [Clones]: n = 103; [Brains]: n = 25; Permuted, [Clones]: n = 103		
Figure 2.13	Measurement	Values	N	Statistical	P value
Figure 2.13A	Likelihood for each number of categories (percentage over total samples)	[1]: 74.95%; [2]: 23.63%; [3]: 0.014%;	[Samples]: n = 4000		
Figure 2.13B	Fraction of cells per layer (percentage over total & mean percentage ± Std)	Experimental data, [II/III]: 29.86%; [IV]: 30.69%; [V]: 14.86%; [VI]: 24.58%; Bayesian Model, [II/III]: 29.77 ± 2.25%; [IV]: 30.76 ± 2.29%; [V]: 14.79 ± 1.80%; [VI]: 24.68 ± 2.15%	Experimental, [Clones]: n = 103; [Brains]: n = 25; Bayesian model, [Samples]: n = 4000		
Figure 2.13C	Fraction of lineages containing 3 to 12 cells (percentage over total & mean percentage ± Std)	Experimental data, [3]: 10.68%; [4]: 14.56%; [5]: 6.80%; [6]: 10.68%; [7]: 11.65%; [8]: 17.48%; [9]: 11.65%; [10]: 3.88%; [11]: 5.83%; [12]: 6.80%; Bayesial Model, [3]: 6.27 ± 2.34%; [4]: 7.91 ± 2.74%; [5]: 9.92 ± 3.03%; [6]: 11.44 ± 3.23%; [7]: 12.17± 3.28%; [8]: 11.83 ± 3.22%; [9]: 10.39% ± 3.02%; [10]: 8.23 ± 2.80%; [11]: 5.99 ± 2.41%; [12]: 3.96 ± 2.02%	Experimental, [Clones]: n = 103; [Brains]: n = 25; Bayesian model, [Samples]: n = 4000		

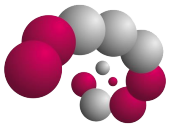

Figure 2.13E	Fraction of translaminar, deep, and superficial lineages (precentage over total)	Experimental data (mean {I.C. 95%}), Translaminar: 77.67 {68.93-84.47}%; Deep: 10.68 {5.83-17.48}%; Superficial: 11.65 {6.8-19.42}%; Bayesian model (median ± intercuartile distance), Translaminar: 82.52 ± 3.88%; Deep: 10.68 ± 3.88%; Superficial: 4.85 ± 2.91	Experimental, [Clones]: n = 103; [Brains]: n = 25; Bayesian model, [Samples]: n = 4000	Chi-square test	p=0.036
Figure 2.13F	Fraction of lineages in each configuration (percentage over total)	Experimental data (mean {I.C. 95%}), [II/III to VI]: 22.33 {14.56-31.07}%; [II/III-IV-VI]: 20.39 {13.59-29.61}%; [II/III-V-VI]: 4.85 {1.94-10.68}%; [II/III to V]: 6.80 {2.91-13.59}%; [II/III-V]: 1.94 {0-6.09}%; [IV-VI]: 7.77 {3.88-14.56}%; [IV to VI]: 7.77 {3.88-14.56}%; [II/III-VI]: 0.97 {0-5.82}%; [IV-V]: 4.85 {1.94-19.71}%; Bayesian model (median ± intercuartile distance), [II/III to VI]: 33.01 ± 6.79%; [II/III-IV-VI]: 15.53 ± 4.85%; [II/III-V-VI]: 2.91 ± 1.94%; [II/III to V]: 6.79 ± 3.88%; [II/III-V]: 0 ± 0.97%; [IV-VI]: 5.83 ± 2.91%; [IV to VI]: 12.62 ± 3.88%; [II/III-VI]: 0.97 ± 0.97%; [IV-V]: 2.91 ± 1.94%	Experimental, [Clones]: n = 103; [Brains]: n = 25; Bayesian model, [Samples]: n = 4000	Chi-square test	p=0.11
Figure 2.14	Measurement	Values	N	Statistical	P value
Figure 2.14B	Fraction of cells per layer (percentage over total & mean percentage ± Std)	Experimental data, [II/III]: 29.86%; [IV]: 30.69%; [V]: 14.86%; [VI]: 24.58%; Model 2, [II/III]: 29.97 ± 2.43%; [IV]: 30.82 ± 1.93%; [V]: 13.95 ± 1.28%; [VI]: 25.26 ± 2.18%	Experimental, [Clones]: n = 103; [Brains]: n = 25; Model 2, [Clones]: n = 103		
Figure 2.14C	Fraction of lineages containing 3 to 12 cells (percentage over total & mean percentage ± Std)	Experimental data, [3]: 10.68%; [4]: 14.56%; [5]: 6.80%; [6]: 10.68%; [7]: 11.65%; [8]: 17.48%; [9]: 11.65%; [10]: 3.88%; [11]: 5.83%; [12]: 6.80%; Model 2, [3]: 13.33 ± 3.24%; [4]: 13.72 ± 3.85%; [5]: 9.50 ± 2.81%; [6]: 9.81 ± 3.06%; [7]: 11.11 ± 3.05%; [8]: 11.10 ± 3.43%; [9]: 9.34% ± 3.07%; [10]: 8.90 ± 2.89%; [11]: 7.12 ± 2.41%; [12]: 6.07 ± 2.22%	Experimental, [Clones]: n = 103; [Brains]: n = 25; Model 2, [Clones]: n = 103		
Figure 2.14E	Fraction of Translaminar, Deep, and Superficial lineages (precentage over total)	Experimental data (mean {I.C. 95%}): Translaminar: 77.67 {68.93-84.47}%; Deep: 10.68 {5.83-17.48}%; Superficial: 11.65 {6.8-19.42}%; Model 2 (median ± intercuartile distance), Translaminar: 78 ± 5.5%; Deep: 11 ± 4.5%; Superficial: 11 ± 5.0%	Experimental, [Clones]: n = 103; [Brains]: n = 25; Model 2, [Clones]: n = 103	Fisher's exact test	p = 0.99
Figure 2.14F	Fraction of lineages in each configuration (percentage over total)	Experimental data (mean {I.C. 95%}), [II/III to VI]: 22.33 {14.56-31.07}%; [II/III-IV-VI]: 20.39 {13.59-29.61}%; [II/III-V-VI]: 4.85 {1.94-10.68}%; [II/III to V]: 6.80 {2.91-13.59}%; [II/III-V]: 1.94 {0-6.09}%; [IV-VI]: 7.77 {3.88-14.56}%; [IV to VI]: 7.77 {3.88-14.56}%; [II/III-VI]: 0.97 {0-5.82}%; [IV-V]: 4.85 {1.94-19.71}%; Model 2 (median ± intercuartile distance), [II/III to VI]: 30 ± 6.0%; [II/III-IV-VI]: 17 ± 5.5%; [II/III-V-VI]: 3 ± 3.0%; [II/III to V]: 7 ± 4.0%; [II/III-V]: 1 ± 1.0%; [IV-VI]: 4 ± 3.0%; [IV to VI]: 11 ± 4.5%; [II/III-VI]: 2 ± 2.0%; [IV-V]: 2 ± 2%	Experimental, [Clones]: n = 103; [Brains]: n = 25; Model 2, [Clones]: n = 103	Chi-square test	p = 0.24
Figure 2.14H	Fraction of cells per layer (percentage over total ± Std)	Fucci quantification, S1: [II/III]: 25.68 ± 2.13%; [IV]: 24.63 ± 0.63%; [V]: 16.61 ± 0.67%; [VI]: 33.09 ± 2.38%; Vi1: [II/III]: 30.39 ± 1.10%; [IV]: 24.31 ± 1.32%; [V]: 21.86 ± 1.22%; [VI]: 23.44 ± 1.58%; Model 2, S1: [II/III]: 24.43 ± 2.12%; [IV]: 24.46 ± 2.04%; [V]: 14.31 ± 1.27%; [VI]: 36.12 ± 2.24%; Vi1; [II/III]: 30.17 ± 2.03%; [IV]: 24.30 ± 1.74%; [V]: 22.13 ± 1.75%; [VI]: 23.40 ± 1.71%	[Brains]: n = 3		
Figure 2.15	Measurement	Values	N	Statistical	P value
Figure 2.15 B	Fraction of cells per layer (percentage over total & mean percentage ± Std)	Experimental data, [II/III]: 29.86%; [IV]: 30.69%; [V]: 14.86%; [VI]: 24.58%; Model 1, [II/III]: 29.21 ± 2.31%; [IV]: 30.36 ± 1.88%; [V]: 15.30 ± 1.29%; [VI]: 25.13 ± 2.04%	Experimental, [Clones]: n = 103; [Brains]: n = 25; Model 1, [Clones]: n = 103		
Figure 2.15C	Fraction of lineages containing 3 to 12 cells (percentage over total & mean percentage ± Std)	Experimental data, [3]: 10.68%; [4]: 14.56%; [5]: 6.80%; [6]: 10.68%; [7]: 11.65%; [8]: 17.48%; [9]: 11.65%; [10]: 3.88%; [11]: 5.83%; [12]: 6.80%; Model 1, [3]: 10.09 ± 3.03%; [4]: 9.97 ± 2.87%; [5]: 10.23 ± 3.07%; [6]: 11.08 ± 3.16%; [7]: 11.35 ± 3.35%; [8]: 12.18 ± 3.08%; [9]: 10.84 ± 3.33%; [10]: 9.86 ± 2.66%; [11]: 8.10 ± 2.70%; [12]: 6.30 ± 2.30%	Experimental, [Clones]: n = 103; [Brains]: n = 25; Model 1, [Clones]: n = 103		
Figure 2.15E	Fraction of Translaminar, Deep, and Superficial lineages (precentage over total)	Experimental data (mean {I.C. 95%}): Translaminar: 77.67 {68.93-84.47}%; Deep: 10.68 {5.83-17.48}%; Superficial: 11.65 {6.8-19.42}%; Model 1 (median ± intercuartile distance), Translaminar: 85 ± 5.0%; Deep: 11 ± 5.0%; Superficial: 4 ± 2.5%	Experimental, [Clones]: n = 103; [Brains]: n = 25; Model 1, [Clones]: n = 103	Fisher's exact test	p = 0.13
Figure 2.15F	Fraction of lineages in each configuration (percentage over total)	Experimental data (mean {I.C. 95%}), [II/III to VI]: 22.33 {14.56-31.07}%; [II/III-IV-VI]: 20.39 {13.59-29.61}%; [II/III-V-VI]: 4.85 {1.94-10.68}%; [II/III to V]: 6.80 {2.91-13.59}%; [II/III-V]: 1.94 {0-6.09}%; [IV-VI]: 7.77 {3.88-14.56}%; [IV to VI]: 7.77 {3.88-14.56}%; [II/III-VI]: 0.97 {0-5.82}%; [IV-V]: 4.85 {1.94-19.71}%; Model 1 (median ± intercuartile distance), [II/III to VI]: 34 ± 6.0%; [II/III-IV-VI]: 17.5 ± 5.5%; [II/III-V-VI]: 4 ± 2.0%; [II/III to V]: 8.5 ± 3.0%; [II/III-V]: 1 ± 1.0%; [IV-VI]: 4 ± 3.5%; [IV to VI]: 11 ± 4.5%; [II/III-VI]: 1.5 ± 1.0%; [IV-V]: 2 ± 2%	Experimental, [Clones]: n = 103; [Brains]: n = 25; Model 1, [Clones]: n = 103	Chi-square test	p = 0.16

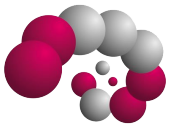

Table 2. Summary of data and statistical analyses for Results: Chaper II

Figure 3.1	Measurement	Values	N	Statistical	P value
Figure 3.1C	Percentage over total of progenitor cells of each morphology, and neurons (mean ± std)	aRG: 30.96 ± 9.56; SNP: 40.37 ± 10.7; bRG: 5.96 ± 5.42; MP: 14.72 ± 0.94; N: 3.39 ± 3.17; IN: 4.71 ± 7.53	[Cells]: n = 171 [Brains] n = 4		
Figure 3.1D	Percentage over total of progenitor cells of each morphology, and neurons (mean ± std)	aRG: 0.72 ± 0.91; SNP: 0.72 ± 0.91; bRG: 1.09 ± 1.09; MP: 11.61 ± 4.37; N: 83.98 ± 4.07; IN: 1.89 ± 1.89	[Cells]: n = 264 [Brains] n = 4		
Figure 3.1E	Percentage over total mitosis in each region (mean ± std)	VS: 48.99 ± 9.38%; VZ: 18.11 ± 3.24 ; SVZ: 32.89 ± 10.59;	[Brains] n = 4		
Figure 3.2	Measurement	Values	N	Statistical	P value
Figure 3.2B	#neurons per lineage (*Top:* mean ± std; *Bottom: m*edian ± IC distance)	Clone size [lineages]: 6.28 ± 3.3 Clone size [hemi-lineages]: 3.17 ± 2.82 Clone size [lineages]: 6.00 ± 4.00 Clone size [hemi-lineages]: 2.00 ± 2.00	[Lineages]: n = 25 [Hemi-lineages]: n = 82 [Brains]: n = 10		
Figure 3.2D	Fraction of lineages containing APs (percentage over total)	Containing APs: 52% Not containing Aps: 48%	[Lineages]: n = 25 [Brains]: n = 10		
Figure 3.2E	Fraction of lineages smaller and larger than 2 cells (percentage over total)	2-cell lineages: 75% >2-cell lineages: 25%	[Lineages]: n = 13 [Brains]: n = 10		
Figure 3.2F	#neurons per lineage (*Top:* mean ± std; *Bottom: m*edian ± IC distance)	Clone size: 4.23 ± 1.54 Clone size: 4.00 ± 2.00	[Lineages]: n = 25 [Brains]: n = 10		
Figure 3.2G	Fraction of 1 cell, 2 cells and >2 cell hemilineages (percentage over total)	1-cell hemi-lineages: 50% 2-cell hemi-lineages: 25% >2-cell hemi-lineages: 25%	[Lineages]: n = 12 [Brains]: n = 10		
Figure 3.3	Measurement	Values	N	Statistical	P value
Figure 3.3C	Percentage over total of cells in the SVZ (mean ± std)	Cortex: [3h]: 0.25 ± 0.43; [6h]: 0.12 ± 0.2; [14h]: 33.75 ± 4.13; [24h]: 30.15 ± 4.66 MGE: [3h]: 0.00 ± 0.00; [6h]: 2.02 ± 1.48; [14h]: 42.45 ± 4.23; [24h]: 49.26 ± 3.38	[Brains]: 3h: n = 3; 6h: n = 3; 14h: n = 4; 24h: n = 3	Paired t-Student test	[14h]: 0.00104 [24h]: 0.0372
Figure 3.3D	Percentage of progenitor cells over total cells in the SVZ (mean ± std)	Cortex: [14h]: 40.89 ± 3.99; [24h]: 35.26 ± 3.51 MGE: [14h]: 72.58 ± 10.18; [24h]: 51.68 ± 8.77	[Brains]: 3h: n = 3; 6h: n = 3; 14h: n = 4; 24h: n = 3	Paired t-Student test	[14h]: 0.0023 [24h]: 0.0327
Figure 3.5	Measurement	Values	N	Statistical	P value
Figure 3.5B	Fraction of recombinad cells (mean ± std)	[P-FAS]: 0.0042 ± 0.0042; [N-FAS]: 0 ± 0; [2272-FAS]: 0.0027 ± 0.0039; [FAS-FAS]: 0.7643 ± 0.0829; [C+]: 0.8409 ± 0.0309; [C-]: 0.0112 ± 0.0105	[Cultures]: n = 3	t-Student test with Welch´s correction	[P-FAS]: 0.0028 [N-FAS]: 0.005 [2272-FAS]: 0.0007 [FAS-FAS]: 0.2466
Figure 3.5C	Fraction of recombinad cells (mean ± std)	[P-P]: 0.6779 ± 0.0172; [2272-2272]: 0.6973 ± 0.023; [N-N]: 0.6792 ± 0.1485; [FAS-FAS]: 0.6843 ± 0.0683;	[Cultures]: n = 3		
Figure 3.7	Measurement	Values	N	Statistical	P value
Figure 3.7C	Percentage of cells with one or multiple reporters over total labeled cells (mean ± std)	One reporter: 44.64 ± 2.89 Multiple reporters: 55.35 ± 2.89	[Cultures]: n = 3		
Figure 3.7D	Percentage of cells with two, three or all reporters over total labeled cells (mean ± std)	Two reporters: 10.09 ± 0.59 Three reporters: 11.62 ± 2.03 All reporters: 33.64 ± 3.71	[Cultures]: n = 3		
Figure 3.7E	Percentage of sinlge reporter cells expressing each reporter (mean ± std)	TagBFP: 32.36 ± 3.46 EGFP: 17.50 ± 1.99 tdTomato: 27.58 ± 1.19 LacZ: 22.56 ± 2.69	[Cultures]: n = 3		
Figure 3.7H	Percentage of cells with one or multiple reporters over total labeled cells (mean ± std)	One reporter: 61.76 ± 7.69 Multiple reporters: 38.24 ± 7.69	[Brains]: n = 3		
Figure 3.7I	Percentage of cells with two, three or all reporters over total labeled cells (mean ± std)	Two reporters: 20.58 ± 4.34 Three reporters: 10.88 ± 3.27 All reporters: 6.77 ± 2.12	[Brains]: n = 3		
Figure 3.7J	Percentage of sinlge reporter cells expressing each reporter (mean ± std)	TagBFP: 40.47 ± 8.93 EGFP: 19.54 ± 2.53 tdTomato: 19.4 ± 5.82 LacZ: 20.59 ± 1.19	[Brains]: n = 3		
Figure 3.7K	Fraction of colonies recombined each configuration (percentage over total)	TagBFP: 25.47% EGFP: 30.19% tdTomato: 22.64% LacZ: 21.69%	[Colonies]: n = 106		